Some Investigations on Distribution Systems Resources Optimization

Ph.D. Thesis

NAND KISHOR MEENA

ID No. 2013REE9560

DEPARTMENT OF ELECTRICAL ENGINEERING

MALAVIYA NATIONAL INSTITUTE OF TECHNOLOGY JAIPUR

June 2018

Some Investigations on Distribution Systems Resources Optimization

Submitted in

fulfillment of the requirements for the degree of

Doctor of Philosophy

by

Nand Kishor Meena

ID: 2013REE9560

Under the Supervision of

Dr. Anil Swarnkar

DEPARTMENT OF ELECTRICAL ENGINEERING

MALAVIYA NATIONAL INSTITUTE OF TECHNOLOGY JAIPUR

June 2018

Declaration

I, **Nand Kishor Meena** declare that this thesis titled, ***"Some Investigations on Distribution Systems Resources Optimization"*** and work presented in it, is my own. I confirm that:

- This work was done wholly or mainly while in candidature for a research degree at this university.
- Where any part of this thesis has previously been submitted for a degree or any other qualification at this university or any other institution, this has been clearly stated.
- Where I have consulted the published work of others, this is always clearly attributed.
- Where I have quoted from the work of others, the source is always given. With the exception of such quotations, this thesis is entirely my own work.
- I have acknowledged all main sources of help.
- Where the thesis is based on work done by myself, jointly with others, I have made clear exactly what was done by others and what I have contributed myself.

Date:

Nand Kishor Meena

(2013REE9560)

Certificate

This is to certify that the thesis entitled ***"Some Investigations on Distribution Systems Resources Optimization"*** being submitted by ***Nand Kishor Meena (ID: 2013REE9560)*** is a bonafide research work carried out under my supervision and guidance in fulfillment of the requirement for the award of the degree of **Doctor of Philosophy** in the Department of Electrical Engineering, Malaviya National Institute of Technology, Jaipur, India. The matter embodied in this thesis is original and has not been submitted to any other University or Institute for the award of any other degree.

Dr. Anil Swarnkar

Associate Professor
Department of Electrical Engineering
Malaviya National Institute of Technology Jaipur

June 2018

The thesis is dedicated to

My respected teachers so far and beloved family

Acknowledgements

The research is driven by the motivation, dedication, determination, honesty, constant hard work and support of many individuals. My doctoral thesis is the outcome of many efforts that have been made by me and a number of individuals who have supported me time to time during my stay and in research work at MNIT Jaipur. I would like to express my sincere acknowledgement and thankfulness towards them.

First, I would like to express my sincere gratitude to my mentor **Dr. Anil Swarnkar** for his constant and valuable supervision during the years of my Ph.D. research work. He has allowed me to work in the area of my interest and motivated to explore it. He has always provided me a platform to express new ideas and gave meaningful shape to those, which made my Ph.D. research work possible. It is really a great opportunity for me to work with him. Again, I really thank him for all his help and support.

I am genuinely thankful to **Prof. K. R. Niazi** and **Dr. Nikhil Gupta** for being my inspiration, and their constant motivational support to make my Ph.D. interesting and successful. I have always enjoyed the fruitful discussions with them, which enhanced my knowledge of Electrical Engineering.

I am deeply grateful to **Prof. I. K. Bhat**, former Director and **Prof. Udaykumar R Yaragatti**, Director, MNIT, for extending all kinds of infrastructural facilities required for pursuing my Ph.D. I would like to thank **Prof. Manoj Fozdar**, former Head of Department; **Dr. Vikas Gupta**, Head of the Department; **Dr. Rajesh Kumar**, former Convener, DPGC and **Dr. Harpal Tiwari**, Convener, DPGC for encouraging me in all possible manners during the course of my Ph.D.

Further, I would like to thank all faculty members, Department of Electrical Engineering, MNIT Jaipur for their constant support and encouragement during the stay. I specially express my sincere gratitude towards the other members of my DREC **Dr. Kusum Verma** and **Dr. Rajive Tiwari** for time to time evaluations of my research work. I am also thankful to the examiners for devoting their valuable time to review this thesis in such a short-time duration and providing important suggestions/feedback to improve the quality of the thesis.

I really thankful to my wonderful friends at MNIT, Dr. Narayan K., Dr. V. K. Jadoun, Dr. N. Kanwar, Mr. M. Kumawat, Shalini, Ajeet, Pankaj, Sujil, Sonam, Venu, Akanksha, Pradeep, Pranda, Jayprakash, Abhilash, Bhanu, Satyendra and other fellow

who made my stay enjoyable. I am thankful to Rayees and Sachin for helping me to identify and remove typos in the report.

Finally, I would like to thank my family for their constant support and encouragement. I am specially thankful to my wife **Geeta**, children **Dhruv** & **Mitali**, father **Mr. Kajod Mal Meena**, mother **Mrs. Sharwani Devi**, brothers **Prahlad** and **Chetan** for their patience, encouragement, cooperation and understanding during my Ph.D. work.

(Nand K. Meena)

Abstract

The deregulation and restructuring of modern power industry along with several advancements in small-sized generation technologies have led to the concept of active distribution grids. The worldwide energy crisis and global warming have prompted change in national & international policies in order to increase the share of renewables. The changing trend and policies to include clean and sustainable resources have motivated system planners for a paradigm shift. In recent years, the integration of Distributed Resources (DRs) in distribution networks has received lot of attention from industry and academia due to its distinctive benefits and subsequent effects. However, the legacy distribution networks were not designed to accommodate active sources; therefore, non-optimal integration of DRs may produce counter-productive results. In order to minimize some of the issues, DRs are optimally planned as it may produce numerous techno-economic and social benefits for Distribution Network Operators (DNOs), DR owner and customers while improving system performance. Considering the number, location, size and type along with numerous constraints, the optimal DR integration problem turns out to be a complex mixed-integer, non-convex and non-linear optimization problem which requires powerful optimization techniques to solve it.

The purpose of this thesis is two-fold. One is to develop various optimization frameworks by modeling the effect of different DRs and various techno-economic & social benefits of optimal DR integration planning and operations. Initially, the single and multiobjective DR accommodation problems of distribution systems are investigated in deterministic frameworks to improve the system performance. Furthermore, to incorporate the variability and uncertainty of renewables and load demand in DR planning, multi-year optimization frameworks are proposed to maximize the net present value of the project in deterministic, probabilistic and stochastic environments. A multi-year operational framework is also developed to perform the optimal and online active network managements of distribution systems over the lifetime of various DRs. To accommodate the high penetration of renewables with the help of Battery Energy Storage Systems (BESSs), AI-based bi-level optimization framework is developed for optimal accommodation and operational management of BESS. Finally, an optimization framework is developed to optimally deploy the Electric Vehicle (EV) charging stations and to perform real-time operational management of growing EV fleet in smart city environment. The proposed frameworks for optimal planning and operations of DRs have uncovered various non-tangible benefits for DNO, consumer and DR owner. The simulation results obtained are compared with that of the

same available in the literature and found that the proposed approaches are providing promising results.

The another goal of the thesis is to develop new or improve existing optimization methods to solve proposed DR planning and operation problems of distribution systems. Two optimization methods i.e., Taguchi method and genetic algorithm are adopted while suggesting some improvements to overcome some of the limitations observed in their standard variants. The improved variants are alternatively used to solve the proposed DR planning and operation problems. Besides, two node priority lists are proposed to provide an engineering input to these optimization methods namely, static and dynamic node priority lists. The proposed lists are found to be very effective when compared with the same available in existing literature.

The proposed DR planning and operational frameworks are investigated on two standard test distribution systems i.e., 33-bus and 118-bus test distribution systems along with two real-life distribution systems i.e., 108-Indian and 201-bus Portugalian distribution systems. The simulation results reveal that proposed optimal DR planning and operational models are improved the system performance significantly while maximizing the monetary benefits of DR integration. Moreover, the two improved optimization methods are found to be promising when simulation results are compared with the same available in the literature. The comparison shows that the suggested improvements are meaningful and improved the methods performance significantly.

Contents

List of Tables

List of Figures

Abbreviations

AI	**A**rtificial **I**ntelligence
ANOM	**AN**alysis **O**f **M**ean
ANOVA	**AN**alysis **O**f **VA**riance
BESS	**B**attery **E**nergy **S**torage **S**ystem
BM	**B**io**M**ass
CS	**C**harging **S**tation
DG	**D**istributed **G**eneration
DE	**D**iesel **E**ngine
DER	**D**istributed **E**nergy **R**esource
DNO	**D**istribution **N**etwork **O**perator
DNPL	**D**ynamic **N**ode **P**riority **L**ist
DOE	**D**esign **O**f **E**xperiment
DR	**D**istributed **R**esources
DSSE	**D**istribution **S**ystem **S**tate **E**stimation
EV	**E**lectric **V**ehicle
FC	**F**uel **C**ell
GA	**G**enetic **A**lgorithm
GE	**G**as **E**ngine
GHG	**G**reen **H**ouse **G**as
IoT	**I**nternet **o**f **T**hings
LDC	**L**ine **D**rop **C**ompensation
LMP	**L**oad **M**ultiplying **F**actor
LPF	**L**agging **P**ower **F**actor

MOTA	**M**ulti-**O**bjective **T**aguchi **A**pproach
MT	**M**icro **T**urbine
NIS	**N**egetive **I**deal **S**olution
NPC	**N**et **P**resent **C**ost
NPV	**N**et **P**resent **V**alue
OA	**O**rthogonal **A**rray
OLTC	**O**n **L**oad **T**ap **C**hanger
PCC	**P**oint of **C**ommon **C**oupling
PDF	**P**robability **D**istribution **F**unction
PDN	**P**ower **D**istribution **S**ystem
PIS	**P**ositive **I**deal **S**olution
PV	**P**hoto-**V**oltaic
RCI	**R**elative **C**loseness **I**ndex
RTU	**R**emote **T**erminal **U**nit
RWS	**R**oulette **W**heel **S**election
SC	**S**hunt **C**apacitor
SMES	**S**uperconducting **M**agnetic **E**nergy **S**torage
SNPL	**S**tatic **N**ode **P**riority **L**ist
SOC	**S**tate **O**f **C**harge
TM	**T**aguchi **M**ethod
TOPSIS	**T**echnique for **O**rder of **P**reference by **S**imilarity to **I**deal **S**olution
UPF	**U**nity **P**ower **F**actor
VRD	**V**oltage **R**egulation **D**evice
VSI	**V**oltage **S**tability **I**ndex
VSM	**V**oltage **S**tability **M**argin
VVC/VVM	**V**olt-**V**Ar **C**ontrol/**M**anagement
WT	**W**ind **T**urbine

Symbols

CF_{t_p}	Capacity factor of t_p type DG
$\mathrm{CO}_2^{\mathrm{Max}}$	Maximum allowed CO_2 emission from PDN activities (kg/kWh)
$E_{Grid}/E_{DG_{t_p}}$	CO_2 emission associated in grid/DG energy (kg/kWh)
f	Degree of freedom
h	Hours
H_l	Number of hours in lth load level
i, j	System buses
I_{ij}^{Max}/I_u^{Max}	Maximum current limits of branch u, between bus i and j (p.u.)
I_{ij}/I_u	Current in branch u, between bus i and j (p.u.)
$I_{Spc.}/I_G^h$	Maximum allowed reverse current/Reverse current in hth hour (p.u.)
$K_{e,l}/C_E(h)$	Grid energy price during lth load level or hth hour (\$/kWh)
K_{em}	Cost of CO_2 taxation (\$/kg)
$K_{t_p}^{Inst}$	Turnkey cost of t_p type DG (\$/kW)
$K_{t_p}^{OM}/C_{OM}^{t_p}$	Operation and maintenance cost of t_p type DG (\$/kWh)
l	Load levels
L	Taguchi factor level
m, q	Number of factors and levels in DOE
N	Set of buses
N_{DG}	Number of DGs
N_L	Number of load levels
N_{t_p}	Number of DG types
N_{OLTC}/N_{SC}	Maximum number of OLTC/SC tap operations in a day
pf_{t_p}	Operating power factor of t_p type DG

$\underline{P_B}/\overline{P_B}$	Minimum/maximum charging limits of BESS in an hour(kW)
$\Delta P_{DG}/\Delta S_{DER}$	Discrete sizes of DG units (kW/kVA)
$P_{DER}^{Max}/S_{DER}^{Max}$	Maximum allowed limit of a DG unit in the system (kW/kVA)
P_i/Q_i	Real and reactive power injection at bus i (kW or kVAr)
P_{G_i}/P_{DG_i}	Real power generation at bus i (kW)
P_{L_i}/P_{D_i}	Real power load demand at bus i (kW)
$P_{Min}^{EV}/P_{Max}^{EV}$	Minimum/maximum charging limits of EV in an hour (kW)
$P_{r,i}^{WT/PV}$	Rated power output of WT/PV (kW) deployed at ith bus (kW)
Q_{L_i}/Q_{D_i}	Reactive power load demand at bus i (kVAr)
$Q_{G_i}/Q_{DG_i}/Q_{SC_i}$	Reactive power generation at bus i (kVAr)
r_{ij}/θ_{ij}	Resistance & impedance angle of line b/w bus i and j (p.u./rad.)
R_{int}	Annual interest rate
$\underline{SOC}/\overline{SOC}$	Minimum/maximum specified limits of SOC in BESS (%)
S_{Peak}	Peak demand of the system (kVA)
t_p	DG type
T_p/T_d	Set of Years
v_i^h/s_i^h	Wind speed(m/s)/solar irradiation(W/m^2) at bus i in hth hour
v_r/s_r	Rated wind speed(m/s)/solar irradiation(W/m^2) of WT/PV
v_{cuti}/v_{cuto}	Cut-in/Cut-out wind speed of WT (m/s)
$V_i/V_{il}/V_i^h$	Voltage magnitude at ith bus/during lth load level/in hth hour (p.u.)
$V_{\text{minS}}/V_{\text{maxS}}$	Minimum and maximum specified limits of node voltage (p.u.)
$V_{\min}/V_{\max}$	Minimum and maximum allowed limits of node voltage (p.u.)
W_B^R	Maximum allowed BESS capacity at given bus (kWh)
$\overline{W_B}$	Rated capacity of BESS at a given bus (kWh)
x/z	Set of system states and measured states
y	Years
Y_{ij}	Element of Y-bus matrix
δ_i/δ_i^h	Voltage angle at bus i/in h hour (rad.)
$\sigma_{i_{t_p}}/\alpha_i/\beta_i/\lambda_i/\chi_i$	Binary decision variable for deployment of t_p type DER at bus i
η	BESS efficiency (%)
$\rho_{i_{t_p}}$	Binary decision variable for operation of t_p type DG at bus i

Chapter 1

Introduction

1.1 Introduction

The electrical power system is broadly consisting of generation, transmission and distribution. In conventional system, the power is generated far away from the load centers in thermal, hydro and nuclear power plants due to techno-economic and social reasons. This bulk power is then transmitted at high voltage through transmission lines up to the load centers. Then it is distributed to consumers at desired voltage levels.

The energy demand is continuously increasing due to inclusion of new customers, urban development and living standard improvements, which forced the distribution systems to operate under stressed conditions. In passive distribution networks, due to radial structure, low operating voltage and high line resistances the power loss in feeders is high and tail end node voltages are low. Moreover, the electric distribution systems are becoming large and complex leading to higher system losses and poor voltage regulation. Literature has indicated that as much as 13% of total power generated is consumed as losses at the distribution level [1].

Nowadays, the modern consumers are becoming more concerned in terms of power quality, reliability and cost. At the same time, in the deregulated environment, the un-bundling of generation, transmission and distribution utilities is taking place. Therefore, there is a lot of pressure on distribution companies to meet the consumers need while maximizing the revenue and maintaining various constraints. Therefore, distribution systems need to

be improved and any improvement in distribution system would reflect back to transmission and generation systems; consequently improves the performance of the whole power system.

In the literature, many methods have been suggested to improve the distribution system performance, e.g., distribution network reconfiguration, optimal capacitor placement, phase balancing, load balancing, voltage regulation etc. In this deregulated environment, the integration of Distributed Resources (DRs) is also one of the modern ways to improve the distribution system performance and economics. The DRs may be of two types: passive and active. The passive DRs may include feeder voltage regulators, On Load Tap Changers (OLTCs), various passive demand response programs etc. The term, passive demand response may refers for the measures which encourage voluntarily participation of customers to shift their load demand for a specific period to another i.e., load management The active DRs are also known as Distributed Energy Resources (DERs), which may include Distributed Generations (DGs), Shunt Capacitors (SCs), Battery Energy Storage System (BESS), Superconducting Magnetic Energy Storage (SMES), Electric Vehicles (EVs), some active demand response programs etc. Unlike, passive demand response programs, the active programs reduce load for specific time period when called. It has been suggested that active demand response programs playing vital role to power system reliability and market efficiency. Due to technological innovation over a period of time the efficiency of small units for gas turbines, combined cycle, hydro and fuel cells over that of large ones is improved. Thus, it become possible for the industrial and commercial users of electricity to build and operate their own plants to produce power cheaper than that of utility and sell the excess power to small customers or utility, if available. Advancement in several generation technologies, environmental impacts of electric power generation, rapid increases in electric power demand, tight constraints over the construction of new transmission lines for long distance power transmission, high efficiency of small generating units and high power delivery losses encourage consumers and distribution companies to utilize more local generations support.

Additionally, thermal power generations are mostly depending on conventional energy resources which are limited, emitting toxic gases in the environment and have high sharing among the various causes responsible for global warming. The worldwide energy crisis, pressure of national and international policies aiming to increase the share of renewables to reduce greenhouse gas emissions have forced power system planners to integrate renewable based DGs. Next to environmental advantages, DGs contribute in the application of competitive energy policies, diversification of energy resources, on-peak operating cost

reduction, network upgrades deferral, lower losses, potential increase of service quality to end-users and remote electrification.

Nowadays, renewable and non-renewable DGs are suggested as two possible categories; the non-renewable DG resources may include combined heat & power (CHP), small scale gas fired power generating units and many more with rotating machines (synchronous or asynchronous machines). The prominent renewable DG resources are Photovoltaics (PVs) and Wind Turbines (WTs) with inverter circuitry. Each DG technology has different impacts on power system operation, control and stability. For instance, rotating device based DGs have much more profound effect on protection coordination than inverter based technologies whereas, the inverter circuitry based DGs have more voltage control capability, although they affect the harmonics level of the system more than synchronous machines based DGs [2]. The amount of fault current contributed by each DG technologies is also found to be variable. Generally, the converter based DGs may contribute two times current approximately for a small time period whereas the rotating machines can supply several times rated current for prolonged periods [3]. The synchronous based DGs can be damaged if they remains connected to the system during re-closing interval as out of re-closing may cause transient over voltages in the system. Moreover, the renewable energy resources are dependent on meteorological factors; therefore, these are non-dispatchable by nature. The intermittent and uncertain behaviors of renewable power generation may require frequent adjustments in conventional power plants to compensate the fluctuating power mismatch introduced by variable power generations and further, a suitable reserve requirement may be needed to maintain the system security and reliability. The pressure of variability of renewable generation resources is creating additional complexity on the non-renewable portion of the generation portfolio, with a consequence of net increase in operating costs [4].

In modern distribution systems, the concept of microgrid is also taking shape and it allows various DG technologies together to participate and contribute with or without the integration of grid to maximize the utility/consumer benefits. Microgrid may be grid connected or fulfill the demand independently, known as islanding mode of microgrid. The islanding capability is the most salient feature of a microgrid, which is enabled by using switches at the Point of Common Coupling (PCC) and allows the microgrid to be disconnected from the utility grid in case of upstream disturbances or voltage fluctuations [5]. In case of grid failure, the microgrid may be switched from the grid connected to the islanded mode and a reliable & uninterrupted supply for consumer loads is offered by local DGs.

Recently, EVs have emerged as the most prominent succeeder for conventional combustion engine based vehicles. The traditional transportation sector is also one of the culprits responsible for global warming and biggest consumer of convention fuels, like power industry. Therefore, governments across the globe are trying to increase the share of EVs in transportation sector, which may viewed as the sustainable future of transportation industry. The growing fleet of EVs will need the charging infrastructure to maintain the required State Of Charge (SOC) in vehicle battery, which will be reflected on the distribution feeders. Besides, the EVs may also be used as the source of energy to supply power back to the distribution grid when needed and may participate in electricity energy market. Therefore, the integration of EVs and BESS will further increase the operational complexity of system due to uncertainties in availability of vehicle and BESS SOC.

From above discussion, it may be concluded that the penetration of various DRs will grow in future distribution systems. In order to accommodate such a large penetration of DRs in distribution systems, it is required to develop an intelligent or resilient distribution grid. However, the legacy distribution networks were designed deterministically for unidirectional power flows, rather than to accommodate large amount of DR penetration. Therefore, the quick growth of DR penetration may raise many planning and operational issues for Distribution System Operators (DNOs). The high DG penetration leads to reverse power flows which might affect the operation of protection devices. Inappropriate DG locations and capacities more than certain limits, have negative effects such as increased line losses and over voltages. A DG located close to fault points contribute to the fault currents and might require the replacement of switchgear equipment. Moreover, the renewable DGs generally depend on meteorological factors that make these resources highly unpredictable and create vast volatilities in power generation. This variability is one of the challenges that need to be rectified to allow large integration of renewable energy resources.

The technical limitations of conventional distribution systems are the common causes, which are restricting the DER penetration in distribution systems. For example, in weakly connected rural networks, where large amounts of renewable resources are generally available, voltage rise and thermal capacity of feeder may limit the DG integration. Whereas, in urban networks, the large number of micro-CHP units could potentially be installed but the thermal limits and fault levels are the most common constraining factors [2]. Therefore, inappropriate DG allocation can also increase the network capital and operating cost that may lead utility to lose millions of dollars in longer planning horizon. Alternatively,

the optimal planning of DERs may generate enormous amount of benefits for the system operator, DG owner and consumer.

In deregulated energy market, the stakeholders want to maximize their revenue sufficing the technical & regulatory constraints along with the energy demand. Hence, considering the multiple objectives of DG owner, network operator and consumer, the DG planning problem turns out to be a multiobjective optimization problem comprising many objectives of interest, sometimes conflicting, need to be optimized simultaneously. Further, a compromising solution for different perspectives i.e. DG developer, distribution system operator, regulator etc. has to be obtained.

Now, considering the various aspects of different DR technologies, multiple objectives of stakeholders, DNO & consumers, stochastic nature of load and generation profiles along with DR parameters such as number, site, size and type, the optimal DR planning becomes a complex, mixed-integer, non-linear, non-convex optimization problem. Therefore, finding optimal number, location, capacity and type of DGs, while maintaining various system constraints, out of enormous feasible solutions, is a challenging task. In order to solve such a complex optimization problem, powerful optimization methods are required. It may be observed that analytical techniques are fast in computations; however, provides indicative results since simplified assumptions have been made [2]. Whereas, the meta-heuristic methods are capable to explore the global solutions but at the cost of higher computations. Therefore, new or improved variants of optimization techniques may be developed for better exploration of global optima of DG planning and operation problems in distribution systems.

In this thesis, the optimal planning and operational issues of different DRs are precisely addressed and solved for distribution systems. Besides, two existing optimization techniques have been improved to solve the complex DR integration problem. The thesis is organized in six chapters and the brief description of the chapters are as follows.

Chapter 1 includes the introduction and literature review sections on DR planning and operational management in distribution systems. On the basis of critical review, some research gaps are identified and presented in the chapter followed by proposed objectives.

In Chapter 2, the mathematical modeling of various DRs is presented; later, which are used in optimal planning and operational management of distribution systems in Chapter 4 and 5 respectively. The stochastic modeling of hourly renewable power generation and load demand are also presented in the chapter. In the thesis, backward-forward sweep method

has been adopted for power flow calculations of radial distribution systems; therefore, included at the end of this chapter.

Chapter 3 presents the optimization methodologies adopted to solve the proposed DR planning and operational problems. A classical Taguchi Method (TM) is introduced to solve the DR planning problem for the first time. Further, few improvements are also suggested to overcome some of the limitations of standard TM. Moreover, an improved variant of Genetic Algorithm (GA) is also proposed based on a Dynamic NPL (DNPL), suggested as an engineering input. In order to solve the multiobjective DG integration problems of distribution systems, a Multiobjective TM (MOTA) is also proposed. The method effectively combines Taguchi and Technique for Order of Preference by Similarity to Ideal Solution (TOPSIS) approaches.

In Chapter 4, various planning frameworks have been developed and solved using proposed Taguchi or GA based methods introduced in Chapter 3. The DR integration planning problems of dispatchable and non-dispatchable resources are separately investigated. In dispatchable DR, single and multiobjective DG allocation problems are investigated. In order to validate the suggested improvements, the performance of proposed variants of TM are compared with its standard and another modified variant of TM [6].

A coordinated planning problem of dispatchable DERs is developed considering the effect of OLTCs based voltage regulation schemes already available in grid substation(s). The problem is solved by the proposed DNPL-based GA, introduced in Chapter 3, for standard 33-bus test distribution system and a practical Indian distribution system of 108 buses. Moreover, the proposed MOTA is applied to solve the multiobjective DG integration problem of two standard test distribution systems of 33-bus & 118-bus and a practical Portugaian distribution system of 201 buses.

Finally, to incorporate the variability and uncertainty of renewable power generation and load demand in DR planning, a multi-year optimization framework is proposed to maximize the net present value of long-term DR planning in deterministic, probabilistic and stochastic environments. A pricing based Volt/VAr control of active distribution systems and upstream connected grids is also introduced. The proposed model is investigated on a standard 33-bus distribution system. Besides, various test cases are framed and investigated considering the combination of different DR technologies and types.

Chapter 5 presents various optimization frameworks for optimal operational management of active distribution systems. A Distribution System State Estimation (DSSE) is proposed to perform effective Active Network Management (ANM). Due to the inadequacies of

measurements in existing distribution networks, a Roulette Wheel Selection (RWS) based approach is suggested to generate the feasible pseudo measurements. An online ANM scheme is proposed to minimize the instantaneous operating cost of microgrid over the lifetime of available DRs. To validate the proposed online ANM scheme, the simulation results obtained are compared with the same obtained by traditionally used local ANM (offline) scheme.

A bi-level optimization framework is also developed for optimal integration and operational management of BESS along with wind power generation. The model is developed to minimize the feeder power loss, BESS conversion loss, reverse power flow, node voltage deviation and underutilization of BESS. The problem is implemented on 33-bus distribution system and solved using GA.

Further, the infrastructure planning and operational management of EVs in the smart city context is achieved using the help of Artificial Intelligence (AI) and considering the knowledge of Internet of things (IoTs). The goal of this work is to maximize the profit of utility and EV owners participating in real-time smart city energy market subjected to numerous techno-economic constraints of the EVs and power distribution system.

Finally, Chapter 6 summarizes the thesis highlights followed by the scope of future research in the area.

1.2 Literature Survey

Since last few decades, the DG integration problem has received lots of attention from power industry and academia due to its distinctive and enormous benefits to system operators, regulators and society. The growing interest in renewable energy resources has been observed from several years [7] as these are non-polluting, inexhaustible and freely available in the nature. These attributes make such resources attractive for current need of the power industry. The integration of DGs affects critical and economic operations of distribution networks. The optimally integrated DGs may provide enormous benefits such as minimized power loss [8–10], node voltage deviation [9], operating costs [11], T&D reinforcement cost [12], emission [13] etc. while improving the reliability [14,15] and stability [16,17]. Therefore, the DG integration planning problems have attracted the interest of many stakeholders. On other hand, inappropriate DG location and size may damage customer devices due to abnormal voltage and frequency during islanding operation of power system; it also threatens the utility worker's security during maintenance [18]. In this

section, the literature survey on DG planning is divided in two major categories. In first category, various types of problem formulation addressed in the literature, to maximize the integration benefits by revealing new aspects or objectives of DG accommodation, are discussed. Whereas in second category another important part of DG integration, i.e., optimization techniques adopted for DG planning, are summarized.

1.2.1 Problem Formulation of DRs

The typical DG integration problem deals with determination of optimal sites and sizes of DG units to be installed in existing distribution networks to optimize desired objectives, subject to the various constraints of electrical network operation, DG operation, investment, location etc. Based on objectives, DG variables, load variables, DG technology, constraints etc. considered in the literature, the DG allocation problem formulations may be further categorized as follows.

Objectives of DR Integration

In practice, DNOs need to meet many operational objectives of interest simultaneously. In literature, the optimal DG integration problem is formulated to solve one or more objectives. In deregulated and competitive energy market, the most desired objective of DG integration is to maximize the profit of DNO, stakeholders, regulator and customers. The monetary gain based objectives may include the maximization of profit [19–35] or benefit/cost ratio [22, 29]. The other monetary objectives are to minimize various investment and running costs of the system [11–13, 23, 23–32, 36–64]. Apart from economic aspects, the technical performance of modern active distribution grids has to be maximized. In order to improve the performance of distribution systems using DG integration, the commonly used objectives are minimization of system power loss [10, 12, 13, 15, 16, 19–23, 26, 27, 29, 33, 36–39, 42, 58, 60, 65–120], node voltage deviations [13, 22, 33, 43, 50, 106, 110, 112, 115, 118, 121, 122], reactive power requirement [73, 104], and maximization of Voltage Stability Index (VSI) [16, 20, 66, 68, 70, 84, 93, 118, 123], reliability [11, 14, 22, 37, 40, 41, 48, 49, 52, 60, 71, 73, 86, 97, 120, 124–133], voltage limit loading margin [20, 26, 42, 96] i.e. the maximum loading that can be supplied by the power distribution system while the voltages at all nodes are kept within the limits.

The energy loss minimization of Power Distribution Systems (PDNs) is one of the major concerns of DNOs as it affects the significant amount of revenue. Therefore, annual energy loss minimization of PDNs is also considered as one of the objective functions of DR integration [103,121,122,134–136]. Due to the modern sensitive equipments and machinery,

the consumer becomes more concerned about power quality issues; therefore, some of the power quality indices are optimized while integrating DRs in the system. The commonly adopted power quality objectives are to minimize total harmonic distortion [114, 137] and voltage sag mitigation [36]. The integration of active sources in distribution systems increases the fault current level of the system; therefore, short circuit level of the system is also minimized in [109] while optimally integrating the DERs. Further, some of the researchers have adopted the emission reduction as an objective function of optimal DG integration problem [13, 43]. The quick growth of DRs in distribution system has raised many coordination issues in daily operations; therefore, coordination issues and number of OLTC operation are minimized in [29, 33, 58]. The integration capacity of DGs are minimized in [50, 55, 106, 138, 139].

In single objective optimal DG integration problems of PDNs, only one of the objectives is optimized, whereas, in multiobjective optimal DG integration problems, two or more than two objectives are considered simultaneously. However, the definition and formulation of multiobjective optimization problems are complex. The multiobjective formulations can be classified as: a) multiobjective function with weights [16, 17, 104, 118, 140], where the multiobjective formulation is transformed into a single objective function using the weighted sum of individual objectives; b) goal multiobjective index [141, 142], where the multiobjective formulation is transformed into a single objective function using the goal programming method; c) multiobjective formulation considering more than one often contrasting objectives and selecting the best compromising solution in a set of feasible solutions; d) multiobjective problems transformed into single objective by multiplying all the objectives [8, 9] and e) through normalization of each objective function [143] etc.

DR Variables

The DR variables such as number, location, size and type of DRs are playing crucial role in optimal integration of DRs. In the literature, variety of research works are available in which one or more variables are considered to optimize while keeping others as fixed/constant. The majority of literature considered predefined number of DRs while determining other variables; therefore, such works can be further classified in single [66, 70, 76, 77, 85, 92, 144] and multiple [13, 38, 68, 74, 80, 82–84, 87, 88, 90, 91, 93–96, 100, 104, 107, 112–115, 117, 119–121, 145, 146] DRs deployment. The most desired DR variables are it's site and size which are alternatively computed in combination with other variables [2] such as: i) DR location only [77, 81]; ii) DR size only [78, 147]; iii) DR location & size only [10, 76]; iv) DR type, location & size only; v) DG number, location & size only; vii) DR number, type, location & size etc.

In this section, the DR type refers to DG resources, e.g., wind and solar. In above-mentioned second case where the design variable is only the DR size. This particular class of DR integration problem is very interesting in the smart grid system, where the integration of renewable energy resources are expected to increase. However, sizing and placement of these renewable DGs are greatly influenced by the availability of natural resources. Therefore, it is very important to determine the size of renewable energy when the location is already fixed [34, 148].

Load Variables

Load demand in a distribution system is highly unpredictable and difficult to model. In order to overcome the intricacy, many of the researches have suggested that the optimal integration of DRs may be obtained for single load level [16, 20, 21, 36, 65–67, 70, 72, 76–78, 80, 82, 85, 87, 90, 92, 107, 112, 113, 120, 145] i.e. nominal loading. A compromising DR sites and sizes have been achieved for multi-load levels [10, 19, 37, 43, 49, 53, 63, 69, 73, 83, 101, 114, 121, 144, 149–151]; mainly, three load levels are considered namely light, nominal and peak. Further, to incorporate the timely changing behavior of load demand, time-varying load levels are considered in [14, 25, 71, 100, 103]. Some of the researchers have adopted the probabilistic [27, 117, 139, 152] and fuzzy [38] load levels in order to model the demand uncertainty while optimally integrating the DRs.

Generally, the loads are either distributed along the lines or concentrated on the network buses. In case of concentrated load on buses, the following modeling alternatives have been considered in various research works: 1) constant power; 2) variable power that depends on the magnitude of bus voltage; 3) probabilistic; and 4) fuzzy etc.

DR Technologies

As discussed, when connected to the power system, the DR technologies have different impacts on power system operation, control, and stability [3, 153]. The DERs can be rotating devices such as synchronous or asynchronous machines directly coupled to the network, or they can be rotating or static devices interfaced via electronic converters. The inverter-based DR units, feeder voltage regulators and OLTCs have voltage control capability. However, the inverter based DERs may influence system harmonic levels more than synchronous-based DGs. On the other hand, directly coupled rotating DG units have much more profound effect on protection coordination. Thus, these power system impacts of DR technology affect it's site and size [123, 137].

Constraints

The optimal integration of DRs is subjected to numerous constraints. In literature, different types of constraints have been considered while optimally integrating DRs in distribution systems. Broadly, these can be categorized as technical, economical, regulatory and social constraints. The most commonly used technical constraints of optimal DR integration may include 1) nodal power balance constraints; 2) node voltage limits; 3) feeder or transformer capacity limits; 4) total harmonic voltage distortion limit; 5) short-circuit level limit; 6) reliability constraints; 7) power generation limits, 8) DER with constant power factor; 9) limited buses for DG installation 10) discrete size of DG units 11) DG penetration limit; 12) maximum number of DGs etc. Whereas, the budget limit constraint is the widely adopted economic constraint in optimal DR integration. The most commonly used regulatory constraints may involve voltage regulation of DERs, penetration or percentage share of renewables and provision of reactive power compensation or price. The emission control and safety of humans may come under the category of social constraints.

1.2.2 Optimization Methods Adopted

In previous section, the problem formulations of DR integration in distribution systems have been discussed from various literature. It shows that the optimal integration of DRs is a complex optimization problem; thus, requires powerful optimization techniques to obtain the optimal planning solution. In literature, various optimization methods have been adopted to find optimal solution of DG planning problem. A category wise brief literature review is given below.

Analytical Methods

Gözel and Hocaoglu [76] proposed a loss sensitivity factor, based on equivalent current injection to solve the DG integration problem considering power loss as an objective function. Acharya et al. [77] used a loss sensitivity based analytical approach to identify the single DG location on single load level and type. An analytical method based on the exact loss formula is proposed to obtain the optimal site and size of single DG. On a radial feeder with uniformly distributed load, the analytical method known as the '2/3 rule' suggests to install a DG of 2/3 capacity of the incoming generation at 2/3 of the length of line [79]; however, this technique may not be effective for non-uniformly distributed loads. Two analytical methods for optimal location of a single DG with fixed size is introduced in [81]; the first method is applicable to radial systems where as the second is for meshed systems. Hedayati et al., [83] proposed a method based on the analysis of power flow continuation and determination of most sensitive buses to voltage collapse. It also permits an increase in power transfer capacity, maximum loading, and voltage stability margin.

Analytical expressions for the optimal location and size of one and two DGs are proposed in [86]. An analytical method using a loss sensitivity factor that is based on the equivalent current injection is developed in [76] to find the optimum size and location of a single DG. An analytical method is proposed in [87] for finding the optimal locations of multiple DGs in combination with the Kalman filter algorithm for determining their optimal size. In [88], a loss sensitivity based approach used for different types of DGs allocation while calculating the optimal power factor value at single load level and type. Khan and Choudhry, [89] proposed an analytical approach to maximize the feeder loadability using optimal DG placement. Analytical expressions for finding optimal size and power factor of different types of DGs are suggested in [98]. An analytical method described in [94] computes the optimal location and size of multiple DGs, also considering different types of DGs.

Hung et al., [103] presented three analytical expressions, including two new expressions to minimize the power loss considering renewable DG models comprising time varying load model. In [104, 107, 108], an analytical approach is proposed based on minimizing the loss associated with the active and reactive component of branch currents by placing the DGs at various locations. Elsaiah et al., [105] used a loss sensitivity approach to minimize the real power loss of the system using multiple DGs and type placement considering single load level and type. A continuous power flow based methodology is proposed to maximize the voltage limit loadability (i.e. the maximum loading which can be supplied by the power distribution system while the voltages at all nodes are kept within the limits) [145]. In [116], a loss sensitivity based method is proposed for optimal allocation and sizing of DG units in order to minimize losses and to improve the voltage profile in distribution systems.

Numerical Methods

Gradient Search: Gradient search method is used in [78] and [147] for optimal sizing of DGs in meshed networks while ignoring and considering fault level constraints respectively.

Linear Programming (LP): In [154, 155], LP is used to solve DG integration models to achieve maximum DG penetration and maximum DG energy harvesting respectively.

Sequential Quadratic Programming (SQP): SQP is applied to solve the DG integration problem with and without fault level constraints, in [90] and [147], respectively. In [106], a multiobjective DG placement problem has solved through SQP.

Nonlinear Programming (NLP): A discrete probabilistic generation-load model with all possible operating conditions is reduced into a deterministic model that is solved using a mixed integer nonlinear programming (MINLP) technique for optimally allocating either

only wind DG units [156] or different types of DG units [134]. Various problems are formulated as multi-period AC optimal power flow (OPF) and solved using NLP [135, 139, 157]. The distribution network capacity for the connection of DG is computed by an OPF formulation that is solved by an interior point method [158]. MINLP is employed for optimal allocation of different types of DG units considering electricity market price fluctuation [159]. An DG planning model in hybrid electricity market is evaluated using MINLP [160]. An integrated distribution network planning model, implementing DG integration as an alternative option, is solved by MINLP [59]. Electronically interfaced DGs, with an objective of improving the voltage stability margin are optimally placed and sized using MINLP [123].

Dynamic Programming (DP): DP is applied to solve the DG integration problem to maximize the profit of DNO over considered light, medium and peak load conditions [71].

Ordinal Optimization (OO): An OO method is developed in [161] for specifying the locations and sizes of multiple DGs such that a trade-off between loss minimization and DG capacity maximization is achieved.

Exhaustive Search: The DG integration problem is solved by an exhaustive search that seeks the DG location and optimizes the objective function (maximization of reliability or minimization of system power loss) for a given DG size [14]. An exhaustive search is proposed to solve a DG integration problem for distribution networks with variable power load in [83, 89, 162]. A multiobjective performance index, taking into account the time-varying behavior of both demand and generation, when optimized by an exhaustive search, is suggested in [163].

Heuristic Methods

Genetic Algorithm (GA): GA is presented for optimal location and sizing of DGs on distribution systems [10, 16, 20, 22, 25, 39, 48, 50, 57, 82, 85, 109, 118, 164]. Lezama et al., [72] solved a location and contract pricing based DG allocation problem with GA. In [36], a power quality issue i.e. voltage sag mitigation problem is solved through GA. The GA and an improved Hereford ranch algorithm (variant of GA) are proposed in [15] for DGs optimal sizing. GA is applied to solve an DG integration problem with reliability constraints in [22, 97, 129]. Abdelazeem et al., [114], used GA for harmonics mitigation in rural distribution network. GA is used to solve a DG accommodation problem that considers variable power concentrated load models [165], distributed loads [85] and constant power concentrated loads [165, 166]. A GA is employed to solve DG allocation problem that maximizes the profit of DNO by optimal placement of DGs [19]. A GA methodology has been implemented to optimally allocate the renewable DGs in distribution network to maximize

the worth of connection to the local distribution company as well as the customers connected to the system [34]. A value-based approach, taking into account the benefits and costs of DGs, is developed and solved by a GA that computes the optimal number, type, location, and size of DGs [167]. A GA-based method allocates simultaneously DGs and remote controllable switches in distribution networks [149]. The Chu-Beasley GA solves a nonlinear bi-level programming problem of DG integration that maximizes the profits to the DG owner, subject to the minimization of payments procured by the DNO [72]. Goal programming transforms a multiobjective DG allocation problem into a single objective one, which is solved by GA [141]. GA and decision theory are applied to solve an DG allocation problem under uncertainty including power quality issues [168]. GA and OPF are combined to solve the problem [169]. A fuzzy GA is used in an DG planning model that minimizes the cost of power loss [170]. A fuzzy GA is employed to solve a weighted multiobjective problem [20, 171]. A hybrid GA and fuzzy goal programming is proposed to solve DG integration problem [142]. A combined GA and Tabu search is suggested in [82]. A hybrid GA and immune algorithm solves an DG accommodation problem that maximizes the profit of DNO [21]. GA solves a weighted-sum multiobjective optimization problem of DG integration [35]. Few multiobjective DG allocation problems are solved using a GA and an e-constrained method in [146, 172, 173]. A non-dominated sorting GA (NSGA) is used to maximize the distributed wind power integration [174]. NSGA-II (a variant of NSGA) in combination with a max-min approach solves a multiobjective DG integration problem [143] and also implemented in [41, 52, 53]. In [39, 175], DG planning models with uncertainties are solved by Monte Carlo simulation in conjunction with GA.

Tabu Search (TS): The DG planning problem is solved by a TS method for the case of uniformly distributed loads [80]. A genetic-based TS algorithm is used for optimal DG allocation in distribution networks [82]. A multiobjective TS is used to solve a multiobjective optimization problem of DG integration in distribution networks [109]. A. M. Cossi et al. [11] a TS optimization technique is used for DG planning taking into account reliability, operation and expansion costs under various contingencies. TS simultaneously solve the integration problem of DG and reactive power sources [176]. A continuous stochastic DG planning model is solved by a GA as well as by a combined TS and scatter search [131].

Particle Swarm Optimization (PSO): PSO is applied to solve an DG planning model in distribution system with non-unity power factor considering variable power load models [150]. An improved PSO is proposed for optimal placement of various DG types that inject real power and inject or absorb reactive power [91]. A hybrid GA and PSO is suggested in [16]. Discrete PSO computes the optimal DG location and OPF calculates the optimal DG size [177]. PSO is used for optimal selection of types, locations and sizes of

both inverter-based and synchronous-based DG units to achieve maximum DG penetration considering standard harmonic limits and protection coordination constraints [137]. Kumar et al. [122] proposed discrete PSO (DPSO) method, which utilizes the inherent inability of PSO to solve problems with discrete variables to solve the DG allocation problem. An improved particle swarm optimization (IPSO) has been proposed for the problem considering various load models [73].

Ant Colony Optimization(ACO): An ACO algorithm is proposed in [129] to solve the DG allocation problem. Favuzza et al., [12] used a dynamic ACO algorithm to solve an optimal electrical distribution systems reinforcement planning using gas micro turbines.

Artificial Bee Colony (ABC): An ABC method, with only two control parameters to be tuned, is proposed in [144].

Differential Evolution (DE): The optimal DG locations are computed based on incremental bus voltage sensitivities and the optimal DG sizes are calculated by DE [93]. Arya et al., [133] used DE with PSO for reliability evaluation and enhancement of distribution systems in the presence of distributed generation based on standby mode.

Harmony Search (HS): The optimal DG location is based on loss sensitivity factors and the optimal DG size is obtained by HS algorithm [10]. Nekooei et al., [115] proposed an improved multiobjective harmony search algorithm for DG integrations in distribution systems considering voltage profile and real power loss.

Practical Heuristic Algorithms: A heuristic approach places a single DG based on the ranking of the energy not supplied index or the ranking of the power losses in the network lines [37]. A heuristic cost-benefit approach to solve DG planning problem to serve peak demands optimally in a competitive electricity market is introduced in [178]. A heuristic value-based approach determines the optimum location of a single DG by minimizing the system reliability cost [128]. The DG placement in wholesale electricity market is solved by two heuristic methods that are based on a locational marginal price ranking and a consumer payment ranking [179]. A heuristic iterative search technique is developed that optimizes the weighting factor of the objective function and maximizes the potential benefit of distribution systems [180]. Heuristic methods based on continuation power flow are proposed in [84, 145]. The DG allocation problem is solved by voltage sensitivity analysis and loss sensitivity analysis of power flow equations in combination with a security constrained optimization method [97].

A heuristic method calculates the regions of higher probability for location of DG plants [181]. The DG integration problem of small distribution networks is solved by a heuristic method in [151]. The problem is solved by a heuristic iterative method in two stages, in which clustering techniques and exhaustive search are exploited [121]. A sensitivity test

computes the optimal location and a heuristic curve-fitted technique provides the optimal size of DG [92]. Heuristic methods for sizing wind farms based on modes of voltage instability are developed in [148].

1.3 Critical Review

As found in literature review, various objective functions have been formulated and solved to maximize the benefits of DG integration. In order to solve such complex problems, various optimization techniques proposed are also reviewed. The literature review shows that modern power industry has witnessed many reforms in last few decades to securely and reliably meet the growing energy demand across the globe. The unmanaged expansion of modern colonies especially, in urban areas, has forced distribution system planners to expand the PDN accordingly. Conventionally, various DRs and operational strategies have been deployed to improve the performance of such systems. The popularly used measures can be network reconfiguration, power factor correction, tap control of feeder voltage regulator, OLTCs and switched shunt capacitors etc.

The recent advancements in small-sized generating units and dispersed availability of energy resources have received the attention of DNOs to have their own generation,as optimally accommodated DGs are providing enormous techno-economic benefits to DNO, DG owner and consumer. However, the integration of DGs in distribution systems has changed the conventional structure and topology of existing vertically integrated power system. The unmanaged growth of active sources in PDNs may raise many new operational challenges. Therefore, there is a pressing need to re-investigate the planning and operational strategies of active distribution systems in the present scenario. On the basis of literature review, some crucial gaps have been identified as discussed below.

1.3.1 Optimization Techniques

The optimization techniques are always playing a vital role to solve various complex power system optimization problems. In the literature, numerous optimization techniques have been suggested. It may be observed that analytical methods are computationally fast but provide indicative results, since simplified assumptions have been made [2]. Alternatively, AI-techniques are capable to search the global or near global solution but are found to be computationally demanding. Therefore, new or modified version of optimization methods may be developed to improve the performance of active distribution systems.

1.3.2 Multiobjective Optimization Techniques

The deregulation and restructuring of modern power industry has got the interest of many stakeholders to invest in various developments of power system. The availability of multiple stakeholders at the level of distribution system has created the local competitive energy market. In such framework, every stakeholder wants to maximize his profit. In order to maximize the benefits of DNOs, customers and multiple stakeholders, the optimal DR planning model becomes a complex multiobjective optimization problem. In literature various multiobjective optimization methods have been developed to solve such problems, as discussed in literature review; however, most of these are suffering from some limitations. For example, the optimal solution of weighted sum approaches shows high dependency on selected weights while goal programming requires pre-specified goals defined by the operator. In ϵ-constraint based multiobjective formulation, an objective function is selected as master objective function while other objective functions are considered as slaves. Some of the limitations of such approaches are overcome by fuzzification of the objectives and max-min approach which brings all the objectives on same scale and units. However, it does not consider the even distribution of Pareto solutions.

1.3.3 Optimal Planning of DERs in Coordination with Existing DRs

The contemporary distribution systems are not newly designed or planned, since it is an outcome of time-to-time modifications have taken place in past due to various technological evolutions. It may be observed that most of the existing work available in literature, deploy DERs while ignoring the effect of existing DRs, which might be available in the system. However, such planning models may raise many coordination issues between newly installed and existing DRs. Therefore, it will be beneficial to formulate and re-investigate the DR accommodation problems in coordination with traditional measures.

1.3.4 Multi-year Stochastic Framework for Multiple DRs Planning

Several parameters of DER planning are uncertain, e.g., wind & solar power generation, fuel price, future load growth, market prices, future capital costs, future availability of fuel supply system, and charging of EVs. Very less work has been reported in the literature considering uncertainties and stochastic nature of above mentioned parameters. Therefore,

some research scope may be identified in the development of multi-year stochastic optimization frameworks for multiple DRs planning comprising generation and load demand uncertainties.

1.3.5 Active Network Management

The introduction of DGs enables active operations of distribution system, which certainly involves communication and control infrastructure. The DG can also participate in ANM schemes/strategies to improve the performance of distribution systems. Using real-time information about the operation of network and the nature of connected DG resources, protective relay settings may dynamically change. Moreover, deployment of ANM could reduce the total cost of integrating high penetrations of DGs. The DG planning model with embedded ANM schemes can help to ensure adequate power quality with high penetrations of DGs. In such environment, various new schemes/policies may be proposed and implemented for active networks to perform the Volt/VAr management of distribution and transmission networks simultaneously.

1.3.6 Optimal Planning and Operational Management of BESS

The recent advancements in battery storage technologies have risen the integration of BESS along with renewables to alleviate some of the impact of high renewable penetration, despite being costly. Moreover, the BESS provides an additional degree of flexibility to distribution systems by means of optimizing the way energy is generated from renewables, stored and it's effective utilization. However, the problem of BESS accommodation is more complex than the DG allocation problems, since it behaves like load and generation with uncertain SOC level, which require various estimation algorithms to determine the instantaneous SOC of each BESS. Considering the issues and challenges, the simultaneous optimal accommodation of deep renewables and BESS turns out to be a multi-level, complex mixed-integer, non-linear optimization problem, which may require multi-level optimization model and framework to determine the optimal site and size of renewables and BESS simultaneously.

1.3.7 EV Infrastructure Planning and Operational Management

The growing fleet of EVs will require the charging facilities to maintain the BESS SOCs of EVs. Moreover, various planning and operational management framework may be developed to facilitate the EVs in smart city context. Therefore, an optimization framework may be developed comprising of the AI-based techniques and Internet of Things (IoT) for optimal planning and operational management of mobile power infrastructure in the growing smart city context.

1.4 Research Objectives

From the critical review, following objectives are proposed

1. To carry out literature survey and comparative study of existing objectives, policies, constraints and optimization techniques used for DR planning.
2. To improve existing or apply new optimization methods to solve DR integration problem(s) of distribution systems.
3. To propose new/improve a multiobjective optimization method to solve the multiobjective DR integration problem(s) of distribution systems.
4. To formulate DER integration problem in the presence of conventionally existing devices/strategies in distribution systems i.e. DER planning in-coordination with network reconfiguration, OLTCs, feeder voltage regulator etc.
5. To develop a multi-year optimization framework for multiple DRs planning considering uncertainties associated with power generation and load demand.
6. To develop a multi-year optimization framework for ANM of distribution systems in presence of multiple DRs.
7. To develop an optimization framework for optimal planning and management of high renewable penetration in distribution systems.
8. To develop an optimization framework of mobile power i.e. EV infrastructure planning and operational management for smart city applications.

Chapter 2

Distributed Resources Modeling

2.1 Introduction

Traditionally, various types of DRs have been employed in distribution systems to achieve various techno-economic goals thereby DNOs have to perform many everyday tasks to operate the system in secure, reliable and economic manner. The quick growth of DGs in distribution systems makes the system operations more challenging. Therefore, a sophisticated modeling of modern distribution systems comprising of active and passive DR technologies is required to enhance the system performance. In this chapter, the modeling of various DRs, stochastic behavior of renewable generations and load demand is presented. Later, the backward-forward power flow calculations of radial distribution systems in the presence of DRs is also discussed. These modelings and the power flow method will be used for planning and operation of the active distribution systems in the following chapters.

2.2 Voltage Regulator(s)

The Volt/VAr Control (VVC) has always been an important concern for power system planners and operators in order to maintain steady node voltages across the system under variable load demand and generation. The typical objectives of VVC can include power loss minimization and voltage regulation, normally achieved by optimal tap-settings of OLTCs, feeder voltage regulators, SCs etc. Generally, power demand shows voltage dependency up to some extent, therefore VVC can also play a vital role in demand reduction [182, 183].

In this thesis, it is assumed that the grid substation transformer have the necessary on load tap-changing arrangements. Traditionally, the OLTC taps are being controlled by a local controller assisted by the Line Drop Compensations (LDCs) to estimate the target remote bus voltage. The basic arrangements of local OLTC tap controller are shown in Fig. 2.1(a). The controller adjusts the OLTC taps until the voltage comes in permissible limits as suggested in [184, 185]. Ref. [184, 185] also mentioned that the scheme may be suitable for voltage control in passive distribution systems but may not be a wise choice for active distribution networks due to the coordination issues among multiple Voltage Regulating Devices (VRDs). Moreover, the performance of LDC may be affected if active source is present in the systems resulted into estimation errors. Alternatively, the online OLTC tap control may be adopted to overcome some of the limitations of offline controllers. But, the measurement inadequacy of existing distribution systems makes the implementation more challenging. However, pseudo-measurements may be used to monitor the systems in minimum number of measurement units. Generally, field experience and engineering knowledge are in practice to deploy Remote Terminal Units (RTUs) on some critical nodes, feeders and VRs with various communication links (GPRS/Wi-Fi/LAN etc.). If it is assumed that the system supplies homogeneous loads over a small geographical area then the number of measurements will further reduce as suggested in [186]. The basic modeling of proposed online OLTC tap controller is presented in Fig. 2.1(b). In this work, RTUs are assumed to be deployed on all DER connected nodes, which measure the node voltages, currents in connected feeders and DER injection. For online control, online measurements are used to control the OLTC taps as suggested by the optimization method.

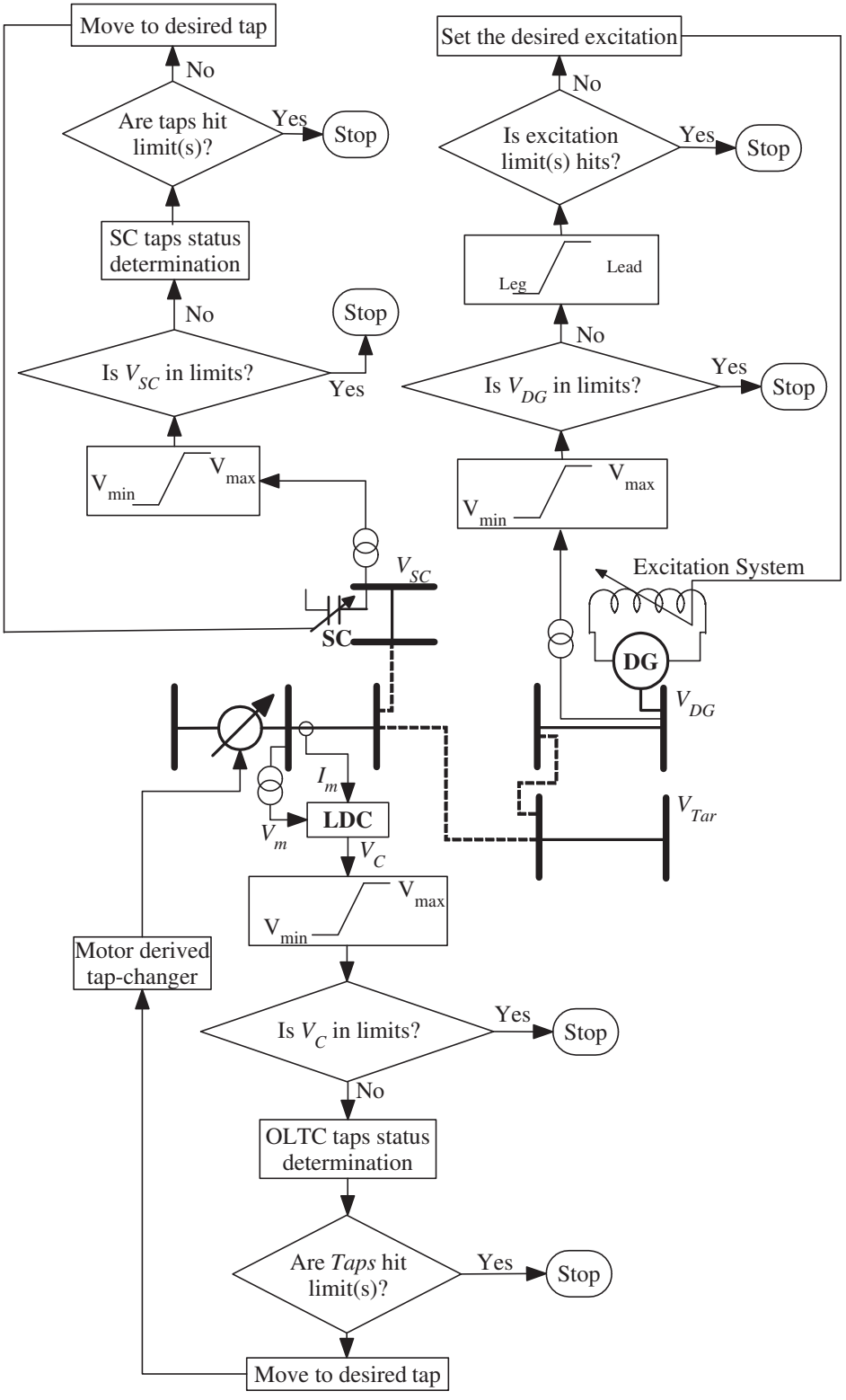

(a) Offline ANM

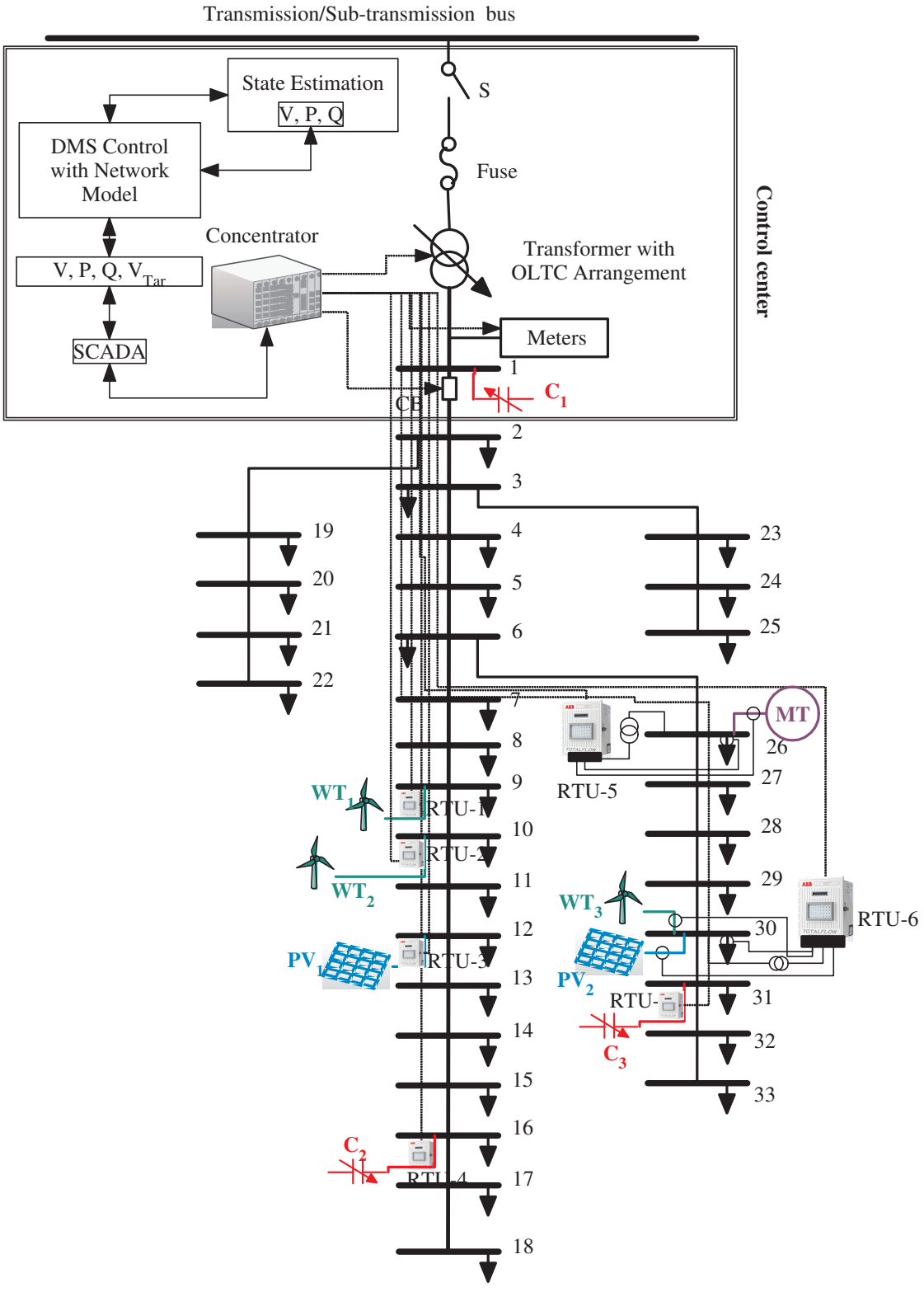

(b) Centralized online ANM

FIGURE 2.1: Basic structure of offline and proposed ANM schemes

2.3 Distributed Energy Resources (DERs)

DERs are capable to make the energy transactions to/from the system. The popularly known DERs are DGs, SCs, BESS, EVs, SMES etc. The individual modeling of the DERs used in the case studies of the thesis are given below.

2.3.1 Distributed Generations (DGs)

Nowadays, DGs are the most widely used DER technologies across the globe, which can be defined as a small-scale power generating unit connected near to load centers with a capacity of 1 kW to fewer MWs [187]. Due to the geographical distribution of natural resources, such types of generation technologies are known as the 'Distributed', 'Dispersed' and embedded generations. The DGs are operating locally, rather than centrally, in order to reduce the complexity, cost and dependencies on distribution and transmission networks while improving their efficiencies associated. The DGs are active source of energy associated with renewable or conventional energy resources. Generally, two types of DG models are studied in power flow calculations i.e. PQ and PV models. In the thesis, PQ models are referred for the DG models which inject pre-specified real and reactive power into the system whereas, PV models are referred for the models which supply and maintain pre-specified real power and PCC voltage respectively. In PQ model, the DG is considered as a negative load while restricting the voltage control capabilities of PCC. However, it is allowed to regulate the PCC voltage, if connected and operated in PV mode as shown in Fig. 2.2.

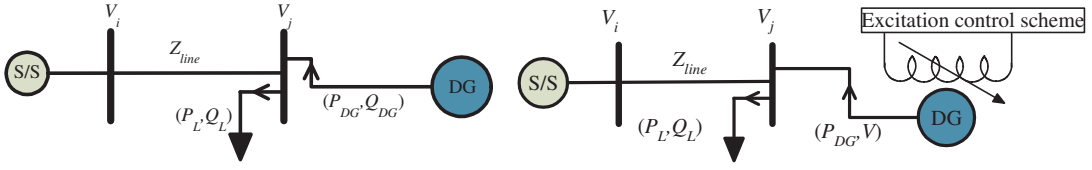

(a) PQ model (b) PV model

FIGURE 2.2: PQ and PV models used for optimal DG integrations in distribution systems

Fig. 2.2(a) shows that bus j is considered as the load bus (PQ-bus) for power flow calculations, if DG is injecting pre-specified amount of real and reactive powers at bus j. Since, the net real, P_j and reactive, Q_j power injections are known for the bus, the equations of power flow calculations in order to determine the bus voltages and angles can be modified

as

$$\begin{aligned} P_j = P_{DG_j} - P_{L_j} = V_j \sum_{i=1}^{N} V_i Y_{ij} cos(\theta_{ij} + \delta_i - \delta_j) \qquad \forall\ j \\ Q_j = Q_{DG_j} - Q_{L_j} = -V_j \sum_{i=1}^{N} V_i Y_{ij} sin(\theta_{ij} + \delta_i - \delta_j) \qquad \forall\ j \end{aligned} \tag{2.1}$$

Alternatively, if the generators are connected in voltage control mode as shown in Fig. 2.2(b), the real power generation and bus voltage will be known. Therefore, the amount of reactive power should be estimated in order to maintain the specified bus voltage. The load flow equations for PV buses can be expressed as

$$Q_j = -Im\Big[V_j \sum_{i=1}^{N} V_i Y_{ij}\Big] = Im\Big[V_j\{Y_{j1}V_1 + Y_{j2}V_2 +, \ldots, Y_{jj}V_j +, \ldots, +Y_{jN}V_N\}\Big] \tag{2.2}$$

However, it may be observed that frequent injection of large amount of reactive power into the system in order to improve node voltages may result in high field current, overheating of generator, triggering the excitation limit and disconnecting the DG from the system [115]. The reactive power dispatch capability of generators is mainly depending on stator current, rotor current and rotor voltage. Therefore, the VAr control capability of generators is limited by the maximum allowable current limits of field & armature windings and the stator core end-region heating limit. Therefore, the excitation is limited by the maximum leading to maximum lagging Power Factor (PF) to protect the generator field and armature winding as shown in Fig. 2.1(a).

For effective utilization of generator excitation control, two types of voltage control schemes, i.e., offline and online, are used in Chapter 5 of the thesis, if the DG is operated in the voltage control mode. In offline voltage control, a local set-point based generator excitation control is used to regulate the PCC voltage only as shown in Fig. 2.1(a). For online Volt/VAr Management (VVM), remote measurement based online voltage control is used to regulate all node voltages on the system unlike offline control. In the scheme, the DG will only allow to control the voltage if other passive voltage regulators such OLTC and SCs are not able to maintain the system node voltages within the pre-specified limits. Besides, an AI technique is used to determine the instantaneous tap status of OLTC, SCs and DGs simultaneously.

2.3.2 Shunt Capacitors (SCs)

Generally, distributed feeder SCs are deployed to maintain the PF and node voltages of system within the pre-specified limits. Besides, the optimal integration of SCs minimizes the real and reactive power loss of the system by providing the local VAr support. The SCs are connected as the negative load as shown in Fig. 2.3.

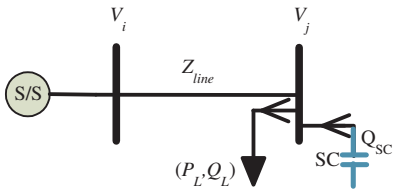

FIGURE 2.3: PQ model used for optimal SC integrations in distribution systems

The figure shows that SCs are injecting the reactive power only, which improves the power factor and node voltage profile while minimizing the real and reactive power loss. The nodal power balance used for power flow calculations for optimal SC integration in distribution systems can be expressed as

$$\begin{aligned} P_j = 0 - P_{L_j} = V_j \sum_{i=1}^{N} V_i Y_{ij} cos(\theta_{ij} + \delta_i - \delta_j) \qquad \forall\ j \\ Q_j = Q_{SC_j} - Q_{L_j} = -V_j \sum_{i=1}^{N} V_i Y_{ij} sin(\theta_{ij} + \delta_i - \delta_j) \qquad \forall\ j \end{aligned} \tag{2.3}$$

It may be stated that a variable SC can provide cheaper VAr support to the system as compared to a DG since the effective per kVAr cost of SC is considerably less as compared to per kVAr cost of any DG operating at lagging power factor. Therefore, technically and economically, the DGs may be lesser utilized to provide the VAr support and simultaneous integration of DGs and SCs may be encouraged as investigated in Chapter 4. The VAr dispatch of SCs can also be controlled through online and offline controllers. In offline Volt/VAr approach, traditional set-point based voltage regulation is adopted in the thesis, which control the PCC voltages within permissible limits. The flowchart of control algorithm provided in Fig. 2.1(a) shows that the controller would send the signal to tap changer if voltage is out of the dead-band limits and taps do not hit its limits.

In online VVM, central remote monitoring based controller is employed to control the reactive power dispatch of SCs, like in DGs. In each measurement sample, node voltages, feeders & transformer loading and system PF are estimated by the state estimator. In

this control, SCs tap status will be determined in coordination with other available voltage regulators, if node voltages or microgrid PF limits are violated. For this purpose, a meta-heuristic optimization method is used to determine the hourly scheduling of all VRDs simultaneously. Fig. 2.1(b) shows the online control arrangement for SCs as used for DG control.

2.3.3 Battery Energy Storage Systems (BESSs)

The recent advancements in energy storage technologies have received lot of attention from industry as well as academia. Besides, the quick growth of renewables and EVs have initiated the BESS deployment in modern distribution systems. The optimal BESS integration is more trickier problem than DGs as it behaves like load and generation both with uncertain SOC level. To perform this, various estimation algorithms are required to determine the instantaneous SOC of each BESS before charging/discharging considering numerous constrains.

In this thesis, BESSs are considered as negative and positive loads when it supplies and consumes power to/from the systems respectively. Fig. 2.4 shows that the BESS supplies/absorbs the real power only connected at node j as negative/positive load only.

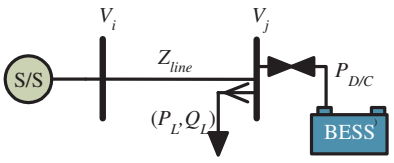

FIGURE 2.4: PQ model used for optimal BESS integrations in distribution systems

After BESS integration at node j, the modified nodal real and reactive power balance used for the power flow calculations may be expressed as

$$\begin{aligned} P_j &= P_{C/D_j} - P_{L_j} = V_j \sum_{i=1}^{N} V_i Y_{ij} cos(\theta_{ij} + \delta_i - \delta_j) \qquad \forall\ j \\ Q_j &= 0 - Q_{L_j} = -V_j \sum_{i=1}^{N} V_i Y_{ij} sin(\theta_{ij} + \delta_i - \delta_j) \qquad \forall\ j \end{aligned} \tag{2.4}$$

Here, P_{C/D_j} is representing the charging/discharging amount of power scheduled for the BESS deployed at node j. The reactive power dispatch from BESS is not considered in the proposed research work.

2.3.4 Electric Vehicles (EVs)

The traditional transportation sector is mainly relying on the conventional fuels such as diesel, petrol and gas which are limited in nature. Besides, the industry is one of the major culprits which are responsible for Green House Gas (GHG) emission. As discussed, the recent advancement in battery energy storage technologies has also stimulated the growth of EV industry. In near future, the quick growth of EVs might have significant impact on contemporary distribution systems. The unscheduled and non-optimal charging and discharging of EVs may increase the operational and economic challenges for DNOs. Therefore, the optimal planning and operational management of EVs may be required to maximize the techno-economic and social benefits for utilities and EV owners. The optimization models and strategies may play a vital role to solve the future mobile power infrastructure planning and management problems. The problem of optimal Charging Station (CS) placement is more complex than the optimal placement of BESS because, the time, availability and SOC status of EV batteries are not under the control of DNO. However, the power flow equations and constraints of batteries employed in EVs will be assumed to be the same as that of the BESS in previous section.

2.4 Probabilistic Modeling of Renewable Power Generation and Load Demand

Mostly, the energy consumption pattern is depending on type of consumers, their usage behavior and environmental factors, which are highly uncertain and difficult to model. Besides, the renewable power generation is also intermittent and uncertain by nature. To overcome the intricacy, some researchers have adopted the deterministic modeling of the system [121, 188]. However, it may provide average integrated benefits while ignoring the system uncertainties. To overcome the limitations, the probabilistic modeling of generation and load is suggested in literature to incorporate associated uncertainties [156, 189, 190], which deals with the generation and load demand uncertainties.

However, these models have treated the renewable power generation and load demand as independent events thereby the concept of combined probability is adopted for generation and load demand. Whereas, the occurrence of one event is affecting the other i.e. change in wind speed or solar irradiation may result into the change in load demand, since both are depending on environmental factors. Besides, complete historical data of load or generations is fitted into a single Probability Distribution Function (PDF) [156, 189, 190].

Such models may be appropriate for planning stage irrespective of hourly occurrence of multiple events thus may provide misleading results in operation.

Therefore, a sophisticated stochastic ad-hoc model is required for complete system, which models the hourly generation and load demand separately in order to extract the actual benefits of DER planning and operations, unlike in [156, 189, 190]. In following sections, the proposed probabilistic modeling of hourly solar irradiation, wind speed and load is presented followed by the stochastic modeling for complete system.

2.4.1 Wind Power Generation

The wind speed is variable and uncertain by nature thereby requires a probabilistic modeling. In literature, the wind power generation is modeled as Weibull PDF to analyze planning and operational aspects of distribution systems [190]. In this thesis, the hourly wind speed is modeled as Weibull distribution function as shown in Fig. 2.5 and expressed for ith bus in hth hour as

$$f(w_i^h) = \frac{\gamma^h}{(\beta_i^h)^\gamma}(w_i^h)^{\gamma-1} exp\left(\frac{w_i^h}{\beta_i^h}\right) \tag{2.5}$$

where, w_i^h is the wind speed (m/s) in hth hour, γ^h and β_i^h are the shape and scale parameters of Weibull probability distribution respectively. The PDF of each hour is divided into N_W segments of equal width. Then the mean wind speed $[v_1, v_2, v_3, \ldots, v_{N_w}]$ and their corresponding areas or probabilities $[p_1^w, p_2^w, p_3^w, \ldots, p_{N_w}^w]$ of segments are obtained for each hour.

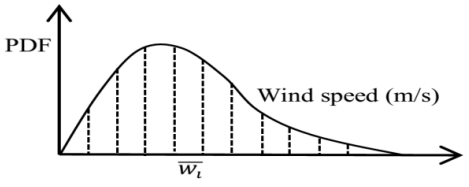

FIGURE 2.5: Weibull probability distribution function of wind speed

2.4.2 Solar Photovoltaic Power Generation

Usually, various forecasting techniques, based on historical data, are adopted to determine the future solar irradiation. The solar irradiation can be modeled as normal or Gaussian

PDFs. Therefore, in this work, hourly solar irradiation is modeled as a normal PDF. The hourly associated PDF used in the thesis work is demonstrated in Fig. 2.6 and expressed for hth hour at ith bus as

$$f(x_i^h) = \frac{1}{\sqrt{2\pi\sigma_h^2}} exp\left(\frac{-(x_k^h - \mu^h)^2}{2\sigma_h^2}\right) \tag{2.6}$$

where μ^h and σ_h are representing mean and standard deviation (Std.) of solar irradiation (W/m^2) or demand for hth hour. In proposed probabilistic model, in each hour, load and generation profiles are considered for statistical analysis and an interval for normal PDF, $\mu^h \pm 3\sigma_h$ is considered with 99.7% probability, which is divided into N_{PV} segments of equal width, like wind speed model. The area of each segment represents the probability of average solar irradiation of that segment. For each hour, average solar irradiation of each segment $[s_1, s_2, s_3, \ldots, s_{N_{PV}}]$ and corresponding probabilities $[p_1^s, p_2^s, p_3^s, \ldots, p_{N_{PV}}^s]$ are kept for the auxiliary analysis.

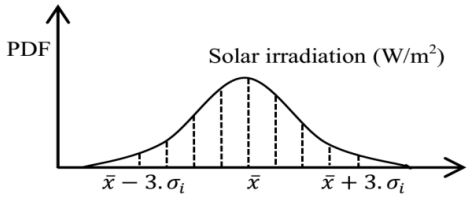

FIGURE 2.6: Gaussian probability distribution function of solar irradiation

2.4.3 Load Demand

Similar to solar irradiation, demand also follows the normal probability distribution [189, 190]. Hence, a similar model is also adopted for probabilistic load modeling. Initially, hourly Load Multiplying Factor (LMF) of given historical data is calculated by dividing the annual data with its corresponding annual peak. Then its hourly PDF is also divided into N_D number of segments of equal width as done for solar PDF. The mean LMF of each segment $[dl_1, dl_2, dl_3, \ldots, dl_{N_D}]$ and their corresponding areas or probabilities $[p_1^d, p_2^d, p_3^d, \ldots, p_{N_D}^d]$ are evaluated for each hour.

2.5 RWS based Stochastic Modeling of Complete System

Following the previous sections, the probabilistic modeling of complete system is framed in this section. In the model, each hour can have N_{PV}, N_W, and N_D set of possible values for solar irradiation, wind speed and load demand respectively along with their corresponding probabilities. In each hour, system can have total $N_{PV} \times N_W \times N_D$ number of possible states and each probable state $[(s, w, d)\epsilon(N_{PV} \times N_W \times N_D)]$ has a combined probability of $(p_d \times p_w \times p_s)$, if events are independent as shown in Fig. 2.7. However, the events might have some dependency as all parameters are depending on weather. Therefore, combined probability approach may be avoided. Here, the probability analysis of each variable is done independently, unlike previously proposed models [156, 189, 190].

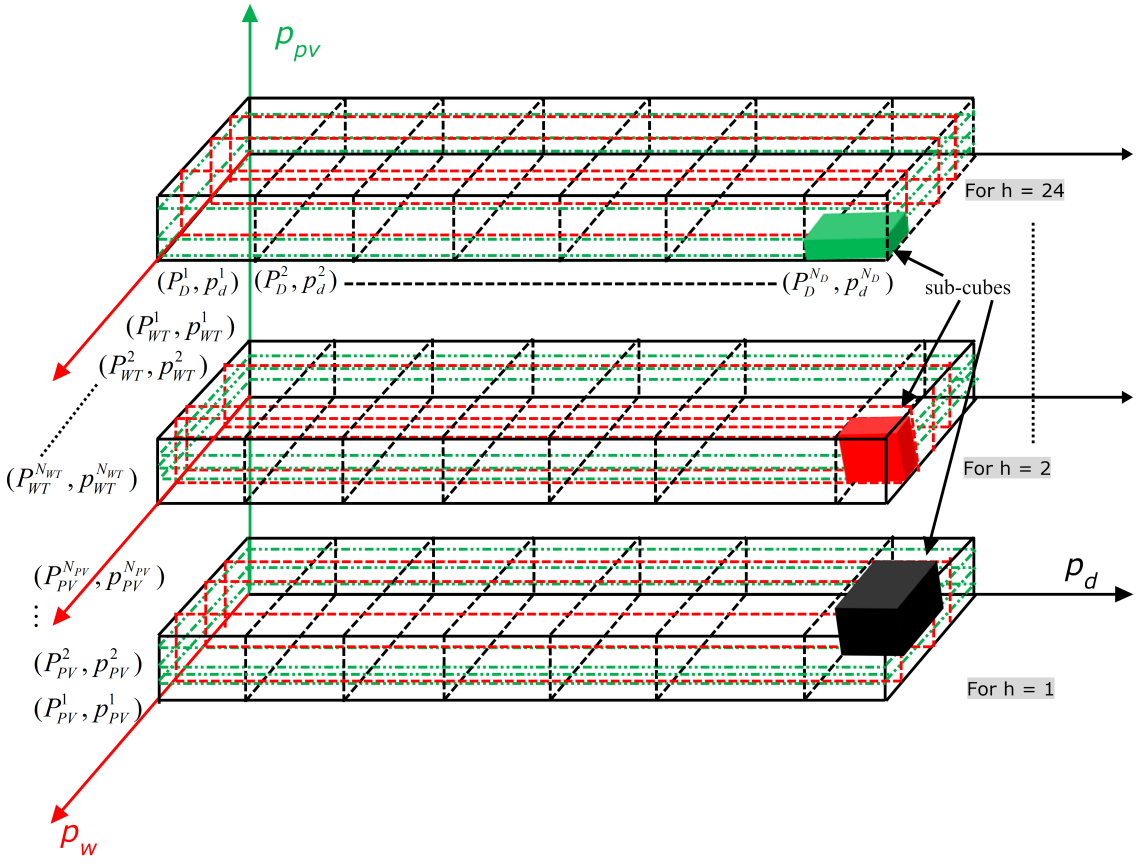

FIGURE 2.7: Probabilistic model structure of complete system

In this work, hourly stochastic data modeling of load demand, solar irradiation and wind speed are obtained; besides, RWS criteria is adopted that itself is a probabilistic approach. For each hour, roulette wheel is spun three times to get probabilistic values, $f^{RWS}(s\epsilon p_s, w\epsilon p_w, d\epsilon p_d)$ of solar irradiation, wind speed and LMF individually. The RWS

criterion selects a more probable outcome among N_{PV}, N_W and N_D possible values respectively based on their corresponding probabilities obtained in previous sections. The variables X^{PV}, X^W, and X^D are representing the selected states of solar irradiation, wind speed and demand using RWS criteria respectively. Now, the stochastically generated kW power of PVs & WTs along with kW demand is discussed below.

2.5.1 Stochastic Wind Power Generation

The WT produces real power as a function of wind speed and other turbine parameter such as swapping area, pitch angle, air density etc. However, these parameters can be assumed to be constant for all hours except wind speed. Therefore, using appropriate transformation, wind speed may be converted into the real power as a cubic function of wind speed

$$PG_i^{Wind} = f(v) = av^3 + b \tag{2.7}$$

where, a and b are the constants. Using (2.7), proposed RWS based stochastic wind power generation at bus i is expressed as

$$PG_i^{WT}(h) = \begin{cases} 0, & 0 \le v_i^h(X^W) < v_{cuti} \text{ or } v_i^h(X^W) \ge v_{cuto} \\ \left[\frac{v_i^h(X^W)}{v_r}\right]^3, & v_{cuti} \le v_i^h(X^W) < v_r \\ P_{r,i}^{WT}, & v_r \le v_i^h(X^W) < v_{cuto} \end{cases} \quad \forall\ h, i \tag{2.8}$$

where, $v_i^h(X^W)$, $X^W \epsilon [1, 2, 3, \ldots, N_W]$ is the probabilistic wind speed obtained by RWS criteria at ith bus in hth hour according to their probabilities $P(X^W)$.

2.5.2 Stochastic Solar Power Generation and Load Demand

Typically, distribution system covers a small geographical area. Hence, due to geographical proximity, the solar irradiation is assumed to be the same for all buses [191]. Therefore, same probability distribution given in (2.6) may be used for all buses for a given time-frame. The PV produces real power as a function of solar irradiation and some solar PV module parameters such as surface area, tilt angle, temperature, efficiency etc. Therefore, without loss of generality and simplicity of the model, module parameters are assumed to be constant in all operating hours except solar irradiation. The PV power generation at

ith bus can be expressed as a linear function of solar irradiation.

$$PG_i^{Solar} = f(s) = es + f \tag{2.9}$$

where, e and f are the constants. Following the assumptions, the hourly power generation from PV power plants can be expressed as the fraction of its installed rated power output at bus i. Using (2.9), the proposed hourly stochastic power generation of a PV plant installed at ith bus is expressed as

$$PG_i^{PV}(h) = \begin{cases} \frac{s_i^h(X^{PV})}{s_r} P_{r,i}^{PV}, & 0 \leq s_i^h(X^{PV}) < s_r \\ P_{r,i}^{PV}, & s_r < s_i^h(X^{PV}) \end{cases} \qquad \forall\ h, i \tag{2.10}$$

where, $s_i^h(X^{PV}),\ X^{PV} \epsilon [1, 2, 3, \ldots, N_{PV}]$ is the probabilistic outcome of solar irradiation obtained by RWS criteria at ith bus in hth hour on the basis of their probabilities $P(X^{PV})$. A similar model is also adopted to synthesize the stochastic load profile of the system. The RWS based hourly stochastic demand at ith bus is expressed as

$$P_i^D(h) = dl_i^h(X^D) \times P_{L,i}^{annual\_peak} \qquad \forall\ i, h \tag{2.11}$$

where, $dl_i^h(X^D),\ X^D \epsilon [1, 2, 3, \ldots, N_D]$ represents the probabilistic LMF obtained by RWS for ith bus in hth hour on the basis of their probabilities $P(X^D)$.

2.6 Power Flow Calculations in Presence of Distributed Resources

In order to determine the steady-state performance of distribution systems, power flow studies are required. It may be observed that the traditional power flow methods such as Newton-Raphson and Gauss Seidel etc. may show ill-conditioning for radial distribution systems. However, modified Newton-Raphson method is used for power flow studies of radial or weakly mesh distribution systems but requires relatively high computations. The backward/forward sweep method is popularly used for power flow studies of radial distribution systems thereby adopted in the thesis for load flow calculations. The method is simple and requires lesser computations for power flow calculations as compared to modified newton methods. In this thesis, the backward/forward sweep method is presented for the power flow studies of passive/active distribution systems as it is utilized in the work. In order to demonstrate the method, a simple radial feeder is used as shown in Fig. 2.8.

The basic steps of the method can be summarized as given below.

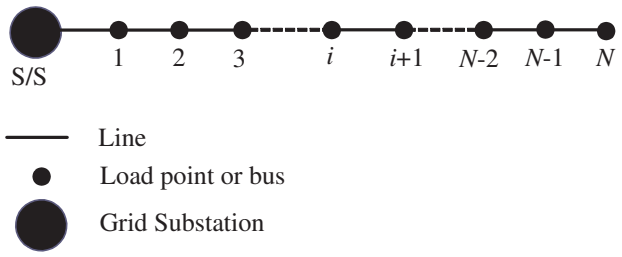

FIGURE 2.8: Single line diagram of a radial distribution system feeder

***Step*-1:** Set input parameters such as base kV, kVA, iterations, line data, bus data etc. and set all node voltages to $1\angle 0$.

***Step*-2:** Calculate the base value of all quantities as given below.

$$\begin{aligned} Z_{base} &= \frac{kV_{base}^2}{MVA_{base}} \\ I_{base} &= \frac{MVA_{base}}{kV_{base}} \end{aligned} \tag{2.12}$$

***Step*-3:** Convert all given quantities into their respective per unit value such as

$$\begin{aligned} Z_{ij}(p.u.) &= \frac{Z_{ij}(\Omega)}{Z_{base}} \qquad \forall\ i,j \\ S_i^{inj}(p.u.) &= \frac{S_i(MVA)}{S_{base}} \qquad \forall\ i \end{aligned} \tag{2.13}$$

where,

$$S_i^{inj} = S_{DER_i} - S_{L_i} \tag{2.14}$$

$$S_{DER_i} = P_{DER_i} + jQ_{DER_i} \tag{2.15}$$

$$S_{L_i} = P_{L_i} + jQ_{L_i} \tag{2.16}$$

***Step*-4:** Determine the terminal and intermediate nodes of the system. For example, node N is the terminal node and all other are considered to be the intermediate nodes.

***Step*-5:** Determine the current injection of all nodes as given below

$$I(i,i) = \left(\frac{S_i^{inj}}{V_i}\right)^* \qquad \forall\ i \tag{2.17}$$

***Step*-6:** Start with end/terminal node i.e. N, reverse sweep is used to calculate the branch currents using the Kirchhoff's current law till the substation node is reached as shown in

Fig. 2.8 and expressed below.

$$I(i-2,i-1) = \left(\frac{S_{i-1}^{inj}}{V_{i-1}}\right)^{*} + I(i-1,i) \qquad \forall\ i \tag{2.18}$$

***Step*-7:** Now, forward sweep is used to update the node voltages by adopting the ohms law till the terminal/end node is touched. Start from the substation by considering the substation node voltage to $1\angle 0$.

$$V_{i+1} = V_i - I(i,i+1) \times Z(i,i+1) \tag{2.19}$$

***Step*-8:** Repeat step-5 to 7 till the specified convergence criteria is reached.

2.7 Summary

The chapter presents the modeling of different DRs which are used in Chapter 4 and 5 for optimal planning and operations of active distribution systems respectively. The controlling schemes of DRs i.e. offline and online are also presented for operational management of distribution systems. The probabilistic behavior of wind speed and solar irradiation are modeled into the wind and solar PV power generation respectively along with the probabilistic modeling of system load demand. Further, a RWS based stochastic model of complete system is proposed to produce hourly stochastic states of solar and wind power generation. In order to determine the steady-state states of active distribution systems comprising of different DRs, backward/forward power flow method is re-introduced and will be used throughout the work for load flow studies.

Chapter 3

Optimization Methods

3.1 Introduction

The optimization methods are playing a crucial role to solve various complex real-life problems. Classically, analytical methods are popularly used to obtain the optimal solution quickly by making some simplified assumptions. However, it may be noticed that the analytical methods are not capable to explore the global optima. Whereas, contemporary method such as meta-heuristic techniques are capable to explore it better, which may be very difficult or sometimes impossible to solve using analytical methods, but at the cost of slightly more computations [2]. The methods are inspired by the self-sustaining characteristics and controlling behavior of various elements of the nature. Nowadays, these behaviors and characteristics are modeled into some set of mathematical equations to develop an artificial intelligence of nature to solve the complex real-life engineering problems. So far, numerous optimization algorithm inspired by genetics, nervous system, swarm intelligence, based on the behavior of birds, fishes, bees, ants, bats, frogs, elephants, cats, wolfs, buffalo etc. have been suggested in the literature. These algorithms are applied to solve various complex power system optimization problems and are found to be very effective to search the global or near-global solutions. To enhance the working of such techniques, various improved or hybrid versions are also available in the literature [8, 9, 16, 115, 140, 192].

As discussed in Chapter 1, the optimal DR integrations and their operational management problems are turned out to be a complex mixed-integer, non-linear, non-convex and combinatorial problem generally comprised of number, location, sizes, taps and type of DRs. In order to solve such complex real-life problems, powerful optimization techniques may

be required. In this thesis, two optimization methods have been used to solve the single and multiobjective DR planning and management as discussed below.

3.2 Taguchi Method (TM)

TM is a statistical method developed by Dr. Genichi Taguchi to improve the product quality in manufacturing industry. It employs Orthogonal Arrays (OAs) to tune the input parameters over different levels to get optimal outcome in minimum number of experiments. It is used when values of input parameters are too large to allow the exhaustive search of every possible input level in shorter time interval. In TM, objective function is recursively optimized while satisfying various system constraints. The method is used for systems having small number of inputs with large range of possible values thus large search space. The basic TM is broadly divided into two essential steps, first is OA construction and second is response analysis [193, 194].

3.2.1 Orthogonal Arrays (OAs)

The OA is an essential part of TM that represents special combinations of factor levels used in Design of Experiments (DOE). These statistically organize the possible levels of factors/parameters at which they can be varied for determining the relationship between process inputs and outputs. The objective is to intelligently gather the information about relationship between inputs and outputs with the least amount of effort. A sample case OA is given in Table 3.1, where each factor has two possible levels [6, 193, 194]. For example,

TABLE 3.1: Orthogonal Array $L_8(2^5)$

Test No.	OA					Fitness
	F_1	F_2	F_3	F_4	F_5	
1	1	1	1	1	1	J_1
2	1	1	1	2	2	J_2
3	1	2	2	1	1	J_3
4	1	2	2	2	2	J_4
5	2	1	2	1	2	J_5
6	2	1	2	2	1	J_6
7	2	2	1	1	2	J_7
8	2	2	1	2	1	J_8

m and q are representing total number of factors & levels for each factor respectively

then maximum possible number of factorial DOE is expressed as q^m. However, maximum number of Taguchi experiments will be $M = m \times f + 1$; where, $f = (q - 1)$ is the degree of freedom for a factor. Here, $M \ll q^m$; therefore, very less number of experiments is required to obtain the near optimal solution using TM. Initially, user randomly set the levels for each factor usually in ascending order (i.e. $Level_1 < Level_2 < Level_3 ... q$).

3.2.2 Response analysis

In basic TM, the goal is to determine the optimal outcome $J = J(L_1, L_2, L_3 \dots L_m)$ and respective optimal factor levels. After experimentations i.e. J_1 to J_8 using OA in Table 3.1, the factor levels are updated for next cycle by using the Analysis of Means (ANOM) and Analysis of Variance (ANOVA), as in [194, 195].

3.3 Improved Taguchi Method

TM is less sensitive to the initial values of parameters and capable to provide near optimal solution in less number of experiments particularly, for large-scale problems [6, 195]. However, the effectiveness of the method depends on proper selection of factors and their levels, which is very difficult. Moreover, the TM as such may not be a proper choice for the problems having factors varying in continuous manner [193, 194]. In this research work, some improvements are suggested to overcome some of the limitations of standard TM to solve optimal DR planning and operation issues.

3.3.1 Improved Taguchi-based Approach–I

The improvement is mainly done in response analysis part and proposed approach is systematically discussed in following steps.

***Step*-1 (*Parameter Initialization*):** All factors are initialized to their respective initial levels and mean positions defined as matrix $Q^c(q \times m)$ and L^c_{avg} respectively. For

maximization problems, all elements of L^c_{avg} are set to zero or vice-versa.

$$Q^c = \begin{pmatrix} x_1^1 & x_1^2 & x_1^3 & \dots & x_1^m \\ x_2^1 & x_2^2 & x_2^3 & \dots & x_2^m \\ \vdots & \vdots & \vdots & \ddots & \vdots \\ x_{q-1}^1 & x_{q-1}^2 & x_{q-1}^3 & \dots & x_{q-1}^m \\ x_q^1 & x_q^2 & x_q^3 & \dots & x_q^m \end{pmatrix} \tag{3.1}$$

$$L^c_{avg} = \Big(Zeros\Big)_{q\times m} \tag{3.2}$$

***Step-2* (*Updating the OA Elements*):** The OA$[L_M(q^m)]$ is updated by replacing the respective levels of each factor defined in (3.1). The initialized OA will look like a matrix OA^c $(M \times m)$ as

$$OA^c = \begin{pmatrix} x_1^1 & x_1^2 & x_1^3 & \dots & x_1^m \\ x_1^1 & x_2^2 & x_2^3 & \dots & x_2^m \\ \vdots & \vdots & \vdots & \ddots & \vdots \\ x_q^1 & x_{q-1}^2 & x_1^3 & \dots & x_{q-2}^m \\ x_q^1 & x_q^2 & x_{q-1}^3 & \dots & x_1^m \end{pmatrix} \tag{3.3}$$

***Step-3* (*Fitness Calculations*):** In this step, fitness/response for each experiment is calculated using OA^c in (3.3) as

$$Fit^c = \Big(J_1, J_2, J_3, \dots, J_{M-1}, J_{M-1}\Big)_{1\times M} \tag{3.4}$$

***Step-4* (*Mean Response of Factors at Respective Levels*):** Then the mean response of all factors at their respective levels is calculated. For example, the mean responses for factor F_4 (see Table 3.1) on each level is expressed as:

$$L^4_{1(avg)} = \frac{J_1 + J_3 + J_5 + J_7}{4}, L^4_{2(avg)} = \frac{J_2 + J_4 + J_6 + J_8}{4} \tag{3.5}$$

Similarly, mean responses for other factors are also calculated and generalized for 'm' factors at their 'q' levels as:

$$L^c_{avg} = \begin{pmatrix} L^1_{1(avg)} & L^2_{1(avg)} & \dots & L^m_{1(avg)} \\ \vdots & \vdots & \ddots & \vdots \\ L^1_{q-1(avg)} & L^2_{q-1(avg)} & \dots & L^m_{q-1(avg)} \\ L^1_{q(avg)} & L^2_{q(avg)} & \dots & L^m_{q(avg)} \end{pmatrix}_{q\times m} \tag{3.6}$$

***Step*-5 (*Calculate the Direction of Movement*):** In order to obtain the direction of next level movement, mean response of each factor at its respective levels are compared with the same of previous cycle, unlike in [6] where, the mean response of each level is compared with best mean response of that factor in the same cycle. For maximization problem, the direction matrix $G^c, \forall\ r \epsilon q$ and $z \epsilon m$ is defined as

$$G^c(r,z) = \begin{cases} +1, & \text{if } L^c_{avg}(r,z) - L^{c-1}_{avg}(r,z) > 0 \\ 0, & \text{if } L^c_{avg}(r,z) - L^{c-1}_{avg}(r,z) = 0 \\ -1, & \text{if } L^c_{avg}(r,z) - L^{c-1}_{avg}(r,z) < 0 \end{cases} \tag{3.7}$$

***Step*-6 (*Update the Levels*):** Using the direction matrix G^c of (3.7), the level of each factor or element of matrix Q^c in (3.1) are updated as follows

$$x^z_r(new) = x^z_r(old) + G^c \Delta x, \quad \forall\ r\ \epsilon\ q\ \&\ z\ \epsilon\ m \tag{3.8}$$

***Step*-7 (*Termination Criteria*):** Step-1 to 6 is repeated until convergence is reached. Here, the algorithm is terminated, if D_P=max$(\Delta D^c_z) \leq 10^{-2}$. The vector ΔD^c_z is defined as:

$$\Delta D^c_z = \max\left[L^c_{avg}(r,z) - L^{c-1}_{avg}(r,z)\right];\ \forall\ r\ \epsilon\ q \tag{3.9}$$

3.3.2 Improved Taguchi-based Approach–II

In this approach, the proposed approach-I is combined with the method given in [6]. The contribution of [6] is inserted between step-4 and 5 of Section 3.3.1. Further, the levels are again updated according to step-5 and 6. In this work, proposed approach-II is adopted and called as the improved TM to solve optimal DER planning and operational problems.

3.4 Optimal DER Integration using Improved Taguchi-based Approach

In this thesis, the improved Taguchi-based approach is introduced to solve the optimal DER integration problems aiming to determine optimal number, location, sizes and types of DERs for a given distribution system. The DERs locations and their variable sizes are considered to be analogous to the factors and their levels in Taguchi DOE respectively. In standard TM, the factors are to be specified by the user. In the thesis, a heuristic based

approach is used to choose the Taguchi DOE factors during the iterative process of the method.

3.4.1 Heuristic-based Static Node Priority List (SNPL)

A new heuristic-based node priority list is proposed to provide engineering input for the optimization technique to enhance its performance. Generally, node sensitivity list is prepared by penetrating small test size DER at all nodes one by one and top few nodes are selected as candidate nodes to reduce the search space [10, 94, 113]. The major drawback of such methods is that they completely ignore other nodes, which may have optimal node(s). The number of top nodes to be selected for the given system are also not specified. Moreover, by changing the test size of DER, the node sensitivity order will change in the list. To overcome these drawbacks, a new heuristic-based approach is proposed to prepare the node priority list. According to which, the test size of DER is varied at each node from zero MW to peak demand of the system in small step size and based on the best fitness achieved, a node priority list is prepared off-line.

3.4.2 Optimal DER Integration using Proposed Improved TM

In proposed approach, a RWS is used to select 'm' number of nodes from the node priority list as factors in proposed TM. Then the improved TM is applied to determine the corresponding DER sizes to these nodes. The process is repeated till the pre-specified number of iterations. Broadly, the proposed approach is divided into following essential steps.

***Step*-1 (*Input Parameters*):** Create an offline SNPL for a given distribution system and objective, as suggested in Section 3.4.1. Set maximum number of iterations, the number of DERs to be installed, N_{DER} etc.

***Step*-2 (*Roulette Wheel Selection*):** Apply the RWS criteria on the proposed static node priority list and spun it for N_{DER} times to select N_{DER} nodes for DER integration.

***Step*-3 (*Apply the Proposed TM*):** Now, apply the proposed TM given in Section 3.3.2 to obtain the optimal sizes on the selected nodes considering them as Taguchi factors.

***Step*-4 (*Best Taguchi Solution*):** Determine the best solution based on its fitness value and compare it with the existing best value. If found better, replace it.

***Step*-5 (*Apply Proposed TM*):** Repeat Step-2 to 4 till the pre-specified number of iterations and print the best solution.

The algorithm of proposed TM for optimal DER integrations in distribution systems is presented in Algorithm 1.

Algorithm 1 Proposed Taguchi-based Approach for Optimal DER Integration

1: **Input:** system data, node priority list, objective function, Max_iter, m, Δx etc.
2: **for** i=1:Max_iter **do**
3: **Node Selection:** The roulette wheel is spun $m = N_{DG}$ times to select N_{DER} nodes from SNPL, the structure of DER locations, served as factors is given as

Loc_1	Loc_2	Loc_3	...	$Loc_{N_{DER}-1}$	$Loc_{N_{DER}}$

4: **Initialization:** set $c = 0$, $D_P = 1$, initialize all factor levels as in (3.1) and (3.2) etc.
5: **while** $D_P > \Delta x$ **do**
6: $c = c + 1$
7: **DER Sizes:** step-1 to 7 of improved Taguchi-based approach given in (3.1)-(3.9) are used to obtain the optimal sizes of DERs at these selected nodes. The DER sizes and their corresponding best fitness for these nodes is structured as

$$M_1(c,:) = \big[\text{DER Sizes (c) fitness value (c)}\big]$$

8: **Termination criteria:** $D_P \leq max(\Delta D_z)$
9: **end while**
10: **Selection of Best Sizes:** On the basis of fitness values evaluated in c cycles, best DER sizes are selected from matrix M_1. In each iteration, the DER sites along with their corresponding sizes and best fitness values are stored in matrix 'M_2' as

$$M_2(i,:) = \big[\text{DER Locations } (i), \text{ DER Sizes } (i), \text{ Fitness } (i)\big]$$

11: **end for**
12: **Output:** Print the best DER nodes, sizes and fitness among Max_iter alternatives given in M_2.

3.5 Genetic Algorithm(GA)

The GA is a powerful meta-heuristic optimization technique inspired by process of natural selection and belongs to the group of evolutionary algorithms. The bio-inspired parameters used in GA are population, parent selection, crossover, mutation etc. Originally, the technique was developed by Prof. John Holland and his students at the University of Michigan during the 1960s and 1970s. As observed by many researchers [8, 9, 196], the standard form of GA has inherent drawbacks related to poor convergence, local trapping etc. though, full potential of the technique can be extracted if internal mechanism alters in such a way that provides self-healing against its intrinsic flaws [9]. Since its development, a variety of improvements have been suggested in literature to overcome some of its limitations. For optimal DER integration problems, initially, random but feasible population of individuals is generated. The individuals will contain the nodes and respective DER sizes for possible integration as the decision variables. The basic structure of an individual used in optimal DER integration problem is shown in Fig. 3.1.

Loc_1	Loc_2	Loc_3	...	$\text{Loc}_{N_{DER}-1}$	$\text{Loc}_{N_{DER}}$

FIGURE 3.1: Individuals' structure in GA for optimal DER integration

During the optimization process, many infeasible descendants are generated, especially for complex optimization problems with large constraints. Therefore, a correction algorithm may be required to convert all infeasible descendants into feasible population. In literature, various analytical and heuristic based correction algorithms have been suggested [8,9,196]. In this work, a DNPL is proposed dynamically changing by following the behavior of nodes in each generation of GA. Then, the list is used in correction algorithm, which helps the GA to leave local trap and improve the convergence.

3.5.1 Dynamic Node Priority List (DNPL)

In literature, objective function or power loss sensitivity-based node priority lists are suggested by perturbing a very small DG/SC sizes at system nodes. Then, the nodes which show high sensitivity towards power loss [10] or objective function [9] are given the top priority for optimal DER integration. However, these lists are created offline therefore it remains unaltered during the optimization process. The offline NPL may be better suited for single DG/SC integration but in the case of multiple DER integration, the optimal solution may depend on the combination of nodes generated in optimization process. Therefore, there is an increasing need to develop a dynamically changing NPL, which will be guided in each generation of GA and updated accordingly.

The proposed DNPL is inspired from the natural process of genetics in which gene retains the best information/carrier during its natural evolution. Similarly, DNPL retains the information of all nodes in terms of their cumulative fitness during the generation process. The cumulative participation of each node in terms of fitness function and DER sizes is dynamically analyzed in each generation. The proposed DNPL is then divided into two sub-priority lists: Cumulative Fitness based Dynamic Node Priority List (CF-DNPL) for site correction and Cumulative Size based Dynamic Node Priority List (CS-DNPL) for size correction in infeasible descendant. Both the lists are updated simultaneously.

In order to demonstrate the proposed formulation of DNPL, a standard 33-bus distribution system given in [197] is adopted. Besides, a population size of N_p=10 is considered for individual shown in Fig. 3.1 and the snapshot of such population is shown in Fig. 3.2.

Pop No.	DG Locations			SC Locations			DG Sizes (kW)			No. of SC Banks			Fitness
1	17	15	08	06	16	33	05	37	60	3	4	0	F01
2	04	17	19	24	05	12	09	06	34	2	0	0	F02
3	04	01	02	31	03	16	33	07	25	2	3	4	F03
4	07	23	22	09	30	28	06	63	05	4	1	2	F04
5	01	17	12	16	22	07	29	67	03	4	0	3	F05
6	16	13	32	19	26	32	24	04	50	2	3	2	F06
7	07	17	24	14	25	31	16	54	50	2	0	0	F07
8	28	08	26	28	06	33	28	20	56	0	1	4	F08
9	18	08	01	04	15	04	14	34	21	3	3	4	F09
10	09	15	27	31	06	06	46	04	62	2	2	2	F10

FIGURE 3.2: A sample population of individuals and their fitness values for 33-bus system

In each generation, the priority of each node in terms of mean fitness attained so far is determined, corresponding to the node for DER site. For example, from Fig. 3.2, the priority of node '1' for DGs location (appearing in pop no. 3, 5, 9 shown in gray color), on the basis of corresponding fitness, is evaluated as

$$\text{CF-DNPL}_1^{DG}(gen) = \frac{\frac{(F03+F05+F09)}{3} + \text{CF-DNPL}_1^{DG}(gen-1)}{2} \tag{3.10}$$

where, gen, represents the current generation.
Similarly, the node priority list for SCs are determined in terms of mean fitness attained so far. For example, the priority of node '6' for SCs location (appearing in pop no. 1, 8, 10 in red color) based on corresponding fitness may be calculated as

$$\text{CF-DNPL}_6^{SC}(gen) = \frac{\frac{(F01+F08+F10)}{3} + \text{CF-DNPL}_6^{SC}(gen-1)}{2} \tag{3.11}$$

The CF-DNPLs, prepared in (3.10) and (3.11) will be used to select the promising nodes, corresponding to DGs and SCs respectively while correcting the infeasible chromosome appeared during the evolutionary process of the proposed GA. In this work, another new DNPL i.e. CS-DNPL is also suggested to select the sizes of DERs corresponding to each node. To prepare it, the mean of DER sizes appeared in previous generations is evaluated for each node. For example, the CS-DNPL of node '1' for DGs appeared in pop no. 3, 5,

9 is expressed as

$$\text{CS-DNPL}_1^{DG}(gen) = \frac{\frac{(07+29+21)}{3} + \text{CS-DNPL}_1^{DG}(gen-1)}{2} \text{ kW} \tag{3.12}$$

Similarly, the CS-DNPL of SCs for node '6' appeared in pop no. 1, 8, 10 of Fig. 3.2 is evaluated as

$$\text{CS-DNPL}_6^{SC}(gen) = \frac{\frac{(3+1+2)}{3} + \text{CS-DNPL}_6^{SC}(gen-1)}{2} \tag{3.13}$$

Likewise, the priorities for all other nodes are also evaluated and updated at the end of each generation.

3.5.2 Optimal DER Integrations using Proposed DNPL-based GA

The proposed DNPL-based GA is discussed in following steps.

***Step*-1 (*Input Parameters*):** Set the algorithm parameters such as chromosome length, lower & upper limits of variables, crossover rate, mutation rate, fitness function, population size N_p, maximum generation G_{max} etc.

***Step*-2 (*Initialization and Population*):** Initially, N_p numbers of random but feasible individuals' are generated as shown in Fig. 3.1 and their respective fitness values are evaluated and kept for auxiliary analysis as shown in Fig. 3.2. Now, the DNPL is prepared as explained in previous Section 3.5.1.

***Step*-3 (*Parents Selection*):** Now, two individuals are selected for crossover using RWS criteria. However, it reduces the natural exploration of algorithm; therefore, only one parent is selected using RWS and second is randomly selected to maintain the diversity.

***Step*-4 (*Crossover*):** The crossover is required to exchange the genetic information among different individuals and to increase the diversity in population. In proposed GA, single-point crossover is used to produce offspring by selecting random crossover-point. In order to improve the average fitness of the group, the fitness value of each offspring is calculated and then compared with the weakest individual in the population rather than to their own parents as suggested in [196]. According to Darwinian's evolution model i.e. "survival of fittest", the offspring will replace the weakest individuals, if they have better fitness values as compared to the weakest individual in the population. This way, the average fitness of the population will improve in each generation.

***Step*-5 (*Proposed Correction Algorithm*):** In crossover, many infeasible descendants may be generated. Therefore, a correction algorithm may be required to transform all infeasible descendants into feasible solution. Generally, a random but feasible gene/chromosome is generated to replace infeasible gene of the offspring. However, the random movement may affect the optimization process. In this work, in order to produce diversified offspring population, a RWS criterion is used to select a feasible gene employing proposed DNPL. Similar to DNPL, the correction algorithm is also divided into two parts: node selection and size selection. If a gene that contains the information of DG and SC sites found to be infeasible then the RWS criteria will be applied on CF-DNPL of DGs and SCs to selected feasible gene for DG and SC respectively. Alternatively, if an infeasible gene that contains the sizing information of DG and SC then the CS-DNPL will be used to select an appropriate average size of DG and SC respectively for corresponding node.

***Step*-6 (*Mutation*):** In order to improve the exploration of algorithm, mutation is used. A chromosome is selected randomly from given population then one gene of that chromosome is mutated. The mutation rate is generally kept between 2 to 10% of population size N_p, as suggested in literature [196]. After mutation, correction algorithm is used to check the feasibility of muted chromosome. The fitness of muted individual is compared with that of weakest individual in population. It will replace the individual if it's fitness is found to better as compared to the fitness of that individual, as done in crossover step.

***Step*-7 (*Update the Proposed DNPL*):** The DNPL shown in Fig. 3.2 will be updated at the end of each generation; the figure shows a snapshot of single generation. In order to update DNPL, the cumulative values of each element of DNPL in current and previous generation will be used to get a final DNPL and so on.

***Step*-8 (*Termination*):** The algorithm is terminated, if all individuals of group attain the same fitness value or reached to pre-defined number of generations. Elitism is used to preserve the best individual and its fitness in the end of each generation.

3.6 TOPSIS Approach

TOPSIS is a multi-criteria decision making approach developed by Hwang and Yoon in 1981 and further improved by Yoon in 1987 [198, 199]. Unlike other approaches, in this approach, two reference points are considered to select the best compromising solution known as Positive Ideal Solution (PIS) and Negative Ideal Solution (NIS). Hence, the chosen best compromising solution should be close to PIS and far from NIS [198–202]. For example, Fig. 3.3 shows n_1 alternatives for objectives Y_1 and Y_2. According to TOPSIS, solution a_1 is the most compromising solution because it has minimum Euclidean distance

from PIS and maximum Euclidean distance from NIS.
A multiobjective problem can be expressed as

$$\text{optimize } [f_1(x), f_2(x), f_3(x), \ldots, f_{n_2}(x)] \tag{3.14}$$

subjected to: $x \epsilon C$ where, $f_j(x) : R^n \rightarrow R$ is jth objective function, $j = 1, 2, \ldots, n_2$, $n_2 > 1$ and C is the feasible searching space.

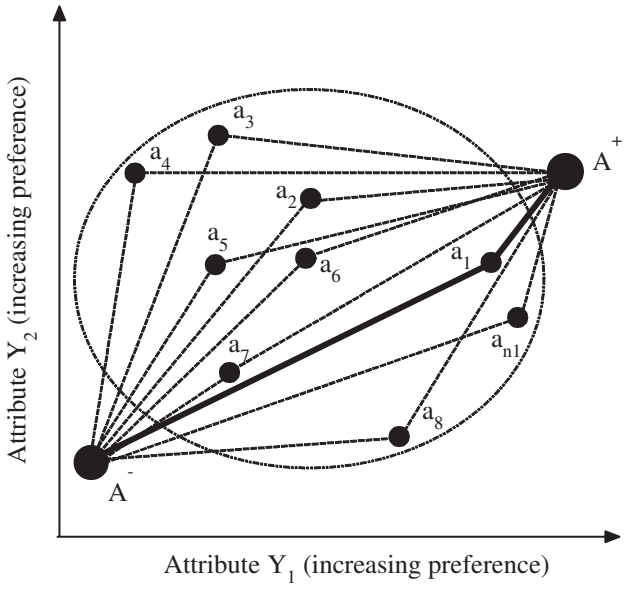

FIGURE 3.3: Multi-decision making criteria of TOPSIS approach

Following steps are used to find the most compromising solution for multiobjective optimization problems.

***Step*-1 (*Construct a Normalized Decision Matrix*):** It is constructed to transform the attributes of different dimensions into non-dimensional attributes for fair comparison across the attributes. The normalized decision matrix element r_{ij} is calculated as

$$r_{ij} = \frac{f_{ij}}{\sqrt{\sum_{i=1}^{n_1} f_{ij}^2}} \quad \forall\ i \epsilon n_1\ \&\ j \epsilon n_2 \tag{3.15}$$

where, n_1 is the number of alternatives and f_{ij} represents the output of ith alternate of jth objective.

***Step*-2 (*Construct the Weighted Normalized Decision Matrix*):** Based on the priorities of various attributes, weighted normalized decision matrix has been constructed. The element v_{ij} of the matrix is expressed as

$$v_{ij} = w_j \times r_{ij} \qquad \forall\ \ i \epsilon n_1\ \&\ j \epsilon n_2. \tag{3.16}$$

where, w_j is the weight of jth objective and $\sum_{j=1}^{n_2} w_j = 1$. For equal priority of attributes this step may be skipped.

***Step*-3 (*Determine PIS & NIS*):** From weighted normalized decision matrix, PIS and NIS are determined, which contain the best and worst values for each objective respectively.

$$PIS = \{v_{1+}, v_{2+}, v_{3+}, \ldots, v_{n_2+}\} \tag{3.17}$$

$$NIS = \{v_{1-}, v_{2-}, v_{3-}, \ldots, v_{n_2-}\} \tag{3.18}$$

where,

$$v_{j+} = \begin{cases} max < v_{ij} > \quad \forall\ i, & \text{if objective represents a benefit} \\ min < v_{ij} > \quad \forall\ i, & \text{if objective represents a cost} \end{cases}$$

$$v_{j-} = \begin{cases} max < v_{ij} > \quad \forall\ i, & \text{if objective represents a cost} \\ min < v_{ij} > \quad \forall\ i, & \text{if objective represents a benefit} \end{cases}$$

for $i = 1, 2, 3, \ldots, n_1$ and $j = 1, 2, 3, \ldots, n_2$.

***Step*-4 (*Calculation of Euclidean Distances from Ideal Solutions*):** Then, the euclidean geometry is applied to measure the distances d_{i+} and d_{i-} for each solution from its corresponding element of PIS and NIS respectively.

$$d_{i+} = \sqrt{\sum_{j=1}^{n_2} (v_{ij} - v_{j+})^2} \quad \& \quad d_{i-} = \sqrt{\sum_{j=1}^{n_2} (v_{ij} - v_{j-})^2} \tag{3.19}$$

***Step*-5 (*Relative Closeness Index Calculation*):** A Relative Closeness Index (RCI) is calculated for each alternative, which indicates the relative significance of alternatives and expressed as

$$C_{i+} = \frac{d_{i-}}{d_{i+} + d_{i-}} \tag{3.20}$$

where, $0 \leq C_{i+} \leq 1$ for $j = 1, 2, 3, \ldots, n_1$.

***Step*-6 (*Rank the Preference Order*):** On the basis of RCI defined in (3.20), a ranking list is created in the descending order of RCI.

3.7 Multi-Objective Taguchi Approach (MOTA) for Optimal DER Integration

In this research work, a new approach is introduced to solve multiobjective DG integration problem using TM that employs TOPSIS approach to select most compromising solution

among multiple solutions in order to determine optimal sites and sizes of DGs in a given distribution system. In proposed MOTA, the number of Taguchi factors 'm' is analogous to the number of DGs required to be installed 'N_{DG}' and their 'q' number of levels are analogous to possible sizes to be installed in ascending order for each DG, i.e., $[L_1, L_2, ..., L_q]$, as done in Section 3.4. The value of which may be decided by the system planner based on the experience. In literature, it has been suggested that three levels for each factor may be sufficient to obtain better results as compared to minimum two levels of OA [6]. Therefore, a suitable OA, $\mathrm{L}_{n_i}(3^{N_{DG}})$ is selected and constructed for N_{DG} number of nodes on the basis of basic rules described in Section 3.2.1. For example, the OA L_9 (3^3) given in Table 3.2 can be used in Taguchi DOE if $N_{DG} = 3$.

TABLE 3.2: Orthogonal Array $L_9(3^3)$ and Decision Matrix

Exp. No.	OA			Decision Matrix ($\boldsymbol{D}$)				
	F_1	F_2	F_3	obj_1	obj_2	obj_3	,. . . ,	obj_{n_2}
1	1	1	1	f_{11}	f_{12}	f_{13}	,. . . ,	f_{1n_2}
2	1	2	2	f_{21}	f_{22}	f_{23}	,. . . ,	f_{2n_2}
3	1	3	3	f_{31}	f_{32}	f_{33}	,. . . ,	f_{3n_2}
4	2	1	2	f_{41}	f_{42}	f_{43}	,. . . ,	f_{4n_2}
5	2	2	3	f_{51}	f_{52}	f_{53}	,. . . ,	f_{5n_2}
6	2	3	1	f_{61}	f_{62}	f_{63}	,. . . ,	f_{6n_2}
7	3	1	3	f_{71}	f_{72}	f_{73}	,. . . ,	f_{7n_2}
8	3	2	1	f_{81}	f_{82}	f_{83}	,. . . ,	f_{8n_2}
9	3	3	2	f_{91}	f_{92}	f_{93}	,. . . ,	f_{9n_2}

The steps of proposed MOTA are given below

***Step*-1 (*Selection of DG Locations*):** For possible DGs installation, N_{DG} nodes are selected using RWS criterion based on SNPL discussed in Section 3.4.1. Hence, all nodes get chance to be selected according to their RCI values, unlike top node selection approaches [10, 77, 94]. Moreover, the approach also reduces the computational burden.

***Step*-2 (*Initialize the Levels*):** The levels of each DG are initialized in this step, generally in ascending order with small increment i.e. $L_1 < L_2 ... < L_q$.

***Step*-3 (*Update OA Elements*):** In this step, the elements of designed OA will be replaced by their corresponding DG levels, i.e., DG sizes. For example, OA $\mathrm{L}_9(3^3)$ given in Table 3.2, the value '1', representing level-1 of factor $F_2 = DG_2$, appeared in exp. no. 1, 4 & 7, will be replaced by the L_1 of F_2. The remaining entries of OA are also updated accordingly.

***Step*-4 (*Taguchi Experimentation*):** It is basically a fitness calculation step. Each row of OA is used to evaluate various objectives and stored in a decision matrix for each

cycle, as shown in Table 3.2

***Step*-5 (*Compromising Sizes Selection*):** Now, TOPSIS approach described in Section 3.6 is adopted to select most compromising sizes based on RCI values of n_1 alternative solutions given in decision matrix $\boldsymbol{D}$. The selected compromising sizes and their corresponding values of objective functions for cth cycle are stored in the cth row of MOTA decision matrix M_1 structured as

$$M_1(c,:) = [\overbrace{S_{c1}, S_{c2}, \ldots, S_{cN_{DG}}}^{\textbf{Sizing Matrix}} \quad \underbrace{f_{c1}, f_{c2}, \ldots, f_{cn_2}}_{\textbf{Decision Marix } (D_2)}]$$

***Step*-6 (*Mean Response Analysis of an Objective Function*):** It is required to analyze the response of all factors at their individual levels in order to guide the factors in next cycle of TM. Suppose, the analysis is carried for obj_1 only; however, it depends on the need and decision of the user. For each factor, the mean of obj_1 corresponding to each level is evaluated, e.g., from Table 3.2, the mean response of factor F_2 for each level can be expressed as

$$\begin{aligned} L^2_{1(avg)} &= (f_{11} + f_{41} + f_{71})/3 \\ L^2_{2(avg)} &= (f_{21} + f_{51} + f_{81})/3 \\ L^2_{3(avg)} &= (f_{31} + f_{61} + f_{91})/3 \end{aligned} \tag{3.21}$$

***Step*-7 (*Update the Levels of Factors*):** In every cycle, levels of each factor will be updated according to their mean responses calculated in previous step. Therefore, a level which shows best mean response would be followed by remaining levels of same factor. Fig. 3.4 shows nine different possible trends of mean response for main objective function at respective levels. In each cycle, Δx amount is adjusted in shown direction. For example, in trend T_5 & T_8, level 1 shows best (minimum) average response therefore, level 2 & 3 will follow the level 1 by decreasing the current levels by predefined amount Δx. The levels of other factors are also updated in similar manner.

***Step*-8 (*Termination Criteria of Proposed TM*):** Step–3 to 7 is repeated until the TM converges. Ideally, convergence is achieved when all levels corresponding to each factor attain the same value; otherwise, the TM is terminated when deviation between best and worst mean responses for each factor is less than certain predefined small value, ϵ. Mathematically, it is expressed as

$$D_p = max\left[\frac{max(L^{N_{DG}}_{r(avg)}) - min(L^{N_{DG}}_{r(avg)})}{max(L^{N_{DG}}_{r(avg)})}\right] \leq \epsilon \quad \forall\ r, N_{DG} \tag{3.22}$$

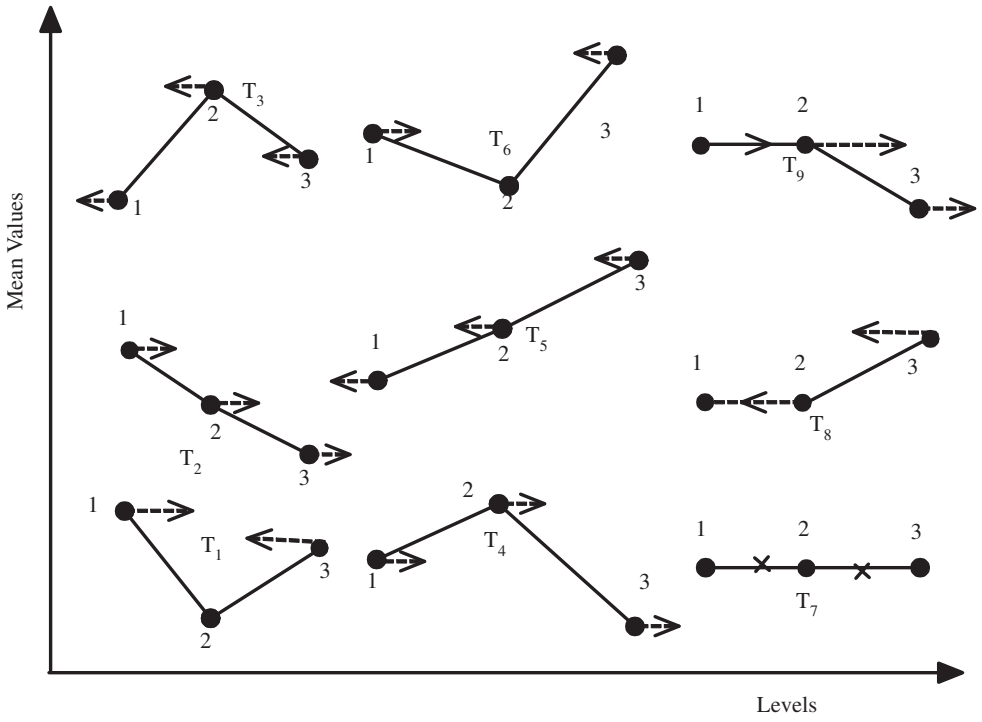

FIGURE 3.4: Nine different trends of fitness function at respective levels

***Step*-9 (*Best Compromising Size Selection*):** Now, the compromising solution will be chosen among multiple solutions in decision matrix D_2 of M_1, expressed in Step-5, using the TOPSIS approach for DG locations obtained in step-1. The best compromising solution for kth iteration of MOTA is stored in kth row of matrix M_2 as structured below

$$M_2(k,:)=[\overbrace{N_{k1}, N_{k2}, \ldots, N_{kN_{DG}}}^{\text{DG Locations}} \quad \underbrace{S_{k1}, S_{k2}, \ldots, S_{kN_{DG}}}_{\text{DG Sizes}} \quad \overbrace{f_{k1}, f_{k2}, \ldots, f_{kn_2}}^{\text{Decision Marix } (D_3)}]$$

***Step*-10 (*Termination of MOTA and Best Compromising Solution Selection*):** Step-1 to 9 is repeated till the predefined maximum number of iterations, N^{iter} is reached. The best compromising solution is selected from MOTA decision matrix M_2 using TOPSIS approach and its corresponding DG locations and sizes are printed. The TOPSIS approach is applied on decision matrix D_3. The pseudo-codes of above discussed steps of MOTA are given in Algorithm 2.

Algorithm 2 MOTA Approach for Optimal DG Integration

1: **Input:** bus data, line data, objective functions, N^{iter}, OA, RCI values from proposed NPL, set N_{DG} etc.
2: **for** $k = 1$ *to* N^{iter} **do**
3: Spun the roulette wheel N_{DG} times to select N_{DG} nodes from NPL that is structured as

DG Locations					
Loc_1	Loc_2	Loc_3	...	$Loc_{N_{DG}-1}$	$Loc_{N_{DG}}$

4: Initialize factor levels and set $c = 0$, $D_P = 1$,.
5: **while** $D_P > \epsilon$ **do**
6: $c = c + 1$
7: Update the OA elements with current levels as in Table 3.2.
8: Carry out the Taguchi experiments for fitness calculations.
9: Selected the best compromising experiment and its outcome among Taguchi experimentation as discussed in Step-5.
10: Analyze the response of each factor at its corresponding levels as in (3.21).
11: Update the levels of each factor based on response analysis in previous step.
12: **Termination criteria:** Calculate D_P given in (3.22).
13: **end while**
14: Select the best compromising DGs sizes obtained using TM on given nodes as discussed in Step-9.
15: **end for**
16: **Output:** Print the best optimal site, size and fitnesses having highest RCI Value in M_2.

3.8 Summary

This chapter is enlightening the optimization tools and techniques used in the thesis to solve the real-life optimal DER integration problems for distribution systems. In the thesis, two optimization techniques are alternatively used to solve the different optimization aspects of active distribution system planning and operational managements. As per the author's knowledge, the thesis introduced a systematic iterative Taguchi method to solve optimal DER allocation problem for the first time. The chapter first discussed about the basic variants of respective optimization technique and its corresponding limitations. Some improvements are also suggested to overcome some of the limitations observed in their standard variants. Further, two node priority lists are also suggested as an engineering input to DR integration problems. The list are used to select the optimal DR nodes in lesser time as compare to their thorough search. The TOPSIS approach is introduced to solve the multiobjective optimal DER integration in distribution systems. Besides, the effective integration of TOPSIS and Taguchi approach is also presented in the chapter.

Chapter 4

Optimal Planning of Distributed Resources

4.1 Introduction

Generally, the monetary gain is the supreme motivation behind any investment along with the improvement of system performance. Similarly, there may be many techno-economic and social goals behind DR deployment in distribution systems, which have to be achieved as per the needs and constraints. The economic goals may include cost minimization of power/energy loss, grid power purchase, DR and various other investments, energy not supplied, renewable power curtailment, various penalties etc. The objectives related to the system performance may be improvement of node voltage profile, various system stability indices, reliability indices and minimization of short circuit current and switching operations in the system etc. The social aspect considers the minimization of various GHG emission caused by traditional power plants and DNO activities such as oxides of carbon, sulfur and nitrogen etc. In this chapter, different planning frameworks are proposed and investigated to maximize the techno-economic and social benefits for active distribution systems comprised of different DR technologies. The aim of such models is to determine the optimal nodes, sizes of different dispatchable and non-dispatchable DERs such that the profit is maximized and system performance is improved.

4.2 Optimal Integration of Dispatchable DERs

The term '*dispatchable*' is referred for the DER technologies, which have ability to provide the controlled power dispatch as per the demand of load or power grid operators. The dispatchable DERs may be of two types, renewable and non-renewable. The dispatchable renewables may include biomass, hydro-power with a reservoir, geothermal energy conversion etc. The most popular non-renewable fuel is '*natural gas*' used in dispatchable DERs. Generally, dispatchable DERs are deployed in load-generation mismatch, voltage & frequency regulations, optimized dispatches, mitigation of congestion, fulfilling the system constraints etc. In literature, various optimal DER planning models have been investigated for distribution systems by considering various dispatchable technologies. Broadly, these can be classified into following categories: 1) optimal DER allocation using single load level, 2) single-year optimization model and 3) multi-year optimization models as discussed in subsequent sections.

4.2.1 Optimal Integration Mix of Diversified DGs using Improved TM

Nowadays, the integration of DGs in distribution networks has received lot of attention from industry and academia due to its distinctive benefits. The impact of various DG technologies would be different in terms of system performance and economics. For example, solar and wind based DGs are non-dispatchable and cannot guarantee fixed power output due to the uncertainties in power availability [203] and require high investment costs and/or space. The integration of non-dispatchable DGs requires the support of dispatchable DGs, e.g. Fuel Cell (FC), Micro-Turbine (MT), Diesel Engine (DE), Gas Engine (GE), Biomass (BM) etc. to participate in competitive electricity market. Therefore, the selection of type of DGs must also be considered for DG integration problems. In oder to maximize the DG integration benefits, the diversified DG technologies should be optimally mixed considering their pros and cons.

The increasing pressure of environment protection agencies to reduce GHG emission tends to be modifying the existing or introduce new policies for electric power industry [204–206]. Similarly, the OFGEM report says that DNOs activities also have a substantial impact in terms of GHG emissions, with 97% of total DNO GHG emissions related to electricity losses alone [205]. The changing trends have directed the system planners to incorporate future environment protection policies along with techno-economic aspects of DG integration in distribution systems.

In this section, the improved TM introduced in Section 3.3.2 has adopted to solve the DG integration problems for distribution networks. A new objective function is formulated comprising of techno-economic and social aspects of diversified dispatchable DG technologies over multiple load levels. The techno-economic objectives considered are annual cost of grid energy transactions, DG investment and running costs along with node voltage deviation. The social aspect considers the recent environment protection policies imposed on DNO activities to reduce the CO_2 emission. The proposed DG planning model is tested on two standard test systems i.e., 33-bus and 118-bus radial distribution systems. The results obtained are validated with same determined by an improved variant of GA in existing literature [196].

Problem Formulation

The proposed DG planning model is formulated and investigated in two stages, in stage-1; DG planning parameters such as number, location, size, and type of different DGs are obtained considering different load levels. The optimal power dispatch of all DGs installed in stage-1 are determined, in stage-2, for all load levels such that the operational benefits of installed DGs are maximized.

Stage–1: *Optimal Allocation of DGs:*
In this stage, different type and number of DGs are modeled considering DG investment cost, operation & maintenance (O&M) cost, CO_2 emission intensity, capacity factor (CF) and Power Factor (PF). The objective function considered for optimal DG-mix is expressed as

$$\max \;\; J_p = \frac{k_1 J_1 + k_3 J_3 + k_4 J_4}{k_5 J_5} - k_2 J_2 \tag{4.1}$$

where, k_1, k_2, k_3, k_4 & k_5 are weighting coefficients, which can be decided by DNOs as per requirements. The objectives J_1, J_2, J_3, J_4 and J_5 are representing the annual, energy loss saving benefit, DG investment cost, benefits of optimal dispatch, carbon taxation saving benefit and voltage penalty factor respectively, as expressed in (4.2)–(4.6).

$$J_1 = J_1^{before} - J_1^{after} \tag{4.2}$$

$$J_2 = \sum_{i=1}^{N} \sum_{t_p=1}^{N_{t_p}} \sigma_{it_p} K_{it_p}^{Inst} S_{DG_{it_p}} T_p^{-1} \big(1 + R_{int}\big)^{T_p} \tag{4.3}$$

$$J_3 = J_3^{before} - J_3^{after} \tag{4.4}$$

$$J_4 = J_4^{before} - J_4^{after} \tag{4.5}$$

$$J_5 = 1 + \sum_{l=1}^{N_L} \sum_{i=1}^{N} \Delta V_{il} \tag{4.6}$$

where,

$$\begin{aligned} J_1^{before} &= \sum_{l=1}^{N_L} K_{e,l} H_l \sum_{i=1}^{N} \sum_{j=1}^{N} \alpha_{ij,l} \big(P_{il} P_{jl} + Q_{il} Q_{jl}\big) + \beta_{ij,l} \big(Q_{il} P_{jl} - P_{il} Q_{jl}\big) \\ &= \sum_{l=1}^{N_L} K_{e,l} H_l \sum_{i=1}^{N} \sum_{j=1}^{N} \alpha_{ij,l} \big(P_{D_{il}} P_{D_{jl}} + Q_{D_{il}} Q_{D_{jl}}\big) \ + \beta_{ij,l} \big(Q_{D_{il}} P_{D_{jl}} - P_{D_{il}} Q_{D_{jl}}\big) \end{aligned} \tag{4.7}$$

$$\alpha_{ij,l} = \frac{r_{ij} \cos(\delta_{il} - \delta_{jl})}{V_{il} V_{jl}} \tag{4.8}$$

$$\beta_{ij,l} = \frac{r_{ij} \sin(\delta_{il} - \delta_{jl})}{V_{il} V_{jl}} \tag{4.9}$$

$$\begin{aligned} J_1^{after} = \sum_{l=1}^{N_L} K_{e,l} H_l \sum_{i=1}^{N} \sum_{j=1}^{N} \alpha_{ij,l} \big[&\big(P_{DG_{il}} - P_{D_{il}}\big)\big(P_{DG_{jl}} - P_{D_{jl}}\big) + \big(Q_{DG_{il}} - \\ &Q_{D_{il}}\big)\big(Q_{DG_{jl}} - Q_{D_{jl}}\big)\big] + \beta_{ij,l} \big[\big(Q_{DG_{il}} - Q_{D_{il}}\big)\big(P_{DG_{jl}} - P_{D_{jl}}\big) \\ &- \big(P_{DG_{il}} - P_{D_{il}}\big)\big(Q_{DG_{jl}} - Q_{D_{jl}}\big)\big] \end{aligned} \tag{4.10}$$

$$\begin{aligned} P_{DG_{il}} &= \sum_{t_p=1}^{N_{t_p}} \rho_{l,it_p} CF_{t_p} S_{DG_{l,it_p}} pf_{l,it_p} \\ Q_{DG_{il}} &= \sum_{t_p=1}^{N_{t_p}} \rho_{l,it_p} CF_{t_p} S_{DG_{l,it_p}} \sqrt{1 - pf_{l,it_p}^2} \end{aligned} \tag{4.11}$$

$$J_3^{before} = \sum_{l=1}^{N_L} \sum_{i=1}^{N} H_l K_{e,l} P_{D_{il}} \tag{4.12}$$

$$\begin{aligned} J_3^{after} = \sum_{l=1}^{N_L} \sum_{i=1}^{N} K_{e,l} H_l \Big(P_{D_{il}} - \sum_{t_p=1}^{N_{t_p}} \rho_{l,it_p} CF_{t_p} S_{DG_{l,it_p}} \times pf_{l,it_p} \Big) \\ + \sum_{l=1}^{N_L} \sum_{i=1}^{N} \sum_{t_p=1}^{N_{t_p}} \rho_{l,it_p} K_{t_p}^{OM} H_l CF_{t_p} S_{DG_{l,it_p}} pf_{l,it_p} \end{aligned} \tag{4.13}$$

$$J_4^{before} = \sum_{l=1}^{N_L} K_{em} E_{Grid} H_l \Big(\sum_{i=1}^{N} P_{D_{li}} + P_{b,l} \Big) \tag{4.14}$$

$$J_4^{after} = \sum_{l=1}^{N_L} K_{em} H_l \Big\{ E_{Grid} \Big(\sum_{i=1}^{N} P_{D_{li}} + P_{a,l} \Big) - \sum_{i=1}^{N} \sum_{t_p=1}^{N_{t_p}} \rho_{l,it_p} CF_{t_p} S_{DG_{l,it_p}} pf_{l,it_p} \times \Big(E_{Grid} - E_{DG_{t_p}} \Big) \Big\} \tag{4.15}$$

$$\Delta V_{il} = \begin{cases} V_{\text{minS}} - V_{il}, & \text{if } V_{il} < V_{\text{minS}} \\ 0, & \text{if } V_{\text{minS}} \leq V_{il} \leq V_{\text{maxS}} \\ V_{il} - V_{\text{maxS}}, & \text{if } V_{il} > V_{\text{maxS}} \end{cases} \tag{4.16}$$

The terms defined in (4.7), (4.12) and (4.14) are representing the cost of annual energy loss, energy supplied to the load and carbon taxation respectively, before DG integration. After DG integration, these are again expressed in (4.10), (4.13) and (4.15) respectively. The node voltage deviation index used in the work is expressed in (4.16). The proposed objective function for active distribution planning, defined in (4.1), is subjected to the following constraints except (4.19) which will be used in the optimal operation of active networks.

Power Balance Constraints

$$P_{G_{il}} - P_{D_{il}} = V_{il} \sum_{j=1}^{N} V_{jl} Y_{ij} \cos(\theta_{ij} + \delta_{jl} - \delta_{il}) \quad \forall\ i, l \tag{4.17}$$

$$Q_{G_{il}} - Q_{D_{il}} = -V_{il} \sum_{j=1}^{N} V_{jl} Y_{ij} \sin(\theta_{ij} + \delta_{jl} - \delta_{il}) \quad \forall\ i, l \tag{4.18}$$

Voltages Limit Constraints

$$V_{\text{minS}} \leq V_{il} \leq V_{\text{maxS}} \qquad \forall\ i, l \tag{4.19}$$

DG Units Limit Constraints

$$P_{DG_{it_p}} \leq P_{DG_{t_p}}^{Max} \qquad \forall\ i, t_p \tag{4.20}$$

Discrete DG Sizes Constraints

$$P_{DG_{it_p}} = a_i \sigma_{it_p} \Delta P_{DG} \qquad \forall\ i, t_p \tag{4.21}$$

DG Penetration Limit Constraint

Maximum DG penetration in the system must be limited to the nameplate kVA rating

(KVA_T) of the respective grid substation transformer [207] or peak demand of the system.

$$\sum_{i=1}^{N}\sum_{t_p=0}^{N_{t_p}} \sigma_{it_p} P_{DG_{it_p}} \leq min(KVA_T, \text{peak demand}) \tag{4.22}$$

Feeders Thermal Limit Constraints

$$I_{lu} \leq I_u^{Max} \qquad \forall\ l, u \tag{4.23}$$

CO_2 Emission Constraints

The future environmental policies would limit the CO_2 emission intensity (kg/kWh) in PDNs [205, 206]. Therefore, the CO_2 emission constraint is also incorporated.

$$Avg.\ CO_2\ intensity \leq CO_2^{\text{MaxS}} \tag{4.24}$$

Stage–2: *Optimal Power Dispatch of Installed DGs and Grid*

In this stage, operational benefits of DNO are maximized by obtaining the optimal dispatch of installed DGs and grid for all load levels. The objective function for optimal dispatch of active distribution systems considers the running costs such as fuel cost, CO_2 taxation and grid energy transaction cost defined in stage-1, except investment cost of DGs, since the DGs has already been deployed. The objective function J_o for optimal dispatch of DGs is expressed as

$$\max \quad J_o = k_1 J_1 + k_3 J_3 + k_4 J_4 \tag{4.25}$$

Objective function defined in (4.25) for optimal operation of installed DGs is subjected to the operational constraints given in (4.17), (4.18), (4.19), (4.23) and (4.24).

Simulation Results

The proposed DG planning model is solved for two standard test systems i.e. 33–bus [197] and 118–bus radial distribution systems [208]. The basic information of the systems are given in Section A.1 and Section A.3 of Appendix A respectively. For simplicity, three load levels ($N_L = 3$) are considered in one year namely light load (50% of nominal for 2000 hrs.), nominal load (for 5260 hours) and peak load (160% & 120% of nominal for system-1&2 respectively for 1500 hrs.) as in [9]. The life of DGs, $T_d = 20$ years, annual rate of interest, $R_{\text{int}} = 12.5\%$, CO_2 emission from convention grid, $E_{\text{Grid}} = 910$ kg/MWh and CO_2 tax, $K_{\text{em}} = 10\$/\text{ton}$ [21]. The minimum (V_{minS}) and maximum (V_{maxS}) permissible voltages limit are considered as 0.95 pu and 1.05 pu respectively. The grid energy prices of

different load levels are referred from [28]. The maximum allowed average CO_2 emission intensity, CO_2^{MaxS} = 459g/kWh [206]. In this work, the weighing coefficients; k_1, k_2, k_3, k_4 & k_5 are considered to be equal and unity. In base case condition, the minimum bus voltages and power loss of 33-bus system for light, nominal & peak loading are [0.96, 0.91, 0.85] p.u. and [47.07, 202.67, 575.31] kW respectively. For 118-bus system, it is [0.94, 0.87, 0.77] p.u. and [297.14, 1298.0, 3797.8] kW respectively. The commercial information of various DG technologies are summarized in Table B.1 of Appendix B.

In this problem, five different dispatchable DG technologies are considered with their CFs [28] given in Table B.1. To examine the response of each type of DG, minimum one DG of each type is made mandatory to be deployed. For 33-bus system, optimization is done for five sites, one for each type of DG. For 118-bus system, approximately 10% buses, i.e., 12 locations (2-DEs, 2-GEs,2-MTs, 3-BMs and 3-FCs) are considered for DG integration. It may be noted that the share of biomass based DG locations is kept more to restrict carbon emission within the specified limit.

In order to validate the simulation results obtained by proposed approach, an improved variant of GA [196], without considering heuristic spark, is used to solve the proposed DG planning model of stage-1. In validation, the population size of 500 and 1000 are used in GA for 33-bus and 118-bus systems respectively, in order to achieve the fitness as close as to that of proposed approach-II in Section 3.3.2. Some performance parameters of proposed approach-II and GA are summarized in Table 4.1. The table shows that the proposed approach is capable to solve constrained optimal DG integration problem in less number of experiments as compared to an improved variant of GA. The approach takes 9357 and 44066 number of fitness evaluations whereas; the GA takes 26489 and 72043 number of fitness evaluations for 33-bus and 118-bus systems respectively. Moreover, the proposed approach performs better compared to applied GA in terms of best fitness, mean fitness, worst fitness and standard deviation.

Table 4.1: Comparison of Proposed Approach and GA for 100 Runs

Parameters	33-bus distribution system		118-bus distribution system	
	improved GA	proposed TM	improved GA	proposed TM
Best fitness (J_p)	0.3233	0.3327	1.5014	1.5050
Mean fitness (J_p)	0.2125	0.3145	1.4479	1.4692
Worst fitness (J_p)	0.1549	0.2890	1.2655	1.4324
Standard deviation	0.0544	0.0081	0.0411	0.0122
Average no. of fitness evaluation	26489	9357	72043	44066

Moreover, in order to substantiate the improvements in basic TM, the convergence characteristics of different variants of TM and proposed approach are shown in Fig. 4.1. It shows that suggested improvements are able to search the global optimal in less number of experiments whereas, the basic TM seems less efficient to explore it while taking more number of experiments. Besides, the proposed method-II shows high global search capability with the inclusion of both the improvements.

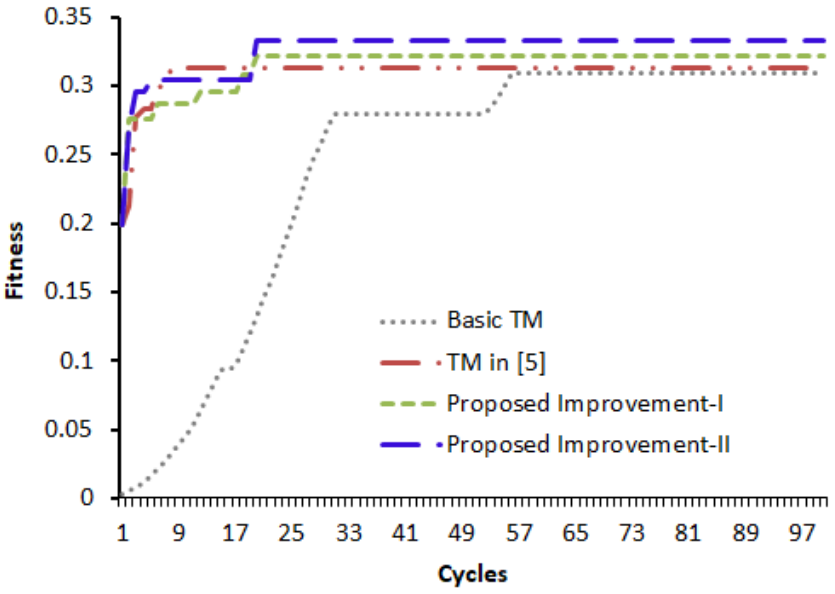

FIGURE 4.1: Convergence characteristics of various Taguchi based methods

After the establishment of proposed optimization method, now, the proposed DG mix model is explored. Table 4.2 shows the simulation results obtained for proposed DG planning and operational models. As mentioned, optimal locations and sizes of each DG technology are determined in stage-1. The DG sizes during peak load hours are representing the original installed sizes of each DG technology. The maximum hosting capacity of dispatchable DGs (98.67% of peak demand) is achieved without violating the system constraints. In future, high DG penetration may allow DNOs to operate PDNs in islanding mode, when needed. For 33-bus system, the optimal mixing of various installed DGs such as DEs, GEs, MTs, BMs and FCs are about 12%, 24%, 48%, 12%, and 4% respectively. For 118-bus system, it is about 10.90%, 32.73%, 15.45%, 11.82% and 29.09% respectively.

In the work, it has been assumed that DNOs are not allowed to export power back to the main grid. Therefore, in stage-2 optimal dispatch of each installed DG for each load level is determined to increase the operational benefit J_o, as shown in Table 4.2. The

table shows that significant amount of power loss reduction is achieved in all load levels for both systems, although it is a multiobjective optimization problem. All node voltages are found to be within specified limit for both test systems as can be observed from the table. Moreover, the results show that no system is violating the average CO_2 emission intensity limit expressed in (4.24).

TABLE 4.2: Simulation Results After DG Integration

Systems	Parameters	Optimal Solutions After DG Integration
33 bus system	DG type (site)	DE(1), GE(30), MT(19), BM(12), FC(17)
	DG Outputs (MVA)	(0.252, 0.594, 1.116, 0.279, 0.114)[a] (0.576, 1.296, 1.944, 0.666, 0.228)[b] (0.900, 1.800, 3.600, 0.900, 0.300)[c]
	Power Loss (kW)	(10.06[a], 34.76[b], 116.68[c])
	Min. bus voltages (p.u.)	(0.9867[a], 0.9790[b], 0.9508[c])
	Max. bus voltages (p.u.)	(1.0010[a], 1.0015[b], 1.0030[c])
	Total CO_2 Intensity (kg/kWh)	0.4101
118 bus System	DG type (site)	DE(5, 36), GE(7, 107), MT(85, 70), BM(53, 34, 75), FC(9, 33, 3)
	DG Outputs (MVA)	(0.126, 0.132, 2.520, 3.840, 0.096, 1.080, 1.512, 0.048, 0.378, 2.400, 0.108, 1.560)[a] (0.300, 0.264, 6.000, 4.800, 2.400, 2.700, 0.504, 1.200, 0.900, 2.260, 2.700, 3.900)[b] (0.300, 3.300, 6.000, 4.800, 2.400, 2.700, 1.800, 1.200, 0.900, 3.000, 2.700, 3.900)[c]
	Power Loss (kW)	(126.36[a], 368.58[b], 504.27[c])
	Min. bus voltages (p.u.)	(0.9789[a], 0.9614[b], 0.9529[c])
	Max. bus voltages (p.u.)	(1.0210[a], 1.0099[b], 1.0092[c])
	Total CO_2 Intensity (kg/kWh)	0.4354

[a]light loading, [b]nominal loading and [c]peak loading

Table 4.3 shows various annual monetary benefits achieved from optimal DG mix approach. It shows that maximum benefit is achieved by optimizing the annual energy purchase from DGs and main grid. Figs. 4.2 and 4.3 demonstrate the annual percentage share of energy generation, carbon emission, monetary benefit and DG investment of various DG technologies for 33-bus and 118-bus systems respectively. For 33-bus system, it may be observed that the share of MTs and GEs in all above mentioned factors is large due to lesser installation and running costs. Although the investment cost of DEs is also less, but their share is less due to high running cost and emission. Similarly, BMs and FCs are also having less sharing due to their high investment cost in-spite of less running cost and

emission. For 118-bus system, the number of renewable DGs (i.e., BMs and FCs) is more as compared to 33-bus system thereby the share of FCs has been increased due to less installation and running cost compared to BMs. The annual share of MTs is reduced due to the mutual advantages from BMs and GEs. The share of GEs is increased due to their less investment and running cost in-spite of high carbon emission, which is compensated by BM based DGs. Therefore, the DG-mix strategy comprising different pros and cons of various DG technologies maximizes the total annual benefits of DNOs and DGOs.

Fig. 4.2 shows that for 33-bus system, the annualized DG investment line is below the maximum monetary benefit for all DGs (benefit-to-cost ratio is more than unity), except BMs and FCs, same is true for 118-bus system as shown in Fig. 4.3. The BM and FC based DGs have proven to be less economical due to their high investment cost. However, in future, the advancement in such technologies may reduce various investment costs and increase the share of such DGs. In Fig. 4.3, for 118-bus system the benefit-to-cost ratio of DEs is also less than unity because DEs are mainly contributing to meet the peak load demand, which can be observed from Table 4.3. The fact is that DEs are having high running cost and emission hence, less preferred for large systems.

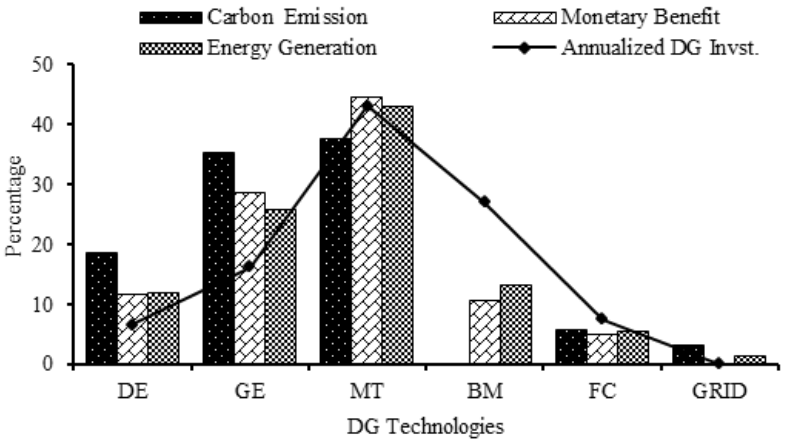

FIGURE 4.2: Share of various DG technologies in annual benefit (33-bus system)

In this research work, simple but powerful optimization technique is introduced to solve the DG integration in distribution systems. The technique is based on TM that employs statistical designed OAs. Further, few improvements are also suggested to overcome some of the limitations of basic TM. The new heuristic-based SNPL proposed in 3.4.1 is providing an engineering input to the method. The simulation results are found to be promising when compared with the same obtained by an existing variant of GA. The proposed TM

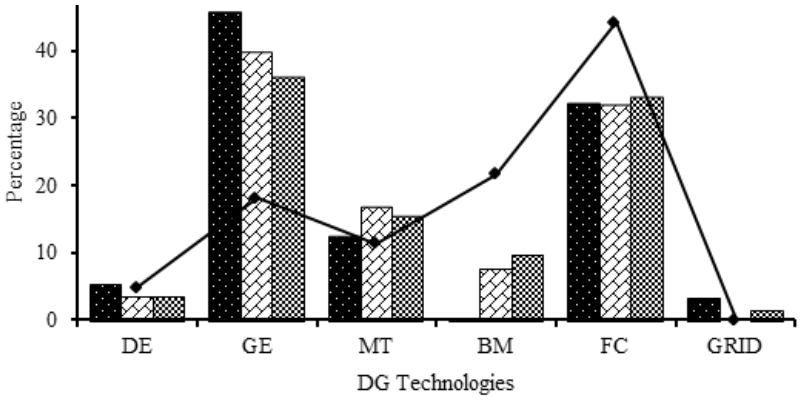

FIGURE 4.3: Share of various DG technologies in annual benefit (118-bus system)

TABLE 4.3: Annualized Monetary Analysis of Distribution Systems

Systems	Costs (in M$)	Before DG	After DG	Profit (M$)
33-bus System	Energy loss (J_1)	1.596	00.385	01.210
	DG Investment (J_2)	0.000	04.041	04.041
	Energy supplied (J_3)	0.000	23.266	23.266
	CO_2 tax (J_4)	0.311	00.156	00.156
	Benefit (M$)		20.885	
118-bus System	Energy loss (J_1)	7.870	2.215	5.655
	DG Investment (J_2)	0.0	21.766	21.766
	Energy supplied (J_3)	0.0	134.374	134.374
	CO_2 tax (J_4)	1.760	0.815	0.945
	Benefit (M$)		119.212	

recursively maximizes the DG integration benefits faster than the population based AI-techniques e.g., GA. The new objective function is proposed comprising techno-economic and social aspects of different DG technologies. It has been found that optimal DG-mix approach is better suited to solve technical, economic and environmental issues of deregulated power system.

4.2.2 Optimal Integration of DERs in Voltage Regulated Framework

Voltage regulation and energy loss minimization have always been the major concerns for distribution network operators therefore, many conventional voltage regulation schemes are dedicatedly employed in the distribution networks. In this section, a new DER integration problem is investigated by simultaneously modeling the effect of OLTC based VR-schemes to improve the distribution system performance with adequate DER penetration. The

objective function is defined to minimize the cost of annual energy loss and voltage deviation for multiple load levels. Unlike previous section, one of the popular optimization techniques, Genetic Algorithm (GA) is adopted, to solve the proposed DER integration problem, due to its proven abilities to solve complex power system optimization problems. Further, a Dynamic Node Priority List (DNPL) proposed in Section 3.5.1, analogous to genetic information carriers, is adopted, which is dynamically updated in each generation of GA; unlike existing static node priority lists [8–10, 94]. The proposed DNPL is used to correct the infeasible solutions generated during the evolutionary process as suggested in Section 3.5.2. The effectiveness of proposed DER integration model and DNPL-based GA are demonstrated on standard 33-bus test distribution system and a practical 108-bus Indian distribution system for multiple test scenarios. The simulation results obtained are found to be inspiring when compared with other existing optimal DER integration models and optimization techniques.

Problem Formulation

In practice, the energy price varies as the demand varies so does the cost of energy loss. In such situation, minimization of annual energy loss in 'kWh' may not be justified. Therefore, in proposed DER integration model, the cost of annual energy loss minimization with variable tariff is considered as one of the objectives. The modern power consumer is becoming more concerned about the quality of supply voltage. Therefore, node voltage regulation is an essential duty of DNOs to provide regulated node voltages to the consumers. In proposed optimal DER integration model, node voltage regulation is considered as the second objective function. The combined objective function of the proposed DER integration model is expressed as

$$\min\ f = k_1 f_1[1 + k_2 f_2] \tag{4.26}$$

where,

$$\min\ f_1 = \sum_{l=1}^{N_L} K_{e,l} H_l \sum_{i=1}^{N}\sum_{j=1}^{N}[\alpha_{ij,l}(P_{il}P_{jl} + Q_{il}Q_{jl})\ + \beta_{ij,l}(Q_{il}P_{jl} - P_{il}Q_{jl})] \tag{4.27}$$

$$\min\ f_2 = \max\langle \Delta V_{il} \rangle \qquad \forall\ i, l \tag{4.28}$$

$$\Delta V_{il} = \begin{cases} |1 - V_{il}|, & \text{if } V_{\text{minS}} \le V_{il} \le V_{\min} \\ 0, & \text{if } V_{\min} \le V_{il} \le V_{\max} \qquad \forall\ i, l \\ \text{A very large number}, & \text{Else} \end{cases} \tag{4.29}$$

where, $\alpha_{ij,l} = \frac{r_{ij}\cos(\delta_{il}-\delta_{jl})}{V_{il}V_{jl}}$, $\beta_{ij,j} = \frac{r_{ij}\sin(\delta_{il}-\delta_{jl})}{V_{il}V_{jl}}$ and $P_{il} = P_{DG_{il}} - P_{D_{il}}$, $Q_{il} = Q_{DG_{il}} - Q_{D_{il}}$; Besides, $P_{DG_{il}}$, $Q_{DG_{il}}$. $P_{D_{il}}$, $Q_{D_{il}}$, V_{il} and δ_{il} are representing real power capacity of DG, reactive power capacity of DG, real power demand, reactive power demand, voltage magnitude and voltage angle respectively at bus i during load level l. Similarly, r_{ij} and x_{ij} are representing resistance and reactance of line connected between bus i and j. N, N_L, H_l and $K_{e,l}$ are representing total number of buses, number of load levels considered, number of hours and energy price during lth load level respectively. V_{il} represents the ith node voltage during lth load level. V_{minS}, $V_{\min}$, $V_{\max}$ are the minimum specified, minimum and maximum permissible node voltages in p.u.

The objective function expressed in (4.26) is subjected to following constraints

$$\begin{aligned} P_{il} &= V_{il}\sum_{j=1}^{N} V_{jl}Y_{ij}\cos(\theta_{ij}+\delta_{jl}-\delta_{il}) \\ Q_{il} &= -V_{il}\sum_{j=1}^{N} V_{jl}Y_{ij}\sin(\theta_{ij}+\delta_{jl}-\delta_{il}) \end{aligned} \qquad \forall\ i,l \tag{4.30}$$

$$S_{DER_i} \le S_{DER}^{\text{Max}} \qquad \forall\ i \tag{4.31}$$

$$S_{DER_{il}} = a_i \times \rho_{il} \times \Delta S_{DER} \qquad \forall i \tag{4.32}$$

$$\sum_{i=1}^{N} \sigma_i S_{DER_i} \le S_{Peak} \tag{4.33}$$

$$I_{ij,l} \le I_{ij}^{\text{Max}} \quad \forall \quad i,j,l \tag{4.34}$$

In (4.26), objective function f_2 is considered as a penalty factor for the cost of annual energy loss. Equations expressed in (4.30)–(4.34) are representing nodal power balance, maximum specified DER installation size at a bus, DER dispatch at node i during lth load level, DER penetration limit of the system and thermal limit of feeders constraints respectively. Where, k_1, k_2, ΔS_{DER}, a_i, ρ_{il}, σ_i, S_{Peak}, are representing the weighting coefficients, discrete size of DER, integer variable, binary decision variable of DER dispatch during lth load levels, binary decision variable of DER installation at node i, peak demand of the system respectively.

In this work, dispatchable DGs and variable SCs are considered since the goal of this work is to investigate the effect of existing voltage control schemes on DER planning. The DGs are assumed to be operated at fixed PF and considered as negative load thereby not allowed to participate in voltage control schemes to regulate the PCC voltages, as also suggested in [115]. Furthermore, a traditional OLTC-based voltage control is assumed to

be employed in proposed optimal DER integration model as discussed in Section 2.2 and presented in Fig. 2.1(b).

Simulation Results

In order to demonstrate the effectiveness of proposed DNPL based GA and optimal DER integration in VR framework, it has been tested on benchmark 33-bus and practical Indian 108-bus radial distribution systems. In order to validate the proposed DNPL based GA, initially, a simple optimal DG integration problem is solved to minimize the real power loss for standard 33-bus distribution system for nominal load level only. However, the effect of OLTC-based VR is ignored to highlight the effect of the proposed GA. The simulation results of optimal DG integration problem obtained by DNPL based GA are compared with the same available in literature and summarized in Table 4.4. The comparison shows that the proposed GA is very effective for optimal DG integration problems as the real power loss obtained by proposed method is minimum.

TABLE 4.4: Comparative Analysis of Various Optimization Methods

Method	Optimal DG Nodes (Sizes in MW)	Loss (MW)
TLBO [17]	12(1.183), 28(1.191), 30(1.186)	0.1246
GA [16]	11(1.500), 29(0.423), 30(1.071)	0.1063
PSO [16]	08(1.177), 13(0.982), 32(0.830)	0.1053
GA/PSO [16]	11(0.925), 16(0.863), 32(1.200)	0.1034
QOTLBO [17]	13(1.083), 26(1.187), 30(1.199)	0.1034
LSF [94]	18(0.720), 25(0.900), 33(0.810)	0.0851
IA [94]	06(0.900), 12(0.900), 31(0.720)	0.0811
Analytical [104]	06(1.730), 16(0.530), 25(0.770)	0.0795
ELF [94]	13(0.900), 24(0.900), 30(0.900)	0.0743
Proposed GA	14(0.752), 24(1.101), 30(1.074)	0.0714

Further, to analyze the role of DNPL in proposed GA the CF-DNPL and CS-DNPL of the final generation are shown in Figs. 4.4(a) and 4.4(b) respectively. It may be noticed that the DG locations obtained in the optimal solution of the proposed method are among the best nodes suggested by CF-DNPL. Moreover, most of the optimal locations obtained by other methods of the table are also the subset of top priority nodes of CF-DNPL only. Therefore, the proposed DNPL can play a vital role as an engineering input for meta-heuristic optimization techniques to solve DG integration problems effectively. Above investigation ensured that the proposed GA can be used to solve the proposed DER integration problem.

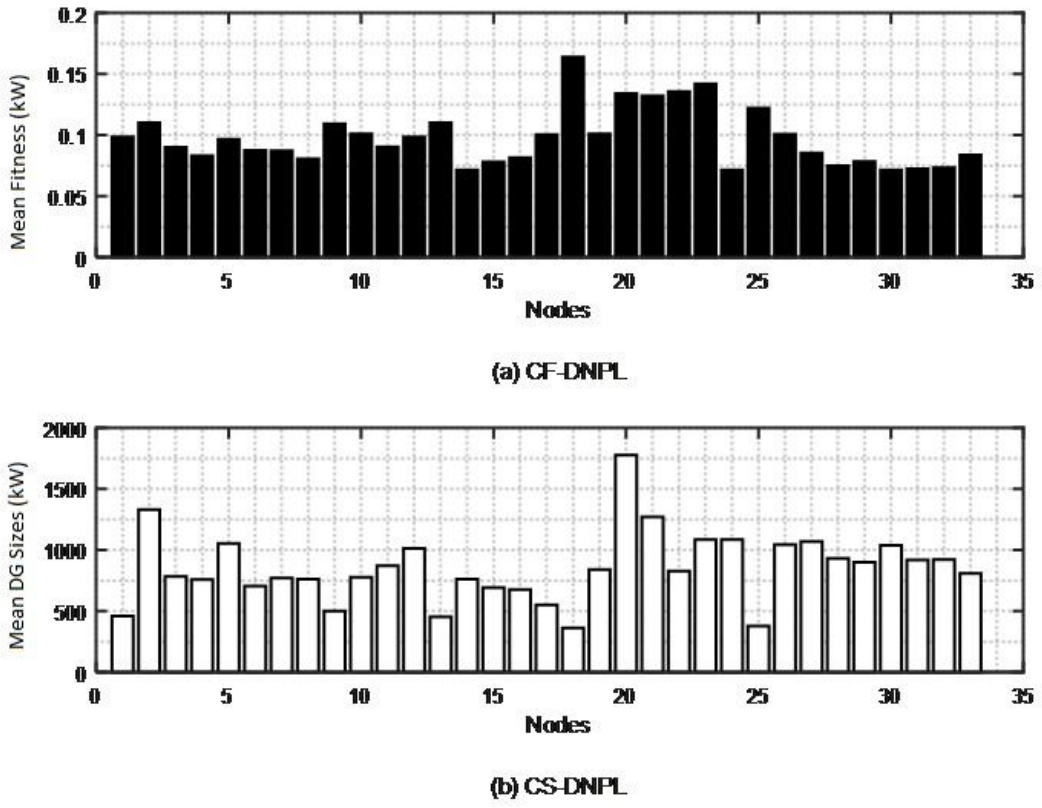

FIGURE 4.4: Proposed DNPLs (a) CF-DNPL and (b) CS-DNPL

Now, the proposed DNPL-based GA is applied to minimize the cost of annual energy loss using optimal DER integrations over multiple load levels. Various load levels suggested in [9, 10, 69] along with their energy price are summarized in Table 4.5. The problem is broadly solved in two stages, optimal integration followed by their optimal operation. In first stage, optimal siting and sizing of DERs are determined considering different load levels; whereas, their optimal dispatches are obtained in second stage for individual load levels. In order to show the effect of already existing voltage control schemes on optimal integration of different DERs, two cases are investigated: (a) optimal integration of DGs only and (b) simultaneous optimal integration of DGs and SCs. Each case is further explored for following scenarios.

Scenario–I: without considering the OLTC in both planning and operation

Scenario–II: considering the OLTC in operation only

Scenario–III: considering the OLTC in both planning and operations

The proposed DER integration problem is investigated on benchmark 33-bus test distribution system and a practical 108-bus Indian distribution system. The network and load information of the systems are given in Appendix A.

TABLE 4.5: Various Parameters used in the Study

Load Levels	Load Multiplying Factor	Load Duration (H)	Energy Price (USD/MWh)
Light (L)	0.5	2000	55
Nominal (N)	1.0	5260	72
Peak (P)	1.6	1500	120

Study System–1 (33-Bus Radial Distribution System): It is a 12.66 kV benchmark test distribution system with total nominal real and reactive power demand of 3.715 MW and 2.300 MVAr respectively [197]. The DNPL-based GA is applied to solve the proposed optimal DER integration problem and simulation results for various simulated scenarios are presented in Table 4.6. The table contains the information of optimal sites and sizes of DERs, power loss and minimum voltage appeared for different load levels, the installed DER penetration, annual energy loss and its cost. The DER penetration is calculated as the fraction of system demand considered in peak load hours.

From the table, it may be observed that in Scenario–I of Case (a) and Case (b), where the effect of OLTC based voltage regulation is ignored, the annual energy loss is drastically reduced by the proposed DNPL-based GA as compared to other similar methods [9,10,69] available in the literature, which may be unable to integrate the adequate amount of DER penetration. It may be observed that the proposed DER integration model provides more power loss reduction in peak load hours due to different energy price consideration for different load levels. The node voltage of the system is also found to be satisfactory.

In Scenario–II, the optimal dispatch of DERs installed in Scenario–I are again obtained in coordination with existing OLTC to maximize the operational benefits. The simulation results of Scenario–II shows that OLTC changes its tap position during peak load hours only when DGs are unable to bring the node voltages within limits; however, the taps remain unchanged in simultaneous integration of DG and SCs as no voltage violation is detected by OLTC control scheme as shown in Table 4.6. It may be possible that DERs have already explored their voltage control potential therefore, the existing OLTC resources are underutilized in system operations.

Therefore, in Scenario–III, DER deployment and optimal dispatches are determined in coordination with existing OLTC-based voltage control schemes in planning and operational stages respectively. It may be observed that less DER penetration is required under this strategy while providing more techno-economic benefits as compared to previous two scenarios. Moreover, OLTC is efficiently participating in voltage regulations in coordination

TABLE 4.6: Simulation Results of Study System–1

Scenarios	Method	Optimal Nodes of [DGs] & {SCs}	Optimal Sizes [DGs in MW)] {SCs in MVAr}	OLTC Tap Position	Power Loss in kW (f_1)	V_{Min} (p.u.)	Total Cost of Annual Energy Loss (USD)
Base case		–	–	NA	047.06^{L} 202.67^{N} 575.27^{P}	0.96^{L} 0.91^{N} 0.85^{P}	185,480
Case–(a) Integration of DGs Only							
I	HSA [10]	[17, 18, 33]	$[0.178, 0.130, 0.503]^{L}$ $[0.572, 0.107, 1.046]^{N}$ $[0.911, 0.194, 1.612]^{P}$	NA	023.29^{L} 096.76^{N} 260.97^{P}	0.98^{L} 0.97^{N} 0.94^{P}	86,181
	FWA [69]	[14, 18, 32]	$[0.295, 0.095, 0.507]^{L}$ $[0.590, 0.190, 1.015]^{N}$ $[0.944, 0.301, 1.678]^{P}$	NA	021.37^{L} 088.68^{N} 238.07^{P}	0.98^{L} 0.97^{N} 0.95^{P}	78,788
	Proposed GA	[14, 24, 30]	$[0.374, 0.543, 0.527]^{L}$ $[0.754, 1.100, 1.071]^{N}$ $[0.842, 1.201, 1.246]^{P}$	NA	017.33^{L} 071.46^{N} 221.03^{P}	0.98^{L} 0.97^{N} 0.93^{P}	68,753
II	Proposed GA	[14, 24, 30]	$[0.374, 0.543, 0.527]^{L}$ $[0.754, 1.100, 1.071]^{N}$ $[0.842, 1.201, 1.246]^{P}$	0^{L} 0^{N} 2^{P}	017.33^{L} 071.49^{N} 208.89^{P}	0.98^{L} 0.97^{N} 0.95^{P}	66,569
III	Proposed GA	[14, 24, 30]	$[0.374, 0.543, 0.528]^{L}$ $[0.763, 1.062, 0.865]^{N}$ $[0.869, 1.062, 1.168]^{P}$	0^{L} 2^{N} 3^{P}	017.33^{L} 069.15^{N} 208.68^{P}	0.98^{L} 0.99^{N} 0.96^{P}	65,659
Case–(b) Optimal Integration of DG & SC Simultaneously							
I	ITLBO [8]	[14, 24, 30] {15, 24, 30}	$[0.374, 0.540, 0.517]^{L}$ $\{0.200, 0.300, 0.500\}^{L}$ $[0.747, 1.074, 1.054]^{N}$ $\{0.300, 0.500, 1.000\}^{N}$ $[0.823, 1.074, 1.067]^{P}$ $\{0.300, 0.600, 1.200\}^{P}$	NA	003.02^{L} 011.94^{N} 081.99^{P}	1.00^{L} 0.99^{N} 0.95^{P}	19,612
	Proposed GA	[14, 24, 30] {14, 24, 30}	$[0.373, 0.538, 0.522]^{L}$ $\{0.200, 0.300, 0.500\}^{L}$ $[0.748, 1.078, 1.047]^{N}$ $\{0.400, 0.500, 1.000\}^{N}$ $[0.829, 1.191, 1.164]^{P}$ $\{0.300, 0.600, 1.200\}^{P}$	NA	002.95^{L} 011.73^{N} 073.70^{P}	1.00^{L} 0.99^{N} 0.95^{P}	18,033
II	Proposed GA	[14, 24, 30] {14, 24, 30}	$[0.373, 0.538, 0.522]^{L}$ $\{0.200, 0.300, 0.500\}^{L}$ $[0.748, 1.078, 1.047]^{N}$ $\{0.400, 0.500, 1.000\}^{N}$ $[0.829, 1.191, 1.164]^{P}$ $\{0.300, 0.600, 1.200\}^{P}$	0^{L} 0^{N} 0^{P}	002.95^{L} 011.73^{N} 073.70^{P}	1.00^{L} 0.99^{N} 0.95^{P}	18,033
III	Proposed GA	[13, 24, 30] {14, 24, 30}	$[0.388, 0.536, 0.516]^{L}$ $\{0.200, 0.300, 0.500\}^{L}$ $[0.779, 1.073, 1.035]^{N}$ $\{0.300, 0.500, 1.000\}^{N}$ $[0.848, 1.177, 1.143]^{P}$ $\{0.300, 0.600, 1.200\}^{P}$	0^{L} 0^{N} 3^{P}	002.95^{L} 011.86^{N} 069.63^{P}	1.00^{L} 0.99^{N} 0.99^{P}	17,350

with DG and improves the system voltage profile for all load levels. The most important benefit of this scenario is that it reduces the amount of DER penetration required to achieve more or same integration benefits. Besides, the lesser DER penetration helps the operators to alleviate many operation challenges such as reduced reverse power flow and fault current etc.

Study System–2 (Indian 108-Bus Radial Distribution System): This system is an 11kV real Indian radial distribution system of Jhalawar city, India comprising of five main feeders. It originates from 33/11 kV transformer with OLTC arrangement that is installed in 220 kV GSS. The nominal real and reactive demand of the system is 12.132 MW and 9.099 MVAr respectively. The nominal real and reactive power losses of the base system are 645.020 kW and 359.416 kVAr respectively. The proposed approach is applied to obtain the optimal allocation of DERs for various scenarios and the simulation results obtained are summarized in Table 4.7.

For the practical system, very similar facts are observed as in previous case study. In Scenarios–I, the optimal integration of DERs has significantly reduced the annual energy loss while improving voltage profile of the system. In Scenarios–II, the optimal dispatch of DERs deployed in Scenario–I are again determined in coordination with OLTC tap movement for operational stage. The simulation result reveals that annual energy loss of the system is further reduced. Similar to previous case study, it is observed that OLTC is moving its tap position for peak load level only because the voltage violation is occurring in peak load hours only.

In Scenario–III, simultaneous optimal integration of DGs and SCs are determined in coordination with OLTC tap movements. The simulation result shows that the cost of annual energy loss is less for the scenario. However, the annual energy loss is slightly higher as compared to Scenario–II because the loss reduction achieved in peak load hours due to high energy price is more. Moreover, the better node voltage profile is obtained in Scenario–III as compared to the other scenarios. The OLTC moves its tap for all load levels except light load level thus utilized effectively.

From Scenario–I, it may be concluded that the proposed DNPL-based GA has capability to explore better site and size of DERs. Whereas, from scenarios II and III, it is observed that the proposed optimal DER integration model considering the coordinated effect of OLTC based voltage regulation, generates more techno-economic benefits for distribution network operators and customers as well. Moreover, it finds the adequate hosting capacity of DERs to achieve more or same energy loss reduction.

TABLE 4.7: Simulation Results of Study System–2

Scenarios	Optimal Nodes of [DGs] & {SCs}	Optimal Sizes [DGs in MW)] {SCs in MVAr}	OLTC Tap Position	Power Loss in kW (f_1)	V_{Min} (p.u.)	Total Cost of Annual Energy Loss (USD)
Base case	–	–	NA	0151.53^{L} 0645.02^{N} 1828.62^{P}	0.95^{L} 0.89^{N} 0.82^{P}	585,457
Case–(a) Integration of DGs Only						
I	[85, 102, 60, 30, 63, 21, 67]	$[0.380, 0.567, 0.776, 0.498, 1.208, 1.286, 0.495]^{L}$ $[0.765, 1.159, 1.574, 0.999, 2.429, 2.601, 1.005]^{N}$ $[0.844, 1.513, 1.738, 1.113, 2.664, 2.820, 1.065]^{P}$	NA	0061.92^{L} 0253.09^{N} 0753.60^{P}	0.99^{L} 0.97^{N} 0.94^{P}	238,313
II	-do-	$[0.380, 0.567, 0.776, 0.498, 1.208, 1.286, 0.495]^{L}$ $[0.765, 1.159, 1.574, 0.999, 2.429, 2.601, 1.005]^{N}$ $[0.844, 1.513, 1.738, 1.113, 2.664, 2.820, 1.065]^{P}$	0^{L} 0^{N} 3^{P}	0061.92^{L} 0253.09^{N} 0733.17^{P}	0.99^{L} 0.97^{N} 0.95^{P}	234,635
III	[60, 63, 85, 97, 102, 24, 67]	$[0.776, 1.208, 0.379, 0.473, 0.367, 1.539, 0.496]^{L}$ $[1.573, 2.427, 0.763, 0.962, 0.745, 2.492, 1.003]^{N}$ $[1.737, 2.602, 0.828, 0.962, 0.871, 2.990, 1.089]^{P}$	0^{L} 1^{N} 3^{P}	0061.19^{L} 0245.93^{N} 0715.71^{P}	0.98L 0.98N 0.96P	228,701
Case–(b) Optimal Integration of DG & SC Simultaneously						
I	[60, 19, 63, 67, 30, 84, 102] {67, 63, 85, 102, 60, 20, 30}	$[0.769, 1.318, 1.203, 0.478, 0.531, 0.433, 0.561]^{L}$ $\{0.400, 0.900, 0.300, 0.400, 0.600, 1.000, 0.400\}^{L}$ $[1.537, 2.644, 2.399, 0.943, 1.063, 0.876, 1.132]^{N}$ $\{0.700, 1.800, 0.600, 0.800, 1.200, 1.900, 0.800\}^{N}$ $[1.676, 2.941, 2.624, 0.945, 1.105, 1.046, 1.239]^{P}$ $\{0.900, 2.100, 0.600, 0.900, 1.200, 2.100, 0.900\}^{P}$	NA	0014.70^{L} 0059.21^{N} 0298.77^{P}	0.99^{L} 0.98^{N} 0.94^{P}	77,819
II	-do-	$[0.769, 1.318, 1.203, 0.478, 0.531, 0.433, 0.561]^{L}$ $\{0.400, 0.900, 0.300, 0.400, 0.600, 1.000, 0.400\}^{L}$ $[1.537, 2.644, 2.399, 0.943, 1.063, 0.876, 1.132]^{N}$ $\{0.700, 1.800, 0.600, 0.800, 1.200, 1.900, 0.800\}^{N}$ $[1.676, 2.941, 2.624, 0.945, 1.105, 1.046, 1.239]^{P}$ $\{0.900, 2.100, 0.600, 0.900, 1.200, 2.100, 0.900\}^{P}$	0^{L} 0^{N} 1^{P}	0014.70^{L} 0059.21^{N} 0291.00^{P}	0.99^{L} 0.98^{N} 0.96^{P}	76,395
III	[29, 102, 60, 63, 85, 97, 20] {102, 63, 83, 60, 19, 28, 67}	$[0.561, 0.364, 0.767, 1.203, 0.411, 0.461, 1.244]^{L}$ $\{0.400, 0.900, 0.400, 0.600, 0.900, 0.500, 0.300\}^{L}$ $[1.136, 0.749, 1.539, 2.400, 0.890, 0.891, 2.492]^{N}$ $\{0.800, 1.800, 0.700, 1.200, 1.800, 1.000, 0.600\}^{N}$ $[1.300, 0.813, 1.680, 2.622, 0.977, 0.891, 2.644]^{P}$ $\{0.900, 2.100, 0.900, 1.200, 1.800, 1.200, 0.600\}^{P}$	1^{L} 1^{N} 3^{P}	0015.00^{L} 0060.60^{N} 0287.76^{P}	1.00^{L} 0.99^{N} 0.98^{P}	76,367

The section presents a cost effective strategy for optimal DERs integration in distribution networks incorporating the effect of existing OLTC based voltage regulation schemes. The effect of OLTC based VR reduces the amount of DER penetration required to attain the same or higher benefits of DG integration in distribution networks. The lesser DG penetration may alleviate many other operational challenges raised in active distribution networks. Moreover, it also maximizes the utilization of existing voltage-regulating infrastructure of distribution system, which was not fully utilized when ignored in planning stage. A DNPL-based GA is proposed that preserves the hereditary information of genetic evolution of each generation and is used to improve the future generations.

4.2.3 Multiobjective DG Integration Problem using Proposed MOTA

In practice, DNOs have to meet many objectives simultaneously, some of them may be conflicting in nature. Considering two or more than two objectives, the optimal DG integration turns-out to be a complex multiobjective optimization problem, aiming to determine optimal number, location, size, and type of DGs. It is difficult to optimize multiple objectives simultaneously, as each objective is equally important with different units and scales. Therefore, a trade-off is required to obtain a compromising solution. The selection of best compromising solution among Pareto solutions is very difficult for optimization techniques, which are originally designed to optimize a single objective. In this section, a new multiobjective optimization technique introduced in Section 3.7 has been demonstrated to solve the multiobjective DG integration problems. The method effectively combines the Taguchi and TOPSIS approaches.

Problem Formulation

In this study, optimal location and size of DGs is determined for nominal loading condition to maximize DG integration benefits. Five objectives are considered to formulate a multiobjective DG allocation problem such as minimization of real power loss, minimization of reactive power loss, minimization of node voltage deviation, maximization of voltage stability margin and maximization of voltage stability index respectively expressed as

$$\min\ f_1 = \sum_{i=1}^{N}\sum_{j=1}^{N}[\alpha_{ij}^{p}(P_iP_j + Q_iQ_j)\ + \beta_{ij}^{p}(Q_iP_j - P_iQ_j)] \tag{4.35}$$

$$\min\ f_2 = \sum_{i=1}^{N}\sum_{j=1}^{N}[\alpha_{ij}^{q}(P_iP_j + Q_iQ_j)\ + \beta_{ij}^{q}(Q_iP_j - P_iQ_j)] \tag{4.36}$$

$$\min\ f_3 = \sum_{i=1}^{N}(V_i - 1)^2 \tag{4.37}$$

$$\min\ f_4 = max\langle L_{ij}\rangle \qquad \forall\ \ i,j \tag{4.38}$$

$$\max\ f_5 = min\langle VSI_i\rangle \qquad \forall\ i \tag{4.39}$$

where,

$$L_{ij} = \frac{4[(P_jx_{ij} - Q_jr_{ij})^2 + (P_jr_{ij} + Q_jx_{ij})V_j^2]}{V_i^4} \tag{4.40}$$

$$VSI_i = V_j^4 - 4(P_ir_{ij} + Q_ix_{ij})V_j^2 - 4(P_ix_{ij} - Q_ir_{ij})^2 \qquad \forall\ j \tag{4.41}$$

Equation (4.35)–(4.39) are denoting the objective functions of real power loss, reactive power loss, node voltage deviation, line and node voltage stability indices respectively. The proposed multiobjective DG integration problem is subjected to the following constraints.

Generation Limit Constraint:

$$0 \leq P_{DG_i} \leq P_{DG}^{Max} \quad \forall\ i \tag{4.42}$$

Bus Voltage Limit Constraint:

$$V_{Min} \leq V_i \leq V_{Max} \quad \forall\ i \tag{4.43}$$

Power Balance Constraint:

$$P_{G_i} - P_{D_i} = V_i \sum_{j=1}^{N} V_j Y_{ij} cos(\theta_{ij} + \delta_j - \delta_i) \quad \forall\ i \tag{4.44}$$

$$Q_{G_i} - Q_{D_i} = -V_i \sum_{j=1}^{N} V_j Y_{ij} sin(\theta_{ij} + \delta_j - \delta_i) \ \ \forall\ i \tag{4.45}$$

Thermal Limit Constraint:

$$I_{ij} \leq I_{ij}^{\max} \ \ \forall \ \ i, j \tag{4.46}$$

DG Penetration Constraint:

$$\sum_{i=1}^{N_{DG}} P_{DG_i} \leq \sum_{i=1}^{N} P_{D_i} \tag{4.47}$$

where, $\alpha_{ij}^{p} = \frac{r_{ij} cos(\delta_i - \delta_j)}{V_i V_j}$, $\beta_{ij}^{p} = \frac{r_{ij} sin(\delta_i - \delta_j)}{V_i V_j}$, $\alpha_{ij}^{q} = \frac{x_{ij} cos(\delta_i - \delta_j)}{V_i V_j}$, $\beta_{ij}^{q} = \frac{x_{ij} sin(\delta_i - \delta_j)}{V_i V_j}$
Also, P_{DG_i}, Q_{DG_i}. P_{D_i}, Q_{D_i}, V_i and δ_i are representing real power capacity of DG, reactive power capacity of DG, real power demand, reactive power demand, voltage magnitude and voltage angle respectively at bus i. Similarly, r_{ij}, x_{ij}, θ_{ij}, I_{ij}, I_{ij}^{Max} are representing resistance, reactance, impedance angle, flow of current, maximum thermal limit of line respectively connected between bus i and bus j. N, N_{DG}, V_{Min} and V_{Max} are representing total number of buses, number of DGs, minimum and maximum allowable voltage limits respectively in the system.

Simulation Results

The MOTA presented in Section 3.7 is adopted to solve this multiobjective DG integration problems for two benchmark test distribution systems of 33 [197] & 118 buses [208] and

one real-life Portugalian distribution system of 202 buses [209]. The line and bus data of the systems are given in Appendix A. The case studies are discussed below.

33-bus Test Distribution System: For this system, the multiobjective DG integration problem is solved for three different cases as suggested in the literature i.e. 3 DG with Unity Power Factor (UPF), 4 DG with UPF and 3 DG with 0.85 Lagging Power Factor (LPF). In order to validate the performance of proposed MOTA, it is also compared with basic TM. For this purpose, the basic TM presented in Section 3.2 is applied to solve the multiobjective DG integration problem formulated in [16,17,140] using weighted sum approach presented in [16].

Initially, three UPF DGs are considered to be installed at three different nodes in the network similar to [16, 17]. The multiobjective DG integration problem is solved using proposed MOTA for five different objectives expressed in (4.35)–(4.39). The simulation results obtained are compared with that of other methods presented in [16, 17] and are summarized in Table 4.8. The best value for each objective is shown bold. From the table, it is clear that the proposed MOTA provides most compromising solution as the values for three objectives are best among all other methods; whereas, none or at the most two objectives are best for other methods. It should be noted that [16, 17] are solving the problem only for three objectives. The DG penetration for the methods of [16] and TM is less but inadequate, as the results obtained are poor. The DG penetration for the proposed MOTA is less than that of the methods of [17]. The CPU time of proposed MOTA is significantly less.

Now, four UPF DGs are considered to be installed optimally at four different nodes as in [115,140]. The comparison results are summarized in Table 4.8. From the table, it can be observed that the values for two objective functions are best for the proposed MOTA and basic TM. However, proposed MOTA provides better values for three objective functions as compared to basic TM. Therefore, the MOTA is capable to provide most compromising solution for multiobjective DG allocation problems in significantly less computational time with comparable DG penetration. Although, in [115] and [140] the problem is solved only for two and three objectives respectively.

In this investigation, three DGs with 0.85 LPF are considered to be installed as in [68,104]. The comparison result of different optimization methods for the scenario is presented in Table 4.8. It has been found that MOTA provides most compromising solution as values for all objectives are found to be the best among all techniques presented in [68, 104], in very less computational time.

TABLE 4.8: Comparison Results for 33-bus Radial Test Distribution System

Case	Method	Values of objective functions					DG sites	DG sizes (MVA)	DG Penet. (%)	CPU time (s)
		f_1^*	$f_2^\#$	f_3	f_4	f_5				
Base		0.2027	0.1351	0.1171	0.0760	0.6988	—	—	00.00	—
3 DG with UPF	GA [16]	0.1063	0.0751	0.0407	0.0266	0.9490	11, 29, 30	1.5000, 0.4228, 1.0714	50.37	–
	PSO [16]	0.1053	0.0776	0.0335	0.0266	0.9255	13, 32, 08	0.9816, 0.8297, 1.1768	50.27	–
	GA/PSO [16]	0.1034	0.0818	0.0124	0.0266	0.9508	32, 16, 11	1.2000, 0.8630, 0.9250	50.27	–
	TLBO [17]	0.1247	0.0884	**0.0011**	**0.0265**	0.9503	12, 28, 30	1.1826, 1.1913, 1.1863	59.90	12.63
	QOTLBO [17]	0.1034	0.0705	**0.0011**	**0.0265**	0.9530	13, 26, 30	1.0834, 1.1876, 1.1992	58.38	12.55
	TM	0.1023	0.0775	0.0040	0.0267	0.9371	15, 26, 33	0.7199, 0.7199, 1.4397	47.99	7.92
	MOTA	**0.0963**	**0.0698**	0.0014	0.0266	**0.9551**	30, 07, 14	1.3400, 0.9800, 0.9600	55.18	**0.30**
4 DG with UPF	GA [140]	0.0701	0.0488	0.0115	0.0244	0.8776	6, 13, 24, 30	0.643, 0.857, 0.857, 0.738	52.07	–
	PSO [140]	0.0713	0.0495	0.0109	0.0266	0.8776	6, 15, 25, 31	0.830, 0.833, 0.541, 0.648	47.98	–
	GA/PSO [140]	0.0682	0.0475	0.0130	0.0261	0.8903	32,14, 24, 26	0.664, 0.663, 1.023, 0.867	54.12	–
	IMOHS [115]	0.0678	0.0474	0.0111	**0.0242**	0.8891	6, 14, 24, 31	0.937, 0.667, 1.012, 0.731	56.31	–
	TM	0.0899	0.0647	**0.0029**	0.0266	**0.9509**	7, 15, 29, 33	0.748, 0.748, 0.748, 0.748	49.89	**8.61**
	MOTA	**0.0663**	**0.0458**	0.0111	0.0257	0.8907	24, 7, 32, 15	0.960, 1.000, 0.680, 0.560	53.84	**0.33**
3 DG with LPF	Analytical [104]	0.0261	0.0224	0.0086	0.0240	0.8678	06, 31, 25	1.8100, 0.9300, 0.8400	60.22	–
	LSFSA [68]	0.0267	0.0218	0.0013	0.0265	0.9323	06, 18, 30	1.3829, 0.5517, 1.0629	50.43	–
	TM	0.0274	0.0204	0.0010	0.0266	0.9545	16, 27, 30	0.7052, 0.7052, 1.4104	47.01	7.88
	MOTA	**0.0157**	**0.0127**	**0.0004**	**0.0152**	**0.9760**	14, 25, 30	0.8800, 0.9200, 1.5600	56.53	**0.30**

f_1^*– in MW and $f_2^\#$ – in MVAr

From the above discussed scenarios for 33-bus system, it may be observed that proposed MOTA provides most compromising solution for the multiobjective DG integration problems as compared to other techniques, in drastically reduced computational time. The voltage profiles for the optimal solutions obtained by the proposed MOTA for all three cases of the study system are plotted in Fig. 4.5. From the figure, it may be noted that

voltage profile is significantly improved as compared to the base case and it is the best for scenario of DGs with 0.85 LPF as it provides real and reactive power support to the system.

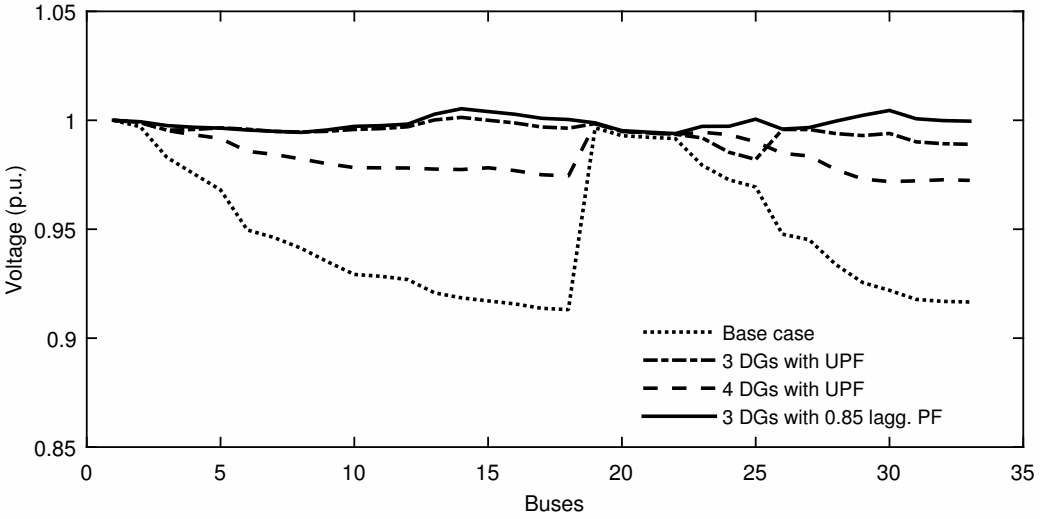

FIGURE 4.5: Voltage profiles obtained by proposed MOTA for 33-bus system

118-bus Test Distribution System: This is a large, 11 kV, 118-bus radial distribution system with total nominal real and reactive power demand of 22.71 MW and 17.04 MVAr respectively [208]. The other system data is given in Appendix A. For the system, two cases are investigated; in first case, 7 UPF DGs are considered to maximize the integration benefits as suggested in [17, 68]. The comparison result of proposed MOTA and other optimization techniques available in literature is summarized in Table 4.9. From the table, it can be observed that the proposed method is competent to provide the best compromising solution among the methods compared with since, it provides three best values of objective functions. The DG penetration obtained by the proposed method is almost equal to the same obtained by ITLBO of [17]. However, none of the objective function value is best for SA [68] and TLBO [17]. Although, the method of [68] solves the problem to minimize real power loss only and the methods of [17] are applied to optimize three objective functions. The computation time of proposed method is significantly less than other methods compared.

Now, 7 DGs with 0.85 LPF are considered to be installed at 7 different nodes in the system [68]. The comparison result of the scenario is presented in Table 4.9. From the Table, it can be observed that MOTA provides better results for all objectives considered as compared to [68]. Although, [68] solves the the problem for power loss minimization

only but the same obtained by the proposed MOTA is significantly less with reduced DG penetration. The CPU time of MOTA is significantly lower than SA [68].

Fig. 4.6 shows the voltage profiles of all discussed scenarios for 118-bus system. It shows that the system's node voltage profiles are significantly improved in both scenarios as compared to base case. It can also be observed that DGs with 0.85 LPF provides best node voltage profile compared to the DGs operated at UPF.

TABLE 4.9: Comparison Results for 118-bus Radial Test Distribution System

Case	Method	Values of objective functions					DG sites	DG sizes (MVA)	DG Penet. (%)	CPU time (s)
		f_1	f_2	f_3	f_4	f_5				
Base		1.2981	0.9787	0.3576	0.1432	0.5703	—	—	00.00	—
7 DG with UPF	SA [68]	0.9001	0.6924	0.1022	0.0631	0.7626	036, 048, 056, 075, 088, 103, 116	7.4673, 0.7109, 3.6739, 2.8246, 2.2979, 5.0803, 0.4606	61.97	25.30
	TLBO [17]	0.7058	0.5553	0.0327	0.0430	0.8548	035, 048, 065, 072, 086, 099, 111	3.2462, 2.8864, 2.4307, 3.3055, 1.9917, 1.6040, 3.5984	52.46	20.91
	QOTLBO [17]	0.6776	0.4955	**0.0233**	**0.0353**	0.8794	043, 049, 054, 074, 080, 094, 111	1.5880, 3.8459, 0.9852, 3.1904, 3.1632, 1.9527, 3.6013	50.44	20.85
	MOTA	**0.6182**	**0.4619**	0.0305	0.0369	**0.8797**	072, 110, 042, 078, 070, 048, 096	1.380, 3.600, 1.920, 2.880, 2.280, 4.380, 1.920	50.53	**3.15**
7 DG with LPF	SA [68]	0.6348	0.4201	0.0562	0.0613	0.8111	036, 048, 056, 075, 088, 103, 116	7.0564, 2.5148, 4.9796, 3.1806, 0.7231, 6.1605, 0.5861	69.36	25.30
	MOTA	**0.2329**	**0.1690**	**0.0138**	**0.0298**	**0.8825**	078, 042, 108, 060, 072, 033, 092	3.420, 1.680, 4.380, 0.960, 3.180, 5.640, 2.100	58.79	**3.21**

201-bus Portugalian Distribution System: After validation of proposed MOTA on two benchmark test systems, it is also validated on a large-scale real life distribution system. This is a large, 201-bus, 10 kV radial distribution system with total demand of 36.10 MW, 27.08 MVAr [209]. The line and bus data is given in Appendix A. The optimal number of DGs for this system is not available in literature for the same problem. Hence, the number of DGs is varied from seven to fifteen in order to determine the optimal number of DGs and it has been found that ten DGs provide best compromising results

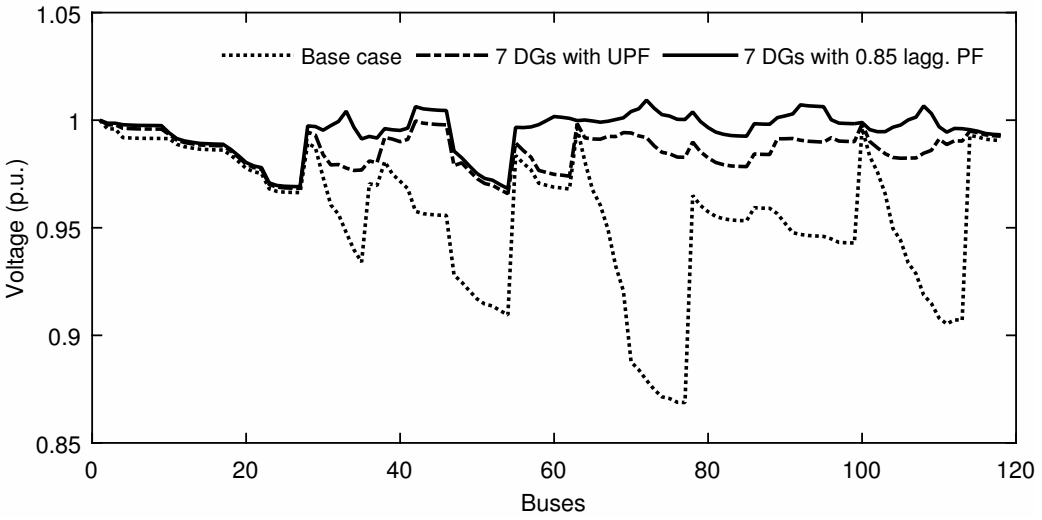

FIGURE 4.6: Voltage profiles obtained by proposed MOTA for 118-bus system.

TABLE 4.10: Comparison Results for 201-bus Portugalian Distribution System

Case	Values of objective functions					DG nodes	DG sizes (MVA)	DG Penet. (%)	Worst Voltage (pu)	CPU time (s)
	f_1	f_2	f_3	f_4	f_5					
Base	2.2387	0.9313	0.5104	0.0860	0.7237	—	—	00.00	0.9221	—
10 DG with UPF	0.9014	0.3716	0.0169	0.0163	0.9337	138, 010, 086, 011, 126, 153, 132, 105, 008, 141	2.802, 2.802, 2.802, 2.802, 5.479, 4.047, 5.790, 4.919, 3.175, 1.183	61.98	0.9820	6.56
10 DG with LPF	0.1856	0.0716	0.0030	0.0086	0.9668	139, 112, 119, 182, 121, 055, 160, 053, 194, 011	2.179, 4.358, 3.113, 6.101, 0.498, 4.670, 2.988, 3.238, 5.230, 2.864	61.01	0.9916	6.51

for the system. Therefore, two different scenarios are considered to maximize the DG integration benefits of the system.

Similar to previous case studies, initially, 10 DGs operating at UPF are assumed to be installed at 10 different nodes in the system. Simulation results of multiobjective DG accommodation problem using proposed MOTA are shown in Table 4.10. It shows that significant power losses and voltage deviation reduction, increased Voltage Stability Margin (VSM) and VSI are achieved using MOTA in comparison to base case scenario.

Now, 10 LPF DGs are considered to be installed on 10 different nodes in the system. Simulation results of multiobjective DG allocations are summarized in Table 4.10. It can be

observed that the reactive power generation from DGs provides high power loss reduction, better voltage regulation, high VSM and VSI compared to UPF DGs for the same system. In the scenario, 91.70% of real power loss reduction is achieved while maintaining all node voltages between 0.99 to 1.01 pu, which is inspiring.

Fig. 4.7 shows the node voltage profiles of real life distribution system for all discussed scenarios. It shows that node voltage profiles are significantly improved for both the scenarios as compared to base case scenario. As observed in other two study systems, LPF-based DGs provide the better voltage profile compared to UPF-based DGs.

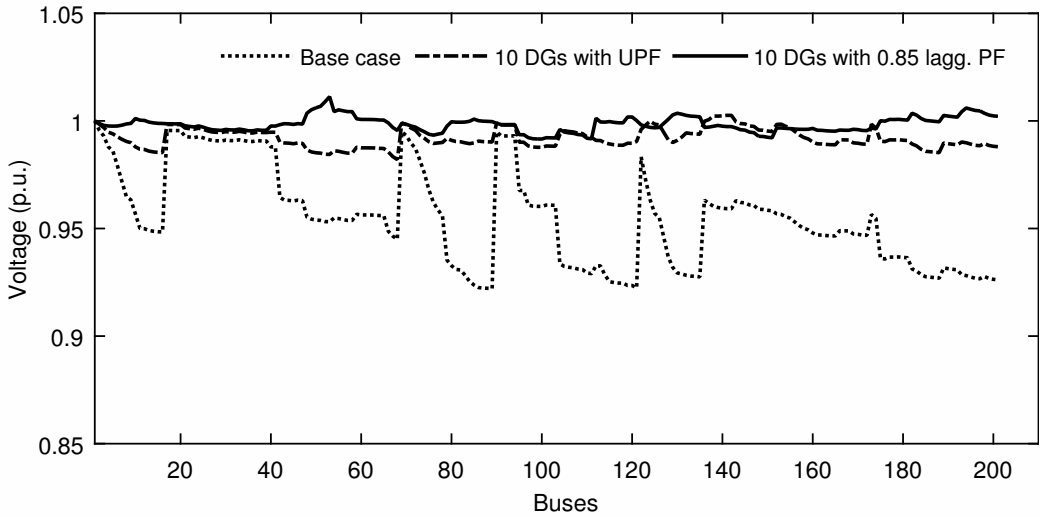

FIGURE 4.7: Voltage profiles obtained by proposed MOTA for 201-bus Portugalian distribution system

After validation on three different PDNs, it has been ensured, that the proposed MOTA is capable to provide compromising solutions for multiobjective DG integration problems for both small and large scale distribution systems. The comparisons show that it has efficiently obtained the optimal or near optimal solution in minimum computations.

Performance Analysis of Proposed MOTA: For multiobjective optimization problems, the definition of quality solution is more complex compared to single objective optimization problems. For any powerful multiobjective optimization technique, the distance between obtained non-dominated set and Pareto front should be minimum [115]. In literature, various techniques or measures are suggested to analyze the quality of multiobjective optimization techniques such as spacing metric (SP-metric), relative convergence metric, diversity metric, etc. The SP-metric is the variance of distance between each solution from its nearest neighbor and is used to check the quality of Pareto solutions [115, 192].

As claimed, TOPSIS approach is capable to minimize the euclidean distances of the solutions from PIS and to maximize it from NIS. Therefore, in order to show the quality of Pareto solutions of MOTA, SP-metric is used. The SP-metric is defined as in [115, 192]

$$S = \sqrt{\frac{1}{N_P - 1} \sum_{i=1}^{N_P} (\bar{d} - d_i)^2} \tag{4.48}$$

where, N_P is the population size, d_i is the distance between ith solution and its nearest neighbour and $\bar{d}$ representing the mean value of d_i among individuals. The d_i and $\bar{d}$ are calculated as follows:

$$d_i = \min \left\{ \sum_{k=1}^{n_2} \frac{|f_k(x_i) - f_k(x_j)|}{f_k^{max} - f_k^{min}} \right\} \qquad \forall\ i, j = 1, 2, \ldots, N_P \tag{4.49}$$

$$\bar{d} = \frac{\sum_{i=1}^{N_P} d_i}{N_P} \tag{4.50}$$

For equidistant solution set, the SP-metric value should be zero, which is an ideal case. Therefore, the value of SP-metric should be minimum for more evenly spaced solution set. A box plot for 100 runs is shown in Fig. 4.8. In each box, the central horizontal

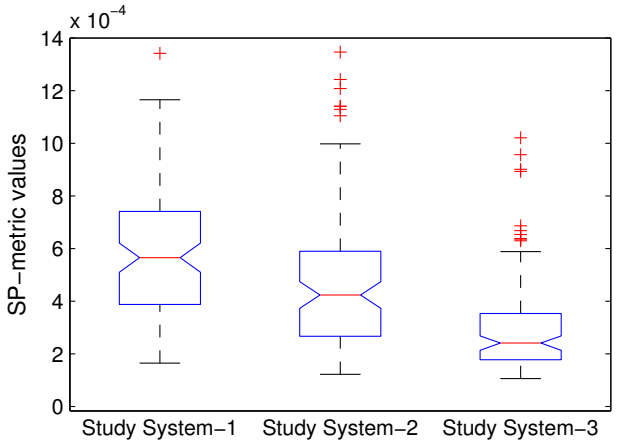

FIGURE 4.8: Box-plot of SP-metric values for 100 runs.

mark represents the median of the SP-metric values. The central box contains the 50% of solution set. The lower and upper boundary lines of the box indicate the 25^{th} and 75^{th} percentiles respectively. The outliers are indicated individually using the '+' symbol. Fig. 4.8 shows that the values of median for system-1, 2 and 3 are 0.0005654, 0.0004238 and 0.0002411 respectively. For study system-1, median is significantly lower than INSGA-II,

NSGA-II, DEMO, SPEA2 in [192], which has considered thee objective only. The reason is that TOPSIS method is based on the minimization of distances between solutions as discussed in section–II. It proves that TOPSIS method provides evenly distributed Pareto-solution sets for multiple objectives.

4.3 Optimal Planning of Non-dispatchable DERs

In Section 4.2, the optimal integration of dispatchable DGs have been investigated for distribution systems. The problem is formulated as single and multiobjective optimization in deterministic framework while ignoring the system uncertainties. It may be noted that the share of renewables is expected to increase in future, which will increase the operational complexity of the system due to associated uncertainty of renewables. Therefore, it is a growing concern to incorporate the stochastic behavior of renewables in DG planning. Here, the optimal integration of renewable DGs is explored considering the hourly stochastic behavior of generation and load. The probabilistic modeling of renewable generation and load demand presented in Section 2.4, followed by the proposed stochastic modeling of complete system in Section 2.5 are used in this section.

Alternatively, the increasing penetration of grid connected DGs and microgrids in distribution networks may attract the attention of transmission system operators to introduce a new energy pricing policies to reduce the irregular amount and types of energy transactions at PCCs. For example, DGs operating at UPF or leading PF may deteriorate the system power factor, as system will import relatively more reactive power in comparison to real power from upstream grid and might affect the voltage stability of the connected grid. Therefore, the energy pricing should incorporate the type and amount of power import/export by the microgrids, DGs or PDNs, since different types of distributed energy resources are being integrated in distribution systems to achieve various techno-economic benefits. Therefore, a DG or system may be rewarded, if it improves the grid performance whereas; a DG/system may be penalized, if it deteriorates the performance of upstream grid. Here, a new PF-based energy pricing policy is introduced to control the irregular and different grid energy transactions among microgrids and its connected distribution grid.

4.3.1 Proposed Pricing based VVC of Microgrids

In this section, an energy pricing based VVC is introduced for microgrids to establish a balance of real and reactive energy transactions from/to connected upstream grid at a

given point of time. However, it is difficult to model the effect of microgrids on connected PDN, while observing it from the PCC. For example, a microgrid owner may be unaware about the need of reactive power requirements of upstream connected grid. In order to reduce the complexity of model, the PF of PCC may be a worthy measure for grid and microgrid performance. Therefore, according to the proposed PF-based energy pricing policy a safe zone of PF (lead/leg) is defined. For an hour h, if the mean PF measured at the PCC is less than the minimum limit of the zone then a penalized energy price will be offered to the microgrid. Whereas, if it is more improved than the specified limit of the zone then a discounted energy price will be offered in that hour.
The PF-based energy pricing may be expressed as

$$C_E^{PF}(h) = [1 + \mu(h)] \times C_E(h) \tag{4.51}$$

where, $\mu(h)$ is PF-based penalty/rebate factor defined as

$$\mu(h) = \begin{cases} pf_{min}^{spec} - pf(h); & \text{if } pf(h) < pf_{min}^{spec} \\ 0; & \text{if } pf_{min}^{spec} \leq pf(h) \leq pf_{max}^{spec} \\ pf_{max}^{spec} - pf(h); & \text{if } pf(h) > pf_{max}^{spec} \end{cases} \tag{4.52}$$

$$pf(h) = \frac{P_{Grid}^{before/after}(h)}{\sqrt{\left(P_{Grid}^{before/after}(h)\right)^2 + \left(Q_{Grid}^{before/after}(h)\right)^2}} \tag{4.53}$$

$$P_{Grid}^{before}(h) = \sum_{i=1}^{N} P_i^D(h) + P_{Loss}^{before}(h) \tag{4.54}$$

$$Q_{Grid}^{before}(h) = \sum_{i=1}^{N} Q_i^D(h) + Q_{Loss}^{before}(h) \tag{4.55}$$

$$P_{Grid}^{after}(h) = \sum_{i=1}^{N} P_i^D(h) + P_{Loss}^{after}(h) - \sum_{i=1}^{N} \left[\alpha_i PG_i^{WT}(h) + \beta_i PG_i^{PV}(h) + \chi_i P_{r,i}^{MT}(h)\right] \tag{4.56}$$

$$Q_{Grid}^{after}(h) = \sum_{i=1}^{N} Q_i^D(h) + Q_{Loss}^{after}(h) - \sum_{i=1}^{N} \gamma_i Q_{r,i}^{SC}(h) \tag{4.57}$$

The hourly mean PF of microgrid is defined in (4.53). Equations (4.54)–(4.57) are representing the real and reactive power transactions between connected grid substation and microgrid before and after DG integration respectively.

4.3.2 Problem Formulation

In this section, a multi-year optimization framework is developed for optimal planning of microgrids considering different DERs. The problem is formulated as a mixed integer, non-linear optimization problem in order to obtain the simultaneous optimal allocation of multiple DERs i.e. PVs, WTs, MT and SCs, such that the Net Present Value (NPV) of the investment is maximized. The NPV calculation comprises of the costs of DER investment, operation, maintenance, grid energy transaction etc. Furthermore, to control the active/reactive power exchange between microgrids and up-stream grid, an energy pricing based VVC for PDNs introduced in previous section is used. The aim is to determine the optimal nodes, sizes of different DGs and SCs simultaneously such that the project NPV is maximized considering their ancillary services. The proposed objective function is expressed as

$$\max\ NPV = \frac{PVC^{before}_{\text{Outflows}} - PVC^{after}_{\text{Outflows}}}{1 + K\sum_{y=1}^{T_P}\sum_{h=1}^{24}\sum_{i=1}^{N}\Delta V_i(y,h)} \tag{4.58}$$

such that

$$PVC^{before}_{\text{Outflows}} = \sum_{y=1}^{T_P}\frac{\phi}{(1+d)^y}\Big[\sum_{h=1}^{24} C^{PF}_E(y,h)P^{before}_{Grid}(y,h)\Big] \tag{4.59}$$

$$PVC^{after}_{\text{Outflow}} = \overbrace{\sum_{i=1}^{N}\alpha_i P^{WT}_{r,i}C^{WT}_{Ins} + \beta_i P^{PV}_{r,i}C^{PV}_{Ins} + \chi_i P^{MT}_{r,i}C^{MT}_{Ins} + \lambda_i Q^{SC}_{r,i}C^{SC}_{Ins}}^{\text{Installation cost of DGs and SCs}} +$$
$$\sum_{y=1}^{T_P}\frac{\phi}{(1+d)^y}\times\Bigg[\overbrace{\sum_{h=1}^{24}\sum_{i=1}^{N}+\beta_i P^{PV}_{r,i}C^{PV}_{Ins} + \chi_i P^{MT}_{r,i}C^{MT}_{Ins} + \lambda_i Q^{SC}_{r,i}C^{SC}_{Ins}}^{\text{O\&M cost of DGs and SCs}} + \tag{4.60}$$
$$\overbrace{\sum_{h}^{24}\sum_{i=1}^{N}\chi_i P^{MT}_{r,i}\eta\alpha^{MT}_E(y)}^{\text{Emission cost of MT}} + \overbrace{\sum_{h}^{24}C^{PF}_E(y,h)P^{after}_{Grid}(y,h)}^{\text{Grid energy transaction cost}}\Bigg]$$

$$C^{MT}_{OM}(y) = \alpha^{MT}_E(y) + m^{MT}(y) \tag{4.61}$$

$$\Delta V_i(y,h) = \begin{cases} V^{spec}_{min} - V_i(y,h), & \text{if } V_i(y,h) < V^{spec}_{min} \\ 0, & \text{if } V^{spec}_{min} \le V_i(y,h) \le V^{spec}_{max} \\ V_i(y,h) - V^{spec}_{max}, & \text{if } V_i(y,h) > V^{spec}_{max} \end{cases} \tag{4.62}$$

The objective function expressed in (4.58) is subjected to the following constraints

$$NPV > 0 \tag{4.63}$$

$$\alpha_i PG_i^{WT}(y,h) + \beta_i PG_i^{PV}(y,h) + \chi_i P_{r,i}^{MT} - P_i^D(y,h) = V_i(y,h)\sum_{j=1}^{N} V_j(y,h)Y_{ij}\cos\big(\theta_{ij} + \delta_j(y,h) - \delta_i(y,h)\big) \tag{4.64}$$

$$\gamma_i Q_{r,i}^{SC} - Q_i^D(y,h) = -V_i(y,h)\sum_{j=1}^{N} V_j(y,h)Y_{ij}\sin\big(\theta_{ij} + \delta_j(y,h) - \delta_i(y,h)\big) \tag{4.65}$$

$$I_{ij}(y,h) \leq I_{ij}^{Max} \qquad \forall\ i,j \tag{4.66}$$

$$\sum_{i=1}^{N} \alpha_i P_{r,i}^{WT} + \beta_i P_{r,i}^{PV} + \chi_i P_{r,i}^{MT} \leq \sum_{i=1}^{N} P_{L,i}^{Peak} + P_{Loss}^{Peak} \tag{4.67}$$

$$\sum_{i=1}^{N} \gamma_i Q_{r,i}^{SC} \leq \sum_{i=1}^{N} Q_{L,i}^{Peak} + Q_{Loss}^{Peak} \quad y{=}1 \text{ or year of commissioning} \tag{4.68}$$

where, (4.59)–(4.62) are representing the Net Present Costs (NPCs) of total future cash outflows in planning horizon before and after DG integration, O&M cost of MTs and voltage penalty factor respectively. The future cash outflows of microgrid includes the cost of DER investment, their operation & maintenance, pollution treatment/emission and energy purchase from the main grid over the considered planning horizon T_P. The objective function expressed in (4.58) is subjected to the NPV, instantaneous nodal power balance, feeder current limit, DG and SC penetration limit constraints, given in (4.63)–(4.68) respectively.

In order to solve the proposed optimal DER planning problem, a meta-heuristic optimization technique has been adopted i.e. improved GA presented in Section 3.5. The basic structure of chromosome or an individual used in the GA to solve the proposed DER planning problem is shown in Fig. 4.9.

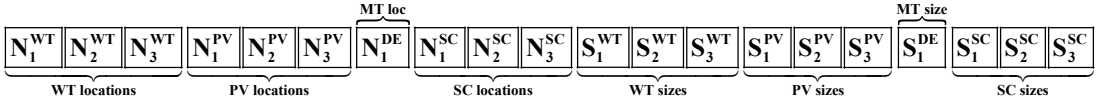

FIGURE 4.9: Structure of an individual used in GA

4.3.3 Simulation Results

In order to demonstrate the applicability and techno-economic feasibility of proposed stochastic model, the standard 33-bus test distribution system [197] is considered as a microgrid system given in Appendix A. The annual peak demand of microgrid is assumed

to be 1.6 times of nominal demand with 3% annual peak-load growth [210]. The other parameters used in this study such as cost of DG investment, operation, maintenance, variable grid energy transaction, annual increment rate of monetary parameters etc. are referred from [30,203,210] and collectively, various technical and initial economical parameters used in this work are summarized in Table B.2 of Appendix B.

In order to validate the proposed hourly-based stochastic model for microgrid planning and operations, it is compared with the models available in literature [134,156,189,190,211]. As it is difficult to compare all models in stochastic environment [189]; therefore, all compared in deterministic framework. For fair comparison, single objective problem i.e. annual energy loss minimization is considered for optimal allocation of SCs as in [156,189,190,211]. However, it is difficult to get the exact historical load and generation data used in above references; therefore, to bring all models on the common platform, a common historical data is used for all simulations, as suggested in [189]. The results obtained for all models are summarized in Table 4.11 for comparison. From the table, it may be observed that the total optimal size of SCs obtained for all the methods is equal; however, the proposed method provides maximum annual energy loss reduction as compared to all other methods. The method of [156], provide results very close to the proposed model. The annual energy loss reduction obtained by the method of [189] is less and the estimated energy loss for the base case is high, however, it is applied for three load levels based deterministic model. Hence, the proposed model is validated and found to be an efficient method for optimal SC planning problem and may be applied for proposed stochastic DER planning and operational problems.

Table 4.11: Comparison of Different Methods in Deterministic Framework

Methods (N_D=1)	Cases	Optimal SC Nodes (kVAr)	Annual Energy Loss (MWh)	Annual Energy Loss Reduction (%)
3-load levels [189]	Base Case	–	2318.98	–
	After SC Integration	14(0300) 24(0600) 30(1200)	1565.09	32.50
1-load level [156]	Base Case	–	1775.45	–
	After SC Integration	10(0600) 24(0600) 30(0900)	1166.20	34.32
Proposed 24 hours model	Base Case	–	1767.82	–
	After SC Integration	14(0300) 24(0600) 30(1200)	1155.29	34.65

Now, the proposed hourly-based DER planning model is thoroughly investigated in deterministic, probabilistic and stochastic frameworks. In deterministic framework, hourly single states of generation and load i.e. $N_W = 1$, $N_{PV} = 1$, $N_D = 1$ are considered for each hour to synthesize the generation and load data. For proposed probabilistic model, the hourly generation and load is synthesized by selecting the event with highest probability in that hour using probability distributions discussed in Section 2.4. In proposed stochastic model, heuristic approach based on RWS criteria is presented to introduce the uncertainty and variability in hourly generation and load demand as discussed in Section 2.5. The hourly stochastic solar irradiation, wind speed and LMF are synthesized for 24×365 hours for each year of the planning horizon, T_p then the annual mean of each hour of synthesized generation and load data is used for every year separately. The hourly annual mean of stochastically generated data for LMF, solar irradiation and wind speed for first year are shown in Fig. 4.10.

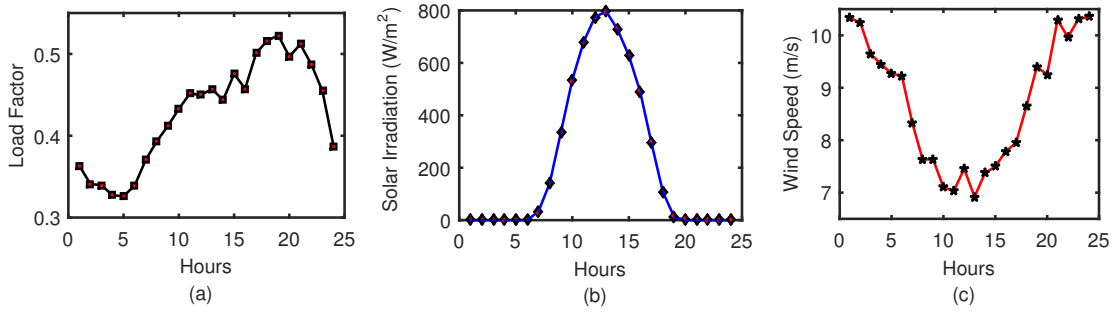

FIGURE 4.10: Hourly synthesized data for (a) load multiplying factor (b) solar irradiation and (c) wind speed in first year

From above figure, it may be observed that hourly power generation profile of each renewable resource is very different from others. For example, wind farms are producing more power during light load hours or in night when wind speed is high, whereas PV generates power in daytime. Fig. 4.10(c) shows that WT produces more fluctuating power compared to PV, which may affect the VVC schemes in different manner. However, the availability of solar irradiation is low as compared to wind, since it is only available during the day. Therefore, in order to investigate the pros and cons of different DER technologies on microgrid planning, seven practically possible test cases are framed as given below.

Case–I: Optimal integration of SCs only

Case–II: Optimal integration of WTs only

Case–III: Simultaneous optimal integration of WTs and SCs

Case–IV: Simultaneous optimal integration of PVs and SCs

Case–V: Simultaneous integration of WTs, MT and SCs

Case–VI: Simultaneous integration of PVs, MT and SCs
Case–VII: Simultaneous integration of WTs, PVs, MT and SCs

Due to the consideration of high investment cost of PVs as compared to WTs, the integration of only PVs is not considered in this work, as it provides negative NPV for given parameters. In order to reduce the effect of intermittent power generation from PV and WTs, one biofuel-based dispatchable MT is also considered in cases V to VII. In planning, all DGs are assumed to be operated at UPF and modeled as the negative load [13, 115]. The simulation results of deterministic, probabilistic and stochastic models for optimal VVC planning in microgrids for all cases are summarized in Table 4.12. The table shows the optimal sites and sizes of different DERs along with their respective NPVs.

The results show that the installed DER penetration is almost equal for all three models. However, deterministic modeling of microgrid planning is unable to explore the maximum profit compared to probabilistic and stochastic models. It may be due to the consideration of hourly annual mean value for generation and load while ignoring load and generation uncertainties. The stochastic approach is found to be better as compared to other two as maximum NPV is produced for all cases except Case II & V. Moreover, this is more realistic since hourly variability is taken into consideration for renewables and load. It is noticed that installed PV penetration is very low compared to WTs because of their high investment cost. Similarly, the share of MTs is also low due to their high installation and running charges as compared to WTs. However, the successive improvement and timely reducing cost of PV technology may increase the share of PVs in future microgrids. The case-III is found to be more beneficial due to the comparatively low investment and running cost of WTs and simultaneous integration of WTs and SCs.

It has been observed that WTs are proved to be promising in terms of monetary benefits but at high DER penetration, which could raise the operational challenges. Therefore, a detailed comparison of various technical and monetary factors of microgrid is archived in Table 4.13. The table shows the mean and standard deviation of microgrid node voltages and PF appeared in planning horizon, T_p. The bifurcation of future cash outflows/inflows of microgrid due to energy loss, PF penalty/rebate, grid energy transaction and emission in their Present-Worth (PW) are also shown in the table. It has been observed that microgrid node voltages are significantly improved as compared to base case in all frameworks and cases. It can also be observed that high penetration of WTs only in case-II, III & V deteriorates the Std. of microgrid node voltages for all models as compared to base case.

TABLE 4.12: Optimal Siting and Sizing of Various DERs in Planned Microgrid System

Model	Case	WT sites (Size in kW)	PV sites (Size in kW)	MT site (Size in kW)	SC sites (Sizes in kVAr)	NPV (M$)
Deterministic Framework	I	–	–	–	14(0600), 17(0300), 31(1200)	03.685
	II	02(2010), 11(1830), 31(1890)	–	–	–	20.162
	III	07(2010), 20(1950), 28(2010)	–	–	4(0900), 8(0300), 11(0600)	25.655
	IV	–	33(0030)	–	13(0900), 31(0300), 32(0900)	03.724
	V	06(1470), 24(1410), 28(1500)	–	15(0150)	6(1200), 30(0600)	19.392
	VI	–	08(0120)	18(0030)	16(0600), 17(0300), 32(1200)	03.261
	VII	18(0900), 25(0840), 33(0900)	16(0030)	30(0060)	5(0900), 29(0900)	13.368
Probabilistic Framework	I	–	–	–	10(0600), 17(0600), 32(1200)	04.322
	II	9(1980), 24(1950), 29(1980)	–	–	–	22.295
	III	1(2010), 05(2010), 08(1860)	–	–	15(0600), 30(0900), 31(0600)	27.685
	IV	–	29(0030)	–	12(0300), 14(0900), 31(1200)	04.259
	V	06(1500), 19(1500), 30(1440)	–	13(0030)	16(0600), 26(1500)	21.840
	VI	–	17(0030), 31(0030)	–	15(1200), 31(0900)	04.302
	VII	01(0870), 15(0900), 30(0900)	5(0030), 15(0120)	–	6(0300), 11(0600), 30(1200)	15.007

continued on next page...

Model	Case	WT sites (Size in kW)	PV sites (Size in kW)	MT site (Size in kW)	SC sites (Sizes in kVAr)	NPV (M$)
Stochastic Framework	I	–	–	–	14(1200), 30(0900), 32(0600)	04.522
	II	10(2010), 25(1980), 31(1770)	–	–	–	21.401
	III	01(1950), 06(1890), 07(2010)	–	–	12(1200), 33(0900)	27.971
	IV	–	33 (0150)	–	13(0900), 18(0300), 31(1200)	04.640
	V	06(2910), 23(1410)	–	14(0300)	05(0900), 16(0300), 32(0900)	21.599
	VI	–	31(0060)	17(0180)	14(0900), 29(1200), 31(0300)	04.758
	VII	09(0900), 10(0900), 30(0900)	12(0030), 30(0060)	26(0030)	01(0600), 16(0600), 31(0900)	15.936

The box plots of microgrid node voltages of proposed stochastic model through planning horizon are shown in Fig. 4.11. From the figure, it can be observed that high voltages appeared in cases II, III and V, due to high renewable penetration. Alternatively, the mean PF of microgrid before DER integration was 0.8494, which attracted the heavy penalty on the energy purchased by the microgrid in planning horizon, due to the proposed PF-based energy pricing scheme, as can be seen from the table. In case-I, SCs improve the average PF of microgrid significantly that allows microgrid to receive rebate on grid energy transaction for providing balanced VAr power support. In case-II, WTs operated at unity PF deteriorates the mean PF of microgrid, even compared to base case since it majorly imports the reactive power from the upstream grid. However, the shortcomings are overcome in case-III by integrating WTs and SCs simultaneously, which offers simultaneous VVC in microgrid and connected grid while maximizing the NPV. It is interesting to notice that the mean PF of microgrid for case-VII is poor but still microgrid receives rebate on energy transaction. It may be possible that the energy transaction is very low during poor PF for long duration and amount of energy transaction is very high during improved PF. For all frameworks, the PW of total energy purchased by the microgrid is very less or

TABLE 4.13: Values of Various Objectives for Stochastic Volt/VAr Planning of Microgrids

Model	Cases	Node Voltages Mean	Node Voltages Std.	Power factor Mean	Power factor Std.	PW of energy loss (M$)	PW of PF Penalty/ rebate (M$)	PW of grid energy transaction (M$)*	PW of MT pollution cost ($)
Deterministic	Base	0.9582	0.0061	0.8495	0.0002	1.8023	2.0051	37.8374	–
	I	0.9814	0.0056	0.9853	0.0216	1.6289	-1.5898	37.8374	–
	II	0.9935	0.0102	0.5128	0.2501	1.1751	0.8525	-05.1818	–
	III	0.9995	0.0078	0.8866	0.1981	0.9412	0.3512	-06.9837	–
	IV	0.9807	0.0056	0.9852	0.0218	1.5978	-1.5803	37.7218	–
	V	0.9979	0.0072	0.8849	0.2001	0.4451	0.3424	03.1342	1576.80
	VI	0.9829	0.0055	0.9850	0.0219	1.6557	-1.5468	37.0110	315.36
	VII	0.9915	0.0076	0.8834	0.2092	0.4532	-0.5151	17.1736	630.72
Probabilistic	Base	0.9554	0.0064	0.8494	0.0002	2.3559	2.4047	45.112	–
	I	0.9817	0.0058	0.9804	0.0276	2.1800	-1.8363	45.1120	–
	II	0.9901	0.0106	0.5190	0.2402	1.3717	1.3297	-00.7348	–
	III	0.9972	0.0077	0.8819	0.1934	0.9595	0.0880	-00.5021	–
	IV	0.9816	0.0058	0.9803	0.0277	2.1756	-1.8269	44.9955	–
	V	0.9942	0.0080	0.8652	0.2221	0.9290	-0.3246	10.2680	329.13
	VI	0.9800	0.0059	0.9890	0.0152	2.1714	-1.9132	44.8790	–
	VII	0.9925	0.0075	0.8876	0.2189	0.7645	-0.7234	23.8170	–
Stochastic	Base	0.9529	0.0069	0.8494	0.0002	2.7290	2.6444	49.4181	–
	I	0.9819	0.0062	0.9723	0.0369	2.6144	-1.8700	49.4181	–
	II	0.9889	0.0108	0.5098	0.2136	1.4449	5.8810	04.6920	–
	III	0.9971	0.0082	0.9086	0.1605	1.1728	-0.1355	03.9931	–
	IV	0.9802	0.0061	0.9838	0.0238	2.4138	-2.0589	48.8268	–
	V	0.9938	0.0075	0.8736	0.2023	0.6697	-0.0906	11.6955	3153.60
	VI	0.9820	0.0061	0.9805	0.0292	1.9335	-1.9029	46.6748	1892.16
	VII	0.9926	0.0084	0.9022	0.2053	0.7836	-0.7151	27.6801	315.36

negative for case-II and III because the penetration of WTs is high in these cases thereby small amount of energy will be purchased by the microgrid. Table 4.13 shows that the insertion of MTs improves the node voltage regulation but slightly deteriorates the PF.

In order to analyze the effect of proposed energy pricing based VVC, the export/import of real and reactive power by the microgrid along with its PF are investigated and shown in Figs. 4.12 and 4.13 for 1st and 20th year of planning horizon respectively. It has been found that the microgrid is operated in different modes during a day. Therefore, proposed analysis can be divided into four major operating modes of microgrid as discussed below.

Microgrid operation mode–1 $[P_{Grid}^{After}(h) \geq 0 \ \& \ Q_{Grid}^{After}(h) \geq 0]$

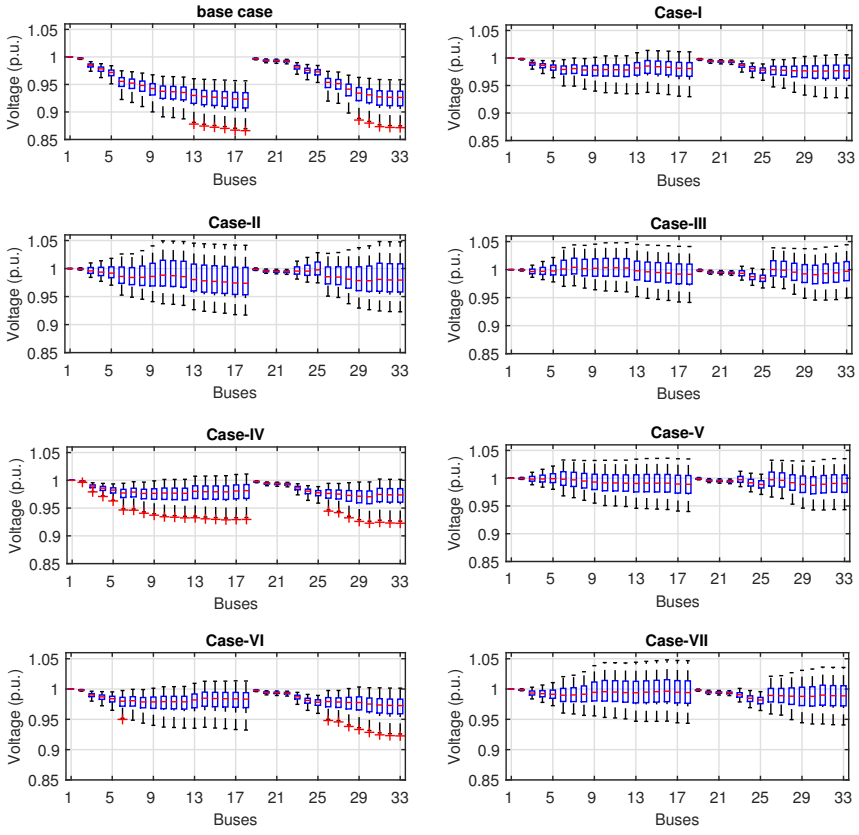

FIGURE 4.11: Box plot of node voltages in planning period for all cases obtained by proposed stochastic model

In this mode, microgrid imports both real and reactive powers from the connected distribution system. In these hours, the total generated real and reactive powers from DGs and SCs respectively would be less than the microgrid's total demand. Hence, the microgrid will act like a load for the connected PDN. For base case, the microgrid behaves like a LPF load, as shown in Fig. 4.12(a). Fig. 4.12(c) shows that DGs operated at UPF further deteriorates the microgrid PF. This mode appears throughout for base case and during 08th to 18th hours for case-II; though, PF is poor for these cases. However, in 20th year, the mode mostly appeared in all cases but with improved PF as compared to base case.

Microgrid operation mode–2 $[P_{Grid}^{After}(h) \geq 0 \ \& \ Q_{Grid}^{After}(h) < 0]$

In this mode of operation, microgrid acts like a leading PF load since total VAr generation in the microgrid is higher than its total VAr demand. Hence, the extra amount of VAr is supplied to the upstream grid. In the first year, this is the major mode of operation of microgrid as observed from Figs. 4.12(b) to Fig. 4.12(h) except Fig. 4.12(c). The microgrid acts like a synchronous motor for PDN operating at leading PF and receives a huge rebate

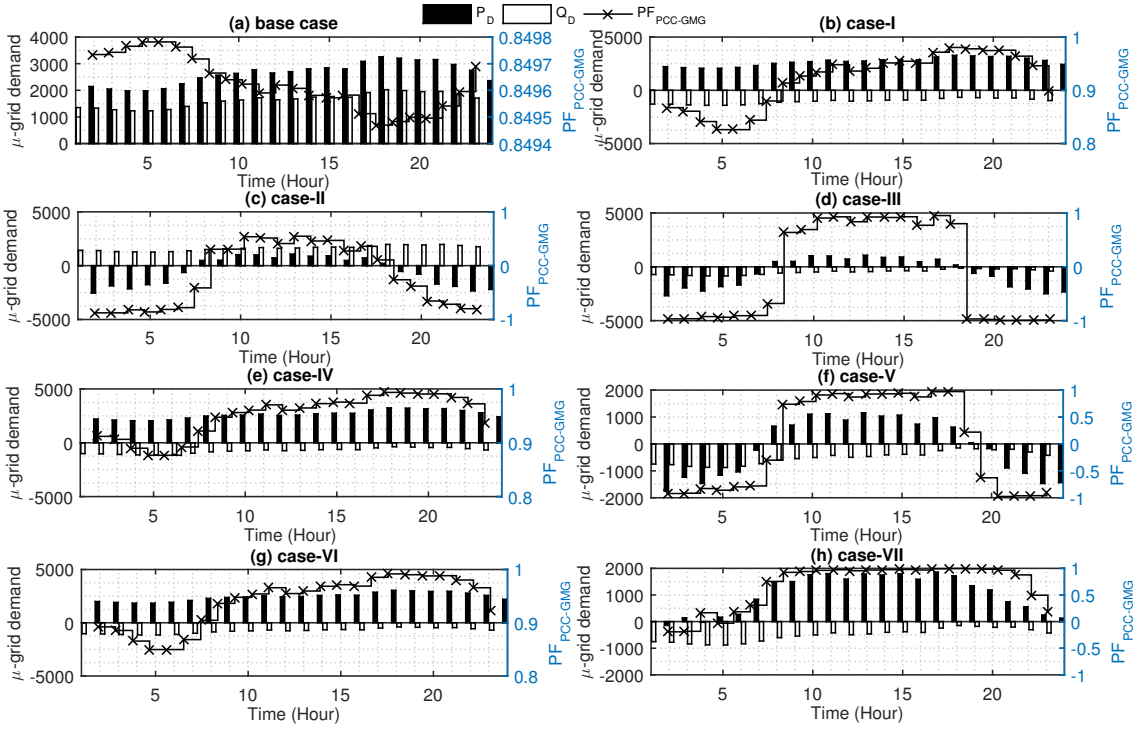

FIGURE 4.12: Hourly PF and load demand variations of the system in 1st year of planning period using proposed stochastic DG planing model

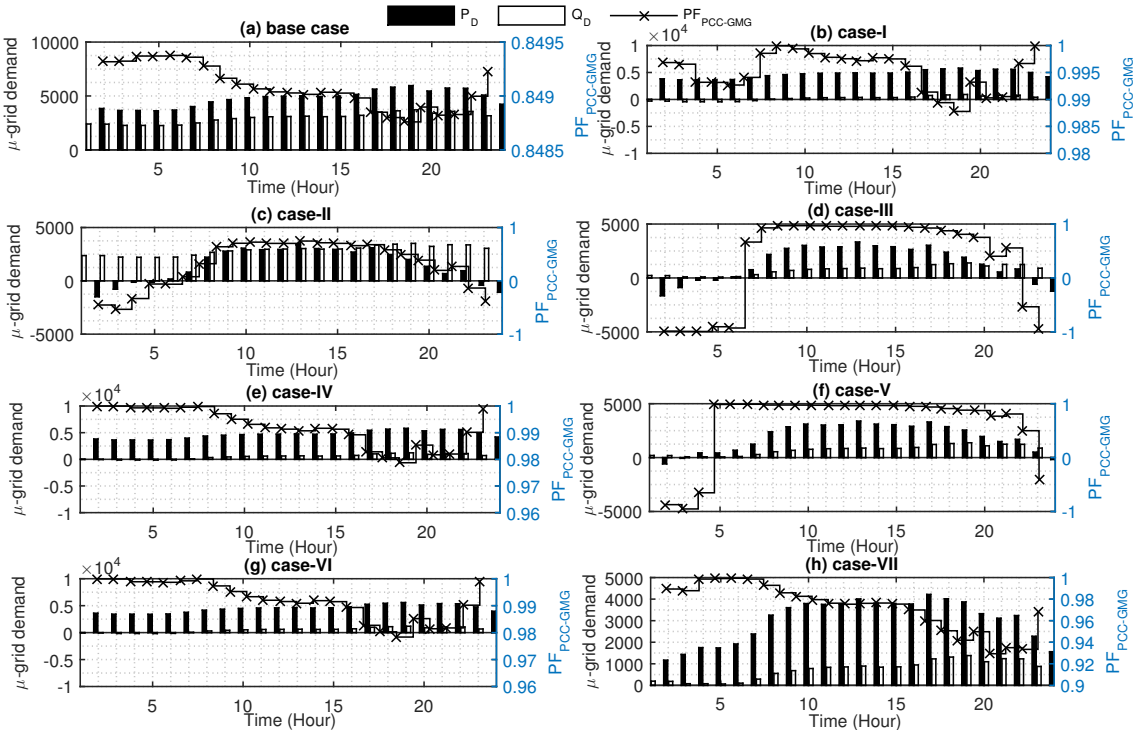

FIGURE 4.13: Hourly PF and load demand variation of the system in 20th year of planning period using proposed stochastic DG planning model

for maintaining the UPF for most of the time. As annual demand increases, the number of operating hours of this mode will decrease and in 20th year of the planning, almost vanishes as observed from Fig. 4.13. This mode is very important in terms of voltage stability of upstream connected grid in peak hours.

Microgrid operation mode–3 $[P_{Grid}^{After}(h) < 0 \ \& \ Q_{Grid}^{After}(h) > 0]$
There may be few hours in which microgrid exports real power and imports reactive power with main grid like an induction generator. This mode appears when total real power demand of microgrid is less than total real power generation and total VAr demand is more than total VAr generation e.g., 19th to 7th hours of case-II in Fig. 4.12(c). In this mode, a very less amount of VAr is permitted to import from the main grid as most of the countries are having kW based energy pricing. The proposed energy pricing based VVC may help the DNOs to limit the VAr drawn by microgrids by maintaining the specified PF; the negative PF represents the leading PF. Therefore, a simultaneous integration of DGs and SCs may be encouraged. Alternatively, DGs can be operated in lagging PF to provide VAr support, if SCs are not present in the system but not suggested.

Microgrid operation mode–4 $[P_{Grid}^{After}(h) < 0 \ \& \ Q_{Grid}^{After}(h) < 0]$
In this mode, microgrid behaves like a Synchronous Generator (SG) for upstream grid since the total kW and kVAr generation from DGs will be more than the total microgrid kW and kVAr demand. The mode appears in case-III and case-V during 19th to 7th hour for first year of planning in Figs. 4.12(d) and 4.12(f) respectively. From the figures, it can be observed that the microgrid is operated in lagging PF generation mode as SG. However, the PF is very poor during mode-switching hour(s) but for less duration.

From above discussion, it has been concluded that emerging microgrids may raise many operational challenges for distribution system operators. In this case, the proposed energy pricing policy would help the operators to perform the optimal Volt/VAr control in the system as shown in Figs. 4.12 and 4.13. These results are obtained using the full installed DER capacities; however, the optimal operation of such microgrids further improve the performance of microgrids as investigated in Chapter 5.

4.4 Summary

In this chapter, various DER planning frameworks have been investigated to maximize the integration benefits of dispatchable and non-dispatchable DGs. A DG allocation problem is formulated to determine the optimal mix of diversified dispatchable DG technologies to

maximize the annual techno-economic and social benefits. Some new objective functions and constraints are also introduced in this proposed DG planning model for PDNs. The improved TM introduced in Chapter 3 is adopted to solve the problem for standard test distribution systems of 33 and 118 buses.In order to validate the suggested improvements, the performance of proposed approach has compared with standard TM and with another variant available in the literature. The comparison shows that the suggested improvements are promising. To validate the simulation results of proposed approach, these have been validated with the same obtained by an improved variant of GA in existing literature.

A new DER integration problem is developed in existing voltage regulation framework to minimize the cost of annual energy loss of PDNs. The proposed DG planning problem is solved by an DNPL-based GA proposed in Chapter 3. Initially, the DNPL-based GA is validated with some optimization techniques available in the literature. The comparison reveals that the proposed DNPL has improved the performance of GA. The simulation results obtained are found to be promising when compared with same in existing literature. After validation of the algorithm, it is applied to solve the proposed DER integration problem for 33-bus test and 108-bus Indian radial distribution systems under different scenarios. The simulation results show that the consideration of existing OLTC-based VR schemes in DER integration generates more techno-economic benefits at lesser DER penetration as compared to the conventional DER planning models compared with. Moreover, the proposed DER integration model is effectively utilizing the existing infrastructure of PDNs.

Finally, a multi-year optimization framework has been developed for optimal planning of microgrids with the inclusion of renewable & non-renewable DGs and SCs. In order to show the impact of intermittent renewable power generation and load demand on VVC, three planning models viz, deterministic, probabilistic and stochastic, have been investigated under seven different cases. For stochastic model, hourly stochastic load and generation profiles are synthesized using an RWS criteria based on historical data. Moreover, an energy pricing based VVC scheme is introduced to limit the VAr import/export between microgrids and connected grid. The significant improvements have been observed in microgrid performance parameters such as PF, voltage profile, energy loss etc. The energy pricing based VVC efficiently controls the amount and type of energy exchange between upstream grid and microgrid.

Chapter 5

Optimal Operational Management of Distributed Resources

5.1 Introduction

In recent years, the quick growth of various DRs in distribution systems has raised many operational issues and challenges for system operators. Besides, the modern power consumers are more concerned about the quality of power supply. Therefore, the ANM is one of the integral parts of modern distribution management system, which involves various algorithms to control voltages (Volt), reactive power (VAr) and power dispatch of DERs in the system via centralized and decentralized controllers. However, the complexity of system and solution algorithms limits the capabilities of local automatic controllers associated with voltage regulators in existing Distribution Networks [212]. Moreover, the emergent integration of DRs has further increased the complexity of control algorithms, especially renewables. The uncertainty of renewable power generation and load demand may cause unnecessary tap movements of automatic voltage regulators. The frequently changing taps may cause voltage transients in the system, which can affect the smooth operation of consumers. Moreover, excessive tap operation of these switching devices may not be desirable due to the mechanical wear at tap-point [212]. Therefore, efficient and fast control algorithms are required for each regulator to accomplish its associated tasks in minimum tap-changes in coordination with other regulators present in system.

With the recent advances in battery technologies, the BESS can play a vital role to alleviate the impact of renewables, despite of its high cost. However, the operational management

of BESS is slightly more complex than DGs as it behaves like load and generation with uncertain SOC level and numerous charging/discharging constrains. Various algorithms are also required to estimate the instant SOC. Considering above discussed issues and challenges, the optimal integration and operational management of BESS turns out to be a complex multi-level, mixed-integer, non-linear optimization problem, which may require multi-level optimization framework to determine the optimal site and size of BESS while simultaneous considering the operational management of BESS.

Alternatively, the penetration of EVs is expected to increase in future thereby need the CSs to charge the EVs. Mostly, the CSs will be deployed in distribution systems, which will change the demand profile and variability. Besides, the concept of smart city development is also taking shape across the globe. Therefore, it is growing need to investigate the problem of mobile power infrastructure deployment and operational management i.e. EVs, in context of smart city development.

Considering the above discussed facts, some optimization frameworks are proposed in this chapter for operational management of active distribution networks. Initially, an online ANM scheme is proposed to minimize the hourly operating cost of microgrid throughout the considered planning horizon. For online monitoring and control of the system, a RWS-based scheme is used in the DSSE to generate feasible pseudo measurements. The order to demonstrate the effectiveness of proposed model, the simulation results are compared with that of the same obtained by a traditional local ANM scheme, which has found to be promising. An energy pricing based VVM of microgrid and its coupled distribution grids is also proposed to improves the system performance.

A bi-level optimization framework is also developed for optimal accommodation and operations of BESS such that the penetration of renewables has maximized while maintaining the system security constraints within limits. To achieve this, some new objective and security constraints have been proposed. The simulation results reveals that the proposed BESS management scheme increases the penetration of renewables in distribution systems, without violating the system security constraints considered. Furthermore, some optimal planning and operational management schemes have been proposed to optimally manage the growing EV penetration in smart city context. The proposed aggregator based operational management of EVs generates techno-economic benefits of DNO, EV owners and aggregator. In this chapter, the goal is to perform the ANM of distribution systems considering different DRs; therefore, some minor planning problems of DRs allocation is also presented to make the system active.

5.2 Proposed Online Active Network Management

In this section, a multi-year optimization model is developed in a stochastic framework to perform online ANM of distribution systems comprised of multiple DRs over their lifetime. Due to the lack of measurement adequacy in existing PDNs, pseudo-measurements are used for DSSE. A new heuristic-based approach is proposed to generate feasible pseudo-measurements, which employs RWS criteria based on historical data of load and generation. These pseudo-measurements are used for state estimation using Weighted-Least Square (WLS) method. The basic arrangements of local and proposed online ANM are presented in Fig. 2.1(b) and discussed in Section 2.2.

5.2.1 Distribution System State Estimation (DSSE)

In the era of smart grid, the state estimator plays a vital role in wide area monitoring and control of modern power system. In order to operate the system in normal or secure state, a continuous monitoring is required. In control centers, multiple tasks can assigned to state estimators such as state estimation, topology processing, observability analysis, bad data processing, error processing etc. based on measurement data obtained from various Remote Monitoring Units (RMUs). The large-scale deployment of Phasor Measurement Units (PMUs) along with the existing conventional measurement units is taking place across the globe for continuous monitor and control of modern power system [213, 214].

The transmission networks are designed to be operate in mesh structure, which is advantageous to obtain the unknown system states in minimum number of measurements via state estimators. Whereas, most of existing PDNs are operating in radial configuration and very small number of measurement units are present in PDNs, which result into poor convergence of DSSE. To overcome some of its limitations, one way is to deploy required number of measurement units along with the existing units; however, economically not recommended. Secondly, the DSSE can use pseudo or virtual measurements, which can be generated using historical system data, load and generation forecasting, user experience, some heuristics etc. Mostly, the accuracy of DSSE depends upon the pseudo-measurements selection algorithms hence, low weights may be assign to such measurements.

In this section, the goal is to develop an efficient DSSE to estimates the system states. The algorithm minimizes the weighted sum of errors between measured and calculated values.

The WLS estimator is used and the objective function is as expressed in [214]

$$\begin{aligned} J(x) &= \sum_{p=1}^{m} \frac{[z_p - h_p(x)]^2}{R_{pp}} \\ &= \sum_{p=1}^{m} [z_p - h_p(x)]^T R^{-1} [z_p - h_p(x)] \end{aligned} \tag{5.1}$$

s. t.

$$x^{k+1} = x^k - \Big[G(x^k)\Big]^{-1}.g(x^k) \tag{5.2}$$

$$\begin{aligned} G(x^k) &= \frac{\partial J(x^k)}{\partial x} = H^T(x^k).R^{-1}.H(x^k) \\ g(x^k) &= -H^T(x^k)R^{-1}\Big[z - h(x^k)\Big] \\ H(x^k) &= \left.\frac{\partial h(x^k)}{\partial x}\right|_{x=x^k} \end{aligned} \tag{5.3}$$

$$R = diag\{\sigma_1^2, \sigma_2^2, \sigma_3^2, \ldots, \sigma_m^2\} \tag{5.4}$$

$$P_i = V_i \sum_{j=1}^{N} V_j \big(G_{ij}\cos\theta_{ij} + B_{ij}\sin\theta_{ij}\big) \tag{5.5}$$

$$Q_i = -V_i \sum_{j=1}^{N} V_j \big(G_{ij}\sin\theta_{ij} - B_{ij}\cos\theta_{ij}\big) \tag{5.6}$$

where, H shown in (5.3) is the Jacobian of $h(x)$ and R is a diagonal matrix that consists the diagonal elements of measurement covariance. In this work, the weights are selected as the inverse of error covariance. Equations (5.5) is representing the nodal power balance.

In order to improve the accuracy of DSSE, a new heuristic-based algorithm is proposed to generate pseudo-measurements. The approach uses the RWS criteria proposed in Section 2.5 to predict their current states in each hour, which employs hourly historical data of load, wind speed and solar irradiation. The proposed approach is recursively minimize the error between predicted and measured states. The convergence is achieved when predicted states nearly matches the measured states. These predicted states are using as pseudo-measurements for DSSE. The flowchart of proposed DSSE is presented in Fig. 5.1. The proposed heuristic for pseudo measurement is shown in subroutine block–A.

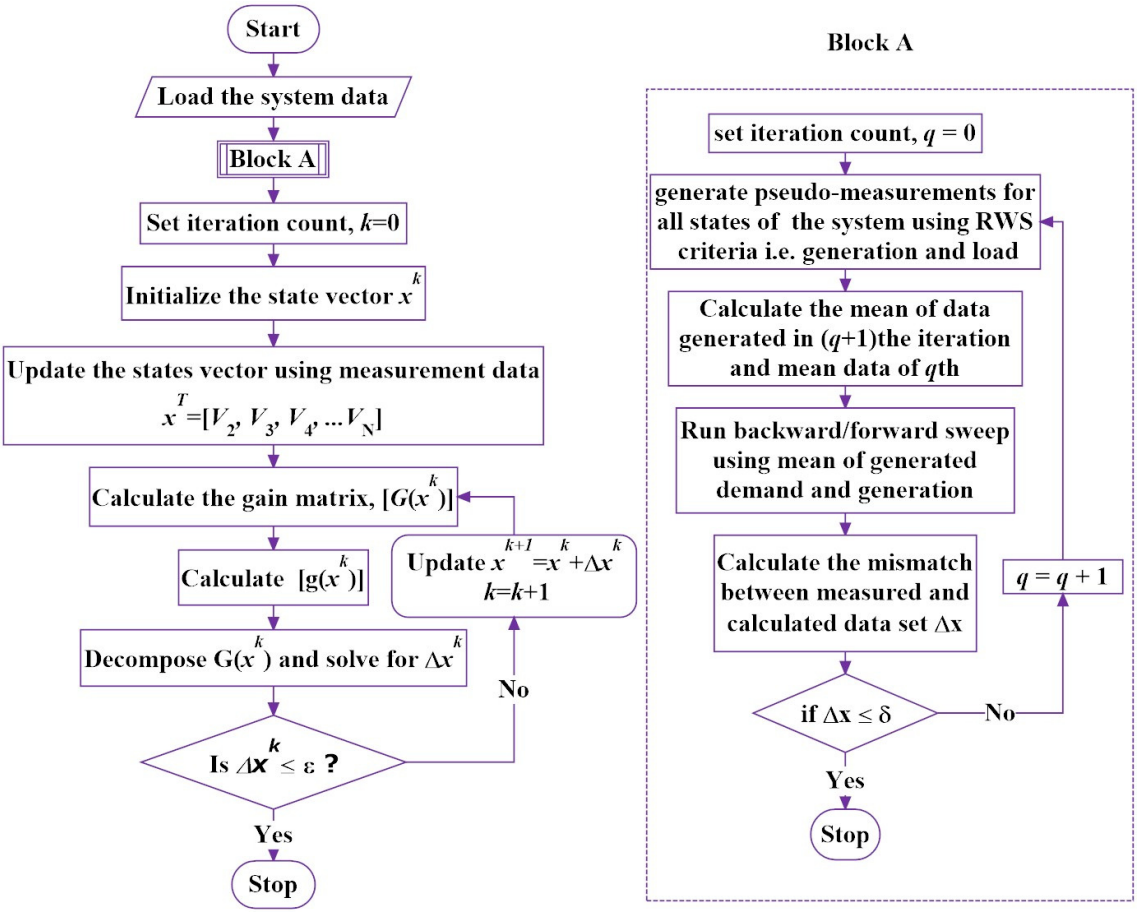

FIGURE 5.1: Flow chart of proposed heuristic based DSSE.

5.2.2 Proposed Objective Function for ANM

In Section 4.3.3, optimal planning of microgrid is performed to maximize the NPV by optimizing the optimal sites and sizes of various DERs considering dynamically changing system states for the complete planning horizon. However, the contribution of other existing VRDs such as OLTCs and feeder voltage regulators has been ignored in the planning, which could have been traditionally employed in PDNs to perform VVM. The increasing number and type of different voltage regulators may raise coordination issues during operations. Therefore, there is an increasing need to establish an optimal coordination between these regulators and to maximize operational benefits. Here, the operational benefits of PDN are maximized via optimizing the ancillary services of DGs, SCs and OLTCs simultaneously.

In proposed ANM, the instantaneous operating cost of the system is minimized while keeping node voltages, PF and other constraints within the limits. If any node voltage or

microgrid PF are found beyond the permissible limits, optimal tap setting of OLTC (Volt) and dispatch of controllable DERs i.e. MT and SCs (VAr) are determined to minimize the instantaneous operating cost of the system. Hence, the objective function to minimize the instantaneous operating cost of microgrid at time t, is expressed as

$$\min Cost^{OPR} = \sum_{i=1}^{N} \overbrace{\alpha_i P_{r,i}^{WT} C_{OM}^{WT}}^{\text{OM cost of WTs}} + \underbrace{\beta_i P_{r,i}^{PV} C_{OM}^{PV}}_{\text{OM cost of PVs}} + \overbrace{\chi_i P_i^{MT}(t) C_{OM}^{WT}}^{\text{OM cost of MT}} + \underbrace{\gamma_i Q_{r,i}^{SC} C_{OM}^{SC}}_{\text{OM cost of SCs}} + \underbrace{\big[1+\mu(t)\big] \times C_E(t) P_{Grid}^{after}(t)}_{\text{Grid energy transaction cost}} \tag{5.7}$$

s. t.

$$P_i = V_i(t) \sum_{j=1}^{N} V_j(t) Y_{ij} \cos\big(\theta_{ij} + \delta_j(t) - \delta_i(t)\big) \tag{5.8}$$

$$Q_i = -V_i(t) \sum_{j=1}^{N} V_j(t) Y_{ij} \sin\big(\theta_{ij} + \delta_j(t) - \delta_i(t)\big) \tag{5.9}$$

$$0.95 \leq V_i(t) \leq 1.05 \qquad \forall\ i \tag{5.10}$$

$$\sum_{t=1}^{24} \big| TAP_t^{OLTC} - TAP_{t-1}^{OLTC} \big| \leq N_{OLTC} \tag{5.11}$$

$$\sum_{t=1}^{24} \big| TAP_t^{SC} - TAP_{t-1}^{SC} \big| \leq N_{SC} \tag{5.12}$$

Equation (5.8)–(5.12) are representing the nodal power balance, feeders thermal limit, node voltage limits, maximum number of OLTC and SC tap change limit constraints respectively. The remaining expression/factors may be referred from Section 4.3.2.

5.2.3 Simulation Results

In order to demonstrate the effectiveness of proposed DSSE and online ANM, a standard 33-bus distribution network shown in Fig. 2.1(b) is adopted. The optimal sites and sizes of different DERs obtained in Chapter 4 are considered to demonstrate the proposed stochastic ANM to minimize the hourly operating cost of the network throughout planning horizon i.e., 20 years. In order to determine the future states of various VRDs based on obtained measurements, an improved variant of GA is adopted from [196], as it has the capability to solve such complex-combinatorial nature of the problems. In order to

demonstrate the effectiveness of proposed ANM model, the cases framed in Section 4.3.3 are re-investigated. Initially, the effectiveness of proposed DSSE is demonstrated. Later, the proposed DSSE is used for online ANM of distribution systems.

Validation of Proposed DSSE

In order to demonstrate the effectiveness of proposed DSSE, it is tested on bare system in first year of planning span. The comparison of estimated node voltages and feeder currents with their actual values are shown in Fig. 5.2(a) and Fig. 5.2(b) respectively. The figures show that the generated pseudo measurements using proposed RWS improve the accuracy of DSSE since it estimates the system states near to their actual values. The validation confirms that proposed DSSE can be used for online monitoring and control of distribution systems.

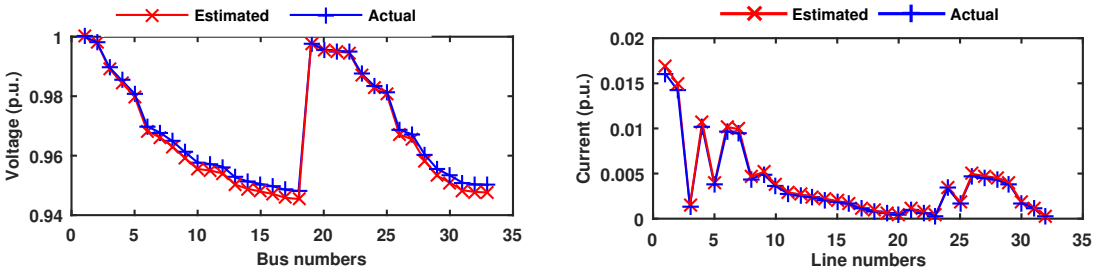

(a) Node voltages (For 1st year)

(b) Line currents (For 1st year)

FIGURE 5.2: Estimated values of bare system using proposed DSSE.

ANM Case Studies and Discussions

Now, the proposed online ANM scheme is applied to minimize the operational cost of DNO over the lifetime of DERs. The results obtained are presented in Table 5.1. The simulation results obtained in Chapter 4 using installed capacity of DERs without any operational management strategy and traditional set-point based local ANM strategy are also presented in the table to highlight the advantages of proposed online strategy. The values estimated at control centers using proposed DSSE and their actual values obtained by power flow calculations are also shown to demonstrate the accuracy of proposed DSSE. The table includes the mean and standard deviation (Std.) of system node voltages over 20 years to realize the voltage management using different strategies. Similarly, the mean and Std. of PF at substation are also presented in the table to show the effectiveness of strategies of reactive power management. Number of OLTC and SCs tap changes required in 20 years of operational management and number of hours of node voltages limit violation are also shown in the table. Finally, all future monetary costs i.e. cash

outflows are converted into their respective NPCs for the period is evaluated and presented in the table.

TABLE 5.1: Various Techno-economic Benefits Obtained by Different ANM schemes

Strategy	Actual/est. values	Case	Voltages		Power Factor		No. of OLTC Tap Change	No. of SCs Tap Change	Voltage limits Viol. Hours	NPC (M$)
			Mean	Std.	Mean	Std.				
Without ANM (Chapter 4)	Base case		0.9529	0.0069	0.8494	0.0002	–	–	165710	54.80
	-	I	0.9819	0.0062	0.9723	0.0369	–	–	18615	50.26
		II	0.9889	0.0108	0.5098	0.2136	–	–	36865	22.55
		III	0.9971	0.0082	0.9086	0.1605	–	–	3285	15.80
		IV	0.9802	0.0061	0.9838	0.0238	–	–	24820	49.54
		V	0.9938	0.0075	0.8736	0.2023	–	–	5475	24.37
		VI	0.9820	0.0061	0.9805	0.0292	–	–	25550	49.37
		VII	0.9926	0.0084	0.9022	0.2053	–	–	2920	33.34
local ANM	OLTC only		0.9968	0.0018	0.8495	0.0002	1460	NA*	20805	54.51
	-	I	0.9880	0.0021	0.9723	0.0369	1460	Nil	Nil	50.22
		II	1.0003	0.0056	0.4980	0.2166	1095	NA	Nil	23.04
		III	0.9990	0.0069	0.9086	0.1605	365	Nil	Nil	15.80
		IV	0.9880	0.0020	0.9840	0.0238	730	Nil	Nil	49.50
		V	0.9954	0.0062	0.8737	0.2023	365	Nil	Nil	24.36
		VI	0.9896	0.0018	0.9805	0.0292	1095	Nil	Nil	49.33
		VII	0.9942	0.0072	0.9022	0.2053	365	Nil	Nil	33.33
Proposed Centralized ANM (online)	OLTC only		0.9992	0.0031	0.8495	0.0002	2160	NA	20805	54.50
	Actual values calc. using Load Flow	I	1.0028	0.0008	0.9928	0.0066	730	730	Nil	49.29
		II	0.9994	0.0034	0.5097	0.2135	8030	NA	Nil	22.50
		III	1.0002	0.0052	0.9087	0.1605	365	365	Nil	15.79
		IV	1.0012	0.0026	0.9903	0.0105	730	730	Nil	49.14
		V	0.9992	0.0029	0.8430	0.2715	365	Nil	Nil	24.01
		VI	0.9959	0.0017	0.9825	0.0255	365	365	Nil	49.17
		VII	0.9951	0.0052	0.9032	0.2041	1825	1460	Nil	33.30
	OLTC only		0.9991	0.0031	0.8495	0.0002	2160	NA	20075	54.48
	Est. values using proposed DSSE	I	1.0028	0.0008	0.9928	0.0067	730	730	Nil	49.28
		II	0.9994	0.0034	0.5097	0.2130	8030	NA	Nil	22.51
		III	1.0002	0.0052	0.9057	0.1697	365	365	Nil	15.80
		IV	1.0013	0.0026	0.9903	0.0100	730	730	Nil	49.15
		V	0.9992	0.0028	0.8487	0.2563	365	Nil	Nil	24.01
		VI	0.9960	0.0017	0.9825	0.0253	365	365	Nil	49.17
		VII	0.9951	0.0052	0.9043	0.2035	1825	1460	Nil	33.20

*NA = Not Available

It may be observed from the table that proposed and traditional approaches improve the system performance significantly while generating monetary gain for microgrid. In traditional approach, VRDs take action only when their PCC node voltages violated their limits; however, all node voltages for the period are well within the permissible limits that

is achieved by controlling the OLTC taps only. Interestingly, no capacitor tap change is required throughout the test period as it does not consider the economic aspects. Whereas, the proposed online ANM enables when any estimated node voltage or PF of microgrid deviates from the specified limits. The node voltage profiles and PFs are better as compared to local control approach in almost all cases. However, both the ANM schemes are able to maintain the system node voltages within limits since there is no hour in which system violates these limits.

It may be noted that additional tap changes have been suggested by the proposed online ANM, as the objective is to minimize the instantaneous cost of microgrid while maintaining the system constraints well with limits. The table also summarizes the estimated values of techno-economic factors for various cases obtained by DSSE, which are very close to their actual values obtained by power flow calculations. In all cases, microgrid NPCs are less for proposed ANM as compared to same obtained by local ANM. Table 5.2 shows the net present profits of microgrid achieved by online and local ANM schemes are more as compared to that of without ANM.

TABLE 5.2: Net Present Profit Achieved by Different ANM Schemes (in USD)

Strategy/ Cases	Local ANM (local)	Centralized ANM (online)
OLTC only	2,86,340	2,92,373
Case-I	39,476	9,71,240
Case-II	-4,90,456	49,242
Case-III	6,240	12,231
Case-IV	50,018	4,08,029
Case-V	4,228	3,635,70
Case-VI	42,124	2,00,477
Case-VII	4,927	37,273

Fig. 5.3 shows hourly mean voltages and OLTC tap settings suggested by both the schemes. In the figure, each 24 hours time slot represents the mean hourly profile of a year in increasing order; therefore, the total number of mean hours in 20 years will be $24 \times 20 = 480$. In order to demonstrate the VAr controlling ability of online and local ANM strategies, the hourly real and reactive power demand along with system PF are shown in Fig. 5.4 and Fig. 5.5 for 1st and 20th years respectively. Finally, the detailed case wise comparison and discussion on findings of different ANM strategy are discussed below.

Base Case with OLTC only: This refers to the bare case and OLTC is associated with the grid sub-station transformer. During planning in Chapter 4, the effect of OLTC was ignored. In this chapter, the case is re-investigated considering the benefit of OLTC for operational management. Table 5.1 shows that online control of OLTC generates

more techno-economic benefits as compared to LDC based control with more number of switching operations but well within the limit. Since, an OLTC has a maximum tap-change limit of 50000 in its life span of 30 years [215]. Both controls are equally reducing the number of hours in which system violates the voltage limits. Fig. 5.3(a) shows that mean voltage profiles for both the strategies are same except in initial years, as OLTC taps are set at higher level for online approach and the same level is obtained in three steps by the conventional approach. The action taken by the online strategy provides more operational benefits as shown in Table 5.2. Fig. 5.3(a) and Fig. 5.4(a) show that OLTC is not able to improve the system PF, as there is no reactive power support in this case.

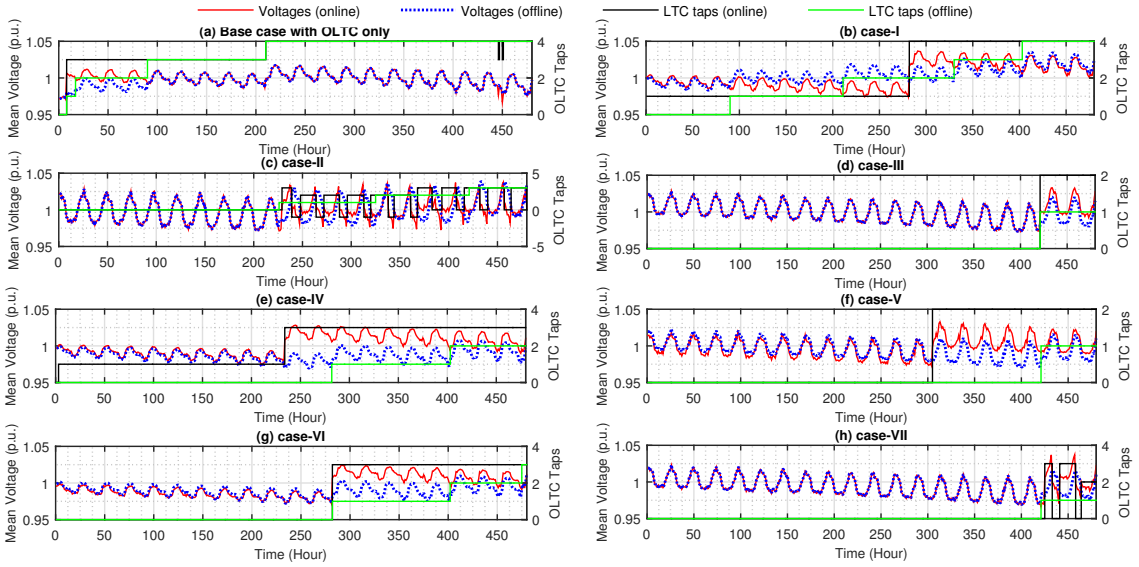

FIGURE 5.3: Hourly mean voltages of the system and OLTC tap positions obtained by online and local ANM schemes for 20 years

Case–I (OLTC and SCs only): In this case, OLTC and SCs are simultaneously performing the coordinated ANM. Table 5.1 & 5.2 show that simultaneous but online control of SCs and OLTC generates more techno-economic benefits as compared to local controllers since it considers monetary aspects too. Table 5.1 shows that voltages are well within limits throughout the considered time frame. In local ANM, OLTC tap setting have been optimized while keeping the SCs at full capacities. In online ANM, tapings of both OLTC and SCs are adjusted to optimized the objective function. Fig. 5.3(b) shows that the centralized ANM suggests larger steps but less number of tap changes for OLTC. Fig. 5.4(b) shows that online VVM approach is found to be very effective to maintain the almost unity PF for initial years however, system PF is improved in both the schemes in last year of the timespan as can be seen from Fig. 5.5(b). However, the local strategy

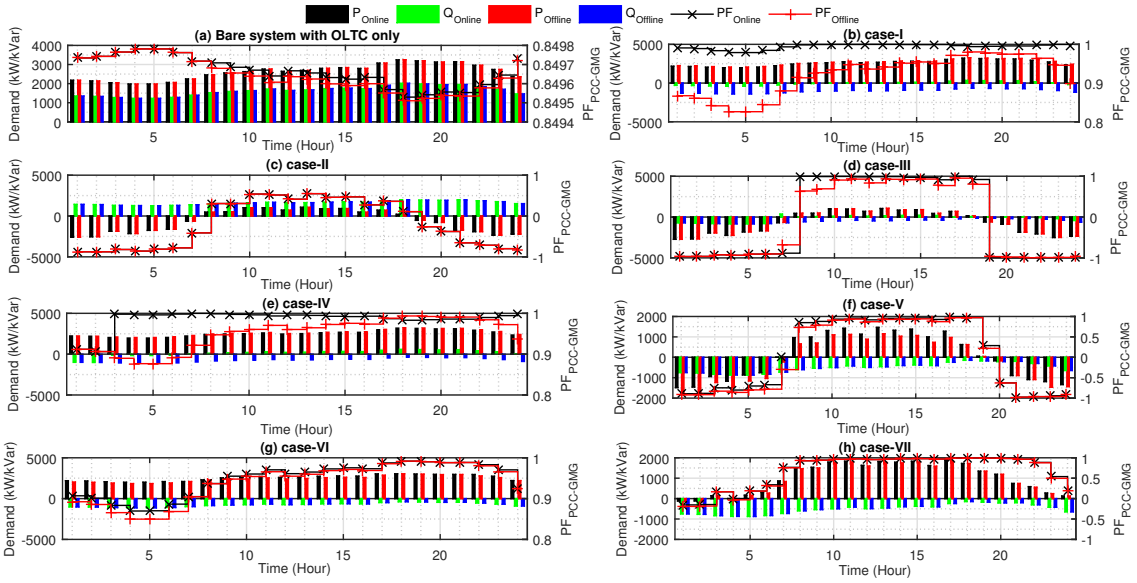

FIGURE 5.4: Real and reactive power demand of the system with its PF for 1st year using different ANM schemes

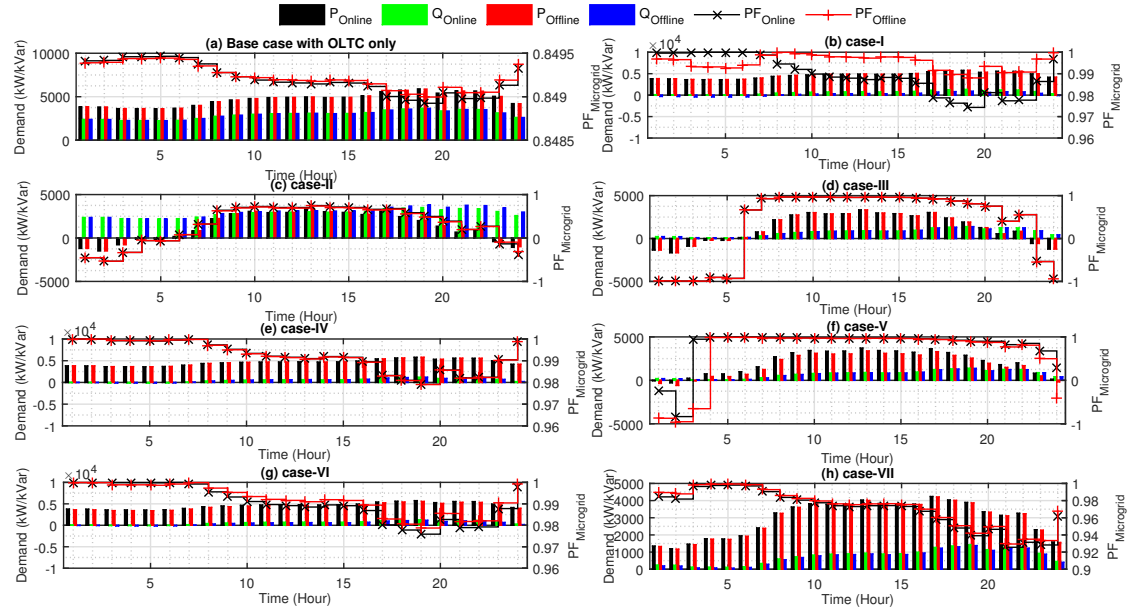

FIGURE 5.5: Real and reactive power demand of the system with its PF for 20th year using different ANM strategies

deteriorates the system PF in initial years since the penetration of SCs is high at that time which allows microgrid to exports excess reactive to the upstream grid.

Case–II (OLTC and WTs only): In this case, OLTC and generator excitation control of WTs are used for online and local ANM. It may be comprehend that in online ANM, OLTC alone is sufficient to retain the system node voltages within permissible limits, as

can be observed from Table 5.1. Whereas in local ANM, the LDC based OLTC control is not able to maintain all nodes voltages within the limits; therefore, generator excitation control is also participated. However, it reduces the number of switching operations of OLTC as compared to the online approach; where, OLTC alone is participating in the voltage control scheme. Alternatively, in online ANM, frequent OLTC tap operations may be observed in peak and light load hours as system demand increases by the years since it is the only VRD employed in the system, unlike local ANM. Fig. 5.4(c) and 5.5(c) show that in both schemes, the microgrid is exporting extra wind power generation to upstream grid during light load hours and always imports the reactive power from upstream grid due to the absence of VAr source. The action is leading to deteriorated system PF and attracted heavy PF penalty on energy transaction price.

As discussed, in the local ANM scheme, the generator excitation of WTs are also participated in coordinated voltage control along with OLTC. Fig. 5.6 shows the voltages at PCC of WTs and their reactive power management. It may be observed that in 325th hour, OLTC tap is moved to higher voltage level to maintain the target bus voltages within limits. However, the action leads to over voltages at PCCs of WTs during light load hours. Therefore, the local ANM scheme associated with WTs senses these over voltages and triggers the excitation controls of WTs, which start absorbing reactive power from the system and further worsens the system PF. Table 5.2 shows that local control of WTs reduces the expected operational benefits even compared to base case.

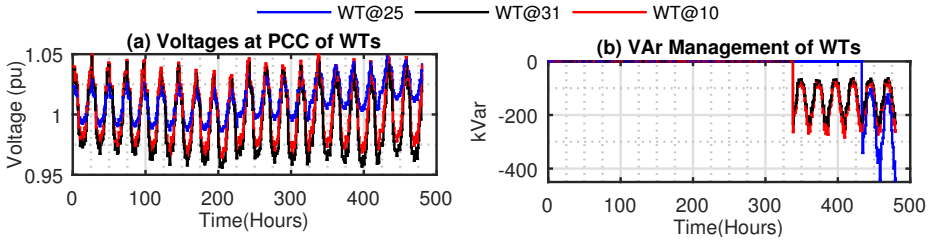

FIGURE 5.6: local ANM using generator excitation control (a) Voltages at PCCs and (b) VAr management of WTs.

Case–III (OLTC, WTs and SCs only): In this case, OLTC, WTs and SCs are simultaneously participating in both ANM schemes. Table 5.1 & 5.2 show that the coordinated switching operations of multiple VRDs are producing more techno-economic benefits, if centrally controlled. Besides, the presence of SCs reduces the number OLTC tap movements in both the control schemes; however, local approach is utilizing the full installed capacities of SCs. Fig. 5.3(d) shows that both schemes suggest OLTC tap move at the

same time towards the end of time horizon but online approach suggests higher tap position as compared to local one. Fig. 5.4(d) shows that initially, microgrid exports both real and reactive power to upstream grid in light load hours; however, at the end of timespan it exports real power only as can be seen from Fig. 5.5(d). It is also observed that online ANM strategy retains the system PF very close to unity operated either in legging or leading PF throughout the time horizon. Alternatively, local ANM provides poor PF sometime during initial years but at the end of time horizon both strategy works similarly as full capacities of DERs are utilized, as shown in Fig. Fig. 5.5(d).

Case–IV (OLTC, PVs and SCs only): A simultaneous ANM of PV, SC and OLTC is investigated in this case. Table 5.1 and 5.2 show that centralized control of DRs are providing more operational benefits as compared to their local control in same number of OLTC tap movements. Moreover, the online ANM scheme utilizes the switched SCs efficiently in order to maximize the operational benefits. The voltage profile and OLTC tap position are shown in Fig. 5.3(e). In both the schemes, hourly mean voltages remain almost same for initial years but after some time centralized approach suggests higher OLTC tap position to maximize the operational benefits as compared to local scheme. Fig. 5.4(e) shows that centralized control maintains the system PF near to unity for initial years, whereas, the local controllers are found to be less efficient to improve the same. However, during last years of considered time horizon, performance of both the strategies are observed to be same from Fig. 5.5(e), like in Case–III.

Case–V (OLTC, WTs, MT and SCs): The presence of high renewable penetration may raise many operational challenges due to their intermittent and uncertain behavior. Therefore, one dispatchable DG i.e. micro-turbine is considered along with WTs, SCs and OLTC to perform more effective ANM in this case. Table 5.1 shows that the presence of MT alleviates the voltage deviation since it vanishes the switching operations of SCs. However, mean PF shown in the table is observed to be less improved as compared to other cases since system PF is deteriorated slightly for very short time duration in light load hours as shown in Fig. 5.4(f) and 5.4(f). Due to less power transaction during the period it does not affect the operating cost. Table 5.2 shows that the online dispatch control of MT is providing more operational benefits as compared to local control as the support of MT will reduce the peak energy charges during peak load hours. Fig. 5.3(f) shows that the online ANM prepones the OLTC tap operation as compared to case–III in which MT was absent; however, it is unaltered in local ANM. This case concludes that the presence of dispatchable DGs along with high renewable penetration may generate more techno-economic benefits when controlled online.

Case–VI (OLTC, PVs, MT and SCs): Similar to previous case, one MT is considered along with OLTC, PVs and SCs to perform coordinated ANM. Table 5.1 shows that the centralized ANM provides more techno-economic benefits in less number of switching operations as compared to local one. The presence of MT slightly reduces the voltage variations as compared to similar Case–IV without MT, as it reduces the switching operations of available VRDs. Moreover, the presence of MT delays the OLTC tap switching operation as compared to similar Case–IV as observed from Fig. 5.3(e) and 5.3(g). Fig. 5.4(g) shows that PF of the system is slightly poor for both the approaches in initial years however; it improves along with the annual load growth as can be observed from 5.5(g).

Case–VII (OLTC, WTs, PVs, MT and SCs): In this case, ANM is performed by considering all DERs and OLTC simultaneously. Table 5.1 and 5.2 show that higher techno-economic benefits are achieved through online VVM as compared to local ANM. The involvement of multiple regulators in ANM schemes, the number of switching operations is found to be more for online approach as compared to other cases, which causes more voltage variations (i.e. high Std.) in the system. However, the Std. is still less as compared to local ANM. Fig. 5.3(h) shows that the node voltage profiles of system provided by both ANM schemes are identical for most of the time except in last few years of time horizon considered. The same is true for system PF as observed from Fig. 5.4(h) and 5.5(h). The case concludes that online control of multiple DRs increase the number of switching operations in the system but provides higher operational benefits as compared to their local control.

From above discussion, it has been observed that the proposed online ANM produces higher techno-economic benefits as compared to traditionally used set point based local ANM. The reason being is that the economic operation of PDNs is only possible when system is completely observable from control centers, so that the operators can take online corrective actions to maximize the operational benefits. The recent advances in communication and information technologies employed in power systems have brought the physical realization of such schemes close to reality. Despite of being costly, the presence of dispatchable MTs increases the operational benefits of microgrid. Moreover, it also alleviates some of the issues of renewable energy resources.

5.3 Optimal Accommodation and Operational Management of BESS with High Renewable Penetration

As per the standard offered programs, utilities have the right to curtail renewable power generation, if any operating constraint is violated [156]. Such preventive action taken by utilities may result into the revenue loss to the DG owner's revenue. Whereas, the alarming GHG emission forced power system planners to increase the renewable penetration in distribution systems. The conflicting aspects of high renewable penetration may create many operational challenges for utilities. Moreover, without utilizing the context of legacy distribution systems, it is quite difficult to accommodate high penetration of renewables to achieve foreseen objectives of smart distribution systems. Therefore, the renewable based DG integration problems need to be strategically addressed, modeled and solved precisely considering the traditional context of existing distribution systems.

In this section, a new bi-level optimization framework is developed for simultaneous optimal accommodation and management of high wind power generation and BESS in distribution networks. The goal is to determine the optimal sites and sizes of predefined number of WTs and BESS simultaneously. To achieve this, new objectives and constraints are introduced to alleviate the effect of intense variable power generation and load demand on system security, e.g., annual energy loss in feeders, reverse power flow into the grid, non-utilized BESS capacities, round-trip conversion losses of installed BESSs and voltage deviation of distribution systems etc. An AI-based optimal energy storage management model is developed for optimal operation of distribution system. To explore the non-tangible benefits of BESSs integration with high renewable penetration, the problem is developed in a deterministic framework for various scenarios. An improved variant of GA has been adopted from [196], as discussed in Section 3.5.2 to solve the problem due to it's ability of finding the global or near global optima.

5.3.1 Problem Formulation

During power delivery, power loss may be found at many stages, among these, maximum power losses may be found in distribution systems which are significantly high as compared to transmission networks. The quick growth of AC/DC conversion devices has introduced many conversion losses in the system which need to be minimized. Therefore, power loss minimization may be an objective of Distribution Network Operators (DNOs) to maximize

the annual revenue. Moreover, node voltage regulation is also an important objective, which needs to be achieved for improved node voltage profile at customer nodes.

The above discussed objectives can be optimized, if controllable energy sources/devices are present in the system; however, it may be difficult under high penetration of renewables. Moreover, the high renewable generation may cause reverse flow into the upstream grid during light load hours, which may create many protection issues. Therefore, reverse power flows should to be restricted and can be seen as one of the objectives. In order to minimize the different power losses, reverse power flow and node voltage deviation of the system under high wind power penetration, the simultaneous optimal accommodation of WTs and BESS is achieved in this part of work. It may be noted that the installation and running costs of BESS are very high with relatively lesser timespan. Therefore, an optimal BESS nodes and capacities needed to be identified such that the above discussed issues are minimized.

Objective Function

Considering the above facts, in this work, various annual energy loss and node voltage deviation of the system are minimized subjected to various DG, BESS and system constraints. For this purpose, following objective function is minimized using optimal accommodation and management of wind power generation and BESS simultaneously.

$$\min\ f = \phi\Big(1 + \sum_{h=1}^{24} \Delta V^h\Big)(1 + \Delta W_B) \times \sum_{h=1}^{24}(P^h_{Del.} + P^h_{Rev.} + P^h_{Conv.}) \tag{5.13}$$

where,

$$\Delta V^h = \begin{cases} |\underline{V} - V_i^h|, & \text{if } V_i^h < \underline{V} \\ 0, & \text{if } \underline{V} \le V_i^h \le \overline{V} \\ \text{a large number}, & \text{if } V_i^h > \overline{V} \end{cases} \tag{5.14}$$

$$\Delta W_B = \left| \sum_{h=1}^{24} P^h_{C_i} - \sum_{h=1}^{24} P^h_{D_i} \right| \qquad \forall\ i \tag{5.15}$$

$$P^h_{Del.} = \sum_{i=1}^{N}\sum_{j=1}^{N} \alpha^h_{ij}(P^h_i P^h_j + Q^h_i Q^h_j) + \beta^h_{ij}(Q^h_i P^h_j - P^h_i Q^h_j) \tag{5.16}$$

$$\alpha^h_{ij} = \frac{r_{ij} cos(\delta^h_i - \delta^h_j)}{V^h_i V^h_j} \quad \text{and} \quad \beta^h_{ij} = \frac{r_{ij} sin(\delta^h_i - \delta^h_j)}{V^h_i V^h_j} \tag{5.17}$$

$$P^h_{Rev.} = \begin{cases} 0, & \text{if } I^h_G \geq I_{\text{Spc.}} \\ Re(V^h_G I^{h*}_G), & \text{if } I^h_G < I_{\text{Spc.}} \end{cases} \tag{5.18}$$

$$P^h_{Conv.} = (1-\eta) P^h_{C/D_i} \quad \forall\ i \tag{5.19}$$

$$P^h_{C/D_i} = \begin{cases} 0, & \text{if } SOC^h_i = \overline{SOC} \text{ or } I^h_G \geq 0 \\ \overline{P_B}, & \text{if } SOC^h_i + \frac{\eta \overline{P_B}}{W^R_B} \leq \overline{SOC} \ \&\ I^h_G < 0 \\ (\overline{SOC} - SOC^h_i) W^R_B, & \text{if } I^h_G < 0 \ \& \\ & \overline{SOC} - SOC^h_i < \frac{\eta \overline{P_B}}{W^R_B} \\ 0, & \text{if } SOC^h_i \leq \underline{SOC} \text{ or } I^h_G \leq 0 \\ -\underline{P_B}, & \text{if } SOC^h_i - \frac{\eta \underline{P_B}}{W^R_B} \geq \underline{SOC} \ \&\ I^h_G > 0 \\ -(SOC^h_i - \underline{SOC}) W^R_B, & \text{if } I^h_G > 0 \ \& \\ & SOC^h_i - \underline{SOC} < \frac{\eta \underline{P_B}}{W^R_B} \end{cases} \tag{5.20}$$

Equations (5.14), (5.15), (5.16), (5.18) and (5.19) represents the node voltage deviation penalty function, under/over energy utilization penalty of BESS, feeders power loss, amount of reverse power flow into the grid and conversion losses of BESS respectively. Where, V^h_i & δ^h_i, P^h_i & Q^h_i, SOC^h_i and P^h_{C/D_i} are denoting voltage magnitude & angle, real & reactive power injection, SOC status of BESS and charging/discharging dispatch of BESS at ith node in hth hour respectively; V^h_G & I^h_G are the voltage and current magnitude in secondary winding of grid substation transformer respectively. r_{ij} is the resistance of branch connecting node i and j. Further, η, ϕ, N, $I_{Spc.}$, $\underline{V}$ & $\overline{V}$, $\underline{SOC}$ & $\overline{SOC}$, $\underline{P_B}$ & $\overline{P_B}$ and W^R_B are representing, charging/discharging efficiency of BESS, daily to annual conversion factor, total number of nodes in the system, specified reverse current limit into the grid, minimum & maximum allowable node voltage limits, minimum & maximum specified SOC limits of BESS, minimum & maximum allowable charging/discharging power limits of BESS and rated energy storage capacity of BESS respectively.

Constraints

The objective function expressed in (5.13) is subjected to the following constraints.

Generation Limit Constraints:

$$0 \leq P_{DG_i} \leq \overline{P_{DG}} \quad \forall\ i \tag{5.21}$$

BESS Limit Constraints

$$0 \leq W_{B_i} \leq \overline{W_B} \quad \forall\ i \tag{5.22}$$

BESS Charging/Discharging limit Constraints

$$\underline{P_B} \leq P^h_{C/D_i} \leq \overline{P_B} \quad \forall\ i,h \tag{5.23}$$

SOC Limit Constraints of BESS

$$\underline{SOC} \leq SOC^h_i \leq \overline{SOC} \quad \forall\ i,h \tag{5.24}$$

Feeders Thermal Limit Constraint:

$$I^h_{ij} \leq \overline{I_{ij}} \ \ \forall \ \ i,j,h \tag{5.25}$$

Real and Reactive Nodal Power Balance Constraints:

$$P^h_i = V^h_i \sum_{j=1}^{N} V^h_j Y_{ij} cos(\theta_{ij} + \delta^h_j - \delta^h_i) \quad \forall\ i \tag{5.26}$$

$$Q^h_i = -V^h_i \sum_{j=1}^{N} V^h_j Y_{ij} sin(\theta_{ij} + \delta^h_j - \delta^h_i) \ \ \forall\ i \tag{5.27}$$

SOC Balance Constraint

$$SOC^h_i = SOC^{h-1}_i + \frac{\eta P^h_{C/D_i}}{W^R_B} \quad \forall\ i,h \tag{5.28}$$

where, P_i, Q_i, P_{DG_i}, W_{B_i}, $\overline{P_{DG}}$ and $\overline{W_B}$ are representing real power injection, reactive power injection, real power generation of DG, energy dispatch of BESS, maximum power and energy generation limit of DG and BESS respectively at bus i. Similarly, θ_{ij}, Y_{ij}, I^h_{ij} and $\overline{I_{ij}}$ are representing impedance angle, element of Y-bus matrix, flow of current in hth hour and maximum thermal limit of line respectively connected between bus i and bus j.

5.3.2 Proposed Bi-level Optimization

In this section, the proposed strategies and algorithm have been discussed and explained for optimal accommodation and management of high wind power generation in distribution systems. In order to solve the proposed mixed-integer, non-linear and non-convex optimization problem formulated in previous section, an improved variant of GA suggested in Section 3.5.2 is adopted. In this work, two GAs are used to solve the optimal accommodation and management problems simultaneously: 1) simultaneous optimal accommodation of WTs and BESSs, which will act as the main optimization method; 2) optimal management of BESS, which is used as the subroutine technique to determine hourly optimal scheduling of BESS based on available SOCs and update its SOC status. The chromosome structure used in main GA is shown in Fig. 5.7

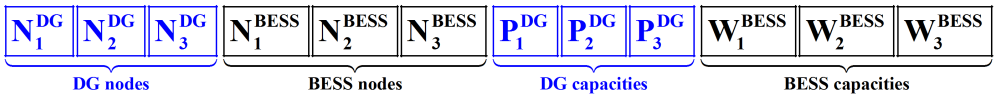

FIGURE 5.7: The chromosome structure of used in GA-1

The chromosome structure for GA-2 will contain the BESS capacities only as the decision variables. The flow chart of basic steps of proposed optimal accommodation and management strategies for WTs and BESS are shown in Fig. 5.7.

5.3.3 Simulation Results

In order to validate the proposed simultaneous optimal accommodation of WTs and BESS, it is implemented on standard 33-bus test distribution system given in Appendix A. Following test cases are investigated to show it's effectiveness: I) Base case II) optimal accommodation of WTs only, III) simultaneous optimal accommodation of WTs & BESSs. Further, the simulation parameters used in the study are summarized in Table B.3 of Appendix B.

The simulation results obtained using proposed approach are presented in Table 5.3 for all investigated cases. The table contains optimal nodes and sizes of DGs/BESSs along with respective annual energy loss and DG penetration. The DG penetration is calculated as the fraction of system's peak demand which is assumed to be 1.6 times of nominal demand of the system. The table shows that case-III provides highest annual energy loss

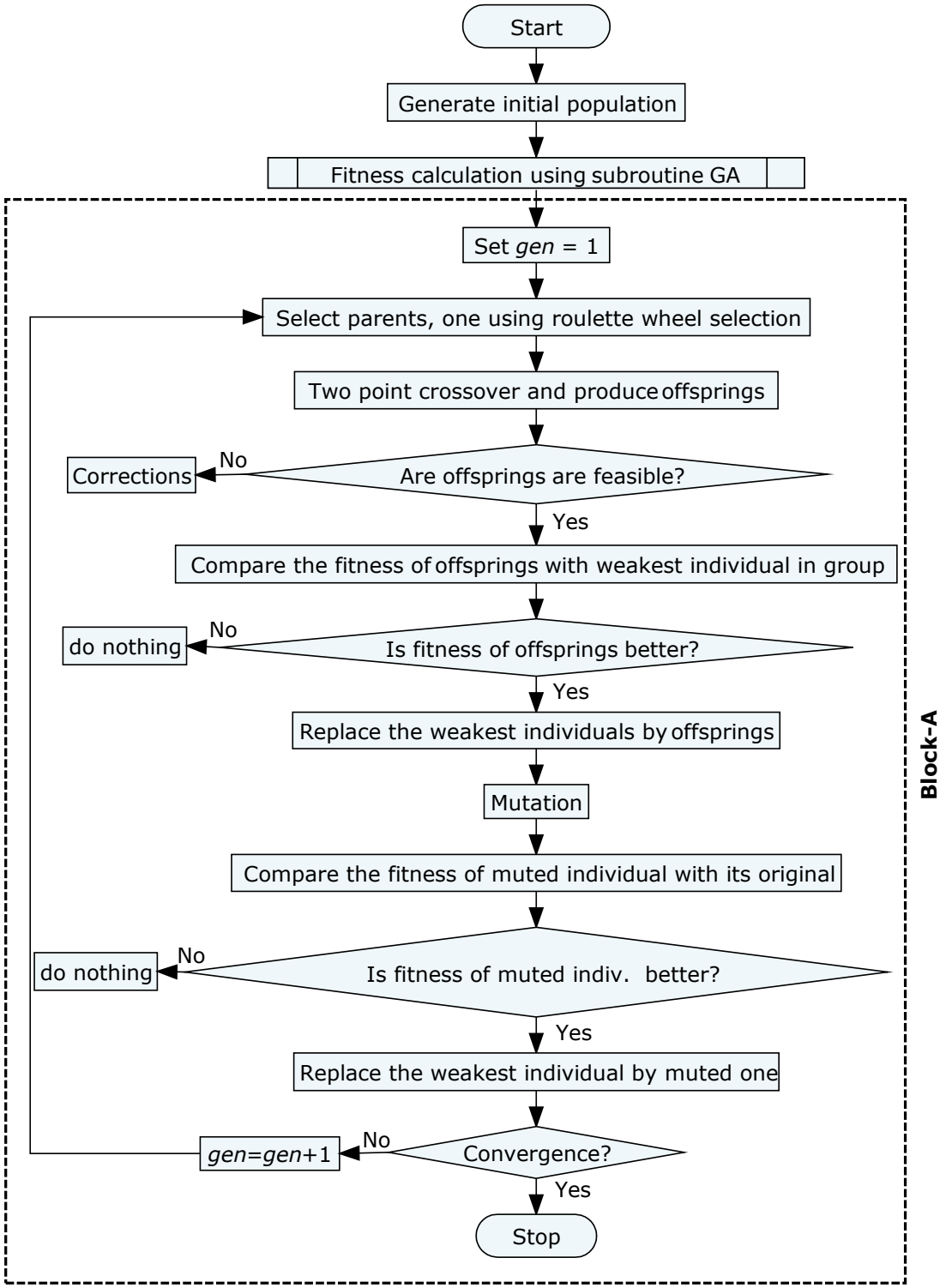

(a) Genetic Algorithm-1 for optimal accommodation

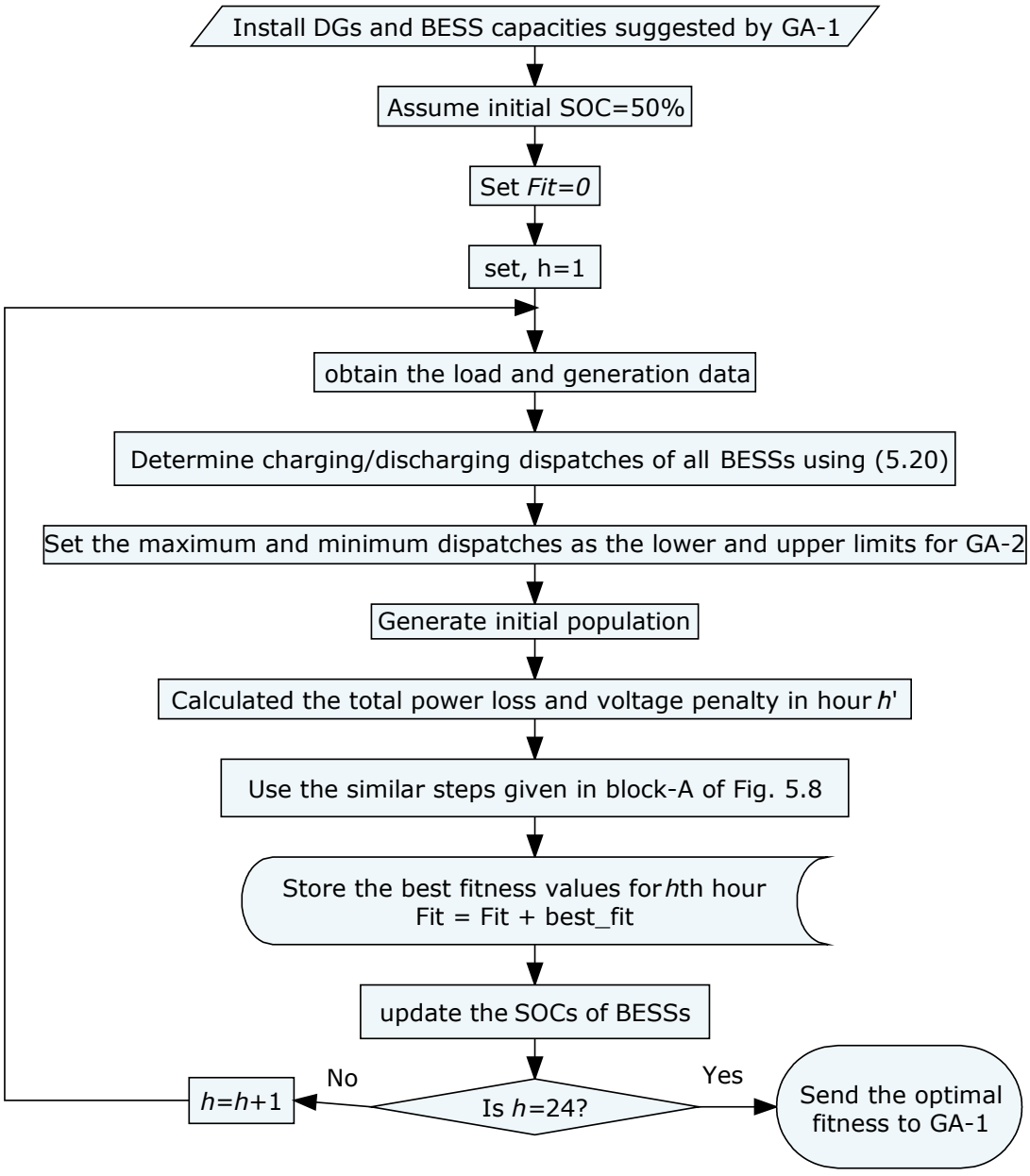

(b) Genetic Algorithm-2 for optimal management

FIGURE 5.7: Flow charts of proposed optimal accommodation and management of high renewable generation with BESS

reduction as compared to case-II, even at high DG penetration while maintaining the system, generation and BESS security constraints. The loss shown in case-III has already included the round-trip conversion loss of BESSs but still, the power losses are found to be 476.74 MWh lesser than the case-II. The simulation results of case-III show that BESS is installed at DG node or near to that node. It may be installed to minimize the electrical

TABLE 5.3: Simulation Results Obtained by Proposed Approach

Case(s)	Optimal nodes (Sizes in kW) of WTs	Optimal nodes (Sizes in kWh) of BESSs	DG penetration (%)	Annual energy loss (MWh)	Annual energy loss reduction (%)
Base case	–	–	00.00	3493.27	00.00
optimal accommodation of WTs only	14(939) 17(909) 32(1651)	–	58.87	1887.54	45.97
simultaneous optimal accommodation of WTs & BESSs	11(1539) 16(719) 30(1941)	10(4494) 16(2743) 30(4411)	70.64	1410.80	59.61

distance between DGs and BESSs so that the energy transaction losses are minimum in charging/discharging cycles.

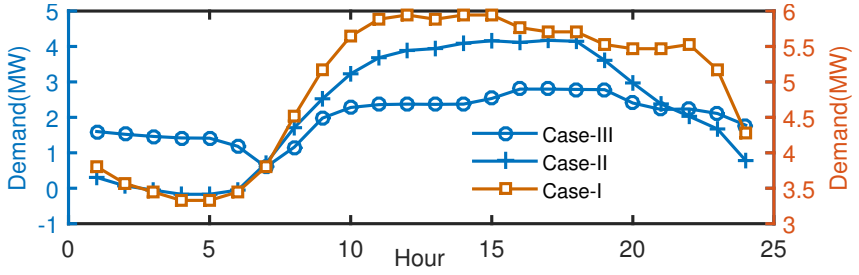

FIGURE 5.8: System demand for all investigated cases

In Fig. 5.8, the hourly system demands are compared for all cases, which shows that BESS shifts the peak demand and reduced the variations in power imported from main grid even at higher DG penetration. The daily hourly power loss observed in all cases are shown in Fig. 5.9. The node voltage profiles for all cases are shown in Fig. 5.10, which ensures that node voltages are significantly improved in case-II & III and no node voltage violation is observed. Similarly, Fig. 5.11 shows the SOC status for all BESSs to minimize the hourly power loss and variability effect of WTs. It may be observed that the installed BESSs are fully utilized because SOCs of all BESS are daily varying from '0' to '1'. It also indicates that minimum required amount of energy storage has been installed which is necessary manage the system operations under high renewable penetration. It shows that all BESSs are charged during night hours (i.e. 21:00 to 7:00) when load demand is low and wind power generation is high.

The proposed bi-level optimization model successfully manages the high wind power generation without violating the system security constraints. New objectives and security

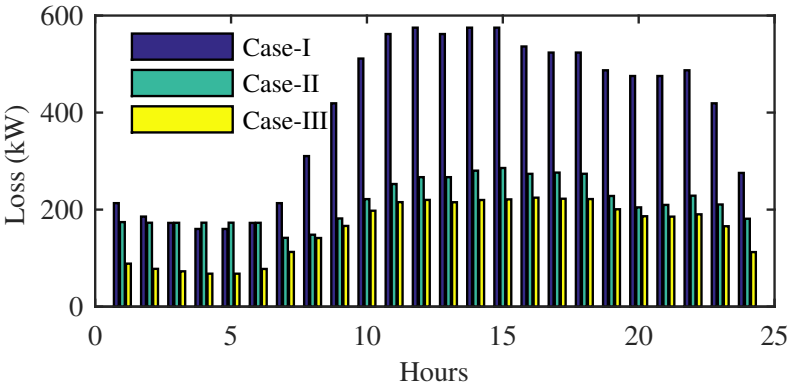

FIGURE 5.9: Daily hourly power loss of the system for all investigated cases

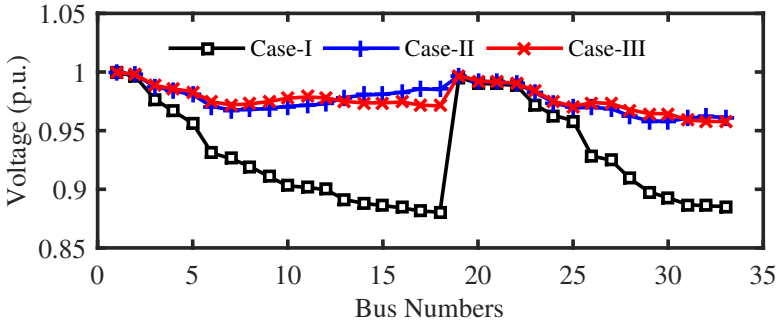

FIGURE 5.10: Mean node voltage profiles of the system for all cases

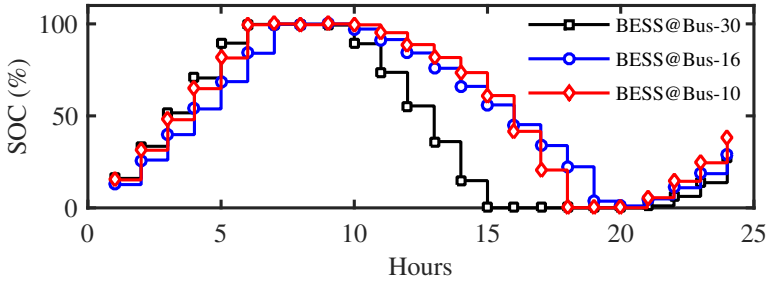

FIGURE 5.11: SOC status of all BESSs

constraints introduced are minimizing the annual energy loss in feeders, reverse power flow into the grid, non-utilized BESS capacities, round-trip conversion losses of BESSs and voltage deviation effectively. The proposed strategies are able to mitigate the reverse power flow problems caused by high wind power generation. It has been observed that proposed approach shifts the system's peak demand and reducing the variability in power imported from main grid. Moreover, the optimal utilization of installed BESS has been ensured to optimize the necessary initial investment cost.

5.4 Operational Management of EVs in Smart City Environment

The growing urbanization, global energy crisis, greenhouse gases emission, depleting conventional resources etc. has led to the vision of smart city deployment. Currently, cities are the major energy consumers and greenhouse gas emitters, which significantly affects the climate and energy security [216]. The key motivation behind smart city deployment may be the optimal utilization of available resources, which are necessary for survival of the society. However, the definition of smart cities is not yet standardized due to the broad vision of smart city deployments [217]. The common scope of smart city deployment may be to increase the living standard of inhabitants by facilitating with basic needs such as electricity, water, gas, transportation, information & communication, traffic & pollution control, basic medical services, etc. Among these, the smart electricity infrastructure planning and management may play a vital role in smart city deployment, which may include the optimal management of EVs i.e. a type of DR and its charging infrastructure, as it provide a wide range of benefits for utility and consumer.

Nowadays, the conventional transportation sector is moving towards a smart and sustainable sector due to limiting conventional energy sources. Recently, a study reports that almost 27% of total energy consumption and 33% of greenhouse gas emissions across the globe are related to transportation sector [218]. The emerging EVs can be called as 'green technology' since it may alleviate energy security and environment related issues while charging from renewables. The future rapid growth of EVs may raise many challenges and issues for future distribution system operators as it will introduce more uncertainties in the system. In order to alleviate some of the issues, artificial intelligence, optimization models and strategies may play a vital role in the future mobile power infrastructure planning and management. In following section, an artificial intelligence and IoT based EV charging infrastructure is proposed for smart city applications.

5.4.1 Proposed Mobile Power Infrastructure Model for Smart City Applications

In this section, a set of strategies and algorithms are proposed for future mobile power, i.e. EV, infrastructure planning and operational management in the context of growing smart cities. The efforts have been made to develop a resilient EV infrastructure for smart city applications. The goal of this work is to maximize the profit of utility and EV owners

participating in real-time smart city energy market subjected to numerous techno-economic constraints of EVs and power distribution systems. For effective real-time applications, the knowledge of AI and IoTs have been used. A prototype of proposed mobile power infrastructure planning and management model based on artificial intelligence and IoTs is shown in Fig. 5.12.

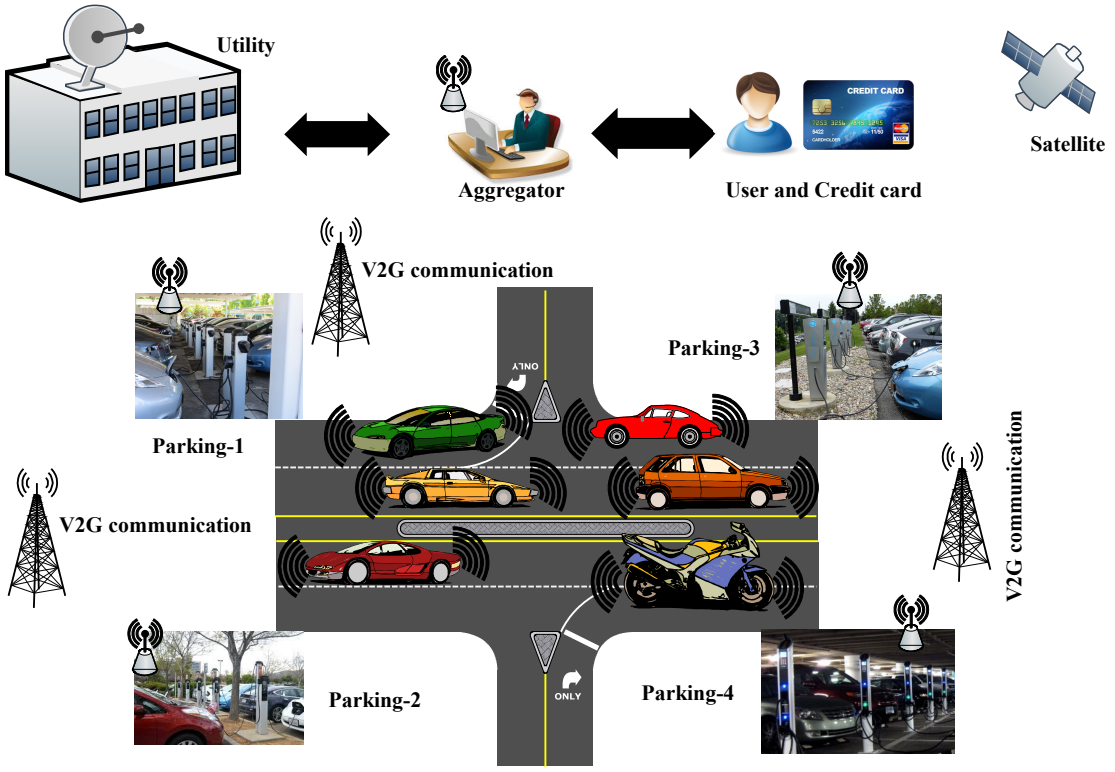

FIGURE 5.12: Basic structure of proposed mobile power infrastructure planning and operational management in smart cities

It may be observed that majority of professionals or car owners are found to be in commercial and industrial areas in daytime. Furthermore, it can be analyzed that many vehicles are generally found to be in the parking lots of restaurants, hotels, bars, discos and shopping complexes in evening hours and weekends. Following this information, it will be advantageous to deploy charging stations in such parking lots to provide the flexibility to EVs and distribution utilities. Such EV charging points can help the distribution system operators to shave the peak load demand as most of the countries are having their peak load demand in these hours.

In proposed work, each EV is assumed to be associated with unique smart ID and IoT chip with the information and communication modules, which could be linked to public

or private networks in smart cities. The smart ID will also link to the credit card of respective EV owner for immediate daily transactions. It is also suggested that each EV should be associated with an aggregator to efficaciously manage the SOC level and energy transactions between EV and distribution grids. The EV chargers available in car parking are assumed to have power line/wireless communication link to communicate with aggregator/utility servers. According to the proposed model, each EV will contain the information of distance traveled, SOC, the mean price of energy stored in EV, associated IoT infrastructure etc. It has also been assumed that each EV will be connected to the chargers in parking lots, but charging/discharging will depend on the decision algorithms of associated aggregator. According to the proposed model, aggregators will continuously receive/monitors the utility energy price and SOC levels of EVs associated with them. It is suggested that the aggregator will send the charging signal to the EVs which are having low SOC levels or below the threshold value. On other hand, it sends a discharging signal to the EVs which have high SOC levels during high utility energy prices.

5.4.2 Objective Function

Here, the problem is formulated as a multiple objectives comprising of utility and consumer objectives simultaneously. The utility objective includes the cost of instantaneous power loss minimization i.e. $f_u(t)$, whereas the objective of EV owner is to minimize the instantaneous cost of total energy stored in BESS of EV i.e. $f_c(t)$ subjected to various system and storage operating constraints Therefore, the aim of an aggregator is to maximize the real-time profit of distribution utility and EV owners. The objective function of aggregator combining the objectives of power distribution utility and EV owner can be expressed as

$$\min\ F(t) = k_1 f_u(t) + k_2 f_c(t) \tag{5.29}$$

where

$$f_u(t) = K_e(t) \sum_{i=1}^{N} \sum_{j=1}^{N} \alpha_{ij}(t)[P_i(t)P_j(t)+Q_i(t)Q_j(t)] + \beta_{ij}(t)[Q_i(t)P_j(t)-P_i(t)Q_j(t)] \tag{5.30}$$

$$f_c(t) = W_{EV}^{Stored}(t) K_e^{Avg.} \pm P^{EV}(t) K_e(t) \tag{5.31}$$

$$\alpha_{ij}(t) = \frac{r_{ij}}{V_i(t)V_j(t)} \cos(\delta_i(t) - \delta_j(t)) \tag{5.32}$$

$$\beta_{ij}(t) = \frac{r_{ij}}{V_i(t)V_j(t)} \sin(\delta_i(t) - \delta_j(t)) \tag{5.33}$$

The objective function expressed in (5.29) is subject to the following constraints

$$P_i(t) = V_i(t) \sum_{j=1}^{N} V_j(t) Y_{ij} \cos(\theta_{ij} + \delta_j(t) - \delta_i(t)) \quad \forall\ i, t \tag{5.34}$$

$$Q_i(t) = -V_i(t) \sum_{j=1}^{N} V_j(t) Y_{ij} \sin(\theta_{ij} + \delta_j(t) - \delta_i(t)) \quad \forall\ i, t \tag{5.35}$$

$$V_{Min} \leq V_i(t) \leq V_{Max} \quad \forall\ i, t \tag{5.36}$$

$$I_{ij}(t) \leq I_{ij}^{\max} \quad \forall \quad i, j, t \tag{5.37}$$

$$P_{k,Min}^{EV} \leq P_k^{EV}(t) \leq P_{k,Max}^{EV} \quad \forall \quad k, t \tag{5.38}$$

Equations (5.34)–(5.38) are the constraints of nodal active power balance, nodal reactive power balance, node voltage limits, feeder current limit and charging/discharging power limits respectively. Where, k_1 and k_2 are the weighing coefficients; $P_i(t)$, $Q_i(t)$, $V_i(t)$, $\delta_i(t)$ are representing the instantaneous real & reactive power injection, voltage magnitude and angle respectively at bus i. Similarly, r_{ij}, x_{ij}, θ_{ij}, $I_{ij}(t)$, I_{ij}^{Max} are denoting the resistance, reactance, impedance angle, flow of current, maximum thermal limit of line respectively connected between bus i and bus j. $W_{EV}^{Stored}(t)$, $K_e^{Avg.}(t)$ and $K_e(t)$ are the instantaneous energy stored in EV, average energy price of stored energy in the EV, charging or discharging power of EV and grid energy price respectively. N, N_b, V_{Min}, V_{Max}, $P_{k,Min}^{EV}$ and $P_{k,Max}^{EV}$ are the total number of buses, number of branches, minimum and maximum allowable voltage limits of the system nodes respectively, minimum and maximum allowable charging/discharging limits of the EV respectively.

5.4.3 AI-based Mobile Power Infrastructure Planning and Operational Management

The proposed mobile power infrastructure planning and operational management problems for smart city applications are solved in two stages. In stage-I, the electrically optimal allocation of EV charging enabled parking lots are determined. Whereas, the optimal operational management of EVs charging are performed in stage-II. The GA, proposed in Section 3.5.2 has been adopted to solve the proposed optimization framework. The chromosome structure of GA used in the study comprises of the system nodes and maximum charging capacities of respective parking lots as decision variables is shown in Fig. 5.13.

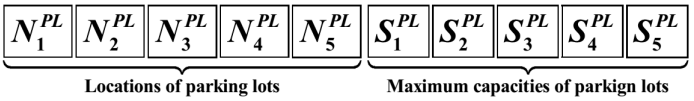

FIGURE 5.13: Chromosome structure of GA for optimal allocation of EV parking lots

In stage-I, the optimal allocation of CSs are obtained such a way that the daily energy loss is minimized for the installed capacity. In this stage, it has been assumed that the EVs will charge if the instantaneous energy price is detected to be less than the average daily energy price otherwise EVs will discharge. Therefore, the EVs will export power to the grid in peak hours and vice-versa.

In stage-II, optimal operational management of EVs is performed in which instantaneous optimal charging/discharging of each EV is determine to minimize the instantaneous profit of EV owner and utility both. The flowchart of adopted GA and the algorithm introduced for stage-II are shown in Fig. 5.14(a) and 5.14(b) respectively; where, t and 0.01η are the time and instantaneous converter power loss factor associated with BESS of each EV respectively. In stage-II, the optimal dispatches of EVs are also determined using the GA. The chromosome structure used in this GA will be the second half section of the chromosome shown in 5.13.

5.4.4 Simulation Results

In order to demonstrate the applicability and effectiveness of proposed model for optimal planning and operational management of mobile power infrastructure in smart cities, a standard 33-bus radial distribution network given in Table A.1 is adopted as a smart city power network. Initial, CSs have been allocated to perform the optimal operational management of EVs. In stage-I, optimal location and maximum allowable charging capacities of five parking lots are identified. The minimum and maximum charging capacity limits of each CS is assumed to be 100 kW and 1000 kW respectively.

For electrically optimal allocation of CSs, the EV is considered to be discharging the energy during peak demand and charging during light load hours. Therefore, in planning stage, the EV will assumed to be charged if grid energy price is found to be less than the mean energy price of 24 hours and vice-versa. This is the commonly used strategy for EV charging/discharging management i.e. called as no strategy case in the work. The motivation behind the optimal accommodation of CSs is to minimize the cost of energy loss under the penetration of EVs in distribution system. The GA is applied to obtain the optimal sites and sizes of CSs. The simulation results are presented in Table 5.4, which

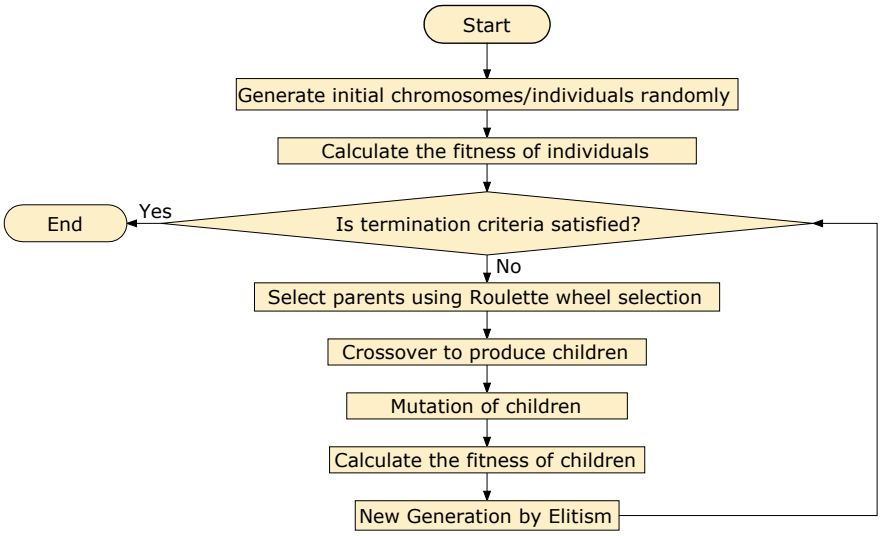

(a) adopted GA

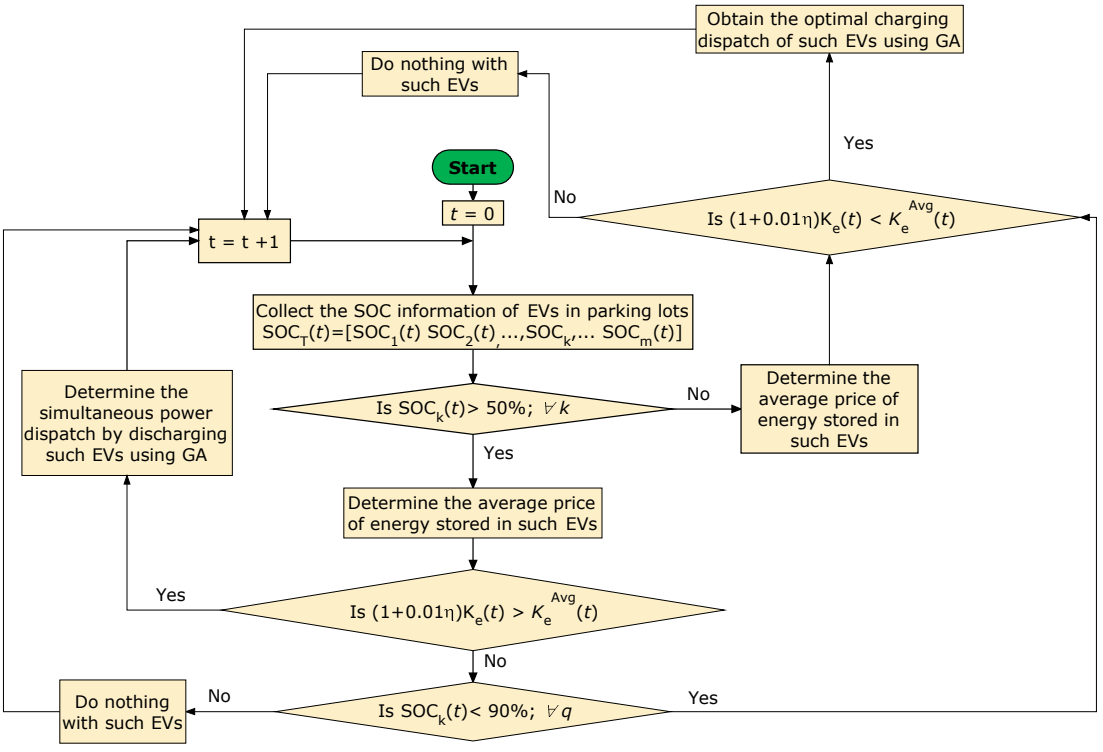

(b) proposed operational management of EVs

FIGURE 5.14: Flow chart of proposed AI and IoT based operational management of EVs

shows that the proposed strategy provides reduced cost of energy loss as compared to the base case while generating the profit to EV owners.

TABLE 5.4: Optimal Sites and Charging Capacities (Peak) of Charging Stations

Cases	Optimal node (Sizes in kW)	Cost of energy loss (USD)
Base case	-	212.206
After allocation of EV CSs	6(413), 14(214), 24(234), 25(196), 31(266)	170.842

The optimal allocation of CSs are determined such that the cost of daily energy loss is minimized. Now, the optimal operational management of EVs in a smart city is performed. Without loss of generality and simplicity of the model, 550 EVs of Nissan leaf are considered as given in [219]. Each EV has a storage capacity of 24 kWh and can travel up to 160 km, if fully charged. Moreover, equal numbers of vehicles are parked in above obtained five parking lots. It is assumed that maximum EVs will remain in any of the parking lots for small geographical towns such as in offices, shopping complexes, restaurants, institutions, residential complexes etc. Therefore, the model shown in Fig. 5.14 is applied for 24 hours by randomly generating the initial SOC of EVs between 40 to 100% with K_e^{Avg} =0.050 \$/kWh.

The simulation results of proposed optimal EVs power management are summarized in Table 5.5. The table shows that proposed approach further reduces the system energy loss. It may be observed that the EV owner benefits are more for conventional approach in which EVs are charged during light load hours and discharged in peak load hours. However, conventional approach increases the variation in the demand as shown in Fig. 5.15(a). Whereas, proposed approach smoothly shifts the peak-demand. Moreover, the minimum node voltage appeared in 24 hours using conventional and proposed approaches are found to be 0.8948 and 0.9345 p. u. respectively. Fig. 5.15(b) shows the charging/discharging powers of five CS which shows that all the CSs are competitively participating in real-time operational management of EVs available in SC.

In proposed approach, daily maximum amount added or deducted to an individual's credit card are found to be 2.4883 and 0.1398 USD respectively which shows that proposed strategy is generating benefits for EV owners. In this case study, 308 vehicles are participated in energy management out of 550 vehicles while the SOC of 242 vehicles remain unaltered due to constraints or not found to be optimal for the scheme. Moreover, the average price of energy stored in the EVs is reduced to 43USD/kWh from 50 USD/kWh.

TABLE 5.5: Optimal Dispatch of EV Parking Lots

Cases	Profit of parking lots location (profit in USD)	Cost of energy loss (USD)	Total profit to EV owners (USD)
Conventional strategy	-	170.842	1042.524
Proposed strategy	25(173.992), 6(177.016), 14(175.524), 31(184.332), 24(158.226)	158.842	0869.090

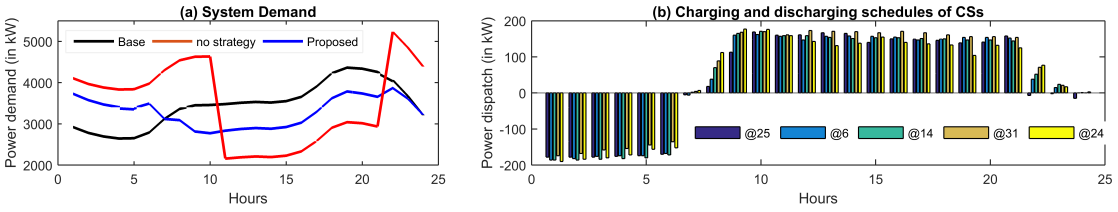

FIGURE 5.15: Hourly system power demand and power dispatch of parking lot with CSs

5.5 Summary

In this chapter, various ANM schemes have been investigated considering diversified DR technologies. An effective online ANM scheme is presented to minimize the hourly operating cost of microgrids, over the lifetime of VRDs, in minimum number of switching operations. To achieve this, a new DSSE algorithm is proposed for online monitoring of the system in minimum number of measurements, which is based on RWS approach employing probabilistic modeling of renewables and load demand. The proposed DSSE has found to be reasonably accurate to perform the ANM of microgrids. The proposed online ANM employing the DSSE is also found to be inspiring when simulation results are compared with that of the same obtained by traditionally used local ANM scheme. Moreover, the proposed energy pricing based VVM of microgrids introduced in 4 provides simultaneous VVM in microgrids and upstream power networks by rewarding the favoring networks and vice versa. The multiple case studies considered are exploring the techno-economic attributes of different DERs.

A bi-level optimization framework is developed for optimal accommodation and operational management of BESS and WTs simultaneously considering various system constraints. In order to alleviate some of impacts of intense wind power penetration, new objectives and system security constraints are introduced. The proposed strategies have mitigated the reverse power flow problem effectively, caused by high wind power penetration in distribution systems. It has been observed that proposed approach shifts the system peak demand and the variability of power imported from main grid is alleviated.

Moreover, the optimal utilization of installed BESS has been ensured to optimize the necessary initial investment cost.

The chapter also presents an effective model of future mobile power infrastructure planning and operational management for smart city applications. To achieve this, various schemes and AI-based algorithms have been developed by using the knowledge of IoTs. The proposed aggregator based model effectively minimizes the system energy losses while simultaneously maximizing the profit of EV owners in real-time. Further, the daily profit of each EV owner has been credited to their credit cards. It also reduces the variation in hourly load demand of the system. The simulation results of proposed model are found to be encouraging when compared with that of the same obtained by conventional scheme. In this chapter, all the proposed frameworks are implemented and investigated on a standard 33-bus test distribution system.

Chapter 6

Conclusions and Future Scope

The chapter is summarizing the findings of this thesis. In the proposed research work, some investigations are carried out to optimize the planning and operational variables of distribution system resources, considering some present trends and realistic scenarios. The investigations reveal some techno-economic and social aspects of optimal DR planning and operational management. In planning stage, various optimization frameworks have been developed to optimally integrate the diversified DR technologies such that the NPV or benefits of DNO, consumer and DR owner are maximized and system performance is improved while maintaining various constraints of the problem. The conclusions and future research scope of the proposed work are addressed in following sections.

6.1 Conclusions

Generally, DR number, type, site, size etc. are the variables, which have to be optimized while planning the DRs in distribution systems. Considering these variables and problem constraints, the DR planning problem turns out to be a complex, mixed-integer, non-linear and non-convex optimization problem; therefore, requires some powerful optimization methods to determine the optimal solution. In this thesis, two optimization methods namely, Taguchi and GA are adopted alternatively to solve the DR planning and operation problems of distribution systems. Further, some improvements are also suggested in these algorithms to overcome few limitations of these methods. In order to provide an engineering input to these techniques, two NPLs are also suggested i.e. static and dynamic NPLs. The NPLs help the optimization methods to search the optimal nodes in lesser time.

In order to validate the suggested improvements, the performance of these methods have been compared with their standard variants and found that the proposed methods are providing promising results. Further, to validate the effectiveness of proposed methods over some existing powerful methods, the simulation results obtained are compared with the same available in existing literature. The comparison shows that the proposed approaches are very effective to solve the DG integration problems.

The suggested modifications in basic TM have significantly improved the performance of TM as compared to its standard variant and another version available in the literature. In order to demonstrate the ability of proposed approach over AI-techniques, it is also compared with an improved variant of GA. The comparison shows that the proposed method provides better solution in very less number of experiments/iterations, as compared to an improved GA. The proposed SNPL has overcome some of the limitations of existing NPLs, as discussed in Section 3.4.1 and helps the TM to select optimal nodes in lesser time.

The proposed new DNPLs, discussed in Section 3.5.1, are providing an efficacious measure to select multiple nodes simultaneously for DR allocation. It also provides the information about DR sizes compatible to the nodes, unlike in SNPLs. In this thesis, the proposed DNPLs are integrated with GA as a genetic information carrier, which stores the tendencies of nodes towards objective function and DR sizes. The simulation results obtained by DNPL-GA are found to be promising when compared with the same available in the literature.

Due to the growing penetration of DRs, the system operators may encounter many operational issues and challenges such as reverse power flow, coordination, over-voltages etc. In order to alleviate some of the operational issues and to maximize the operational benefits of installed DRs, some ANM schemes are also proposed in the thesis. An online ANM scheme, aiming to minimize the hourly operating cost of the microgrids over considered time horizon, is proposed. For the purpose, a DSSE based online monitoring and control scheme has been suggested employing an RWS criteria to generate feasible pseudo measurements due to the inadequacies of measurement units in distribution systems. The scheme is found to be very effective when simulation results obtained are compared with that of the same obtained by a traditionally used offline scheme. The pricing based VVM has improved the system performance significantly.

The bi-level optimization framework developed for optimal accommodation and operational management of BESS has performed well to reduced the impact of intense renewable penetration in distribution systems. The proposed optimization model effectively

manages the optimal operation of deployed BESS such that the techno-economic benefits would be maximum. Moreover, the optimization model proposed for optimal operational management of EVs in smart city context is found to be very encouraging when compared with a case without strategy. The proposed approach may found to be very useful as the penetration of EVs is expected to increase in near future. In order to manage the millions of EVs, proposed aggregator and IoT based strategy will play a vital role.

The point-wise summary of conclusions drawn from the proposed work are presented below.

1. The individual modeling and control schemes of each DR technology adopted in planning and operational management are presented.
2. Basic TM is introduced to solve the optimal DR allocation problems of distribution systems, which shows some promising attributes.
3. Further, improvements are also suggested to overcome some of the limitations of standard TM. The performance of this method is compared with that of basic TM to demonstrate the effectiveness of suggested improvements. The simulation results are also compared with that of improved GA to show the effectiveness of proposed method over meta-heuristic methods. The comparison reveals that the proposed TM is very effective to solve the DR integration problems of distribution systems.
4. A new SNPL is proposed to overcome some of the limitations of existing node priority lists [10, 94, 113]. The proposed SNPL is used to select the promising nodes as Taguchi factors in design of experiments, the SNPL further reduces the computational time of TM.
5. A multiobjective Taguchi method is also introduced to solve the multiobjective DR integration problems of distribution systems. The method combines Taguchi and TOPSIS approaches, which provides most compromising solution of optimal DR integration as compared to the methods available in existing literature.
6. An improved variant of GA is proposed to solve the DG integration problem of distribution systems. A dynamic NPL is proposed, which is dynamically updated in each generation and used as genetic information carrier to improve the performance of GA.
7. A new optimization framework of optimal DR integration is developed under the voltage regulated environment of existing VRDs i.e. OLTCs. The proposed improved variant of GA is used to solve the problem. The simulation results show that the proposed framework provides more benefits at lesser DER penetration as compared to the conventional DER planning models available in the literature.

8. A multi-year optimization framework is developed for optimal planning of multiple DRs in uncertain environment. Besides, a pricing based VVM scheme is also proposed to perform the simultaneous VVM in microgrids and upstream connected grid.

9. A multi-year optimization model is proposed for ANM of microgrids throughout the considered time span with the inclusion of multiple DRs. A centralized online ANM scheme is proposed and simulation results are compared with that of offline ANM scheme to demonstrate the abilities of proposed scheme. The comparison shows that the online ANM provides more techno-economic benefits while improving the system performance.

10. An RWS based DSSE is found to be very effective to perform the online ANM of distribution networks.

11. A bi-level optimization model proposed for optimal accommodation and management of BESS to alleviate the impact of intense renewables is found to be very effective while satisfying various system security constraints.

12. Finally, a smart EV infrastructure planning and network management is proposed for smart city applications. The artificial intelligence based approach is adopted and the knowledge of Internet of things is utilized to find the optimal scheduling of EV charging/discharging in real-time. The proposed scheme is generating more techno-economic benefits for aggregator, DNOs and EV owners.

13. Collectively, various optimization frameworks have been developed for active distribution system planning and operational management under some realistic scenarios.

14. New objective functions and constraints of DR integration have been identified and modeled to maximize the benefits of optimal DR allocation.

15. Diversified DR technologies have been investigated to reveal their pros and cons.

6.2 Future Scope

In present work, the optimal solution for planning and operational management problems of dispatchable and non-dispatchable DRs are obtained for distribution systems. In this thesis, the multiobjective DG integration problem has been investigated for dispatchable DGs thereby may be extended the work for renewables also. Further, the coordinated

planning of dispatchable DERs have been achieved considering the effect of existing OLTC-based VR schemes. The problem may be re-investigated considering the renewable based DGs also.

The ANM of systems are playing an important role to perform the daily techno-economic operations. In proposed ANM, the optimal operations have been investigated for different cases of grid connected microgrids. In future, the growing penetration of microgrids may require islanded operations to improve the reliability of distribution systems; therefore, the ANM of islanded microgrid may also be performed. The proposed bi-level optimization framework for operational management of BESS may be extended for microgrid islanded operations while considering/ignoring the load shedding in the system. In order to reduce the computational burden of bi-level algorithm, a faster optimization techniques such as analytical/Taguchi method may be used in the inner-layer.

An optimization framework can be developed to study and optimize the benefits high penetrations of BESS in the integrated transmission & distribution (T&D) systems. A coupled T&D systems analysis framework can be developed through a co-optimization approach. The following objective functions can be considered in the proposed optimization approach: 1) Real power losses (PL); 2) Voltage deviation (VD) at load buses; and 3) loading margin (LM) or loadability of the system. The framework can be utilized to investigate the impacts of high penetrations of DERs with embedded BESS. Simulations can be performed with 50 and 100% of BESS charging capacity. The proposed framework can be examined on the IEEE 118-bus system.

An optimization framework may be developed as a decision-support tool that residential consumers can utilize to optimize their acquisition of electrical energy services. The decision support tool optimizes energy services provision by enabling end users to first assign values to desired energy services, and then scheduling their available DERs to maximize net benefits. PSO can be used to solve the corresponding optimization problem because of its straight-forward implementation and demonstrated ability to generate near-optimal schedules within manageable computation times. Some improvements can be suggested to improve the basic formulation of cooperative PSO by introducing stochastic repulsion among the particles. The improved DER schedules can then be used to investigate the potential consumer value added by coordinated DER scheduling. This can be computed by comparing the end-user costs obtained with the enhanced algorithm simultaneously scheduling all DER, against the costs when each DER schedule can be solved separately. This comparison enables the end users to determine whether their mix of energy service needs, available DER and electricity tariff arrangements might warrant solving the more

complex coordinated scheduling problem, or instead, decomposing the problem into multiple simpler optimizations.

The rapid growth of the demand for computational power by scientific, business and web applications has led to the creation of large-scale data centers consuming enormous amounts of electrical power. Therefore, an energy efficient resource management system can be proposed for virtualized cloud data centers to reduce operational costs and provide required Quality of Services (QoSs). Energy savings can be achieved by continuous consolidation of VMs according to current utilization of resources, virtual network topologies established between VMs and thermal state of computing nodes. He can present results of simulation driven evaluation of heuristics for dynamic reallocation of VMs using live migration according to current requirements for CPU performance.

The proposed mobile power infrastructure planning and operational management may be extended considering the mathematical modeling of information and communication technologies. The optimal allocation and operational management of charging and battery swapping stations may also be achieved by considering the geographical distributions of loads in the cities. In order to manage the growing EV fleet and home charging loads, demand side management schemes may also be explored.

IoT is an emerging concept, which aims to connect billions of devices with each other. The IoT devices sense, collect, and transmit important information from their surroundings. This exchange of very large amount of information amongst billions of devices creates a massive energy need. Green IoT envisions the concept of reducing the energy consumption of IoT devices and making the environment safe. Inspired by achieving a sustainable environment for IoT infrastructure, a new optimization framework can developed by giving an overview of green IoTs and the challenges that are faced due to excessive usage of energy hungry IoT devices. Some strategies can be proposed to minimize the energy consumption in IoT devices, such as designing energy efficient data centers, energy efficient transmission of data from sensors, and design of energy efficient policies. Moreover, critically analysis of green IoT strategies can be carried out. A case study of very important aspect of IoT, i.e., smart phones and provide an easy and concise view for improving the current practices to make the IoT greener for the world in 2020 and beyond.

In this thesis, all DR planning problems and operational management are formulated by assuming the constant power loads. The problem may be re-investigated by considering the other load models such as constant current & impedance, and voltage dependent.

Appendix A

Test Distribution Systems

A.1 Study System–1

It is a 12.66 kV benchmark test distribution system with total real and reactive power demand of 3715 kW and 2300 kVAr respectively [197]. The nominal real and reactive power loss of the system are 202.677 kW and 135.141 kVAr respectively. Other parameters used for load flow studies are given below.

S_{base} = 100 MVA and kV_{base} = 12.66 kV

TABLE A.1: Line and Bus Data of 33-bus Test Distribution System

Br. no.	Sen. nd.	Rec. nd.	R (Ω)	X (Ω)	Rec. nd. Load kW	Rec. nd. Load kVAr	Br. no.	Sen. nd.	Rec. nd.	R (Ω)	X (Ω)	Rec. nd. Load kW	Rec. nd. Load kVAr
1	1	2	0.0922	0.047	100	60	17	17	18	0.732	0.574	90	40
2	2	3	0.493	0.2511	90	40	18	2	19	0.164	0.1565	90	40
3	3	4	0.366	0.1864	120	80	19	19	20	1.5042	1.3554	90	40
4	4	5	0.3811	0.1941	60	30	20	20	21	0.4095	0.4784	90	40
5	5	6	0.819	0.707	60	20	21	21	22	0.7089	0.9373	90	40
6	6	7	0.1872	0.6188	200	100	22	3	23	0.4512	0.3083	90	50
7	7	8	0.7114	0.2351	200	100	23	23	24	0.898	0.7091	420	200
8	8	9	1.03	0.74	60	20	24	24	25	0.896	0.7011	420	200
9	9	10	1.044	0.74	60	20	25	6	26	0.203	0.1034	60	25
10	10	11	0.1966	0.065	45	30	26	26	27	0.2842	0.1447	60	25
11	11	12	0.3744	0.1238	60	35	27	27	28	1.059	0.9337	60	20
12	12	13	1.468	1.155	60	35	28	28	29	0.8042	0.7006	120	70
13	13	14	0.5416	0.7129	120	80	29	29	30	0.5075	0.2585	200	600
14	14	15	0.591	0.526	60	10	30	30	31	0.9744	0.963	150	70
15	15	16	0.7463	0.545	60	20	31	31	32	0.3105	0.3619	210	100
16	16	17	1.289	1.721	60	20	32	32	33	0.341	0.5302	60	40

A.2 Study System–2

This system is an 11kV real Indian radial distribution system of Jhalawar city, India. It originates from 33/11 kV transformer with OLTC arrangement that is installed in 220 kV GSS. The nominal real and reactive demand of the system is 12.132 MW and 9.099 MVAr respectively. The obtained real and reactive power losses of the base system are 645.020 kW and 359.416 kVAr respectively. The parameters used in power flow studies are given below.

S_{base} = 100 MVA and kV_{base} = 11 kV

TABLE A.2: Line and Bus Data of 108-bus Indian Distribution System

Br. no.	Sen. nd.	Rec. nd.	R (Ω)	X (Ω)	Rec. nd. Load kW	Rec. nd. Load kVAr	Br. no.	Sen. nd.	Rec. nd.	R (Ω)	X (Ω)	Rec. nd. Load kW	Rec. nd. Load kVAr
1	1	2	0.0814	0.0921	0	0	55	1	56	0.6660	0.2826	0	0
2	2	3	0.0555	0.0628	0	0	56	56	57	1.5540	0.6594	0	0
3	3	4	0.1443	0.1632	0	0	57	57	58	1.1100	0.4710	0	0
4	4	5	0.2970	0.0470	0	0	58	58	59	0.3330	0.1413	0	0
5	5	6	1.1550	0.1827	96	72	59	59	60	0.3441	0.1460	1200	900
6	6	7	0.2970	0.0470	38.4	28.8	60	57	61	0.8250	0.1305	240	180
7	7	8	0.5940	0.0940	38.4	28.8	61	58	62	1.1550	0.1827	240	180
8	4	9	0.0666	0.0753	60	45	62	1	63	1.0560	0.7128	2400	1800
9	9	10	0.5940	0.0940	0	0	63	1	64	0.3960	0.2673	0	0
10	10	11	0.6270	0.0992	60	45	64	64	65	0.0990	0.0668	0	0
11	11	12	0.2970	0.0470	60	45	65	65	66	0.8580	0.1357	240	180
12	12	13	0.4950	0.0783	60	45	66	66	67	0.6930	0.1096	0	0
13	13	14	0.2970	0.0470	98.4	73.8	67	67	68	1.0230	0.1618	240	180
14	14	15	0.2970	0.0470	60	45	68	68	69	0.8910	0.1409	0	0
15	9	16	0.0814	0.0921	96	72	69	69	70	1.1550	0.1827	0	0
16	16	17	0.0925	0.1046	96	72	70	70	71	0.6930	0.1096	0	0
17	17	18	0.0396	0.0385	96	72	71	71	72	0.7590	0.1201	60	45
18	18	19	0.0352	0.0342	96	72	72	72	73	0.6600	0.1044	60	45
19	19	20	0.0396	0.0385	96	72	73	67	74	0.7260	0.1148	0	0
20	20	21	0.0352	0.0342	96	72	74	74	75	1.0230	0.1618	240	180
21	21	22	0.0999	0.0424	96	72	75	75	76	0.8910	0.1409	0	0
22	22	23	0.0555	0.0236	96	72	76	76	77	0.4950	0.0783	96	72
23	23	24	0.0888	0.0377	96	72	77	65	78	0.3663	0.1554	0	0
24	24	25	0.0888	0.0377	0	0	78	78	79	0.2220	0.0942	0	0
25	25	26	0.1665	0.0707	96	72	79	79	80	0.1980	0.0313	0	0
26	26	27	0.1650	0.0261	96	72	80	80	81	0.4620	0.0731	0	0
27	27	28	0.2970	0.0470	96	72	81	81	82	0.2640	0.0418	0	0
28	28	29	0.2310	0.0365	96	72	82	82	83	0.3630	0.0574	0	0
29	29	30	0.2970	0.0470	0	0	83	83	84	0.4950	0.0783	60	45
30	30	31	0.3960	0.0626	96	72	84	84	85	1.0890	0.1723	240	180
31	31	32	0.3630	0.0574	96	72	85	85	86	0.6600	0.1044	240	180
32	32	33	0.2310	0.0365	96	72	86	78	87	2.9700	0.4698	240	180
33	33	34	0.2640	0.0418	96	72	87	79	88	0.3630	0.0574	240	180
34	34	35	0.3630	0.0574	96	72	88	80	89	0.9240	0.1462	0	0
35	18	36	0.6270	0.0992	96	72	89	89	90	0.4620	0.0731	60	45
36	36	37	0.6270	0.0992	96	72	90	81	91	0.6270	0.0992	96	72
37	37	38	0.6270	0.0992	96	72	91	82	92	0.1650	0.0261	38.4	28.8
38	19	39	0.4950	0.0783	96	72	92	83	93	0.2310	0.0365	60	45
39	39	40	0.1980	0.0313	96	72	93	1	94	0.6549	0.2779	0	0
40	39	41	0.2310	0.0365	96	72	94	94	95	0.6660	0.2826	0	0
41	21	42	0.4950	0.0783	96	72	95	95	96	1.8870	0.8007	0	0
42	42	43	0.1650	0.0261	96	72	96	96	97	0.0999	0.0424	768	576
43	43	44	0.1650	0.0261	96	72	97	97	98	0.8580	0.1357	0	0
44	23	45	0.2970	0.0470	96	72	98	98	99	2.0460	0.3236	0	0

Continued on next page...

Br. no.	Sen. nd.	Rec. nd.	R (Ω)	X (Ω)	Rec. nd. Load kW	Rec. nd. Load kVAr	Br. no.	Sen. nd.	Rec. nd.	R (Ω)	X (Ω)	Rec. nd. Load kW	Rec. nd. Load kVAr
45	45	46	0.2970	0.0470	96	72	99	99	100	0.2970	0.0470	0	0
46	46	47	0.2970	0.0470	96	72	100	100	101	0.6930	0.1096	0	0
47	46	48	0.2310	0.0365	96	72	101	101	102	0.7260	0.1148	151.2	113.4
48	26	49	0.2970	0.0470	192	144	102	102	103	0.8250	0.1305	0	0
49	28	50	0.1980	0.0313	96	72	103	103	104	0.8250	0.1305	0	0
50	50	51	0.3630	0.0574	0	0	104	104	105	0.8580	0.1357	240	180
51	30	52	0.4950	0.0783	96	72	105	95	106	0.2970	0.0470	240	180
52	10	53	0.2970	0.0470	60	45	106	99	107	0.7260	0.1148	151.2	113.4
53	10	54	0.5940	0.0940	60	45	107	102	108	0.0990	0.0157	240	180
54	54	55	0.2970	0.0470	0	0							

A.3 Study System–3

It is a large, 11 kV, 118-bus benchmark test distribution system with total demand of 22.71 MW, 17.04 MVAr [208]. The real and reactive power losses of the system at nominal loading is found to be 1298.1 kW and 978 kVAr respectively. The load flow parameters used are given below.

S_{base} = 100 MVA and kV_{base} = 11 kV

TABLE A.3: Line and Bus Data of 118-bus Test Distribution System

Br. no.	Sen. nd.	Rec. nd.	R (Ω)	X (Ω)	Rec. nd. Load kW	Rec. nd. Load kVAr	Br. no.	Sen. nd.	Rec. nd.	R (Ω)	X (Ω)	Rec. nd. Load kW	Rec. nd. Load kVAr
1	1	2	0.036	0.013	134	101	60	60	61	0.207	0.075	96	91
2	2	3	0.033	0.012	16	11	61	61	62	0.247	0.892	63	48
3	2	4	0.045	0.016	34	22	62	1	63	0.028	0.042	479	464
4	4	5	0.015	0.054	73	64	63	63	64	0.117	0.202	121	52
5	5	6	0.015	0.054	144	69	64	64	65	0.255	0.092	139	100
6	6	7	0.015	0.013	104	62	65	65	66	0.210	0.076	392	194
7	7	8	0.018	0.014	29	12	66	66	67	0.383	0.138	28	27
8	8	9	0.021	0.063	88	51	67	67	68	0.504	0.330	53	25
9	2	10	0.166	0.134	198	107	68	68	69	0.406	0.146	67	39
10	10	11	0.112	0.079	147	76	69	69	70	0.962	0.761	468	395
11	11	12	0.187	0.313	26	19	70	70	71	0.165	0.060	595	240
12	12	13	0.142	0.151	52	23	71	71	72	0.303	0.109	133	84
13	13	14	0.18	0.118	142	118	72	72	73	0.303	0.109	53	22
14	14	15	0.15	0.045	22	29	73	73	74	0.206	0.144	870	615
15	15	16	0.16	0.180	33	26	74	74	75	0.233	0.084	31	30
16	16	17	0.157	0.171	32	25	75	75	76	0.591	0.177	192	122
17	11	18	0.218	0.285	20	12	76	76	77	0.126	0.045	66	45
18	18	19	0.118	0.185	157	79	77	64	78	0.559	0.369	238	223
19	19	20	0.16	0.196	546	351	78	78	79	0.186	0.123	295	162
20	20	21	0.12	0.189	180	164	79	79	80	0.186	0.123	486	438
21	21	22	0.12	0.079	93	55	80	80	81	0.260	0.139	244	183
22	22	23	1.41	0.723	85	40	81	81	82	0.154	0.148	244	183
23	23	24	0.293	0.135	168	95	82	82	83	0.230	0.128	134	119
24	24	25	0.133	0.104	125	150	83	83	84	0.252	0.106	23	28
25	25	26	0.178	0.134	16	25	84	84	85	0.180	0.148	50	27
26	26	27	0.178	0.134	26	25	85	79	86	0.160	0.182	384	257
27	4	28	0.015	0.030	595	523	86	86	87	0.200	0.230	50	21
28	28	29	0.012	0.028	121	59	87	87	88	0.160	0.393	22	12
29	29	30	0.12	0.277	102	100	88	65	89	0.669	0.241	63	43
30	30	31	0.21	0.243	513	319	89	89	90	0.266	0.123	31	35
31	31	32	0.12	0.054	475	456	90	90	91	0.266	0.123	63	67

Continued on next page...

Br. no.	Sen. nd.	Rec. nd.	R (Ω)	X (Ω)	Rec. nd. Load kW	Rec. nd. Load kVAr	Br. no.	Sen. nd.	Rec. nd.	R (Ω)	X (Ω)	Rec. nd. Load kW	Rec. nd. Load kVAr
32	32	33	0.178	0.234	151	137	91	91	92	0.266	0.123	115	82
33	33	34	0.178	0.234	205	83	92	92	93	0.266	0.123	81	67
34	34	35	0.154	0.162	132	93	93	93	94	0.233	0.115	32	16
35	30	36	0.187	0.261	448	370	94	94	95	0.496	0.138	33	60
36	36	37	0.133	0.099	441	322	95	91	96	0.196	0.180	531	225
37	29	38	0.33	0.194	113	55	96	96	97	0.196	0.180	507	367
38	38	39	0.31	0.194	54	39	97	97	98	0.187	0.122	26	12
39	39	40	0.13	0.194	393	343	98	98	99	0.075	0.318	46	30
40	40	41	0.28	0.150	327	279	99	1	100	0.063	0.027	101	48
41	41	42	1.18	0.850	536	240	100	100	101	0.150	0.234	456	350
42	42	43	0.42	0.244	76	67	101	101	102	0.135	0.089	523	449
43	43	44	0.27	0.097	54	40	102	102	103	0.231	0.120	408	168
44	44	45	0.339	0.122	40	32	103	103	104	0.447	0.161	141	134
45	45	46	0.27	0.178	40	21	104	104	105	0.163	0.059	104	66
46	35	47	0.21	0.138	66	42	105	105	106	0.330	0.099	97	84
47	47	48	0.12	0.079	74	52	106	106	107	0.156	0.056	494	419
48	48	49	0.15	0.099	115	58	107	107	108	0.382	0.137	225	136
49	49	50	0.15	0.099	918	1205	108	108	109	0.163	0.059	509	387
50	50	51	0.24	0.158	210	147	109	109	110	0.382	0.137	189	173
51	51	52	0.12	0.079	67	57	110	110	111	0.245	0.088	918	899
52	52	53	0.405	0.146	42	40	111	110	112	0.209	0.075	305	215
53	53	54	0.405	0.146	434	283	112	112	113	0.230	0.083	54	41
54	29	55	0.391	0.141	62	27	113	100	114	0.610	0.220	211	193
55	55	56	0.406	0.146	92	88	114	114	115	0.187	0.127	67	53
56	56	57	0.406	0.146	85	55	115	115	116	0.373	0.246	162	90
57	57	58	0.706	0.546	345	332	116	116	117	0.405	0.367	49	29
58	58	59	0.338	0.122	23	17	117	117	118	0.489	0.438	34	19
59	59	60	0.338	0.122	81	49							

A.4 Study System–4

This is a 10 kV Portugalian radial distribution system with 201 buses with total real and reactive demand of 36.10 MW and 27.08 MVAr respectively. The real and reactive power losses of the system at nominal demand are 2.2387 MW and 0.9313 MVAr respectively. The load flow parameters used are $S_{base} = 100$ MVA and $kV_{base} = 10$ kV.

TABLE A.4: Line and Bus Data of 201-bus Portugalian Distribution System

Br. no.	Sen. nd.	Rec. nd.	R (Ω)	X (Ω)	Rec. nd. Load kW	Rec. nd. Load kVAr	Br. no.	Sen. nd.	Rec. nd.	R (Ω)	X (Ω)	Rec. nd. Load kW	Rec. nd. Load kVAr
1	1	2	0.0306	0.003	0	0	101	101	102	0.0159	0.0054	221.3	166
2	2	3	0.0122	0.0114	7	5.3	102	102	103	0.0501	0.017	78.3	58.7
3	3	4	0.0316	0.0295	170.4	127.8	103	79	104	0.0694	0.0235	207.4	155.5
4	4	5	0.0122	0.0114	0	0	104	104	105	0.0591	0.02	190.4	142.8
5	5	6	0.0591	0.02	410.8	308.1	105	105	106	0.0206	0.007	207.4	155.5
6	6	7	0.0668	0.0226	192.3	144.3	106	106	107	0.0149	0.005	0	0
7	7	8	0.0668	0.0226	218.7	164	107	107	108	0.036	0.0122	161.1	120.8
8	8	9	0.0154	0.0052	2.7	2	108	108	109	0.0154	0.0052	324	243
9	9	10	0.0771	0.0261	0	0	109	109	110	0.1696	0.0574	455.7	341.8
10	10	11	0.1902	0.0644	207.4	155.5	110	110	111	0.0851	0.0288	254.2	190.6
11	11	12	0.0103	0.0035	148.4	111.3	111	80	112	0.0373	0.0126	55.7	41.8
12	12	13	0.0643	0.0218	225.5	169.1	112	80	113	0.0591	0.02	139.3	104.5
13	13	14	0.0411	0.0139	281.9	211.4	113	83	114	0.0116	0.0039	138.1	103.6
14	14	15	0.0411	0.0139	220	165	114	84	115	0.0122	0.0114	116.8	87.6
15	15	16	0.0257	0.0087	207.4	155.5	115	115	116	0.0514	0.0174	217.2	162.9
16	2	17	0.0296	0.0276	0	0	116	116	117	0.0514	0.0174	324	243

Continued on next page...

Br. no.	Sen. nd.	Rec. nd.	R (Ω)	X (Ω)	Rec. nd. Load kW	Rec. nd. Load kVAr	Br. no.	Sen. nd.	Rec. nd.	R (Ω)	X (Ω)	Rec. nd. Load kW	Rec. nd. Load kVAr
17	17	18	0.0231	0.0078	55.7	41.8	117	117	118	0.0154	0.0052	13.9	10.5
18	18	19	0.054	0.0183	55.7	41.8	118	85	119	0.0365	0.0124	352	264
19	17	20	0.0591	0.02	55.7	41.8	119	119	120	0.0036	0.0004	55.7	41.8
20	3	21	0.0296	0.0276	0	0	120	86	121	0.0347	0.0117	317.8	238.4
21	21	22	0.0591	0.02	0	0	121	1	122	0.0632	0.0589	0	0
22	22	23	0.0643	0.0218	351.1	263.3	122	122	123	0.0638	0.0063	0	0
23	21	24	0.0617	0.0209	55.7	41.8	123	123	124	0.0549	0.0054	47.2	35.4
24	3	25	0.0255	0.0238	140.7	105.6	124	124	125	0.0296	0.0276	0	0
25	25	26	0.0643	0.0218	218.6	164	125	125	126	0.0117	0.0109	657.1	492.8
26	26	27	0.0643	0.0218	99.3	74.5	126	126	127	0.09	0.0305	0	0
27	27	28	0.0231	0.0078	208.7	156.5	127	127	128	0.09	0.0305	8	6
28	28	29	0.0265	0.0247	324	243	128	128	129	0.0565	0.0191	121	90.7
29	25	30	0.0925	0.0313	324	243	129	129	130	0.0591	0.02	0	0
30	30	31	0.0224	0.0209	518.4	388.8	130	130	131	0.0334	0.0113	0	0
31	31	32	0.0411	0.0139	55.7	41.8	131	131	132	0.0437	0.0148	207.4	155.5
32	3	33	0.0796	0.0741	139.7	104.8	132	132	133	0.0308	0.0104	518.4	388.8
33	33	34	0.0488	0.0165	72.6	54.4	133	133	134	0.0283	0.0096	0	0
34	34	35	0.0797	0.027	447.1	335.3	134	134	135	0.0553	0.0187	324	243
35	35	36	0.0308	0.0104	0	0	135	124	136	0.0143	0.0133	101.9	76.4
36	33	37	0.0463	0.0157	230.6	172.7	136	124	137	0.0561	0.0523	207.4	155.5
37	37	38	0.0386	0.0131	340.8	255.6	137	137	138	0.0745	0.0252	324	243
38	38	39	0.0112	0.0105	43.3	32.5	138	138	139	0.0411	0.0139	324	243
39	4	40	0.0112	0.0105	27.4	20.6	139	139	140	0.0386	0.0131	324	243
40	40	41	0.0255	0.0238	55.7	41.8	140	140	141	0.036	0.0122	71.9	53.9
41	8	42	0.0514	0.0174	518.4	388.8	141	141	142	0.0036	0.0033	324	243
42	9	43	0.0257	0.0087	0	0	142	124	143	0.0112	0.0105	170.4	127.8
43	43	44	0.0617	0.0209	131.6	98.7	143	143	144	0.054	0.0183	170.4	127.8
44	43	45	0.1054	0.0357	272.7	204.5	144	144	145	0.0154	0.0052	18.7	14
45	9	46	0.0164	0.0056	207.4	155.5	145	145	146	0.072	0.0244	0	0
46	46	47	0.0565	0.0191	324	243	146	146	147	0.0206	0.007	309.4	232.1
47	10	48	0.0488	0.0165	145.8	109.3	147	147	148	0.1902	0.0644	207.4	155.5
48	48	49	0.0745	0.0252	160.9	120.7	148	148	149	0.0154	0.0052	44	33
49	49	50	0.0386	0.0131	281.4	211	149	149	150	0.0643	0.0218	316.4	237.3
50	50	51	0.0257	0.0087	0	0	150	150	151	0.1516	0.0513	129.6	97.2
51	51	52	0.0797	0.027	408.2	306.2	151	125	152	0.0463	0.0157	212.3	159.2
52	52	53	0.0745	0.0252	101	75.8	152	125	153	0.0103	0.0035	0	0
53	48	54	0.0163	0.0152	324	243	153	153	154	0.0257	0.0087	0	0
54	54	55	0.0231	0.0078	165.7	124.3	154	154	155	0.018	0.0061	131.6	98.7
55	55	56	0.0488	0.0165	324	243	155	155	156	0.0475	0.0161	131.6	98.7
56	56	57	0.0745	0.0252	324	243	156	156	157	0.0488	0.0165	131.6	98.7
57	57	58	0.009	0.003	93.3	70	157	157	158	0.0386	0.0131	131.6	98.7
58	10	59	0.0077	0.0026	324	243	158	158	159	0.0231	0.0078	32.4	24.3
59	59	60	0.0386	0.0131	518.4	388.8	159	159	160	0.0591	0.02	1.3	1
60	60	61	0.0064	0.0022	22	16.5	160	160	161	0.0514	0.0174	0	0
61	61	62	0.0275	0.0257	55.7	41.8	161	161	162	0.0051	0.0017	324	243
62	59	63	0.054	0.0183	270.7	203.1	162	162	163	0.0204	0.019	186.3	139.7
63	63	64	0.0418	0.039	207.4	155.5	163	163	164	0.0173	0.0162	207.4	155.5
64	64	65	0.0437	0.0148	55.7	41.8	164	164	165	0.0133	0.0124	207.4	155.5
65	11	66	0.072	0.0244	207.4	155.5	165	159	166	0.0643	0.0218	135.1	101.3
66	66	67	0.1085	0.1011	324	243	166	166	167	0.0173	0.0162	253.1	189.8
67	67	68	0.0952	0.0886	842.4	631.8	167	167	168	0.0308	0.0104	53	39.7
68	1	69	0.051	0.005	0	0	168	160	169	0.0565	0.0191	324	243
69	69	70	0.0112	0.0105	0	0	169	169	170	0.0463	0.0157	257.2	192.9
70	70	71	0.0235	0.0219	131.6	98.7	170	161	171	0.0206	0.007	231.5	173.6
71	71	72	0.0163	0.0152	0	0	171	171	172	0.0386	0.0131	152.7	114.5
72	72	73	0.0383	0.0356	207.4	155.5	172	153	173	0.0257	0.0087	139.3	104.5
73	73	74	0.0565	0.0191	189	141.8	173	155	174	0.0745	0.0252	131.6	98.7
74	74	75	0.0758	0.0257	324	243	174	128	175	0.0732	0.0248	207.4	155.5
75	75	76	0.0607	0.0205	324	243	175	175	176	0.0308	0.0104	518.4	388.8
76	76	77	0.045	0.0152	55.7	41.8	176	128	177	0.0231	0.0078	58	43.5
77	77	78	0.0378	0.0128	55.7	41.8	177	177	178	0.0283	0.0096	101	75.8
78	78	79	0.2724	0.0922	207.4	155.5	178	128	179	0.0463	0.0157	0	0
79	79	80	0.054	0.0183	0	0	179	128	180	0.0463	0.0157	146.5	109.9
80	80	81	0.0386	0.0131	322.6	242	180	180	181	0.0707	0.0239	189.5	142.1
81	81	82	0.0045	0.0042	152	114	181	129	182	0.0231	0.0078	518.4	388.8
82	82	83	0.0617	0.0209	133.1	99.8	182	182	183	0.0386	0.0131	324	243
83	83	84	0.0822	0.0278	131.6	98.7	183	183	184	0.0822	0.0278	324	243

Continued on next page...

Br. no.	Sen. nd.	Rec. nd.	R (Ω)	X (Ω)	Rec. nd. Load kW	Rec. nd. Load kVAr	Br. no.	Sen. nd.	Rec. nd.	R (Ω)	X (Ω)	Rec. nd. Load kW	Rec. nd. Load kVAr
84	84	85	0.0694	0.0235	102.7	77	184	184	185	0.0617	0.0209	648	486
85	85	86	0.0668	0.0226	321	240.7	185	185	186	0.0308	0.0104	0	0
86	86	87	0.0283	0.0096	0	0	186	186	187	0.0308	0.0104	207.4	155.5
87	87	88	0.0103	0.0035	518.4	388.8	187	187	188	0.054	0.0183	324	243
88	88	89	0.0668	0.0226	129.6	97.2	188	129	189	0.0283	0.0096	112.5	84.4
89	69	90	0.0158	0.0147	55.7	41.8	189	189	190	0.0488	0.0165	207.4	155.5
90	70	91	0.0367	0.0342	0	0	190	190	191	0.0643	0.0218	1	0.8
91	91	92	0.0154	0.0052	207.4	155.5	191	191	192	0.0617	0.0209	324	243
92	70	93	0.0464	0.0432	179.7	134.7	192	130	193	0.0283	0.0096	324	243
93	93	94	0.0316	0.0107	0	0	193	193	194	0.0386	0.0131	0.6	0.5
94	75	95	0.0463	0.0157	272.5	204.4	194	194	195	0.0668	0.0226	207.4	155.5
95	95	96	0.0424	0.0144	55.7	41.8	195	195	196	0.081	0.0274	207.4	155.5
96	76	97	0.0861	0.0291	324	243	196	196	197	0.0488	0.0165	321	240.7
97	97	98	0.091	0.0308	136.2	102.1	197	193	198	0.0514	0.0174	324	243
98	98	99	0.0308	0.0104	304.4	228.3	198	198	199	0.0822	0.0278	324	243
99	99	100	0.0771	0.0261	0	0	199	199	200	0.0668	0.0226	277.4	208.1
100	97	101	0.0077	0.0026	0	0	200	200	201	0.072	0.0244	207.4	155.5

Appendix B

Commercial and Technical Information

Table B.1: Commercial Information of DGs

Parameter	DE	GE	MT	BM	FC
Turnkey cost ($/kVA)	550	690	915	2293	1900
O&M cost ($/kWh)	0.09	0.009	0.011	0.012	0.005
CO_2 Emission (kg/MWh)	650	560	360	003	430
Capacity factor (CF)	0.92	0.92	0.92	0.92	0.92
Power factor (PF)	0.85	0.85	0.85	0.85	1.00

Table B.2: The Summary of Techno-economic Parameters used in the Work

Parameters	Values	Parameters	Values
T_P	20	$C_{OM}^{WT,PV}$	0.0100$/kWh
ϕ	365 days	s_r	1000 W/m2
d	5	C_{OM}^{SC}	0.0002$/kVArh
V_{min}^{spec}	0.95 pu	v_r	15 m/s
C_{Inst}^{WT}	1882$/kW	α_{Fuel}^{MT}	0.0630$/kWh
V_{max}^{spec}	1.05pu	v_{cuto}	20 m/s
C_{Inst}^{PV}	4004$/kW	α_{Emis}^{MT}	0.0200$/kg
pf_{min}^{spec}	0.90 lag/lead	v_{cuti}	4 m/s
C_{Inst}^{WT}	2293$/kW	η	0.0030kg/kWh
pf_{max}^{spec}	0.95 lag/lead	C_E	55-120$/MWh
C_{Inst}^{SC}	900$/bank	m^{MT}	0.0120$/kWh

TABLE B.3: Simulation parameters used in the study

Parameter(s)	Value
ϕ	365
$\underline{V}$, $\overline{V}$	0.95 p.u., 1.05 p.u.
$I_{Spc.}$	5% of grid transformer rated current
η	85%
$\underline{P_B}$, $\overline{P_B}$	1 MW, 1 MW
$\underline{SOC}$, $\overline{SOC}$	0, 1
$\overline{P_{DG}}$, $\overline{W_B}$	2 MW, 5 MWh
v_{cutin}, v_{cutout}, v_r	4 m/s, 20 m/s, 15 m/s

Bibliography

[1] H. N. Ng, M. M. A. Salama, and A. Y. Chikhani, "Classification of capacitor allocation techniques," *IEEE Trans. on Power Del.*, vol. 15, no. 1, pp. 387–392, Jan 2000.

[2] P. S. Georgilakis and N. D. Hatziargyriou, "Optimal distributed generation placement in power distribution networks: Models, methods, and future research," *IEEE Trans. on Power Syst.*, vol. 28, no. 3, pp. 3420–3428, Aug 2013.

[3] R. A. Walling, R. Saint, R. C. Dugan, J. Burke, and L. A. Kojovic, "Summary of distributed resources impact on power delivery systems," *IEEE Trans. on Power Del.*, vol. 23, no. 3, pp. 1636–1644, July 2008.

[4] M. M. Begovic, I. Kim, B. Vidakovic, P. Djuric, and V. Jeremic, "Impact of short-term variations in the generation output of geographically dispersed pv systems," in *2017 the 50th Hawaii International Conference on System Sciences*, 2017, pp. 3003–3010.

[5] S. Parhizi, H. Lotfi, A. Khodaei, and S. Bahramirad, "State of the art in research on microgrids: A review," *IEEE Access*, vol. 3, pp. 890–925, 2015.

[6] D. Liu and Y. Cai, "Taguchi method for solving the economic dispatch problem with nonsmooth cost functions," *IEEE Trans. on Power Syst.*, vol. 20, no. 4, pp. 2006–2014, Nov 2005.

[7] B. S. Borowy and Z. M. Salameh, "Optimum photovoltaic array size for a hybrid wind/pv system," *IEEE Trans. on Energy Conv.*, vol. 9, no. 3, pp. 482–488, Sep 1994.

[8] N. Kanwar, N. Gupta, K. Niazi, and A. Swarnkar, "Simultaneous allocation of distributed resources using improved teaching learning based optimization," *Energy Conv. and Manag.*, vol. 103, pp. 387–400, 2015.

[9] ——, "Improved meta-heuristic techniques for simultaneous capacitor and dg allocation in radial distribution networks," *Int. Journ. of Electr. Power & Energy Syst.*, vol. 73, pp. 653–664, 2015.

[10] R. S. Rao, K. Ravindra, K. Satish, and S. V. L. Narasimham, "Power loss minimization in distribution system using network reconfiguration in the presence of distributed generation," *IEEE Trans. on Power Syst.*, vol. 28, no. 1, pp. 317–325, Feb 2013.

[11] A. M. Cossi, L. G. W. D. Silva, R. A. R. Lazaro, and J. R. S. Mantovani, "Primary power distribution systems planning taking into account reliability, operation and expansion costs," *IET Gen., Trans. Distr.*, vol. 6, no. 3, pp. 274–284, March 2012.

[12] S. Favuzza, G. Graditi, M. G. Ippolito, and E. R. Sanseverino, "Optimal electrical distribution systems reinforcement planning using gas micro turbines by dynamic ant colony search algorithm," *IEEE Trans. on Power Syst.*, vol. 22, no. 2, pp. 580–587, May 2007.

[13] T. Niknam, S. I. Taheri, J. Aghaei, S. Tabatabaei, and M. Nayeripour, "A modified honey bee mating optimization algorithm for multiobjective placement of renewable energy resources," *Applied Energy*, vol. 88, no. 12, pp. 4817–4830, 2011.

[14] D. Zhu, R. P. Broadwater, K.-S. Tam, R. Seguin, and H. Asgeirsson, "Impact of dg placement on reliability and efficiency with time-varying loads," *IEEE Trans. on Power Syst.*, vol. 21, no. 1, pp. 419–427, Feb 2006.

[15] J. Kim, S. Nam, S. Park, and C. Singh, "Dispersed generation planning using improved hereford ranch algorithm," *Elect. Power Syst. Res.*, vol. 47, no. 1, pp. 47–55, 1998.

[16] M. Moradi and M. Abedini, "A combination of genetic algorithm and particle swarm optimization for optimal dg location and sizing in distribution systems," *Int. Jour. of Elect. Power & Energy Syst.*, vol. 34, no. 1, pp. 66–74, 2012.

[17] S. Sultana and P. K. Roy, "Multi-objective quasi-oppositional teaching learning based optimization for optimal location of distributed generator in radial distribution systems," *Int. Jour. of Elect. Power & Energy Syst.*, vol. 63, pp. 534–545, 2014.

[18] N. H. Kan'an, L. A. Farouk, H. H. Zeineldin, and W. L. Woon, "Effect of dg location on multi-parameter passive islanding detection methods," in *IEEE PES Gen. Meet.*, July 2010.

[19] R. Singh and S. Goswami, "Optimum allocation of distributed generations based on nodal pricing for profit, loss reduction, and voltage improvement including voltage rise issue," *Int. Jour. of Elect. Power & Energy Syst.*, vol. 32, no. 6, pp. 637–644, 2010.

[20] M. F. Akorede, H. Hizam, I. Aris, and M. Z. A. A. Kadir, "Effective method for optimal allocation of distributed generation units in meshed electric power systems," *IET Gen., Trans. Distr.*, vol. 5, no. 2, pp. 276–287, Feb 2011.

[21] A. Soroudi, M. Ehsan, R. Caire, and N. Hadjsaid, "Hybrid immune-genetic algorithm method for benefit maximisation of distribution network operators and distributed generation owners in a deregulated environment," *IET Gen., Trans. Distr.*, vol. 5, no. 9, pp. 961–972, Sept 2011.

[22] C. L. Borges and D. M. Falcão, "Optimal distributed generation allocation for reliability, losses, and voltage improvement," *Int. Jour. of Elect. Power & Energy Syst.*, vol. 28, no. 6, pp. 413–420, 2006.

[23] G. P. Harrison, A. Piccolo, P. Siano, and A. R. Wallace, "Exploring the tradeoffs between incentives for distributed generation developers and dnos," *IEEE Trans. on Power Syst.*, vol. 22, no. 2, pp. 821–828, May 2007.

[24] D. Pudjianto, G. Strbac, and J. Mutale, "Access and pricing of distribution network with distributed generation," in *2007 IEEE Power Eng. Soc. Gen. Meet.*, June 2007, pp. 1–3.

[25] R. Ebrahimi, M. Ehsan, and H. Nouri, "A profit-centric strategy for distributed generation planning considering time varying voltage dependent load demand," *Int. Jour. of Elect. Power & Energy Syst.*, vol. 44, no. 1, pp. 168–178, 2013.

[26] K. D. Mistry and R. Roy, "Enhancement of loading capacity of distribution system through distributed generator placement considering techno-economic benefits with load growth," *Int. Jour. of Elect. Power & Energy Syst.*, vol. 54, pp. 505–515, 2014.

[27] H. A. Gil and G. Joos, "Models for quantifying the economic benefits of distributed generation," *IEEE Trans. on Power Syst.*, vol. 23, no. 2, pp. 327–335, May 2008.

[28] S. Wong, K. Bhattacharya, and J. D. Fuller, "Long-term effects of feed-in tariffs and carbon taxes on distribution systems," *IEEE Trans. on Power Syst.*, vol. 25, no. 3, pp. 1241–1253, Aug 2010.

[29] Z. Hu and F. Li, "Cost-benefit analyses of active distribution network management, part i: Annual benefit analysis," *IEEE Trans. on Smart Grid*, vol. 3, no. 3, pp. 1067–1074, Sept 2012.

[30] H. A. Hejazi, A. R. Araghi, B. Vahidi, S. H. Hosseinian, M. Abedi, and H. Mohsenian-Rad, "Independent distributed generation planning to profit both utility and dg investors," *IEEE Trans. on Power Syst.*, vol. 28, no. 2, pp. 1170–1178, May 2013.

[31] M. J. Rider, J. M. Lopez-Lezama, J. Contreras, and A. Padilha-Feltrin, "Bilevel approach for optimal location and contract pricing of distributed generation in radial distribution systems using mixed-integer linear programming," *IET Gen., Trans. Distr.*, vol. 7, no. 7, pp. 724–734, Jul 2013.

[32] P. Siano, L. F. Ochoa, G. P. Harrison, and A. Piccolo, "Assessing the strategic benefits of distributed generation ownership for dnos," *IET Gen., Trans. Distr.*, vol. 3, no. 3, pp. 225–236, Mar 2009.

[33] H. Hosseinpour and B. Bastaee, "Optimal placement of on-load tap changers in distribution networks using sa-tlbo method," *Int. Jour. of Elect. Power & Energy Syst.*, vol. 64, pp. 1119–1128, 2015.

[34] M. F. Shaaban, Y. M. Atwa, and E. F. El-Saadany, "Dg allocation for benefit maximization in distribution networks," *IEEE Trans. on Power Syst.*, vol. 28, no. 2, pp. 639–649, May 2013.

[35] A. A. El-Ela, S. M. Allam, and M. Shatla, "Maximal optimal benefits of distributed generation using genetic algorithms," *Elect. Power Syst. Res.*, vol. 80, no. 7, pp. 869–877, 2010.

[36] S. Biswas, S. K. Goswami, and A. Chatterjee, "Optimum distributed generation placement with voltage sag effect minimization," *Energy Conv. and Manag.*, vol. 53, no. 1, pp. 163–174, 2012.

[37] H. Hamedi and M. Gandomkar, "A straightforward approach to minimizing unsupplied energy and power loss through dg placement and evaluating power quality in relation to load variations over time," *Int. Jour. of Elect. Power & Energy Syst.*, vol. 35, no. 1, pp. 93–96, 2012.

[38] A. Soroudi, M. Ehsan, R. Caire, and N. Hadjsaid, "Possibilistic evaluation of distributed generations impacts on distribution networks," *IEEE Trans. on Power Syst.*, vol. 26, no. 4, pp. 2293–2301, Nov 2011.

[39] Z. Liu, F. Wen, and G. Ledwich, "Optimal siting and sizing of distributed generators in distribution systems considering uncertainties," *IEEE Trans. on Power Del.*, vol. 26, no. 4, pp. 2541–2551, Oct 2011.

[40] A. Saif, V. R. Pandi, H. Zeineldin, and S. Kennedy, "Optimal allocation of distributed energy resources through simulation-based optimization," *Elect. Power Syst. Res.*, vol. 104, pp. 1–8, 2013.

[41] P. Murugan, S. Kannan, and S. Baskar, "Nsga-ii algorithm for multi-objective generation expansion planning problem," *Elect. Power Syst. Res.*, vol. 79, no. 4, pp. 622–628, 2009.

[42] A. Piccolo and P. Siano, "Evaluating the impact of network investment deferral on distributed generation expansion," *IEEE Trans. on Power Syst.*, vol. 24, no. 3, pp. 1559–1567, Aug 2009.

[43] M. E. Jahromi, M. Ehsan, and A. F. Meyabadi, "A dynamic fuzzy interactive approach for dg expansion planning," *Int. Jour. of Elect. Power & Energy Syst.*, vol. 43, no. 1, pp. 1094–1105, 2012.

[44] H. A. Gil and G. Joos, "On the quantification of the network capacity deferral value of distributed generation," *IEEE Trans. on Power Syst.*, vol. 21, no. 4, pp. 1592–1599, Nov 2006.

[45] V. Méndez, J. Rivier, J. de la Fuente, T. Gómez, J. Arceluz, J. Marín, and A. Madurga, "Impact of distributed generation on distribution investment deferral," *Int. Jour. of Elect. Power & Energy Syst.*, vol. 28, no. 4, pp. 244–252, 2006.

[46] T. E. Hoff, H. J. Wenger, and B. K. Farmer, "Distributed generation," *Energy Policy*, vol. 24, no. 2, pp. 137–147, 1996.

[47] D. T. C. Wang, L. F. Ochoa, and G. P. Harrison, "Dg impact on investment deferral: Network planning and security of supply," *IEEE Trans. on Power Syst.*, vol. 25, no. 2, pp. 1134–1141, May 2010.

[48] C. L. T. Borges and V. F. Martins, "Multistage expansion planning for active distribution networks under demand and distributed generation uncertainties," *Int. Jour. of Elect. Power & Energy Syst.*, vol. 36, no. 1, pp. 107–116, 2012.

[49] M. Sedghi, M. Aliakbar-Golkar, and M.-R. Haghifam, "Distribution network expansion considering distributed generation and storage units using modified pso algorithm," *Int. Jour. of Elect. Power & Energy Syst.*, vol. 52, pp. 221–230, 2013.

[50] T.-H. Chen, E.-H. Lin, N.-C. Yang, and T.-Y. Hsieh, "Multi-objective optimization for upgrading primary feeders with distributed generators from normally closed loop to mesh arrangement," *Int. Jour. of Elect. Power & Energy Syst.*, vol. 45, no. 1, pp. 413–419, 2013.

[51] S. N. Ravadanegh and R. G. Roshanagh, "On optimal multistage electric power distribution networks expansion planning," *Int. Jour. of Elect. Power & Energy Syst.*, vol. 54, pp. 487–497, 2014.

[52] S. Nejadfard-Jahromi, M. Rashidinejad, and A. Abdollahi, "Multistage distribution network expansion planning under smart grids environment," *Int. Jour. of Elect. Power & Energy Syst.*, vol. 71, pp. 222–230, 2015.

[53] P. Dehghanian, S. H. Hosseini, M. Moeini-Aghtaie, and A. Arabali, "Optimal siting of dg units in power systems from a probabilistic multi-objective optimization perspective," *Int. Jour. of Elect. Power & Energy Syst.*, vol. 51, pp. 14–26, 2013.

[54] A. Ameli, S. Bahrami, F. Khazaeli, and M. R. Haghifam, "A multiobjective particle swarm optimization for sizing and placement of dgs from dg owner's and distribution company's viewpoints," *IEEE Trans. on Power Del.*, vol. 29, no. 4, pp. 1831–1840, Aug 2014.

[55] W. Ouyang, H. Cheng, X. Zhang, and F. Li, "Evaluation of distributed generation connecting to distribution network based on long-run incremental cost," *IET Gen., Trans. Distr.*, vol. 5, no. 5, pp. 561–568, May 2011.

[56] G. Celli and F. Pilo, "Mv network planning under uncertainties on distributed generation penetration," in *2001 Power Engg. Soc. Summer Meet. Conf.*, vol. 1, Jul 2001, pp. 485–490 vol.1.

[57] E. Naderi, H. Seifi, and M. S. Sepasian, "A dynamic approach for distribution system planning considering distributed generation," *IEEE Trans. on Power Del.*, vol. 27, no. 3, pp. 1313–1322, Jul 2012.

[58] Z. Hu and F. Li, "Cost-benefit analyses of active distribution network management, part ii: Investment reduction analysis," *IEEE Trans. on Smart Grid*, vol. 3, no. 3, pp. 1075–1081, Sept 2012.

[59] W. El-Khattam, Y. G. Hegazy, and M. M. A. Salama, "An integrated distributed generation optimization model for distribution system planning," *IEEE Trans. on Power Syst.*, vol. 20, no. 2, pp. 1158–1165, May 2005.

[60] I. Ziari, G. Ledwich, A. Ghosh, and G. Platt, "Optimal distribution network reinforcement considering load growth, line loss, and reliability," *IEEE Trans. on Power Syst.*, vol. 28, no. 2, pp. 587–597, May 2013.

[61] S. Haffner, L. F. A. Pereira, L. A. Pereira, and L. S. Barreto, "Multistage model for distribution expansion planning with distributed generation—part i: Problem formulation," *IEEE Trans. on Power Del.*, vol. 23, no. 2, pp. 915–923, Apr 2008.

[62] ——, "Multistage model for distribution expansion planning with distributed generation—part ii: Numerical results," *IEEE Trans. on Power Del.*, vol. 23, no. 2, pp. 924–929, Apr 2008.

[63] P. Siano and G. Mokryani, "Assessing wind turbines placement in a distribution market environment by using particle swarm optimization," *IEEE Trans. on Power Syst.*, vol. 28, no. 4, pp. 3852–3864, Nov 2013.

[64] K. Vinothkumar and M. Selvan, "Hierarchical agglomerative clustering algorithm method for distributed generation planning," *Int. Jour. of Elect. Power & Energy Syst.*, vol. 56, pp. 259–269, 2014.

[65] B. H. Dias, L. W. Oliveira, F. V. Gomes, I. C. Silva, and E. J. Oliveira, "Hybrid heuristic optimization approach for optimal distributed generation placement and sizing," in *2012 IEEE Power and Energy Society General Meeting*, July 2012, pp. 1–6.

[66] A. Parizad, A. Khazali, and M. Kalantar, "Optimal placement of distributed generation with sensitivity factors considering voltage stability and losses indices," in *2010 18th Iranian Conference on Electrical Engineering*, May 2010, pp. 848–855.

[67] M. I. A and K. M, "Optimal distributed generation and capacitor placement in power distribution networks for power loss minimization," in *2014 International Conference on Advances in Electrical Engineering (ICAEE)*, Jan 2014, pp. 1–6.

[68] S. K. Injeti and N. P. Kumar, "A novel approach to identify optimal access point and capacity of multiple dgs in a small, medium and large scale radial distribution systems," *Int. Jour. of Elect. Power & Energy Syst.*, vol. 45, no. 1, pp. 142–151, 2013.

[69] A. M. Imran, M. Kowsalya, and D. Kothari, "A novel integration technique for optimal network reconfiguration and distributed generation placement in power distribution networks," *Int. Jour. of Elect. Power & Energy Syst.*, vol. 63, pp. 461–472, 2014.

[70] M. Aman, G. Jasmon, H. Mokhlis, and A. Bakar, "Optimal placement and sizing of a dg based on a new power stability index and line losses," *Int. Jour. of Elect. Power & Energy Syst.*, vol. 43, no. 1, pp. 1296–1304, 2012.

[71] N. Khalesi, N. Rezaei, and M.-R. Haghifam, "Dg allocation with application of dynamic programming for loss reduction and reliability improvement," *Int. Jour. of Elect. Power & Energy Syst.*, vol. 33, no. 2, pp. 288–295, 2011.

[72] J. M. López-Lezama, J. Contreras, and A. Padilha-Feltrin, "Location and contract pricing of distributed generation using a genetic algorithm," *Int. Jour. of Elect. Power & Energy Syst.*, vol. 36, no. 1, pp. 117–126, 2012.

[73] S. Abdi and K. Afshar, "Application of ipso-monte carlo for optimal distributed generation allocation and sizing," *Int. Jour. of Elect. Power & Energy Syst.*, vol. 44, no. 1, pp. 786–797, 2013.

[74] F. Ugranlı and E. Karatepe, "Multiple-distributed generation planning under load uncertainty and different penetration levels," *Int. Jour. of Elect. Power & Energy Syst.*, vol. 46, pp. 132–144, 2013.

[75] F. S. Abu-Mouti and M. E. El-Hawary, "Optimal distributed generation allocation and sizing in distribution systems via artificial bee colony algorithm," *IEEE Trans. on Power Del.*, vol. 26, no. 4, pp. 2090–2101, Oct 2011.

[76] T. Gozel and M. H. Hocaoglu, "An analytical method for the sizing and siting of distributed generators in radial systems," *Elect. Power Syst. Res.*, vol. 79, no. 6, pp. 912–918, 2009.

[77] N. Acharya, P. Mahat, and N. Mithulananthan, "An analytical approach for dg allocation in primary distribution network," *Int. Jour. of Elect. Power & Energy Syst.*, vol. 28, no. 10, pp. 669 – 678, 2006.

[78] N. S. Rau and Y.-H. Wan, "Optimum location of resources in distributed planning," *IEEE Trans. on Power Syst.*, vol. 9, no. 4, pp. 2014–2020, Nov 1994.

[79] H. L. Willis, "Analytical methods and rules of thumb for modeling dg-distribution interaction," in *2000 Power Engg. Soc. Summer Meet.*, vol. 3, 2000, pp. 1643–1644 vol. 3.

[80] K. Nara, Y. Hayashi, K. Ikeda, and T. Ashizawa, "Application of tabu search to optimal placement of distributed generators," in *2001 IEEE Power Engg. Soc. Winter Meet.*, vol. 2, 2001, pp. 918–923 vol.2.

[81] C. Wang and M. H. Nehrir, "Analytical approaches for optimal placement of distributed generation sources in power systems," *IEEE Trans. on Power Syst.*, vol. 19, no. 4, pp. 2068–2076, Nov 2004.

[82] M. Gandomkar, M. Vakilian, and M. Ehsan, "A genetic–based tabu search algorithm for optimal dg allocation in distribution networks," *Elect. Power Comp. and Syst.*, vol. 33, no. 12, pp. 1351–1362, 2005.

[83] D. Singh, R. K. Misra, and D. Singh, "Effect of load models in distributed generation planning," *IEEE Trans. on Power Syst.*, vol. 22, no. 4, pp. 2204–2212, Nov 2007.

[84] H. Hedayati, S. A. Nabaviniaki, and A. Akbarimajd, "A method for placement of dg units in distribution networks," *IEEE Trans. on Power Del.*, vol. 23, no. 3, pp. 1620–1628, July 2008.

[85] R. K. Singh and S. K. Goswami, "Optimum siting and sizing of distributed generations in radial and networked systems," *Elect. Power Comp. and Syst.*, vol. 37, no. 2, pp. 127–145, 2009.

[86] P. M. Costa and M. A. Matos, "Avoided losses on lv networks as a result of microgeneration," *Elect. Power Syst. Res.*, vol. 79, no. 4, pp. 629–634, 2009.

[87] S. H. Lee and J. W. Park, "Selection of optimal location and size of multiple distributed generations by using kalman filter algorithm," *IEEE Trans. on Power Syst.*, vol. 24, no. 3, pp. 1393–1400, Aug 2009.

[88] D. Q. Hung, N. Mithulananthan, and R. C. Bansal, "Analytical expressions for dg allocation in primary distribution networks," *IEEE Trans. on Energy Conv.*, vol. 25, no. 3, pp. 814–820, Sept 2010.

[89] H. Khan and M. A. Choudhry, "Implementation of distributed generation (idg) algorithm for performance enhancement of distribution feeder under extreme load growth," *Int. Jour. of Elect. Power & Energy Syst.*, vol. 32, no. 9, pp. 985 – 997, 2010.

[90] M. F. AlHajri, M. R. AlRashidi, and M. E. El-Hawary, "Improved sequential quadratic programming approach for optimal distribution generation deployments via stability and sensitivity analyses," *Elect. Power Comp. and Syst.*, vol. 38, no. 14, pp. 1595–1614, 2010.

[91] W. Prommee and W. Ongsakul, "Optimal multiple distributed generation placement in microgrid system by improved reinitialized social structures particle swarm optimization," *Euro. Trans. on Elect. Power*, vol. 21, no. 1, pp. 489–504, 2011.

[92] F. S. Abu-Mouti and M. E. El-Hawary, "Heuristic curve-fitted technique for distributed generation optimisation in radial distribution feeder systems," *IET Gen., Trans. Distr.*, vol. 5, no. 2, pp. 172–180, Feb 2011.

[93] L. Arya, A. Koshti, and S. Choube, "Distributed generation planning using differential evolution accounting voltage stability consideration," *Int. Jour. of Elect. Power & Energy Syst.*, vol. 42, no. 1, pp. 196–207, 2012.

[94] D. Q. Hung and N. Mithulananthan, "Multiple distributed generator placement in primary distribution networks for loss reduction," *IEEE Trans. on Indus. Electro.*, vol. 60, no. 4, pp. 1700–1708, April 2013.

[95] H. J. Wenger, T. E. Hoff, and B. K. Farmer, "Measuring the value of distributed photovoltaic generation: final results of the kerman grid-support project," in *1994 IEEE 1st World Conf. on PV Energy Conv.*, vol. 1, Dec 1994, pp. 792–796 vol.1.

[96] M. Aman, G. Jasmon, A. Bakar, and H. Mokhlis, "A new approach for optimum simultaneous multi-dg distributed generation units placement and sizing based on maximization of system loadability using hpso (hybrid particle swarm optimization) algorithm," *Energy*, vol. 66, pp. 202–215, 2014.

[97] D. Popović, J. Greatbanks, M. Begović, and A. Pregelj, "Placement of distributed generators and reclosers for distribution network security and reliability," *Int. Jour. of Elect. Power & Energy Syst.*, vol. 27, no. 5, pp. 398–408, 2005.

[98] F. M. Gonzalez-Longatt, "Impact of distribution generation over power losses on distribution system," in *9th Int. Conf., Elect. Power Quality and Utiliz., Barcelona*, Oct 2007.

[99] R. Prenc, D. Škrlec, and V. Komen, "Distributed generation allocation based on average daily load and power production curves," *Int. Jour. of Elect. Power & Energy Syst.*, vol. 53, pp. 612–622, 2013.

[100] V. V. S. N. Murty and A. Kumar, "Mesh distribution system analysis in presence of distributed generation with time varying load model," *Int. Jour. of Elect. Power & Energy Syst.*, vol. 62, pp. 836–854, 2014.

[101] P. Karimyan, G. Gharehpetian, M. Abedi, and A. Gavili, "Long term scheduling for optimal allocation and sizing of dg unit considering load variations and dg type," *Int. Jour. of Elect. Power & Energy Syst.*, vol. 54, pp. 277–287, 2014.

[102] S. R. Gampa and D. Das, "Optimum placement and sizing of dgs considering average hourly variations of load," *Int. Jour. of Elect. Power & Energy Syst.*, vol. 66, pp. 25–40, 2015.

[103] D. Q. Hung, N. Mithulananthan, and R. C. Bansal, "Analytical strategies for renewable distributed generation integration considering energy loss minimization," *Applied Energy*, vol. 105, pp. 75–85, 2013.

[104] S. N. G. Naik, D. K. Khatod, and M. P. Sharma, "Analytical approach for optimal siting and sizing of distributed generation in radial distribution networks," *IET Gen., Trans. Distr.*, vol. 9, no. 3, pp. 209–220, 2015.

[105] S. Elsaiah, M. Benidris, and J. Mitra, "Analytical approach for placement and sizing of distributed generation on distribution systems," *IET Gen., Trans. Distr.*, vol. 8, no. 6, pp. 1039–1049, June 2014.

[106] W. Sheng, K. yan Liu, and S. Cheng, "Optimal power flow algorithm and analysis in distribution system considering distributed generation," *IET Gen., Trans. Distr.*, vol. 8, no. 2, pp. 261–272, February 2014.

[107] R. Viral and D. Khatod, "An analytical approach for sizing and siting of dgs in balanced radial distribution networks for loss minimization," *Int. Jour. of Elect. Power & Energy Syst.*, vol. 67, pp. 191–201, 2015.

[108] Z. Ghofrani-Jahromi, Z. Mahmoodzadeh, and M. Ehsan, "Distribution loss allocation for radial systems including dgs," *IEEE Trans. on Power Del.*, vol. 29, no. 1, pp. 72–80, Feb 2014.

[109] R. S. Maciel, M. Rosa, V. Miranda, and A. Padilha-Feltrin, "Multi-objective evolutionary particle swarm optimization in the assessment of the impact of distributed generation," *Elect. Power Syst. Res.*, vol. 89, pp. 100–108, 2012.

[110] M. Jamil and S. Kirmani, "Optimal allocation of spv based dg system for loss reduction and voltage improvement in radial distribution systems using approximate reasoning," in *2012 IEEE 5th India Int. Conf. on Power Electro. (IICPE)*, Dec 2012, pp. 1–5.

[111] V. V. S. N. Murthy and A. Kumar, "Comparison of optimal dg allocation methods in radial distribution systems based on sensitivity approaches," *Int. Jour. of Elect. Power & Energy Syst.*, vol. 53, pp. 450–467, 2013.

[112] Z. Moravej and A. Akhlaghi, "A novel approach based on cuckoo search for dg allocation in distribution network," *Int. Jour. of Elect. Power & Energy Syst.*, vol. 44, no. 1, pp. 672–679, 2013.

[113] J. A. M. García and A. J. G. Mena, "Optimal distributed generation location and size using a modified teaching–learning based optimization algorithm," *Int. Jour. of Elect. Power & Energy Syst.*, vol. 50, pp. 65–75, 2013.

[114] A. A. Abdelsalam and E. F. El-saadany, "Probabilistic approach for optimal planning of distributed generators with controlling harmonic distortions," *IET Gen., Trans. Distr.*, vol. 7, no. 10, pp. 1105–1115, October 2013.

[115] K. Nekooei, M. M. Farsangi, H. Nezamabadi-Pour, and K. Y. Lee, "An improved multi-objective harmony search for optimal placement of dgs in distribution systems," *IEEE Trans. on Smart Grid*, vol. 4, no. 1, pp. 557–567, March 2013.

[116] P. Alemi and G. B. Gharehpetian, "Dg allocation using an analytical method to minimize losses and to improve voltage security," in *2008 IEEE 2nd Int. Power and Energy Conf.*, Dec 2008, pp. 1575–1580.

[117] S. H. Lee and J. W. Park, "Optimal placement and sizing of multiple dgs in a practical distribution system by considering power loss," *IEEE Trans. on Indus. Appl.*, vol. 49, no. 5, pp. 2262–2270, Sept 2013.

[118] M. H. Moradi, A. Zeinalzadeh, Y. Mohammadi, and M. Abedini, "An efficient hybrid method for solving the optimal sitting and sizing problem of dg and shunt capacitor banks simultaneously based on imperialist competitive algorithm and genetic algorithm," *Int. Jour. of Elect. Power & Energy Syst.*, vol. 54, pp. 101 – 111, 2014.

[119] S. Kaur, G. Kumbhar, and J. Sharma, "A minlp technique for optimal placement of multiple dg units in distribution systems," *Int. Jour. of Elect. Power & Energy Syst.*, vol. 63, pp. 609–617, 2014.

[120] D. Kumar, S. R. Samantaray, I. Kamwa, and N. C. Sahoo, "Reliability-constrained based optimal placement and sizing of multiple distributed generators in power distribution network using cat swarm optimization," *Elect. Power Comp. and Syst.*, vol. 42, no. 2, pp. 149–164, 2014.

[121] F. Rotaru, G. Chicco, G. Grigoras, and G. Cartina, "Two-stage distributed generation optimal sizing with clustering-based node selection," *Int. Jour. of Elect. Power & Energy Syst.*, vol. 40, no. 1, pp. 120–129, 2012.

[122] P. Kumar, N. Gupta, A. Swarnkar, and K. R. Niazi, "Discrete particle swarm optimization for optimal dg placement in distribution networks," in *18th National Power Syst. Conf.*, Dec 2014, pp. 1–6.

[123] R. S. A. Abri, E. F. El-Saadany, and Y. M. Atwa, "Optimal placement and sizing method to improve the voltage stability margin in a distribution system using distributed generation," *IEEE Trans. on Power Syst.*, vol. 28, no. 1, pp. 326–334, Feb 2013.

[124] I. S. Bae and J. O. Kim, "Reliability evaluation of distributed generation based on operation mode," *IEEE Trans. on Power Syst.*, vol. 22, no. 2, pp. 785–790, May 2007.

[125] Y. M. Atwa and E. F. El-Saadany, "Reliability evaluation for distribution system with renewable distributed generation during islanded mode of operation," *IEEE Trans. on Power Syst.*, vol. 24, no. 2, pp. 572–581, May 2009.

[126] P. M. Costa and M. A. Matos, "Economic analysis of microgrids including reliability aspects," in *2006 Int. Conf. on Probab. Methods Applied to Power Syst.*, June 2006, pp. 1–8.

[127] M. C., "Microgrids and heterogeneous power quality and reliability," *Int. Jour. of Distr. Energy Res.*, vol. 4, no. 4, pp. 281–295, 2008.

[128] B. Banerjee and S. M. Islam, "Reliability based optimum location of distributed generation," *Int. Jour. of Elect. Power & Energy Syst.*, vol. 33, no. 8, pp. 1470–1478, 2011.

[129] L. Wang and C. Singh, "Reliability-constrained optimum placement of reclosers and distributed generators in distribution networks using an ant colony system algorithm," *IEEE Trans. on Syst., Man, and Cyber., Part C (Appl. and Reviews)*, vol. 38, no. 6, pp. 757–764, Nov 2008.

[130] A. A. Chowdhury, S. K. Agarwal, and D. O. Koval, "Reliability modeling of distributed generation in conventional distribution systems planning and analysis," *IEEE Trans. on Indus. Appl.*, vol. 39, no. 5, pp. 1493–1498, Sept 2003.

[131] C. Novoa and T. Jin, "Reliability centered planning for distributed generation considering wind power volatility," *Elect. Power Syst. Res.*, vol. 81, no. 8, pp. 1654–1661, 2011.

[132] M. Moradi and A. Khandani, "Evaluation economic and reliability issues for an autonomous independent network of distributed energy resources," *Int. Jour. of Elect. Power & Energy Syst.*, vol. 56, pp. 75–82, 2014.

[133] R. Arya, S. Choube, and L. Arya, "Reliability evaluation and enhancement of distribution systems in the presence of distributed generation based on standby mode," *Int. Jour. of Elect. Power & Energy Syst.*, vol. 43, no. 1, pp. 607–616, 2012.

[134] Y. Atwa, E. El-Saadany, M. Salama, and R. Seethapathy, "Optimal renewable resources mix for distribution system energy loss minimization," *IEEE Trans. on Power Syst.*, vol. 25, no. 1, pp. 360–370, 2010.

[135] L. F. Ochoa and G. P. Harrison, "Minimizing energy losses: Optimal accommodation and smart operation of renewable distributed generation," *IEEE Trans. on Power Syst.*, vol. 26, no. 1, pp. 198–205, Feb 2011.

[136] N. Agarwal, K. Verma, K. R. Niazi, A. Swarnkar, and N. Gupta, "Optimal penetration of renewable sources for distribution system performance improvement," in *2015 IEEE Power Energy Soc. Gen. Meet.*, July 2015, pp. 1–5.

[137] V. R. Pandi, H. H. Zeineldin, and W. Xiao, "Determining optimal location and size of distributed generation resources considering harmonic and protection coordination limits," *IEEE Trans. on Power Syst.*, vol. 28, no. 2, pp. 1245–1254, May 2013.

[138] I. T. Papaioannou and A. Purvins, "A methodology to calculate maximum generation capacity in low voltage distribution feeders," *Int. Jour. of Elect. Power & Energy Syst.*, vol. 57, pp. 141 – 147, 2014.

[139] C. J. Dent, L. F. Ochoa, and G. P. Harrison, "Network distributed generation capacity analysis using opf with voltage step constraints," *IEEE Trans. on Power Syst.*, vol. 25, no. 1, pp. 296–304, Feb 2010.

[140] M. H. Moradi and M. Abedinie, "A combination of genetic algorithm and particle swarm optimization for optimal dg location and sizing in distribution systems," in *2010 Conf. Proc. IPEC*, Oct 2010, pp. 858–862.

[141] K. Vinothkumar and M. P. Selvan, "Distributed generation planning: A new approach based on goal programming," *Elect. Power Comp. and Syst.*, vol. 40, no. 5, pp. 497–512, 2012.

[142] K.-H. Kim, K.-B. Song, S.-K. Joo, Y.-J. Lee, and J.-O. Kim, "Multiobjective distributed generation placement using fuzzy goal programming with genetic algorithm," *Int. Trans. on Elect. Energy Syst.*, vol. 18, no. 3, pp. 217–230, 2008.

[143] M. R. Haghifam, H. Falaghi, and O. P. Malik, "Risk-based distributed generation placement," *IET Gen., Trans. Distr.*, vol. 2, no. 2, pp. 252–260, March 2008.

[144] F. S. Abu-Mouti and M. E. El-Hawary, "Optimal distributed generation allocation and sizing in distribution systems via artificial bee colony algorithm," *IEEE Trans. on Power Del.*, vol. 26, no. 4, pp. 2090–2101, Oct 2011.

[145] N. G. Hemdan and M. Kurrat, "Efficient integration of distributed generation for meeting the increased load demand," *Int. Jour. of Elect. Power & Energy Syst.*, vol. 33, no. 9, pp. 1572–1583, 2011.

[146] R. K. Singh and S. K. Goswami, "Multi-objective optimization of distributed generation planning using impact indices and trade-off technique," *Elect. Power Comp. and Syst.*, vol. 39, no. 11, pp. 1175–1190, 2011.

[147] P. N. Vovos and J. W. Bialek, "Direct incorporation of fault level constraints in optimal power flow as a tool for network capacity analysis," *IEEE Trans. on Power Syst.*, vol. 20, no. 4, pp. 2125–2134, Nov 2005.

[148] A. A. Tamimi, A. Pahwa, and S. Starrett, "Effective wind farm sizing method for weak power systems using critical modes of voltage instability," *IEEE Trans. on Power Syst.*, vol. 27, no. 3, pp. 1610–1617, Aug 2012.

[149] M. Raoofat, "Simultaneous allocation of dgs and remote controllable switches in distribution networks considering multilevel load model," *Int. Jour. of Elect. Power & Energy Syst.*, vol. 33, no. 8, pp. 1429 – 1436, 2011.

[150] A. M. El-Zonkoly, "Optimal placement of multi-distributed generation units including different load models using particle swarm optimisation," *IET Gen., Trans. Distr.*, vol. 5, no. 7, pp. 760–771, July 2011.

[151] G. Koutroumpezis and A. Safigianni, "Optimum allocation of the maximum possible distributed generation penetration in a distribution network," *Elect. Power Syst. Res.*, vol. 80, no. 12, pp. 1421 – 1427, 2010.

[152] A. S. A. Awad, T. H. M. El-Fouly, and M. M. A. Salama, "Optimal distributed generation allocation and load shedding for improving distribution system reliability," *Elect. Power Comp. and Syst.*, vol. 42, no. 6, pp. 576–584, 2014.

[153] T. Ackermann and V. Knyazkin, "Interaction between distributed generation and the distribution network: operation aspects," in *IEEE/PES T&D Conf. and Exhib.*, vol. 2, Oct 2002, pp. 1357–1362.

[154] A. Keane and M. O'Malley, "Optimal allocation of embedded generation on distribution networks," *IEEE Trans. on Power Syst.*, vol. 20, no. 3, pp. 1640–1646, Aug 2005.

[155] ——, "Optimal utilization of distribution networks for energy harvesting," *IEEE Trans. on Power Syst.*, vol. 22, no. 1, pp. 467–475, Feb 2007.

[156] Y. M. Atwa and E. F. El-Saadany, "Probabilistic approach for optimal allocation of wind-based distributed generation in distribution systems," *IET Renew. Power Gen.*, vol. 5, no. 1, pp. 79–88, January 2011.

[157] L. F. Ochoa, C. J. Dent, and G. P. Harrison, "Distribution network capacity assessment: Variable dg and active networks," *IEEE Trans. on Power Syst.*, vol. 25, no. 1, pp. 87–95, Feb 2010.

[158] G. P. Harrison and A. R. Wallace, "Optimal power flow evaluation of distribution network capacity for the connection of distributed generation," *IEE Proceedings–Gen., Trans. and Distr.*, vol. 152, no. 1, pp. 115–122, Jan 2005.

[159] S. Porkar, P. Poure, A. Abbaspour-Tehrani-fard, and S. Saadate, "Optimal allocation of distributed generation using a two-stage multi-objective mixed-integer-nonlinear programming," *Int. Trans. on Elect. Energy Syst.*, vol. 21, no. 1, pp. 1072–1087, 2011.

[160] A. Kumar and W. Gao, "Optimal distributed generation location using mixed integer non-linear programming in hybrid electricity markets," *IET Gen., Trans. Dist.*, vol. 4, no. 2, pp. 281–298, 2010.

[161] R. Jabr and B. Pal, "Ordinal optimisation approach for locating and sizing of distributed generation," *IET Gen., Trans. Dist.*, vol. 3, no. 8, pp. 713–723, 2009.

[162] S. Kotamarty, S. Khushalani, and N. Schulz, "Impact of distributed generation on distribution contingency analysis," *Elect. Power Syst. Res.*, vol. 78, no. 9, pp. 1537–1545, 2008.

[163] L. F. Ochoa, A. Padilha-Feltrin, and G. P. Harrison, "Evaluating distributed time-varying generation through a multiobjective index," *IEEE Trans. on Power Del.*, vol. 23, no. 2, pp. 1132–1138, 2008.

[164] D. T. C. Wang, L. F. Ochoa, and G. P. Harrison, "Modified ga and data envelopment analysis for multistage distribution network expansion planning under uncertainty," *IEEE Trans. on Power Syst.*, vol. 26, no. 2, pp. 897–904, May 2011.

[165] D. Singh and K. Verma, "Multiobjective optimization for dg planning with load models," *IEEE Trans. on Power Syst.*, vol. 24, no. 1, pp. 427–436, 2009.

[166] T. Shukla, S. Singh, V. Srinivasarao, and K. Naik, "Optimal sizing of distributed generation placed on radial distribution systems," *Elect. Power Comp. and Syst.*, vol. 38, no. 3, pp. 260–274, 2010.

[167] J.-H. Teng, Y.-H. Liu, C.-Y. Chen, and C.-F. Chen, "Value-based distributed generator placements for service quality improvements," *Int. Jour. of Elect. Power & Energy Syst.*, vol. 29, no. 3, pp. 268–274, 2007.

[168] G. Carpinelli, G. Celli, F. Pilo, and A. Russo, "Embedded generation planning under uncertainty including power quality issues," *Euro. Trans. on Elect. Power*, vol. 13, no. 6, pp. 381–389, 2003.

[169] G. P. Harrison, A. Piccolo, P. Siano, and A. R. Wallace, "Hybrid ga and opf evaluation of network capacity for distributed generation connections," *Elect. Power Syst. Res.*, vol. 78, no. 3, pp. 392–398, 2008.

[170] K.-H. Kim, Y.-J. Lee, S.-B. Rhee, S.-K. Lee, and S.-K. You, "Dispersed generator placement using fuzzy-ga in distribution systems," in *2002 IEEE Power Engg. Soc. Summer Meet.*, vol. 3. IEEE, 2002, pp. 1148–1153.

[171] K. Vinothkumar and M. P. Selvan, "Fuzzy embedded genetic algorithm method for distributed generation planning," *Elect. Power Comp. and Syst.*, vol. 39, no. 4, pp. 346–366, 2011.

[172] G. Celli, E. Ghiani, S. Mocci, and F. Pilo, "A multiobjective evolutionary algorithm for the sizing and siting of distributed generation," *IEEE Trans. on Power Syst.*, vol. 20, no. 2, pp. 750–757, May 2005.

[173] G. Carpinelli, G. Celli, S. Mocci, F. Pilo, and A. Russo, "Optimisation of embedded generation sizing and siting by using a double trade-off method," *IEE Proceedings–Gen., Trans. and Distr.*, vol. 152, no. 4, pp. 503–513, July 2005.

[174] L. F. Ochoa, A. Padilha-Feltrin, and G. P. Harrison, "Time-series-based maximization of distributed wind power generation integration," *IEEE Trans. on Energy Conv.*, vol. 23, no. 3, pp. 968–974, Sept 2008.

[175] E. Haesen, J. Driesen, and R. Belmans, "Robust planning methodology for integration of stochastic generators in distribution grids," *IET Renew. Power Gen.*, vol. 1, no. 1, pp. 25–32, March 2007.

[176] M. E. H. Golshan and S. Ali Arefifar, "Optimal allocation of distributed generation and reactive sources considering tap positions of voltage regulators as control variables," *Int. Trans. on Elect. Energy Syst.*, vol. 17, no. 3, pp. 219–239, 2007.

[177] M. Gomez-Gonzalez, A. López, and F. Jurado, "Optimization of distributed generation systems using a new discrete pso and opf," *Elect. Power Syst. Res.*, vol. 84, no. 1, pp. 174–180, 2012.

[178] W. El-Khattam, K. Bhattacharya, Y. Hegazy, and M. M. A. Salama, "Optimal investment planning for distributed generation in a competitive electricity market," *IEEE Trans. on Power Syst.*, vol. 19, no. 3, pp. 1674–1684, Aug 2004.

[179] D. Gautam and N. Mithulananthan, "Optimal dg placement in deregulated electricity market," *Elect. Power Syst. Res.*, vol. 77, no. 12, pp. 1627–1636, 2007.

[180] S. Ghosh, S. P. Ghoshal, and S. Ghosh, "Optimal sizing and placement of distributed generation in a network system," *Int. Jour. of Elect. Power & Energy Syst.*, vol. 32, no. 8, pp. 849–856, 2010.

[181] H. Khodr, M. R. Silva, Z. Vale, and C. Ramos, "A probabilistic methodology for distributed generation location in isolated electrical service area," *Elect. Power Syst. Res.*, vol. 80, no. 4, pp. 390–399, 2010.

[182] M. E. Baran and M.-Y. Hsu, "Volt/var control at distribution substations," *IEEE Trans. on Power Syst.*, vol. 14, no. 1, pp. 312–318, Feb 1999.

[183] Z. Shen, Z. Wang, and M. E. Baran, "Optimal volt/var control strategy for distribution system with multiple voltage regulating devices," in *PES T & D 2012*, May 2012, pp. 1–7.

[184] K. M. Muttaqi, A. D. T. Le, M. Negnevitsky, and G. Ledwich, "A coordinated voltage control approach for coordination of oltc, voltage regulator and dg to regulate voltage in a distribution feeder," in *2013 IEEE Indus. Appl. Soc. Annual Meet.*, Oct 2013, pp. 1–8.

[185] ——, "A novel tuning method for advanced line drop compensator and its application to response coordination of distributed generation with voltage regulating devices," *IEEE Trans. on Indus. Appl.*, vol. 52, no. 2, pp. 1842–1854, March 2016.

[186] A. Bernieri, G. Betta, C. Liguori, and A. Losi, "Neural networks and pseudo-measurements for real-time monitoring of distribution systems," *IEEE Trans. on Instrum. and Measur.*, vol. 45, no. 2, pp. 645–650, Apr 1996.

[187] T. Ackermann, G. Andersson, and L. Söder, "Distributed generation: a definition," *Elect. Power Syst. Res.*, vol. 57, no. 3, pp. 195–204, 2001.

[188] D. Ranamuka, A. P. Agalgaonkar, and K. M. Muttaqi, "Examining the interactions between dg units and voltage regulating devices for effective voltage control in distribution systems," *IEEE Trans. on Indus. Appl.*, vol. 53, no. 2, pp. 1485–1496, March 2017.

[189] A. Dukpa, B. Venkatesh, and L. Chang, "Fuzzy stochastic programming method: Capacitor planning in distribution systems with wind generators," *IEEE Trans. on Power Syst.*, vol. 26, no. 4, pp. 1971–1979, Nov 2011.

[190] M. Dadkhah and B. Venkatesh, "Cumulant based stochastic reactive power planning method for distribution systems with wind generators," *IEEE Trans. on Power Syst.*, vol. 27, no. 4, pp. 2351–2359, Nov 2012.

[191] Z. Liu, F. Wen, and G. Ledwich, "Optimal siting and sizing of distributed generators in distribution systems considering uncertainties," *IEEE Trans. on Power Del.*, vol. 26, no. 4, pp. 2541–2551, Oct 2011.

[192] W. Sheng, K. Y. Liu, Y. Liu, X. Meng, and Y. Li, "Optimal placement and sizing of distributed generation via an improved nondominated sorting genetic algorithm ii," *IEEE Trans. on Power Del.*, vol. 30, no. 2, pp. 569–578, April 2015.

[193] R. K. Roy, "A primer on the taguchi method, competitive manufacturing series," *New York*, pp. 7–80, 1990.

[194] ——, *A primer on the Taguchi method.* Society of Manufacturing Engineers, 2010.

[195] H. M. Hasanien and S. M. Muyeen, "A taguchi approach for optimum design of proportional-integral controllers in cascaded control scheme," *IEEE Trans. on Power Syst.*, vol. 28, no. 2, pp. 1636–1644, May 2013.

[196] A. Swarnkar, N. Gupta, and K. Niazi, "A novel codification for meta-heuristic techniques used in distribution network reconfiguration," *Elect. Power Syst. Res.*, vol. 81, no. 7, pp. 1619–1626, 2011.

[197] M. E. Baran and F. F. Wu, "Network reconfiguration in distribution systems for loss reduction and load balancing," *IEEE Trans. on Power Del.*, vol. 4, no. 2, pp. 1401–1407, Apr 1989.

[198] C.-L. Hwang and K. Yoon, *Multiple Attribute Decision Making Methods and Applications: A State-of-the-Art Survey.* Springer, Berlin, Heidelberg, 1981.

[199] K. Yoon, "A reconciliation among discrete compromise solutions," *Journal of the Operational Research Society*, pp. 277–286, 1987.

[200] K. Fiedler, F. Peldschus, and E. K. Zavadskas, *Methoden der bautechnologischen Entscheidung.* Rektor der Technischen Hochschule Leipzig, 1986.

[201] E. K. Zavadskas, F. Peldschus, and A. Kaklauskas, *Multiple criteria evaluation of projects in construction.* Technika,, 1994, vol. 1.

[202] E. Triantaphyllou, "Multi-criteria decision making methods," in *Multi-criteria decision making methods: A comparative study.* Springer, 2000, pp. 5–21.

[203] K. Zou, A. P. Agalgaonkar, K. M. Muttaqi, and S. Perera, "Distribution system planning with incorporating dg reactive capability and system uncertainties," *IEEE Trans. on Sust. Energy*, vol. 3, no. 1, pp. 112–123, 2012.

[204] A. O'Leary, D. Urbaniak, and L. Roussey, "Legal considerations surrounding the introduction of an emissions performance standard at eu level," ClientEarth, Report, Aug 2015.

[205] OFGEM, "Electricity distribution price control review policy paper," Office of Gas and Electricity Markets, Report, Dec 2008. [Online]. Available: http://www.ofgem.gov.uk

[206] A. O'Leary, D. Urbaniak, and L. Roussey, "Legal considerations surrounding the introduction of an emissions performance standard at eu level," ClientEarth, Report 22, Aug, 2015.

[207] HydroOne, "Technical dg interconnection requirements of hydro one," HydroOne, Report, Aug, 2015. [Online]. Available: http://www.hydroone.com

[208] D. Zhang, Z. Fu, and L. Zhang, "An improved ts algorithm for loss-minimum reconfiguration in large-scale distribution systems," *Elect. Power Sys. Res.*, vol. 77, no. 5, pp. 685–694, 2007.

[209] P. M. d. O. de Jesus, "Remuneration of distributed generation: A holistic approach," Ph.D. dissertation, Universidade do Porto (Portugal), 2007.

[210] Z. Wang, B. Chen, J. Wang, J. Kim, and M. M. Begovic, "Robust optimization based optimal dg placement in microgrids," *IEEE Trans. on Smart Grid*, vol. 5, no. 5, pp. 2173–2182, Sept 2014.

[211] I. C. da Silva, S. Carneiro, E. J. de Oliveira, J. de Souza Costa, J. L. R. Pereira, and P. A. N. Garcia, "A heuristic constructive algorithm for capacitor placement on distribution systems," *IEEE Trans. on Power Syst.*, vol. 23, no. 4, pp. 1619–1626, Nov 2008.

[212] I. Roytelman, B. K. Wee, and R. L. Lugtu, "Volt/var control algorithm for modern distribution management system," *IEEE Trans. on Power Syst.*, vol. 10, no. 3, pp. 1454–1460, Aug 1995.

[213] N. K. Meena and S. Chakrabarti, "Multi-criteria pmu placement for observability of power systems," in *6th IASTED Asian Conf. on Power and Energy Syst. (AsiaPES2013)*, Apr 2013, pp. 1–5.

[214] A. Abur and A. G. Exposito, *Power system state estimation: theory and implementation*. CRC press, 2004.

[215] J. Y. Park, J. M. Sohn, and J. K. Park, "Optimal capacitor allocation in a distribution system considering operation costs," *IEEE Trans. on Power Syst.*, vol. 24, no. 1, pp. 462–468, Feb 2009.

[216] J. Yan, B. Chen, R. Wennersten, P. Campana, and J. Yang, "Cleaner energy for transition of cleaner city," *Applied Energy*, vol. 196, no. Supplement C, pp. 97 – 99, 2017.

[217] R. Wenge, X. Zhang, C. Dave, L. Chao, and S. Hao, "Smart city architecture: A technology guide for implementation and design challenges," *China Communications*, vol. 11, no. 3, pp. 56–69, March 2014.

[218] S. F. Tie and C. W. Tan, "A review of energy sources and energy management system in electric vehicles," *Renewable and Sustainable Energy Reviews*, vol. 20, pp. 82 – 102, 2013. [Online]. Available: http://www.sciencedirect.com/science/article/pii/S1364032112006910

[219] T. Donateo, F. Licci, A. D'Elia, G. Colangelo, D. Laforgia, and F. Ciancarelli, "Evaluation of emissions of co2 and air pollutants from electric vehicles in italian cities," *Applied Energy*, vol. 157, no. Supplement C, pp. 675 – 687, 2015.

Publications

Following papers have been published/accepted out of this thesis work.

International Journals

1. N. K. Meena, S. Parashar, A. Swarnkar, N. Gupta and K. R. Niazi, "Improved elephant herding optimization for multiobjective DER accommodation in distribution systems," *IEEE Transactions on Industrial Informatics*, vol. 14, no. 03, pp. 1029-1039, 2018. DOI: 10.1109/TII.2017.2748220.

2. Nand K. Meena, A. Swarnkar, N. Gupta and K. R. Niazi, "Optimal integration of DERs in coordination with existing VRs in distribution networks" *IET Generation, Transmission, Distribution*, vol. 12, no. 11, 2520-2529, 2018. DOI: 10.1049/iet-gtd.2017.1403.

3. N. K. Meena, A. Swarnkar, N. Gupta and K. R. Niazi, "Multi-objective Taguchi approach for optimal DG integration in distribution systems," *IET Generation, Transmission, Distribution*, vol. 11, no. 9, pp. 2418–2428, 2017. DOI: 10.1049/iet-gtd.2016.2126.

4. N. K. Meena, A. Swarnkar, N. Gupta and K. R. Niazi, "Optimal Accommodation and Management of High Renewable Penetration in Distribution Systems," *The Journal of Engineering*, IET, vol. 2017, no. 13, pp. 1890-1895, 2017. DOI: 10.1049/joe.2017.0659.

5. N. K. Meena, S. Parashar, A. Swarnkar, N. Gupta, K. R. Niazi and R. C. Bansal, "Mobile Power Infrastructure Planning and Operational Management for Smart City Applications," *Energy Proceedia, Elsevier*, vol. 142, pp. 2202-2207, 2017. DOI: 10.1016/j.egypro.2017.12.589.

6. N. K. Meena, A. Swarnkar, N. Gupta and K. R. Niazi, "Stochastic Volt/Var planning and operation for microgrids with renewables," *International Journal of Electrical Energy*, vol. 4, no. 3, pp. 159–164, September 2016. DOI: 10.18178/ijoee.4.3.159-164.

International Conferences

1. N. K. Meena, A. Swarnkar, N. Gupta and K. R. Niazi, "Dispatchable Wind Power Generation Planning for Distribution Systems," Proc. *6th IEEE International Conference on Power Systems (ICPS2017)*, Pune, India **(Presented)**

2. N. K. Meena, A. Swarnkar, N. Gupta and K. R. Niazi, "Wind Power Generation Planning by Utilizing the Reactive Power Capabilities of Generators," Proc. *IEEE Asian Conference on Energy, Power and Transportation Electrification (ACEPT2017)*, Singapore, pp.1-6. DOI: 10.1109/ACEPT.2017.8168611.

3. N. K. Meena, A. Swarnkar, N. Gupta and K. R. Niazi, "Dispatchable Solar Photovoltaic Power Generation Planning for Distribution Systems," Proc. *12th IEEE International Conference on Industrial and Information Systems (ICIIS2017)*, Peradeniya, Sri Lanka, pp. 1-6. DOI: 10.1109/ICIINFS.2017.8300337.

4. N. K. Meena, A. Swarnkar, N. Gupta and K. R. Niazi, "A Taguchi-based approach for optimal placement of distributed generations for power loss minimization in distribution system," Proc. *IEEE Power & Energy Society General Meeting (PESGM2015)*, Denver, CO, pp. 1-5. DOI: 10.1109/PESGM.2015.7286180.

Brief bio-data

Nand Kishor Meena received the B.Tech.-M. Tech. (Dual-Degree) degree in electrical engineering from the Indian Institute of Technology, Kanpur, India, in 2011. He is currently working as an Assistant Professor in department of electrical engineering, Govt. Women Engineering College, Ajmer. His research interests include distributed resources planning, and operations and application of AI-techniques in modern power systems. Mr. Meena is member of IEEE, IET and CIGRE.